

**A Performance-based Evaluation of Asphalt Mixtures with High Recycled Asphalt
Material Contents and Recycling Agents**

by

Mawazo Chiyanda Fortunatus

A dissertation submitted to the Graduate Faculty of
Auburn University
in partial fulfillment of the
requirements for the Degree of
Doctor of Philosophy

Auburn, Alabama
December 11, 2021

Keywords: Recycled Asphalt Materials, Recycling Agent dosage, Rejuvenators, Softeners,
Asphalt Mixture Performance

Copyright 2021 by Mawazo Chiyanda Fortunatus

Approved by

Carolina Rodezno, Chair, Associate Research Professor, National Center for Asphalt Technology
Raquel Moraes, Co-chair, Assistant Research Professor, National Center for Asphalt Technology
Fan Yin, Assistant Director and Assistant Research Professor, National Center for Asphalt
Technology

Nam Tran, Assistant Director and Research Professor, National Center for Asphalt Technology
April E. Simons, Assistant Professor, McWhorter School of Building Science

ABSTRACT

It is agreed that the stiffness and rutting resistance of asphalt mixtures containing recycled asphalt material (RAM) increase with increasing their content; however, their cracking resistance and durability decrease due to the heavily aged asphalt binders in RAM. To mitigate these drawbacks, asphalt researchers and practitioners have explored the incorporation of recycling agents (RAs) in asphalt mixtures with high RAM content.

The purpose of this study was to develop a fundamental understanding of the effect of high RAM content on the performance of asphalt binder and mixtures, while evaluating the effectiveness of RAs in restoring the properties of RAM binder and thus, improving the performance of high RAM content mixtures. Finally, a methodology to guide the usage of RAs to produce high RAM content mixtures with satisfactory performance was recommended.

To accomplish the above objectives, three base binders, four RAM sources, three aggregate sources, four-bio-based RAs, and one petroleum-based RA were utilized. Recycled binder blends with different content of RAM binder alone or with RAs were evaluated using the Dynamic Shear Rheometer (DSR) to conduct Superpave performance grading (PG), multiple stress creep recovery (MSCR) test, linear amplitude sweep (LAS) test, and frequency sweep test to determine the Glover-Rowe (G-R) parameter. Bending Beam Rheometer (BBR) test was used to determine the low-temperature performance grade and Delta T_c (ΔT_c) parameter, while the Fourier-Transform Infrared Spectroscopy with the Attenuated Total Reflectance (FTIR-ATR) was used for evaluation of oxidation products. For short-term aging, the Rolling Thin Film Oven (RTFO) was performed, and the Pressure Oven Vessel (PAV) was followed for long-term aging simulation.

The mixtures were designed to meet the volumetric criteria and were subjected to short-term aging (STOA) and long-term aging (LTOA) of 4 and 6 hours, respectively at 135 °C. The mixtures were characterized for rutting resistance using the Hamburg Wheel Tracking Test (HWTT) and the Asphalt Pavement Analyzer (APA) test and moisture susceptibility using the HWTT. Both rutting resistance and moisture susceptibility were performed after STOA. The intermediate temperature cracking resistance and low temperature cracking resistance were evaluated after LTOA using the Indirect Tensile Asphalt Cracking Test (IDEAL-CT) and the Disk-Shaped Compact Tension Test (DCT), respectively. The dynamic modulus ($|E^*|$) was conducted to analyze the viscoelasticity and aging properties of the mixtures after both STOA and LTOA.

Binder testing results showed that the performance of the recycled binder blends was influenced by the RAM type, quantity, and RA type. Based on the DSR testing, the addition of RAM to the base binders improved their rutting and stiffening properties but had a negative impact on fatigue resistance and thermal cracking properties. The addition of RAs improved the fatigue and thermal cracking properties without being detrimental to the rutting properties of the recycled binder blends. Based on the G-R parameter, stiffness and embrittlement properties of the recycled binder blends increased with the addition of RAM binder, but they decreased when RAs were incorporated. Moreover, the ΔT_c showed that recycled binder blends with up to 40% RAP binder met the minimum threshold of -5 °C after RTFO plus 40 hours of PAV that has been recommended to minimize the risk of age-related block cracking.

According to the HWTT, all high RAM content mixtures had improved rutting resistance and were less prone to moisture damage. The APA suggested that RAs did not have a significant impact on the rutting resistance of the high RAM content mixtures. The fracture energy parameter from the DCT test showed that the control mixtures were not statistically significant different from the high

RAM content mixtures with or without RAs. The IDEAL-CT results showed that the CT_{index} values of the control mixtures were significantly higher than all high RAM contents mixtures (with or without RAs). This indicates that mixtures with high RAM contents were expected to have lower intermediate temperature cracking resistance than the control mixtures. The G-R_m aging index showed that high RAM content mixtures with RAs had low or equivalent aging susceptibility as the control mixture.

The results from this study were used to develop a methodology to guide the usage of RAs for production of high RAM content mixtures and materials from Wisconsin were used to demonstrate it. The first part of the methodology involves determination of optimum RA dosage using blending charts. Mixtures are prepared at desired proportions of RAM and aged accordingly, then performance testing of the mixtures in terms of rutting, intermediate and low temperature cracking resistance is conducted to evaluate if they meet the requirements.

Further, analysis of IDEAL-CT parameters, suggested that the CT_{index} had moderate correlation with the post peak slope whereas the relationship with the fracture energy was very poor. In addition, preliminary thresholds for the post peak slope and fracture energy were suggested to facilitate compliance with the CT_{index} criterion.

A limited evaluation using the IDEAL-CT test showed that a combination of RAs with a discount factor to account for the inactive RAM binder could improve the intermediate temperature cracking resistance of high RAM content mixtures. However, this finding needs to be further evaluated using more mixtures with different materials components.

ACKNOWLEDGEMENTS

I am thankful to the Almighty God for giving me life and an opportunity of pursuing my dreams.

I am also grateful to my father who has always believed in me and supported me in every capacity to achieve whatever I wanted. I am truly blessed to have him as my father.

My sincere thanks to my advisors, Dr. Carolina Rodezno (committee chair) and Dr. Raquel Moraes (co-chair), for their supervision, guidance, encouragement, support, and constructive criticism during my doctorate studies. Their patience and dedication to assisting me are highly appreciated.

I extend my gratitude to the member of the committee: Dr. Fan Yin, Dr. Nam Tran, and April Simons (University reader) for reviewing this dissertation and their valuable comments.

Also, I am immensely thankful to the staff of the National Center for Asphalt Technology (NCAT) at Auburn University who took me in as family and have always made my experience in Auburn joyful and memorable. My special thanks are also due to the Wisconsin and South Dakota DOTs for funding the projects which produced this dissertation.

Finally, my sincere gratitude goes to all my friends, colleagues, and every individual who has made my doctorate studies worthwhile. Your support, encouragement, unconditional care, and friendship; have greatly impacted my life.

DEDICATION

This dissertation is dedicated to:

My late lovely mother, Kariba Mashauri Lukiko (1963 – 2005)

My late sweet sister, Zainabu Nyamisi Chiyanda (1992 – 2020)

My late big brother, Stephano Mashauri Chiyanda (1984 – 2020)

I am grateful for your unconditional love, support, and encouragements. You will always be remembered.

TABLE OF CONTENTS

ABSTRACT.....	2
ACKNOWLEDGEMENTS	5
DEDICATION.....	6
LIST OF TABLES	10
LIST OF FIGURES	12
LIST OF ABBREVIATIONS	17
1. INTRODUCTION	19
1.1. Background	19
1.2. Problem Statement	23
1.3. Hypothesis.....	24
1.4. Objectives.....	25
1.5. Scope	25
1.6. Organization of the Dissertation	27
2. LITERATURE REVIEW	28
2.1. Introduction	28
2.2. Use of Softer Binders	30
2.3. Polymer Modified Asphalt Binder	33
2.4. Increasing the Effective Asphalt Binder Content of the Mixture.....	35
2.5. Recycling Agents	36
2.5.1. Classification and Categorization of Recycling Agents	37
2.5.2. Mechanism of Action of Recycling Agents.....	41
2.5.3. Factors Affecting Effectiveness of Recycling Agents	45
2.5.3.1. Type and Dosage of Recycling Agent.....	45
2.5.3.2. Properties of the Virgin and RAM Binders	48
2.5.3.3. Quantity of RAM in Recycled Binder Blends and/or Mixtures	49
2.5.3.4. Mixing Temperature and Conditioning Time.....	50
2.5.3.5. Recycling Agent Addition Methods	52

2.5.4.	Determination of Optimum Recycling Agent Dosage.....	54
2.5.4.1.	Matching the Physical Properties of the Recycled Binder Blends to that of the Target Binder	55
2.5.4.2.	Matching the Rheological Properties of the Recycled Binder Blends to that of the Target Binder	57
2.6.	Blending Efficiency of RAM Binder	61
2.6.1.	Virgin coarse aggregates-Fine RAP mixture	64
2.6.2.	Gap graded mixtures of coarse virgin aggregates and RAP material	67
2.6.3.	Recycled asphalt mixture performance property parameter	68
2.7.	Performance Characterization of Asphalt Binder and/or Mixtures with RAs	69
2.8.	Field Performance of high RAM content Asphalt Binders/ Mixtures with RAs	73
2.9.	Summary	83
2.10.	Knowledge Gaps Identified from Literature	84
3.	METHODOLOGY	86
3.1.	Introduction	86
3.2.	Material Selection	88
3.2.1.	Base Binders and Recycling Agents	88
3.2.2.	Virgin Aggregates and RAM Materials	89
3.3.	Preparation of Recycled Asphalt Binder Blends.....	92
3.4.	Asphalt Binder Testing.....	94
3.4.1.	Performance Grading and ΔT_c Parameter	95
3.4.2.	Multiple Stress Creep Recovery (MSCR) Test.....	96
3.4.3.	G-R parameter.....	96
3.4.4.	Linear Amplitude Sweep (LAS) Test	97
3.4.5.	Extended Bending Beam Rheometer (BBR) Test	97
3.4.6.	Oxidative Aging Products.....	98
3.5.	Determination of Optimum Recycling Agent Dose for Asphalt Mixtures	98
3.6.	Design of Asphalt Mixtures	102
3.7.	Asphalt Mixtures Mixing Procedure	111
3.8.	Short and Long-Term Aging of Asphalt Mixtures.....	112
3.9.	Asphalt Mixture Performance Testing.....	115
3.9.1.	Hamburg Wheel Tracking Test (HWTT)	116
3.9.2.	Asphalt Pavement Analyzer (APA) Test	117

3.9.3.	Indirect Tensile Asphalt Cracking Test (IDEAL-CT)	118
3.9.4.	Disk-shaped Compact Tension (DCT) Test.....	120
3.9.5.	Dynamic Modulus ($ E^* $) Test.....	122
4.	ASPHALT BINDER TESTING RESULTS.....	125
4.1.	Introduction	125
4.2.	Performance Grading and ΔT_c Parameter.....	125
4.3.	Multiple Stress Creep Recovery (MSCR).....	139
4.4.	Viscoelasticity and Aging Properties	148
4.5.	Linear Amplitude Sweep (LAS) Test.....	160
4.6.	Extended Bending Beam Rheometer (BBR) Test.....	165
4.7.	Products of Oxidative Aging.....	167
4.8.	Summary	169
5.	ASPHALT MIXTURES PERFORMANCE RESULTS.....	171
5.1.	Introduction	171
5.2.	Rutting Resistance and Moisture Susceptibility.....	172
5.3.	Intermediate Temperature Cracking Resistance	177
5.4.	Low-Temperature Cracking Resistance	191
5.5.	Viscoelasticity and Aging Properties	194
5.6.	Summary	206
6.	CONCLUSIONS.....	212
7.	RECOMMENDATIONS	216
	REFERENCES.....	221

LIST OF TABLES

Table 2.1: Maximum allowable and recommendations for high RAM content mixtures by Rodezno et al. (2021).....	31
Table 2.2: Types of RAs by NCAT (2014).....	37
Table 2.3: Categorization of RAs by De Bock et al. (2020).....	38
Table 2.4: DoAv results from Yu et al. (2017) study	66
Table 3.1: Physical properties of the RAs	89
Table 3.2: Particle size distribution of Aggregate 1 material	90
Table 3.3: Properties of Aggregate 1 material	90
Table 3.4: Particle size distribution of Aggregate 2 material	91
Table 3.5: Properties of Aggregate 2 material	91
Table 3.6: Particle size distribution of South Dakota material	92
Table 3.7: Properties of South Dakota aggregates.....	92
Table 3.8: Wisconsin's asphalt binder blends combinations.....	93
Table 3.9: South Dakota's asphalt binder blends combination.....	94
Table 3.10: Asphalt binders performance properties and parameters.....	95
Table 3.11: Recycling agents' dosage for Wisconsin Mixtures	101
Table 3.12: Recycling agents' dosages for South Dakota mixtures	101
Table 3.13: Specifications requirements for 12.5 mm-NMAS mixtures for both Wisconsin and South Dakota DOTs.....	102
Table 3.14: Wisconsin's asphalt mixtures combinations	104
Table 3.15: South Dakota's asphalt mixtures combinations	104
Table 3.16: Maximum allowable percent asphalt binder replacement (WisDOT, 2021).....	104
Table 3.17: Recycling agent dosages for Wisconsin mixtures	105

Table 3.18: Wisconsin's Aggregate 1 blends	106
Table 3.19: Wisconsin's Aggregate 2 blends	106
Table 3.20: South Dakota's aggregate blends	106
Table 3.21: Wisconsin's JMF for Aggregate 1 mixtures	108
Table 3.22: Wisconsin's JMF for Aggregate 2 mixtures	109
Table 3.23: South Dakota's JMFs.....	110
Table 3.24: Summary of mixture aging conditions used in this study.....	114
Table 3.25: Asphalt mixtures performance properties and parameters	115
Table 4.1: Performance grading of the recycled binder blends with the PG 58S-28 and PG 58V-28 binders.....	127
Table 4.2: Performance grading of the recycled binder blends with the PG 58S-34 binder	135
Table 4.3: Results of the extended BBR test at T_g conditioning	166
Table 5.1: Preliminary BMD thresholds for Wisconsin mixtures by West et al. (2021b).....	172
Table 5.2: Aggregate 1 HWTT results.....	175
Table 5.3: Aggregate 2 HWTT results.....	176
Table 5.4: Tukey-Kramer grouping of Aggregate 1 mixtures with the PG 58S-28 binder	197
Table 5.5: Tukey-Kramer groupings of Aggregate 2 mixtures.....	200
Table 7.1: Requirements of the constituent binders.....	217
Table 7.2: Preliminary BMD thresholds for Wisconsin mixtures by West et al. (2021b).....	219

LIST OF FIGURES

Figure 2.1: Crack growth of the N1 and N7 test sections from 2015 to 2017	81
Figure 3.1: Experimental testing plan for Wisconsin material	87
Figure 3.2: Experimental testing plan for South Dakota material	88
Figure 3.3: Preparation of recycled binder blends (a) Addition of RAs (b) checking temperature	93
Figure 3.4: Effect of RAS binder increase on true grade.....	100
Figure 3.5: Example of RA dosage determination.....	100
Figure 3.6: HWTT (a) Experimental setup (b) Data analysis.....	117
Figure 3.7: APA (a) Experimental setup (b) Data analysis	118
Figure 3.8: IDEAL-CT (a) Experimental setup (b) Data analysis	119
Figure 3.9: DCT (a) Experimental setup (b) Data analysis	121
Figure 3.10: Dynamic modulus (a) Experimental setup (b) Data analysis.....	123
Figure 4.1: Relationship between temperature properties and RAP1 binder increase for the recycled binder blends with the PG 58S-28 binder	128
Figure 4.2: Relationship between temperature properties and RAP2 binder increase for the recycled binder blends with the PG 58V-28 binder.....	129
Figure 4.3: Relationship between temperature properties and RAS binder increase for the recycled binder blends with the PG 58S-28 binder	129
Figure 4.4: Relationship between temperature properties and the RAS binder increase for the recycled binder blends with the PG 58V-28 binder.....	130
Figure 4.5: Relationship between temperature properties and RAP1 + RAS binder increase for the recycled binder blends with the PG 58S-28 binder.....	130
Figure 4.6: Relationship between temperature properties and the RAP1 + RAS binder increase for the recycled binder blends with the PG 58V-28 binder	131

Figure 4.7: Change in true temperature properties of the 25% ABR blends with the PG 58S-28 binder	132
Figure 4.8: Change in true temperature properties of the 35% ABR blends with the PG 58S-28 binder	133
Figure 4.9: Change in true temperature properties of the 40% ABR blends with the PG 58S-28 binder	133
Figure 4.10: Change in true temperature properties of the 40% ABR blends with the PG 58V-28 binder	134
Figure 4.11: Relationship between temperature properties and the RAP binder increase for the recycled binder blends with the PG 58S-34 binder	136
Figure 4.12: Change in true temperature properties of the 35% ABR blends with the PG 58S-34 binder	138
Figure 4.13: Change in the true temperature properties of the 50% ABR blends with the PG 58S-34 binder	139
Figure 4.14: Effect of increase in ABR on J_{nr} @ 3.2 kPa and 64 °C for recycled binder blends with the PG 58S-28 binder.....	140
Figure 4.15: Effect of increase in ABR on % recovery @3.2 kPa and 64 °C for recycled binder blends with the PG 58S-28 binder	141
Figure 4.16: Effect of increase in ABR on J_{nr} @3.2 kPa and 64 °C for recycled binder blends with the PG 58V-28 binder.....	142
Figure 4.17: Effect of increase in ABR on % recovery @3.2 kPa and 64 °C for recycled binder blends with the PG 58V-28 binder.....	142
Figure 4.18: Effect of addition of RAs on J_{nr} @3.2 kPa and 64 °C	144
Figure 4.19: Effect of addition of RAs on % recovery @3.2 kPa and 64 °C	144
Figure 4.20: Effect of increase in ABR on J_{nr} @3.2 kPa and 58 °C for recycled binder blends with the PG 58S-34 binder.....	145

Figure 4.21: Effect of increase in ABR on % recovery @3.2 kPa and 58 °C for recycled binder blends with the PG 58S-34 binder	146
Figure 4.22: Effect of addition of RAs on J_{nr} @3.2 kPa and 58 °C for recycled binder blends with the PG 58S-34 binder.....	147
Figure 4.23: Effect of addition of RAs on % recovery @ 3.2 kPa and 58 °C for recycled binder blends with the PG 58S-34 binder	147
Figure 4.24: Relationship of J_{nr} and % recovery for all recycled binder blends.....	148
Figure 4.25: Black space diagram of the recycled binder blends prepared with the PG 58S-28 binder and with or without RA1 at the unaged condition.....	150
Figure 4.26: Black space diagram of the recycled binder blends prepared with the PG 58S-28 binder and with or without after RTFO plus 40 hours PAV.....	150
Figure 4.27: Black space diagram of the recycled binder blends prepared with the PG 58S-28 binder and with or without RA2 at the unaged condition.....	151
Figure 4.28: Black space diagram of the recycled binder blends prepared with the PG 58S-28 binder and with or without RA2 after RTFO plus 40 hours PAV	152
Figure 4.29: Black space diagram of the recycled binder blends prepared with the PG 58V-28 binder and with or without RA1 at the unaged condition.....	153
Figure 4.30: Black space diagram of the recycled binder blends prepared with the PG 58V-28 binder and with or without RA1 after RTFO plus 40 hours PAV	153
Figure 4.31: G-R aging index of the recycled binder blends prepared with the PG 58S-28 binder and with or without RA1.....	154
Figure 4.32: G-R aging index of the recycled binder blends prepared with the PG 58S-28 binder and with or without RA2.....	155
Figure 4.33: G-R aging index of the recycled binder blends prepared with the PG 58V-28 binder and with or without RA1.....	156
Figure 4.34: Black space diagram of the recycled binder blends prepared with the PG 58S-34 binder and with or without RAs at the unaged state	158

Figure 4.35: Black space diagram of the recycled binder blends with the PG 58S-34 binder and with or without RAs after RTFO plus 60 hours PAV.....	158
Figure 4.36: G-R aging index of the recycled binder blends prepared with the PG 58S-34 binder and with or without RAs.....	160
Figure 4.37: N_f at 2.5% strain of the recycled binder blends prepared with the PG 58S-28 binder.....	161
Figure 4.38: N_f at 2.5% strain of the recycled binder blends prepared with the PG 58V-28.....	162
Figure 4.39: N_f at 2.5% strain of the recycled binder blends with RAs.....	163
Figure 4.40: $ B $ parameter of the recycled binder blends with and without RAs.....	164
Figure 4.41: Hardening rate of the recycled binder blends with RAs.....	166
Figure 4.42: C=O + S=O areas of the RAs at unaged state.....	167
Figure 4.43: C=O + S=O areas of the recycled binder blends prepared with the PG 58S-28 binder after RTFO plus 40 hours PAV.....	168
Figure 4.44: C=O + S=O areas of the recycled binder blends prepared with the PG 58S-34 binder after RTFO plus 60 hours PAV.....	169
Figure 5.1: HWTT rut depth curves for Aggregate 1 mixtures.....	173
Figure 5.2: HWTT rut depth curves for Aggregate 2 mixtures.....	173
Figure 5.3: APA rut depth results for South Dakota mixtures.....	177
Figure 5.4: CT_{index} results of Aggregate 1 mixtures.....	179
Figure 5.5: CT_{index} results of Aggregate 2 mixtures.....	180
Figure 5.6: CT_{index} results of the South Dakota mixtures.....	182
Figure 5.7: Relationship between CT_{index} and post peak slope for Wisconsin mixtures.....	183
Figure 5.8: Relationship between CT_{index} and fracture energy for Wisconsin mixtures.....	183
Figure 5.9: Relationship between CT_{index} and post peak slope for South Dakota mixtures.....	184
Figure 5.10: Relationship between CT_{index} and fracture energy for South Dakota mixtures.....	185

Figure 5.11: Space diagram of IDEAL-CT parameters for Wisconsin mixtures	186
Figure 5.12: Mean CT_{index} values after an increase of RA dosage	187
Figure 5.13: Mean CT_{index} values of the 35% ABR mixture after an increase in the dosage of RA1	189
Figure 5.14: Mean CT_{index} values of the 35% ABR mixture at different aging levels.....	190
Figure 5.15: Mean CT_{index} values of the 35% ABR mixture with a discount factor.....	191
Figure 5.16: DCT's fracture energy results for the Wisconsin mixtures	192
Figure 5.17: DCT's fracture energy results of South Dakota mixtures.....	194
Figure 5.18: Dynamic modulus master curves of Aggregate 1 mixtures with the PG 58S-28 binder after STOA.....	195
Figure 5.19: Dynamic modulus master curves of Aggregate 1 mixtures with the PG 58S-28 binder after LTOA	196
Figure 5.20: Dynamic modulus master curves of Aggregate 1 mixtures with the PMB after STOA and LTOA.....	198
Figure 5.21: Dynamic modulus master curves of Aggregate 2 mixtures after STOA.....	199
Figure 5.22: Dynamic modulus master curves of Aggregate 2 mixtures after LTOA	199
Figure 5.23: Black space diagram of Aggregate 1 mixtures.....	202
Figure 5.24: Black space diagram of Aggregate 2 mixtures.....	203
Figure 5.25: $G-R_m$ of Aggregate 1 mixtures	204
Figure 5.26: $G-R_m$ of Aggregate 2 mixtures	204
Figure 5.27: $G-R_m$ aging index of Wisconsin mixtures	206

LIST OF ABBREVIATIONS

AASHTO	American Association of State Highways and Transportation Officials
APA	Asphalt Pavement Analyzer
ASTM	American Society for Testing and Materials
BBR	Bending Beam Rheometer
BMD	Balanced Mix Design
CRD	Corrected Rut Depth
CT _{index}	Cracking Tolerance Index
DCT	Disk-Shaped Compact Tension
DoA	Degree of Activity
DoAv	Degree of Availability
DoB	Degree of Blending
DOT	Department of Transportation
DSR	Dynamic Shear Rheometer
FTIR	Fourier-Transform Infrared Spectroscopy
HMA	Hot Mix Asphalt
HTPG	High Temperature Performance Grade
HWTT	Hamburg Wheel Tracking Test
IDEAL-CT	Indirect Tensile Asphalt Cracking Test
I-FIT	Illinois Flexibility Index Test
JMF	Job Mix Formula
LAS	Linear Amplitude Sweep
LTOA	Long-Term Oven Aging

LTPG	Low Temperature Performance Grade
LTOA	Long-Term Oven Aging
MSCR	Multiple Stress Creep Recovery
MW RAS	Manufactured Waste RAS
NCAT	National Center for Asphalt Technology
NCHRP	National Cooperative Highway Research Program
NMAS	Nominal Maximum Aggregate Size
OT	Overlay Test
PAV	Pressure Aging Vessel
PC RAS	Post-Consumer RAS
PG	Performance Grade
PMB	Polymer Modified Binder
RA	Recycling Agent
RAM	Recycled Asphalt Materials
RAP	Reclaimed Asphalt Pavements
RAS	Recycled Asphalt Shingles
RTFO	Rolling Thin Film Oven
SHRP	Strategic Highway Research Program
SN	Stripping Number
STOA	Short-Term Oven Aging
VMA	Voids in Mineral Aggregate
WMA	Warm Mix Asphalt

1. INTRODUCTION

1.1. Background

The use of recycled asphalt materials (RAM) offers significant economic and environmental benefits that encourage the incorporation of high contents in the production of asphalt mixtures. According to the National Asphalt Pavement Association (NAPA), the total estimated tons of reclaimed asphalt pavements (RAP) and recycled asphalt shingles (RAS) used in hot mix asphalt (HMA) in 2019 were 89.2 million tons and 921,000 tons, respectively. Moreover, it was also reported that the combined savings of asphalt binder and aggregates from the usage of RAP and RAS were estimated to be more than \$3.3 billion and about 59 million cubic yards of landfill space (Williams et al., 2020).

The current RAP content in asphalt mixtures produced in the U.S. ranges from 20 percent to 30 percent (Williams et al., 2020), whereas RAS content ranges between 2 percent to 5 percent (Aschenbrener, 2018) by weight of the asphalt mixture. Despite the pressing interest of highway agencies to increase the amount of RAM used in asphalt mixtures, it is recognized that asphalt mixtures with high quantities of RAM tend to be less durable and more susceptible to cracking due to the stiff and heavily oxidized asphalt binder present in RAM (Arámbula-Mercado et al., 2018; Kaseer et al., 2019b; Martin et al., 2019; Mogawer et al., 2013; Tran et al., 2012; Zaumanis et al., 2013).

Several engineering practices and innovative technologies have been employed to account for the drawbacks of RAM to increase their content in asphalt mixtures. These practices and technologies include but are not limited to the use of softer asphalt binders (Arámbula-Mercado et al., 2018; Martin et al., 2019; Tran et al., 2012), incorporation of polymer modified asphalt binders (Kim et al., 2009; West et al., 2018b; Yan et al., 2017), increase the effective asphalt binder content of the mixture (Buchanan, 2018; Tran et al., 2019a; Tran et al., 2019b), and the use of recycling agents (RAs) (Hand and Martin, 2020; Im et al., 2016; Martin et al., 2019; Mogawer et al., 2013).

The use of RAs in asphalt mixtures with high RAM contents has been gaining interest in recent years due to advancement in the technology, their availability, ease of addition in asphalt mixtures, and associated cost savings when high RAM contents are incorporated in asphalt mixtures (Kaseer et al., 2020). Recycling agents are commonly referred to as rejuvenators, and in some cases, these terms are used synonymously; however, in a more general perspective, the term “recycling agent” also includes softeners (Kaseer et al., 2019b; Martin et al., 2019). Softeners are low viscosity oils that reduce the stiffness of aged binders, whereas rejuvenators partially restore the chemical balance, reduce brittleness, and/ or improve aging sensitivity in addition to reducing the stiffness of aged binders (Hand and Martin, 2020).

Several studies have shown that RAs are effective in reducing the stiffness, viscosity, and embrittlement of the heavily aged binders in RAM, thus improving the cracking resistance of asphalt binders and mixtures (Arámbula-Mercado et al., 2018; Garcia Cucalon et al., 2019; Im et al., 2016; Mogawer et al., 2013; Rajib et al., 2020; Tabatabaee and Kurth, 2017; Tran et al., 2012; Valdés et al., 2011; Zaumanis et al., 2013). Moreover, studies have shown that the effectiveness of RAs in recycled binder blends (recycled asphalt binder + virgin asphalt binder) and recycled asphalt mixtures depend on mixture design factors and asphalt mixture production factors.

Mix design factors include the type and dosage of RAs, properties of virgin asphalt binder, and recycled asphalt binder (Garcia Cucalon et al., 2019; Martin et al., 2019; Shen et al., 2007; Zaumanis et al., 2014b). Asphalt mixture production factors include mixing temperature and time, silo conditioning time, and the method by which RAs are added to the mixture (Lu et al., 2019; West et al., 2019; West and Copeland, 2015; Zaumanis et al., 2019).

If all other factors mentioned above remain unchanged, the recycling agent dosage rate is the main factor that balances the rutting and cracking performances of recycled asphalt binders and mixtures (Kaseer et al., 2020). While the designer can take advantage of the stiffened aged binder from RAM to provide rutting resistance of the asphalt mixture, overcapitalization of this benefit would most likely compromise the cracking resistance of the asphalt mixtures. Thus, the RA dosage should aim at balancing both the cracking and rutting performance of the asphalt mixture. A low dosage may partially reduce the stiffness and brittleness of the aged binder from RAM but may not improve the cracking resistance of the asphalt mixture. On the contrary, high dosage may soften the recycled binder too much causing permanent deformation (rutting) related problems especially at early ages of the pavement (Kaseer et al., 2020). Therefore, for the asphalt industry to gain sustainable benefits by using a high amount of RAM in asphalt mixtures, a proper selection and dosage rate of RAs is of paramount importance.

Due to the lack of a standardized RA dosage selection procedure, researchers use either dosages recommended by manufacturers or blending charts developed from properties of blended base asphalt binders, recycled asphalt binders, and RAs. The blending charts are used to match physical properties such as penetration points, softening values, and viscosity (Forton et al., 2020; Guduru et al., 2021; Sánchez et al., 2020; Zaumanis et al., 2014a), or rheological properties such as high-temperature performance grade (HTPG) or low-temperature performance grade (LTPG)

(Arámbula-Mercado et al., 2018; Martin et al., 2019; Zaumanis et al., 2014b) to that of the target asphalt binder to satisfy both climate and traffic requirements of the project.

Recently, the National Cooperative Highway Research Program (NCHRP) completed a project (NCHRP 9-58) that evaluated the effects of RAs on high RAM content asphalt binder blends and mixtures (Martin et al., 2019). This report recommended that RAs dosage rate for recycled asphalt binder blends should be selected to restore the continuous HTPG to that of the target asphalt binder that satisfies both climate and traffic requirements (Martin et al., 2019). To verify the effectiveness of this approach on improving the long-term cracking performance of asphalt mixtures, the current AASHTO R30 was used as a long-term aging protocol. This protocol requires conditioning compacted specimens in an oven set at 85 ± 3 °C for five days to simulate long-term aging of the asphalt mixture in the field. Despite their recommendation, the researchers suggested that a more representative long-term aging procedure was needed to simulate approximately 7 to 10 years when asphalt pavements are most prone to cracking. This suggestion was based on the NCHRP 9-52 project that pointed out that the AASHTO R30 long-term aging procedure only simulates approximately 1 to 2 years of field aging depending on the specific project climate (Newcomb et al., 2015) instead of the 5-10 years as found during the Strategic Highway Research Program (SHRP) study (Bell et al., 1994). In addition, NCHRP 9-23 project showed that conditioning specimen per AASHTO R30 leads to the development of oxidation gradient in the specimen from the center to its periphery; hence, not truly simulating the field condition as oxidation aging in the field is more pronounced at the pavement surface and it decreases with depth (Houston et al., 2005). NCHRP 9-58 project further warns about the potential for moisture susceptibility for asphalt mixtures with RAs dosages determined to match the continuous HTPG of the target binder. The report states that some asphalt mixtures failed the Hamburg Wheel Tracking Test (HWTT)

criteria. However, these same asphalt mixtures passed the rutting criteria when they were conducted under dry conditions, indicating that rutting resistance can be achieved when mixtures are dosed with RAs to match the continuous HTPG for the target climate and traffic, but they may be susceptible to moisture damage.

1.2. Problem Statement

The use of RAM has significant economic and environmental benefits; including cost savings, conservation of natural resources, and reduction in energy consumption and emissions. There is a general agreement that the stiffness and rutting resistance of asphalt mixtures containing RAM increase with increasing RAM content, while their cracking resistance and durability tend to decrease due to the heavily aged asphalt binders in RAM. To help mitigate the stiffening effect of the RAP and/or RAS materials, asphalt researchers and practitioners have explored the incorporation of RAs. Conceptually, the decreased stiffness after RAs incorporation has the potential to be a detriment to early mixture performance due to increased potential for rutting, but a benefit in the long-term due to improved durability.

While the sustainability aspect and potential economic benefits of producing asphalt mixtures with high RAM content and RAs are well understood, the performance implication of high RAM content mixtures with RAs is still unclear due to the various interaction effects of RAs with other mixture components, which will depend on the total binder availability, RA dosage and its chemical composition, among other factors. Furthermore, the poor performance of rejuvenated high content RAM mixtures can be partially attributed to the current design systems due to inadequate characterization of the effect of reclaimed materials and RAs on the performance properties of the mixture.

Therefore, a performance-based evaluation is needed to design asphalt mixtures with high RAM content and RAs that provide durable mixtures with optimized performance in terms of rutting and cracking resistance. For such evaluation, the long-term effectiveness of rejuvenated high RAM content mixtures must be assessed in the laboratory with an aging protocol capable of simulating proper field aging based on climate, while practical and convenient for routine use.

1.3. Hypothesis

The presence of RAs can potentially affect the performance of asphalt mixtures with high RAM content as indicated by changes in the properties of rejuvenated recycled binders. It is hypothesized that the main benefit of using RAs in the aged RAM mixtures is their ability to improve the aged RAM performance by reducing the stiffness and brittleness of the recycled binder. In addition, it is hypothesized that high RAM content mixtures with proper RAs dosage and designed following volumetrics mix design approach are expected to have equivalent performance to control mixtures with low RAM content.

1.4. Objectives

The objectives of this study were to:

1. Evaluate the effect of high RAM contents on the performance of asphalt binders and mixtures.
2. Evaluate the effectiveness of RAs in softening RAM binders and improving the performance of recycled asphalt mixtures by reducing the stiffness and brittleness of the recycled binder.
3. Recommend a methodology to guide the use of RAs to produce high RAM content asphalt mixtures with satisfactory performance.

1.5. Scope

To accomplish the objectives of this research, a comprehensive experimental test matrix including binder and mixture testing was completed to develop a fundamental evaluation of asphalt mixtures with high RAM contents and RAs. Aged asphalt binders from RAM were extracted and recovered, then blended with base binders from Wisconsin and South Dakota. Wisconsin's asphalt binder blends used two different RAP sources and one RAS source, whereas South Dakota's included only one RAP source. In addition, two base binders were used for Wisconsin's binder blends and mixtures: a PG 58S-28 binder and a polymer-modified (PMB) PG 58V-28 binder. The base binder used for South Dakota's asphalt binder blends was PMB with PG 58S-34. In addition, four bio-based and one petroleum-based RAs were included in the evaluation.

Virgin binders and recycled binder blends with and without RAs were subjected to short-term oven aging (STOA) and long-term oven aging (LTOA) and their rheological properties were characterized at high, intermediate, and low-temperature performance. All asphalt binder blends were graded based on both the Superpave PG system and the Multiple Stress Creep Recovery (MSCR) following AASHTO M320 and M332, respectively. Moreover, the Dynamic Shear Rheometer (DSR) was used to conduct the Linear Amplitude Sweep (LAS) test for fatigue resistance evaluation. The DSR frequency sweep test was used to develop master curves and to determine the Glover-Rowe (G-R) parameter which was used to assess the ductility and block cracking potential of the asphalt binder blends. Bending Beam Rheometer (BBR) test for low-temperature rheological properties evaluation was conducted. Furthermore, asphalt oxidation products were characterized using the Fourier-Transform Infrared Spectroscopy with the Attenuated Total Reflectance (FTIR-ATR) technique.

To assess the effectiveness of RAs on high RAM content asphalt mixtures, two approaches were applied for the selection of dosages based on the specific state needs. For Wisconsin, the recycling agent dosages were determined by targeting the LTPG of the virgin binder based on climatic requirements after 40 hours of conditioning in the Pressure Aging Vessel (PAV). For South Dakota, the dosages were recommended by the supplier of each RA product.

Asphalt mixtures with and without RAs used in this study were prepared using materials provided by contractors from the respective state using their job mixture formula (JMF) as baselines. All asphalt mixtures were designed to meet volumetric requirements as specified in their state's specifications. They were characterized to assess their resistance to rutting using the Hamburg Wheel Tracking Test (HWTT) or Asphalt Pavement Analyzer (APA) (after being subjected to STOA, and their resistance to intermediate and low temperature cracking (after being subjected to

STOA + LTOA) using the Indirect Tensile Asphalt Cracking Test (IDEAL-CT) and the Disc-Shaped Compact Tension (DCT) test, respectively. In addition, the dynamic modulus ($|E^*|$) test was conducted at both STOA and LTOA conditions to assess the stiffness characteristics and aging resistance of the mixtures.

Lastly, based on the results of the tests performed on asphalt binder blends and mixtures (with and without RAs), a procedure to guide the use of RAs to produce high RAM content mixtures with improved performance was recommended.

1.6. Organization of the Dissertation

This dissertation is structured into seven chapters. Chapter 1 describes the background, problem statement, hypothesis of the study, and overall scope of this study. Chapter 2 consists of a literature review on the current techniques used to improve the performance of high RAM content mixtures, classifications of RAs and their mechanism of actions, factors affecting their effectiveness, methods used to determine RA dosages, performance characterization of asphalt binders and mixtures with RAs. and the field performance of projects with RAs. Chapter 3 explains the research methodology and summarizes the materials and laboratory binder and mixture tests employed in this study. Chapter 4 and Chapter 5 present the binder and mixture test results and analyses, respectively. Chapter 6 and Chapter 7 present the conclusions and recommendations, respectively.

2. LITERATURE REVIEW

2.1. Introduction

The use of recycled asphalt material (RAM) has significant economic and environmental benefits that include cost savings, conservation of natural resources, and reduction in energy consumption and emissions. In this study, the term RAM is used to refer to both reclaimed asphalt pavement (RAP) and recycled asphalt shingles (RAS). According to the Federal Highway Administration (FHWA), RAP refers to removed and/ or reprocessed pavement materials containing asphalt and aggregates (Chesner et al., 2002) RAP can be obtained from either milling, full-depth pavement demolition, or rejected/ waste asphalt mixtures from the plant (Chesner et al., 2002; West, 2015). West (2015) refers to RAS as material obtained from either tear-off roofing (also referred to as post-consumer (PC) shingles) or rejected manufacturer waste (MW) with air-blown asphalt. The asphalt in the shingles is air brown to stiffen them so that they can sustain harsh weather and sunlight when in service (West, 2015).

The majority of the asphalt mixtures produced in the U.S contain RAP ranging from 20 percent to 30 percent (Williams et al., 2020), and/or RAS between 2 percent to 5 percent (Aschenbrener, 2018) by weight of the total mixture. The quantity of RAM (RAP and/or RAS) in asphalt mixtures is specified by the percentage of the total mixture, by the percentage of aggregates, or by the percentage of asphalt binder replacement (ABR), also known as recycled binder ratio (RBR). Since RAP and RAS have significantly different binder contents with different brittleness and stiffness level, most highway agencies have adopted the use of the ABR concept, but they still specify the type of RAM in the mixture (Rodezno et al., 2021). ABR provides the overall RAM binder

contribution to mixture performance, and it is defined as the percentage of recycled asphalt binders from RAP and/or RAS by weight of the mixture's total asphalt binder content (Equation 2.1).

$$\%ABR_{mix} = \frac{\%RAB * P_{b-RAB}}{P_{b-mix}} * 100\% + \frac{\%RAS * P_{b-RAS}}{P_{b-mix}} * 100\%$$

Equation 2.1

Where,

$\%ABR_{mix}$ = asphalt binder replacement of the mixture;

$\%ABR_{RAP}$ = Asphalt binder replacement from RAP;

$\%ABR_{RAS}$ = Asphalt binder replacement from RAS;

$\%RAP$ = Percentage of RAP by weight of the mixture;

$\%RAS$ = Percentage of RAS by weight of the mixture;

P_{b-RAP} = Asphalt binder content of RAP;

P_{b-RAS} = Asphalt binder content of RAS;

P_{b-mix} = Asphalt binder content of the mixture.

Due to the stiffness of the RAM binders, increased RAM contents in the asphalt mixtures tend to increase their rutting resistance. However, asphalt mixtures with high quantities of RAM are less durable and more susceptible to cracking due to the stiff and heavily aged binder from RAM. Techniques and technologies such as the use of softer binders, incorporation of polymer modified binder, increasing the effective binder content, and use of RAs are employed for mixtures with high RAM contents. They are discussed in the subsequent sections.

2.2. Use of Softer Binders

Typically, the asphalt binder with performance grade (PG) that satisfies both traffic and climate requirements of the specific project is employed for asphalt mixtures with less than 25% asphalt binder replacement from RAP only (Newcomb et al., 2016). However, with the increased amount of RAP in the mixtures, several Department of Transportations (DOTs) have recommended the use of softer binders to mitigate the stiffening effect of aged binder from RAM. Table 2.1 summarizes a few examples of maximum allowable RAM contents in asphalt mixtures and recommendations for mixtures with high RAM contents. In addition, AASHTO M323 suggests grade reduction of binder PG by 6 °C for mixtures with RAP content between 15 and 25 percent and use of blending charts for mixtures with RAP content over 25 percent. (Rodezno et al. (2021)

Table 2.1: Maximum allowable and recommendations for high RAM content mixtures by Rodezno et al. (2021)

DOT	Maximum allowable RAM content	Recommendations for high RAM content
Illinois	Allows the use of RAP, PC RAS, and MW RAS. Maximum limits depend on mixture type but not more than 5% RAS by weight of the mixture is allowed. Also, only 85% of the binder from RAS is considered active.	Both LTPG and HTPG of the virgin are reduced by 6 °C when binder replacement from RAP and/ or RAS exceed 15%.
Iowa	Allows incorporation of RAP, PC RAS, and MW RAS. Maximum limits depend on mixture designation, aggregate quality, and RAP class. Up to 5% of RAS by weight of aggregate is allowed and is considered part of the maximum allowable RAP. Only 67% of the RAS binder is considered active.	For mixtures with ABR over 20% (from RAP only) or ABR between 15% and 25% (from RAP+RAS), both the LTPG and HTPG of the virgin binder are lowered by 6 °C. When the ABR of the mixture exceeds 30% (from RAP only) or 25% (from the RAP and RAS), the DCT criteria are used depending on the traffic ¹
Michigan	Allows up to 17% ABR (from either RAP only or RAP+RAS) without virgin binder adjustments is allowed. The total asphalt binder content of the mixture is obtained at 3% regressed air void contents.	If ABR from RAP only is between 18 and 27%, the virgin binder is adjusted by lowering the LT grade by 6 C or selected using blending charts (AASHTO M323). If ABR from RAP+RAS is between 18 and 27% or exceeds 27%, blending charts are employed to select the virgin binder grade
Missouri	Allows usage of RAP, PC RAS, and MW RAS. Up to 30% effective virgin binder replacement from either RAP or RAP+RAS, no change in the virgin binder grade (i.e., PG 64-22) as long as the resultant recycled asphalt binder meets the project specification.	For mixtures with effective virgin binder replacement between 30 and 40%, the PG 64-22 is replaced by PG 58-28 or modified by the rejuvenator provided that the resultant recycled binder meets the PG 58-28 requirement. DCT testing is required for mixtures containing RAP and RAS,
Virginia	Allows usage of RAP, PC RAS, and MW RAS. The maximum allowable RAP content is 30% by weight of the mixtures for surface and intermediate course mixtures, and 35% for base mixtures. When RAS is used alone, no more than 5% by weight of the mixture is allowed. Moreover, ABR from RAP and RAS cannot exceed 30%.	For mixtures with RAP contents more than 35% or RAS only, PG 64S-22 is required to meet the requirement of a PG 64H-22. In addition, the mixtures are tested using the APA, IDEAL-CT, and Cantabro since the state has implemented the BMD approach. Rejuvenators are allowed for mixtures designed following the BMD approach.

¹Fracture energy per traffic designation: 690 J/m² (very heavy traffic), 460 J/m² (high traffic), and 400 J/m² (standard traffic)

Mogawer et al. (2012) assessed the performance of high RAP (up to 40% RAP) plant-produced mixtures from New York and Vermont. The Asphalt Binder Cracking Device (ABCD) test conducted on extracted and recovered binder from these mixtures showed that softer binders improved their low-temperature cracking resistance. The researchers found that improvement in cracking resistance (tested using the Texas Overlay test) was observed on Vermont's mixtures while none was observed on New York's mixtures. However, they noted that this difference in cracking performance could be attributed to factors like the total binder content of the mixtures, with Vermont's mixtures having a higher total binder content (6.6%) than New York's mixtures (5.2%); and silo conditioning time since Vermont's mixtures were produced in a batch plant, they didn't undergo significant aging while New York's mixtures underwent significant aging at elevated temperatures in the drum plant. Lastly, the softer binder used with Vermont's mixtures (PG 52-34) was one grade softer than that used with the New York's mixtures (PG 58-28).

Willis et al. (2012) and Norouzi et al. (2014) used the linear amplitude sweep (LAS) test and a simplified Viscoelastic Continuum Damage Model, respectively to show that usage of softer binders (PG 58-28 and PG 52-34) improved the fatigue resistance of asphalt mixtures with up to 50 % RAP by weight of aggregates. In line with this finding, Ameri et al. (2018) found that recycled asphalt binder blends prepared using a softer binder and up to 50% RAP binder had a comparable colloidal index as the control blend.

2.3. Polymer Modified Asphalt Binder

Polymer modification is the most common approach used to modify asphalt binder to achieve grades that are not produced straight from the distillation of crude oil. Several varieties of polymer exist; however, the most commonly used in asphalt binder modification are elastomers, plastomers, recycled tire rubber, and to a lesser extent viscosity modifiers and reactive polymers (Hunter et al., 2015). For the modifier to be effective in terms of practicality and economics, it must: (1) blend homogeneously with the asphalt binder using conventional equipment, (2) maintain the properties of the blend during storage, transportation, application, and in-service; and (3) provide a coating or spraying viscosity at normal mixing and placement temperatures (Hunter et al., 2015). In addition, the desirable characteristics of a polymer modified binder (PMB) include improved elastic recovery, viscosity, cohesive strength, ductility, and rigidity (Bahia, 1995; Yildirim, 2007).

Several DOTs including Wisconsin, Minnesota, South Dakota, Florida, Nevada, and Louisiana have recognized the benefits of PMB in resisting multiple modes of climate and stress-induced distresses in asphalt pavements and have incorporated them into their specifications. Researchers have reported improvement in the performance of mixtures produced with PMB. Kim et al. (2009) used the indirect tensile strength (IDT), asphalt pavement analyzer (APA), and DSR test to evaluate the performance of mixtures with 0, 15, and 35% RAP content prepared with a PG 76-22 PMB. They reported that, regardless of the RAP content, all mixtures had acceptable performance. Another study by Yan et al. (2017) on asphalt mixtures with up to 40% RAP by weight of aggregates and a PG 76-22 PMB showed that high RAP content mixtures had acceptable cracking performance, in terms of dissipated creep energy to failure and energy ratio after long term aging and cyclic pore pressure conditioning.

The combination of polymers and RAs in asphalt binder to balance the rutting and cracking performance has been investigated by several researchers. Mogawer et al. (2016) evaluated the performance of asphalt mixtures with up to 50% RAP using three different PMB and five RAs against the control mixture prepared with virgin aggregates only and PG 64-28 and PG 58-28 binders. The performance of the mixtures was evaluated in terms of rutting, fatigue cracking, and low temperature cracking resistance using the HWTT, standard four-point flexural beam test, and thermal stress restrained specimen tests, respectively. Results from the study showed that a combination of PMB binders and RAs had comparable rutting resistance as the control. Moreover, RAs by themselves were able to improve the cracking resistance of the 50% RAP mixture; however, with PMB the level of performance improved significantly. Although the combination of PMB and RAs had a varying effect on the low-temperature cracking behavior of the mixtures, they were all better than the control mixture. Bonicelli et al. (2017) showed that with proper proportions of plastomeric polymers and RAs' dosages, mixtures with 40% RAP by weight of the mixtures had desirable performance in terms of stiffness and rutting resistance. According to the authors, mixtures with RAs only were susceptible to rutting issues. In this study, the RAs dosage ranged from 0.2% to 0.4% by weight of the RAP, and the plastomeric polymer dosages were between 5% and 8% by weight of the mixtures. Contrary to the previous findings, Zhou et al. (2020) used the Illinois Flexibility Index Test (IFIT) and reported that the cracking resistance of the mixtures with up to 50% RAP mixtures decreased after long-term aging compared to the control mixture. They used a PG 76-22 PMB, and the RA dosage was 4% by weight of the RAP. Also, both loose mixture aging (at 135 °C for 12 hours) and compacted specimen (at 85 °C for 5 days) long oven term aging procedures were evaluated in this study.

2.4. Increasing the Effective Asphalt Binder Content of the Mixture

The effective asphalt binder content volume (V_{be}) is the primary mixture design factor that influences both durability and fatigue cracking resistance of the mixture (Bonaquist, 2014). If other variables remain unchanged, increasing the virgin binder content is expected to increase the effective binder content of the mixture.

A survey conducted by Tran et al. (2019b) as part of the NCHRP 20-07/Task 412 project identified changes in the Superpave volumetric mixture design method that can potentially improve the durability of the mixtures by increasing their virgin binder content. Of the changes identified, the use of PMB binders had the most respondents, followed by the regressed air voids approach, and changes to mixture design specifications to increase in-place density. Other options that were selected by at least five respondents were lowering design gyrations, increasing the minimum voids in the mineral aggregates (VMA) requirement, lowering design air voids, and setting a minimum effective binder content (Tran et al., 2019a). Detailed information about these changes and factors affecting their contribution to mixture performance can be found elsewhere (Tran et al., 2019a; Tran et al., 2019b).

Furthermore, Tran et al. (2019b) found that for mixtures containing RAM, some DOTs have implemented the use of discount factors since not all asphalt binder from RAM is available to contribute to mixture performance. For instance, in 2012, the Georgia DOT implemented the corrected optimum asphalt content (COAC) approach in their mixture design to improve their durability. With this approach, it was assumed that only 75% of the recycled binder from RAP contributes to the performance of the mixtures, therefore 25% of the RAP binder was added as a virgin binder (Tran, 2020). In 2019, the DOT revised the COAC approach to 60:40; whereby 60% of the RAP binder is assumed to be blended, and 40% of it is added as a virgin binder (GDOT,

2019; Tran, 2020). Other DOTs such as Delaware, South Carolina, and Louisiana account for approximately 90, 75, and 92 percent, respectively of RAP binder available during mixture production (Martin et al., 2021). Moreover, a similar approach of reducing the available binder content of RAM is applied to RAS in asphalt mixtures in Delaware, Tennessee, New York, and Ohio accounting for about 80, 75, 60, and 60 percent, respectively of the RAS binder available during production (Martin et al., 2021). By employing discount factors, the virgin binder content of the mixtures increases which is expected to increase the effective binder content and ultimately improve their performance and durability.

2.5. Recycling Agents

Recycling agents (RAs) are products with chemical and physical behaviors designed to restore the properties of aged binders from RAM by improving the asphaltene to maltene ratio, reducing the size of the asphaltenes, increasing molecular mobility, and improving the dispersive power of the continuous maltenes phase (Kaseer et al., 2019b). RAs include softeners which act by reducing the stiffness of the aged binder; and rejuvenators which can partially restore the chemical balance of the aged binder in addition to decreasing their stiffness (Hand and Martin, 2020; Martin et al., 2019).

Studies have shown that RAs improve the cracking resistance of asphalt mixtures (Hajj et al., 2013; Im and Zhou, 2014; Tran et al., 2012; Zhou et al., 2015) and decrease their moisture susceptibility (Hajj et al., 2013; Im and Zhou, 2014). On the other hand, Tran et al. (2012) and Zhou et al. (2015) reported that RAs decreased the rutting resistance whereas Mogawer et al. (2017) and Yin et al. (2017) found that RAs increase the aging susceptibility of the mixtures.

2.5.1. Classification and Categorization of Recycling Agents

Classification of RAs dates back to the 1970s and 1980s when petroleum-based RAs earned popularity due to the increase of asphalt binder price as a result of the Nixon and Carter Oil embargoes (Hand and Martin, 2020). They were classified in the American Society for Testing and Materials (ASTM) D4552 based on their viscosity in addition to other physical properties such as flash point, specific gravity, percent of saturates, and several tests on residues. Advancement in technology has led to the development of RAs with different origins other than the typical petroleum-based. ASTM D 4552 has been revised to also include bio-based RAs (ASTM, 2020).

Another classification was presented by NCAT (NCAT, 2014). The RAs were classified into five major groups (aromatic oils, naphthenic oils, paraffinic oils, triglycerides/fatty acids, and tall oils) based on their chemistry. Table 2.2 shows the NCAT classification with examples of commercially available rejuvenators.

Table 2.2: Types of RAs by NCAT (2014)

Category	Examples of Commercially Available	Description
<i>Aromatic Oils</i>	Hydrolene [®] ValAro 130A [®]	Refined crude oil products with polar aromatic oil components
<i>Naphthenic Oils</i>	Cyclogen L [®] HyPrene BO150 [®] Reclamite [®]	Engineered hydrocarbons for asphalt modification
<i>Paraffinic Oils</i>	Valero VP 165 [®] Waste Engine Oil (WEO) Waste Engine Oil Bottoms (WEOB)	Refined lubricants oils
<i>Tall Oils</i>	Sylvaroad [™]	A by-product of the Kraft process of wood pulp manufacture especially coniferous trees
<i>Triglycerides/ Fatty Acids</i>	Anova [®] Delta S [®] Modified Vegetable Oils Recycled Vegetable Oils	Derived from bio-based sources

As part of research conducted by the Belgian Road Research Centre (BRRC) on Rejuvenation of Reclaimed Asphalt in a Circular Economy (Re-RACE) dossier 21, De Bock et al. (2020) provided another classification of RAs based on the origin of the material and whether they are originally manufactured or recycled from waste as shown in Table 2.3.

Table 2.3: Categorization of RAs by De Bock et al. (2020)

Origin	Originally manufactured or derived	Recycling of wastes
Petrochemical industry/ Petroleum-based	Aromatic extracts and naphthenic oils derived from petroleum <i>Example: Hydrolene[®], Cyclogen[®], Reclamite[®]</i>	Recycled machine oils <i>Example: Re-refined engine oil bottoms, Vacuum tower asphalt extender, engine oil residues</i>
Vegetal/ Biological	i. Vegetal oils from agro-industry <i>Example: Anova[®], ReJUVN8[®], RePLAY 18[®], etc.</i> ii. Engineered bio-based oils <i>Example: Sylvaroad[™], Evoflex, and Delta S</i>	Recycling of food oils <i>Example: Waste sunflower, peanut oil, and certain cooking fats</i>
Residual category	Specifically engineered additives <i>Example: Storbit-Storflux, Bioflux, etc.</i>	

Although different classifications may be employed for RAs based on the material source, manufacturing process, or generic composition, it is also important to differentiate among different products based on the asphalt chemical fraction with the most affinity to the recycling agent (Rodezno et al., 2021). According to Hunter et al. (2015), the constituents of asphalt binder are usually classified in terms of the relative quantity of the so-called SARA fractions (Saturates, Aromatics, Resins, and Asphaltenes), which have increasing molecular polarity as listed (saturates have the lowest and asphaltenes the highest). The asphaltenes are dispersed in the maltenes (saturates and aromatics) with resins acting as a peptizing agent of the asphaltene micelles (Mangiafico et al., 2016).

Sun et al. (2016) and Wang et al. (2018) concluded that the interaction between waste cooking oil and asphalt binder is more physical than chemical due to the coincidence of the absorption peaks from the FTIR test. A similar conclusion was reached by Chen et al. (2018a) and Cai et al. (2019) using atomic force microscopy (AFM) and FTIR, respectively on blends of aged RAP binder with bio-based RAs. In addition, the studies found that the dosage rate did not affect the interaction mechanism of the RAs.

To understand the molecular interaction between RAs and aged asphalt binder molecules, Pahlavan et al. (2018) studied the evolution of molecular packing on aged asphalt binder using a bio-based recycling agent from swine manure. Findings from this study indicated that the bio-based RAs restored the microstructure of the aged asphalt binder while reducing the asphaltene-aggregates size. Moreover, the FTIR analysis showed a high concentration of polar chemical groups such as amides, amines, and carboxyl in the bio-based RAs that improve its solubilizing effect on the aged asphalt binder.

Based on studies conducted by Bajaj et al. (2020), De Bock et al. (2020), and Tabatabaee and Kurth (2017). RAs can be classified based on their mechanism of action (affinity) on the SARA fractions in three categories as described below:

- *Softeners*: They exhibit low compatibility with the aromatics, asphaltenes, and resins fractions of the asphalt binder, especially at low temperatures. They include paraffinic oils and saturated materials with high crystalline fractions (Bajaj et al., 2020; Tabatabaee and Kurth, 2017). The dispersion of these lower viscosity additives in the asphalt will reduce the stiffness of the recycled asphalt binder. Besides, their wettability and oily nature improve the workability of the asphalt mixture. However, their effectiveness was found to diminish with aging since these additives can lead to colloidal instability resulting in the

precipitation of the asphaltenes fraction (Johnson and Hesp, 2014). Due to their low compatibility with the aromatics, asphaltenes, and resins fractions of the asphalt binder, softeners are likely to have poor rheological performance (Bajaj et al., 2020).

- *Replenishers*: They supplement the solvent phase of the asphalt colloidal structure since they are most compatible with the aromatics (i.e., low-polarity naphthenic aromatic fraction) of the asphalt binder (Tabatabaee and Kurth, 2017). They reduce the viscosity and modulus of the aged binder by lowering the viscosity of the continuous solvent phase (Tabatabaee and Kurth, 2017). Since they have little effect on the intermolecular agglomeration and self-assembly of the asphalt polar micelles, their rejuvenation effect is highly influenced by the quality of the virgin and aged asphalt binder; thus often requiring high dosage rates which may not be economically feasible (Bajaj et al., 2020; Tabatabaee and Kurth, 2017).
- *Dispersants/ Compatibilizers*: They show an affinity for multiple fractions of the asphalt binder and are produced through careful engineering of the source material, whether petroleum or bio-based (Tabatabaee and Kurth, 2017). They are capable of breaking or disrupting the intermolecular associations among the asphaltenes present due to oxidation (De Bock et al., 2020). This rejuvenation mechanism is observed in modified vegetable oils as their polar carbonyl groups attach themselves to asphaltenes clusters while olefinic chains remain mobile in the maltenes. Tall oils also fall in this category; however, they are prone to oxidation due to unsaturated double bonds (Bajaj et al., 2020).

2.5.2. Mechanism of Action of Recycling Agents

Before selecting any type of RA, it is important to evaluate its efficiency in terms of stability, compatibility, dispersion, and diffusion (Bennert et al., 2015; Kaseer et al., 2019b). The stability of the RA is related to its degree of volatilization when subjected to oxidation and/or high temperatures for an extended time (Bennert et al., 2015); and it refers to both thermal and storage stability. Thermally unstable RAs can be problematic and sometimes pose severe consequences when their flashpoints are around or less than the asphalt mixture production temperatures. However, this may not be an issue as most RA manufacturers indicate the flashpoint and shelf life of their products on the material safety data sheet as required by the regulations.

RAs with lower viscosity tend to diffuse into aged binder faster but they are thermally unstable (Ma et al., 2015). Thermal stability can either be determined using a RA by itself or blended with the virgin binder and recycled binder. Elkashef et al. (2018) used thermogravimetric analysis to determine the thermal stability of a soybean-derived recycling agent blended with virgin and extracted RAP binder. In their study, neat PG 58-28 was dosed with 12% of soybean-derived recycling agent before being blended with the extracted RAP binder at a ratio of 1:5. This composite blend was found to be thermally stable up to 302 °C.

Compatibility among virgin binders, recycled binders, and RAs is required for the production of uniform, workable, and durable asphalt mixtures. Al-Saffar et al. (2021) followed ASTM D5892 to assess both storage stability (phase separation) and compatibility of a hybrid RA from waste engine oils and the maltenes fraction of the asphalt binder. They did not experience any phase separation issue as the resin from the maltenes fraction acted as a stabilizer for the asphaltenes and prevented their aggregation (Al-Saffar et al., 2021; Aske et al., 2002; Lesueur, 2009).

As part of the NCHRP 9-58 project, Martin et al. (2019) applied saturates, aromatics, resins-asphaltene determinant (SAR-AD) technique and modulated differential scanning calorimeter (MDSC) to evaluate the chemical compatibility of different RAs. The colloidal instability index (CII) and the total peri-condensed aromatics (TPA) indices from the SAR-AD technique showed a significant incompatibility when recycled materials were included in the binder blend; however, the benefit in rebalancing the SAR-AD fractions to proportions comparable to those of the base binder was not clear at the dosage used and entirely impossible at any practical dosage. The glass transition temperatures (T_g) and the high-end glass transition temperatures (T_g End) of the MDSC test decreased significantly when a recycling agent was added to the binder blends. Rejuvenated binder blends exhibited lower T_g and LTPG because RAs are significantly less viscous compared to virgin binders (Lei et al., 2016).

Dispersion is associated with the homogeneous distribution of recycling agent particles over both virgin and aged asphalt binder particles. Dispersion is a physical process that is typically achieved during mechanical mixing; for both laboratory and plant-produced asphalt mixtures (Kaseer et al., 2019b).

Diffusion is a gradual transition of constituents due to concentration gradient. For instance, the aged binder absorbs any hydrocarbon-type liquid as soon as it comes in contact with a recycling agent (Kaseer et al., 2019b). According to Carpenter and Wolosick (1980), Tran et al. (2012), and Zaumanis and Mallick (2013), the diffusion process of RAs into aged asphalt binder is manifested into four steps:

- The recycling agent forms a thin viscosity layer surrounding the RAM particles.
- The recycling agent diffuses into the aged asphalt binder and softens the aged binder. As diffusion continues, the quantity of the recycling agent surrounding the RAM particles decreases.
- Diffusion continues to the inner layer, by this time the viscosity is likely to increase if no more raw recycling agent is present on the outside layer of the aged binder
- Lastly, equilibrium is reached, and the viscosity/workability of the blend is maintained for a certain time.

The diffusion of RAs into the aged RAM binder influences its intermolecular agglomeration and self-assembly of the asphaltenes. It is affected by the chemical formulation and compatibility of the RAs with both virgin and aged binder, mixing and compaction temperatures, rheology properties of the virgin and aged binder, amount of recycled material, and method of incorporation into the asphalt mixture (Karlsson and Isacsson, 2003; Kaseer et al., 2019b; Wang et al., 2017).

Ma et al. (2015) conducted a staged extraction on laboratory-prepared RAP aggregates to understand the diffusion of four different RAs using the DSR test. The rejuvenated asphalt mixture was prepared by adding the RAs on 1.5 kg of RAP aggregates at 150 °C for 60 seconds, then left to cool at room temperature. Both RAP samples with and without RAs were immersed into different trichloroethylene solvents for 45 minutes to obtain the outer asphalt layer and another 45 min in new trichloroethylene solvents for the inner asphalt layer surrounding the aggregates. While values of the $G^*/\sin \delta$ from the outer and inner layer of the RAP sample without the recycling agent were similar; those from the rejuvenated RAP were not. For both outer and inner layer values, the RAP sample without the recycling agent had high values than the rejuvenated RAP, indicating the diffusion effect of the recycling agent. However, the RAs' diffusion process did not

reach equilibrium since the $G^*/\sin \delta$ values of the inner layer were significantly greater than those of the outer layer for rejuvenated RAP.

Carpenter and Wolosick (1980) plotted penetration values at 25 °C versus mixing time of binder layers obtained from staged extraction of the rejuvenated asphalt mixture. The study suggested that the diffusion of RAs is a process that starts from mixing, construction, and continues for some time after construction. Wang et al. (2017) used the image stripping analysis program called Imana to establish the time at which RAs reach an equilibrium diffusion. The Imana program uses the stripping ratio concept to characterize the moisture resistance of asphalt mixtures. The stripping ratio reflects the surface area of an aggregate particle covered with binder which is influenced by the regenerating effect of the recycling agent. Before mixing their laboratory RAP manufactured aggregates with dried-virgin aggregates, the researcher first sprayed it with the RAs. After comparing the stripping ratios of covered versus uncovered areas of the virgin aggregates, they found RAs reached optimal diffusion after eight hours of conditioning at a temperature of 50 °C.

Incomplete diffusion of the RAs into the aged binder may cause pavement distresses like premature cracking, rutting, and soft spots on the mat. Premature cracking could be a result of RAs not diffusing fully into the aged binder causing the RAM particle to remain as a black rock; thus, affecting the effective asphalt content which may lead to a stiff and brittle asphalt mixture that is not durable and susceptible to cracking. Not only, partial diffusion of the RAs could lead to soft spots on the pavement surface posing a safety hazard due to reduced skid resistance but also rutting if open to traffic as the RAs on the aged binders' outer layer may provide soft film on the aggregate particles thus reducing their interlock (Kaseer et al., 2019b; Zaumanis et al., 2013).

2.5.3. Factors Affecting Effectiveness of Recycling Agents

Several studies have shown that the effectiveness of RAs in recycled asphalt binder blends and/or mixtures depends on both mixture design factors and mixture production factors. Mixture design factors that affect the effectiveness of RAs include (1) type and dosage of RAs, (2) properties of virgin and RAM binders; and (3) quantity of RAM in recycled asphalt binder blends or mixtures (Garcia Cucalon et al., 2019; Martin et al., 2019; Shen et al., 2007; Zaumanis et al., 2014b). Asphalt mixture production factors include (1) mixing temperature and conditioning time; and (2) the method by which RAs are added in asphalt mixtures (Lu et al., 2019; West et al., 2019; West and Copeland, 2015; Zaumanis et al., 2019).

2.5.3.1. Type and Dosage of Recycling Agent

The type of RAs determines its chemical formulation and compatibility which affects its mechanism of action on both virgin and aged asphalt binder. RAs can be manufactured using a single component (e.g., petroleum) or engineered from organic materials (e.g., modified vegetable oils). According to Xu et al. (2018a), organic RAs also known as bio-based oils tend to be more effective and can rejuvenate more severely aged RAM than single component RAs. A study conducted by Bajaj et al. (2020) found reacted bio-oils to have the best performance followed by modified vegetable oils. In addition, tall oils performed better than petroleum-based RAs, but they were more susceptible to aging. Bio-oils have been found to improve the colloidal stability of the asphalt matrix due to the interaction of amide groups with asphaltenes, which increase the stacking distance of the asphaltenes and change their conformational packing (Zadshir et al., 2018).

The RA's dosage is the only factor that balances the cracking and rutting performance of the recycled asphalt binder blends and/or mixtures (Kaseer et al., 2020). For a particular recycling agent type and proportion of RAM, a low dosage may partially reduce the stiffness and brittleness of the aged binder from RAM but may not improve the cracking resistance of the resultant asphalt mixture. On the contrary, a high recycling agent dosage rate may not be cost-effective and detrimental to the rutting performance of the asphalt mixture due to the over softening of the aged binder from RAM (Kaseer et al., 2020; Kaseer et al., 2019b).

Due to their different chemical formulation and mechanism of action on recycled binder blends, the effectiveness of RAs varies widely. Zaumanis et al. (2014a) found that recycled binder blends with organic-based RAs required lower dosages compared to those with petroleum-based to cause a similar softening effect on the aged RAP. In line with these findings, Osmari et al. (2017) also showed that petroleum-based RAs required a high dosage compared to waste cooking and castor oils to achieve the same viscosity on aged binders. Similar findings were also reported by Martin et al. (2019) and Nsengiyumva et al. (2020) who showed that aromatic extracts (petroleum-based) required more dosage than vegetable oils, tall oils, and bio-based RAs to achieve the same performance grade as that of the target asphalt binder.

To understand the effect of recycling agent type and dosage on diffusion equilibrium, Zaumanis and Mallick (2013) used finite element modeling technique to simulate the plant mixing processes assuming 100% RAP mixture with five different RAs (refined tallow, paraffinic base oil, waste vegetable oil, waste frying oil, and an asphalt flux). Their modeling considered plant mixing process and temperature, rejuvenator parameters such as specific gravity, film thickness, volume, and concentration of the RA, and aged binder parameters like specific gravity, film thickness, thermal conductivity, specific heat capacity, molecular weights, and molecular radius.

According to Zaumanis and Mallick (2013), film thickness and volume of RAs are influenced by the dosage while concentration is a function of RA's molecular weight. Zaumanis and Mallick (2013) found that the diffusion time of the RAs to reach equilibrium depends on their dosage and type. Moreover, refined tallow oil took the least time to reach equilibrium and was most effective in attaining the target viscosity, whereas the waste frying oil and the asphalt flux took the most time and were least effective.

Ideally, the recycling agent should restore the maltenic phase (saturates, aromatics, and resins) in proportions similar to that of a virgin asphalt binder. However, this may not be the case due to the availability of different products with different origins apart from the typical petroleum-based. The SARA analysis conducted on five different generic commercially available RAs by Haghshenas et al. (2020) showed that aromatic extracts had similar maltenic composition as virgin asphalt binder whereas triglyceride/fatty acids have only the resin fraction and tall oils did not have the saturate fraction. Triglyceride/fatty acids and tall oils contain components with similar solubility parameters as aromatics and resins despite being chemically different (Haghshenas et al., 2020). The difference in the generic composition affects their efficiency in restoring the aged binder properties and their mechanism of action. For instance, replenishers (aromatic extracts) supplement the solvent phase of the asphalt binder colloidal structure since they are most compatible with low polarity naphthenic aromatic fraction of the binder; therefore, requiring high dosages to deliver the same impact as compatibilizers (triglyceride/fatty acids) which act by disrupting the intermolecular agglomeration of the asphaltenes formed during oxidation. However, Haghshenas et al. (2020) warn about susceptibility against moisture damage and oxidation for asphalt binder blends/mixtures rejuvenated with triglyceride/fatty acids or tall oils as these RAs contains hydroxyl function groups.

2.5.3.2. Properties of the Virgin and RAM Binders

Generally, virgin or RAM binders with better quality require a low RA dosage to produce recycled binder blends/mixtures with desirable performance. Martin et al. (2019) showed that a PG 64-22 virgin binder with ΔT_c of -4.6 °C required a high recycling agent's dosage compared to one with ΔT_c of -1.2 °C to achieve a similar PG as that of the target binder. Rejuvenated asphalt mixture with a PG 64-22 and ΔT_c of -4.6 °C had significantly higher resilient modulus after long-term aging than the same mixture with a PG 64-28 virgin binder and ΔT_c of 1.4 °C (Kaseer et al., 2017).

A study by Mogawer et al. (2013) showed that mixtures with 5% RAS or 35% RAP plus 5% RAS were stiffer compared to a mixture with 40% RAP when the same quantity of recycling agent was used. Tran et al. (2017) found that 40% RAP mixture required less recycling agent's dosage compared to a 25% RAP plus 5% RAS mixture; moreover, the binder extracted and recovered from these mixtures were PG 82-22 and PG 88-22, respectively indicating that the mixtures with a combination of RAP and RAS was stiffer compared to one with RAP only. Furthermore, while low severity reflective cracking was observed on all test sections, ten months after their construction; the 25% RAP plus 5% RAS test section had many cracks compared to the 40% RAP test section. The poorer effectiveness of RAs on RAS is attributed to the fact that RAS is typically more aged compared to RAP (Kaseer et al., 2019b).

Apart from using RAs for the production of up to 70% RAP mixtures, the U.S. delegation to Japan reported that Japan requires the RAP to have a minimum binder content of 3.8%, maximum penetration of 20 dmm, and a maximum of 5% of RAP material passing the #200 sieve (West and Copeland, 2015). As part of the NCHRP 9-58 findings; Martin et al. (2019) suggested using high-quality virgin binders with $\Delta T_c \geq -3.5$ °C and RAP and RAS with maximum HTPG of 100 °C and 150 °C, respectively to produce high RAP and/or RAS content mixtures with desirable performance.

2.5.3.3. Quantity of RAM in Recycled Binder Blends and/or Mixtures

Recycling agent dosage increases with an increase in RAM contents in recycled binder blends/mixtures. Ideally, high doses are expected to accommodate high RAM contents; however, researchers have found the long-term effectiveness of RAs to be affected by aging (Abdelaziz et al., 2020; Kaseer et al., 2019b; Kaseer et al., 2017; Mogawer et al., 2017; Yin et al., 2017).

Kaseer et al. (2017) used the mixture stiffness parameter as a measure of recycling agent effectiveness. The researchers showed that the effectiveness of a 50% ABR (25% ABR from RAP and RAS) mixture decreased significantly after long term aging compared to the 30% ABR (10% ABR from RAP and 20% ABR from RAS) mixture; even though the dosage was more than double.

Since the long-term effectiveness of RAs is still questionable, most DOTs are hesitant to incorporate RAs in their mixtures. Moreover, for the production of high RAM content mixtures, Martin et al. (2019) proposed a limit of 15% ABR from RAS only and 50% ABR for those containing both RAP and RAS since at typical HMA production temperatures RAS act more like fillers since its stiffer-aged binder is not fully available for blending.

2.5.3.4. Mixing Temperature and Conditioning Time

RAs are expected to decrease the production temperature of high RAM content mixtures. Nevertheless, these temperatures should be higher than the typical virgin mixture production temperature to increase their softening effect, since the dispersion and diffusion of RAs are affected by the production temperature (Kaseer et al., 2019b). Zaumanis et al. (2013) suggested increasing the mixing and compaction temperatures of a 100% RAP mixture with waste engine oil bottoms by 22 °C. However, the mixing and pre-heating temperatures of the RAM should not exceed 155 °C to avoid secondary oxidation of their binder (Rathore and Zaumanis, 2020).

Studies conducted by Xu and Wang (2018) and Xu and Zhang (2020), using molecular dynamics simulations to investigate the diffusion interaction of RAs with aged RAP and virgin binders showed that the distribution of the RAs into the recycled binder blends increased as the temperature increased. Moreover, RAs diffused more in virgin binder due to its associated low viscosity and high aromatic contents compared to the aged asphalt binder.

During the 2015-2017 research cycle of the NCAT test track, a surface mixture with 20% RAP plus 5% PC RAS (0.282 RBR) and 10% of a bio-based recycling agent by weight of the RAM binder was placed on the test section to evaluate the performance of the recycling agent (West et al., 2019). Cracks were observed on the surface after the application of 1.4 million ESALs on the test section, initial investigation indicated that it was due to delamination between the intermediate layer and the surface layer. Since it was inferred that the delamination weakened the pavement structure hence causing the cracking problem; the test section was repaved with increased tack coat (West et al., 2019). Unfortunately, the second repave showed slippage failure a few hours after trafficking began. A forensic investigation on the test section indicated that the slippage (shear) failure was caused by a decreased stiffness and tensile strength in the surface mixture due

to incomplete interactions among the recycling agent, virgin binder, and aged binder from the RAMs (Tran, 2021). To counteract this issue, the test section was reconstructed using a mixture that incorporated 35% RAP (RBR was kept at 0.282) with 5% of a bio-based recycling agent by weight of the RAP binder. Moreover, the mixture was conditioned in a silo for two hours to allow enough interaction between the recycling agent and the aged RAP binder before being hauled to the test track (approximately 10 minutes away from the plant) for paving (Tran, 2021; West et al., 2019). Among others, the study concluded that the bio-based recycling agent should not be used with southeastern PC RAS without enough silo storage time during production as it may soften the virgin binder excessively leading to premature failures in the pavement.

Xu and Zhang (2020) studied the effect of temperatures on the diffusion of petroleum-based RAs and recycled binders using viscosity, SARA, and FTIR tests. The experiment was prepared by pouring the recycled binder into a cylindrical tube (2 cm in diameter and 15 cm in height) and left to cool at room temperature for four hours. Then, the RAs heated to 80 °C were poured into the tube to 12 cm high. The tubes were placed in ovens set at four different temperatures (110, 120, 130, and 140 °C) for four different periods (6, 12, 18, and 24 hours). The samples were subjected to freezing for six hours in a freezer set at -20 °C after the diffusion process to solidify them. Three specimens of 2cm each were cut from the asphalt layer and tested. The researchers found that viscosity which is affected by temperature promotes the Brownian movements of the molecules of the recycled binder and RAs, thus affecting their diffusion rate. At lower viscosity (higher temperatures) the interaction of the molecules is lower, therefore the diffusion process is easier; vice versa is true at higher viscosity (lower temperatures). Besides, aromatics diffuse easily into aged asphalt binder due to high molecular polarity and moderate molecular weight. Since asphaltenes have a high molecular weight, they affect the diffusion process of the RAs (Ding et

al., 2016). An increase in molecular weight increases the diffusion coefficient; therefore dissolving the agglomerated asphaltenes into smaller sizes facilitates the diffusion process (Behnood, 2019; Xu et al., 2019).

2.5.3.5. *Recycling Agent Addition Methods*

There are three common methods a RA can be incorporated in asphalt mixture during the production of high RAM content mixtures at the asphalt plant: (1) in line with the virgin binder, (2) spraying it directly on the RAM either on the conveyor belt or holding bins, and (3) on the mixture itself. When adding RAs to the mixture itself, mixing time should be considered as it is always relatively short (EAPA, 2018); otherwise the RA will not get enough time to interact with the RAM binder.

There is a consensus that effective diffusion of the recycling agent is achieved when it is directly added to the RAMs, as it softens the RAM and maximizes their blending with virgin aggregates and binder (Kaseer et al., 2019b; Zaumanis et al., 2019).

A volumetrics-based laboratory study conducted by Xie et al. (2019) reported that both the recycling agent type and method of addition into the mixture had an impact on the air void content and voids in mineral aggregate parameters of the 50% RAP content mixtures, whilst no substantial effect was observed on the dust to binder ratio criteria. In contrast, Rathore and Zaumanis (2020) showed that the differences in volumetrics components were not statistically significant regardless of the method the recycling agent was incorporated into mixtures. Moreover, Rathore and Zaumanis (2020) reported neither the indirect tensile strength nor the dynamic modulus of the mixtures was affected.

At the plant, RAs can be directly added to RAM through several locations such as the RAM's storage unit, crusher, conveyor belt, dryer inlet chute, or dryer outlet chute (EAPA, 2018; Zaumanis et al., 2019). Nevertheless, Zaumanis et al. (2019) recommended the RAP's conveyor belt, the RAP's outlet chute, and the mixing unit (pugmill) as the most suitable location(s) on the asphalt plant for the addition of RAs for optimal mixture performance with consideration of minimum environmental pollutions and easy of plant operation. Comparison of the asphalt mixtures produced by spraying recycling agent onto the RAP on the conveyer belt and mixing unit showed similar crack propagation resistance results despite the latter having a 0.5% total binder content higher. However, mixtures produced by spraying the recycling agent at the conveyor belt had more fatigue resistance than those produced by adding it in the mixing unit, indicating that the recycling agent had sufficient diffusion time when added at the conveyor belt as compared at the mixing plant (Zaumanis et al., 2019).

In Japan RAs are blended and conditioned with heated RAP in mixing units (pugmills) for several hours before being mixed with virgin aggregates and binder to allow and accelerate the diffusion of RAs into RAP (West and Copeland, 2015). However, this practice may not be viable and/or costly in the U.S. since drum plants are common. NCAT is currently conducting a study that evaluates the feasibility of using foamed RAs to produce high RAM content mixtures as most plants in the U.S. already have the foaming unit used for WMA installed (Yin and Moraes, 2021).

2.5.4. Determination of Optimum Recycling Agent Dosage

The quantity of RAs also plays a significant role in the performance of the recycled asphalt binders and mixtures. Excessive RA dosage may produce mixtures with high susceptibility to rutting issues whereas inadequate dosage may soften the mixture but with no pronounced impact on improving its cracking resistance (Arámbula-Mercado et al., 2018; Kaseer et al., 2020). The optimum dosage of RAs is affected by the source and grade of the virgin asphalt binder as well as the aging level and quantity of the RAM in the asphalt mixture. Most common methods for determining the dosages of RAs include manufacturer recommendation (Ali et al., 2016; Martin et al., 2019; Mogawer et al., 2013; Tran et al., 2017), user experience (Bahia et al., 2018; Zhang and Bahia, 2021), restoring the performance properties of the recycled binders to that of the virgin binder to be used in mixture design (Tran et al., 2012), or using blending charts of blended asphalt binders' properties (Martin et al., 2019; Tran et al., 2012; Zaumanis et al., 2014a).

Using dosages recommended by the manufacturer involves the contractor sending their materials' sample or data of the RAM and base binders' properties to the manufacturer for dosage determination or directly using rates suggested by the manufacturer as most proprietary RAs have a dosage range specified. Determining dosage by user experience comes with the knowledge an engineer/technician has acquired while working with a particular product. RA dosage determined to restore the performance properties of the recycled binder blend to that of the virgin binder to be used in the mixture design, involve dosing the recycled binder with different proportions of RA, and then testing for high, intermediate, and low-temperature properties of the blends. The optimum RA is determined from the correlations between the RA contents and the critical high or low temperature of the blends.

The dosage of RAs into asphalt mixtures using blending charts can be determined by either matching the physical properties (i.e., viscosity, penetration point, and softening value) or rheological properties (i.e., high temperature, low temperature, and ΔT_c) of the recycled asphalt binder blends to that of the target asphalt binder that satisfies both climate and traffic.

2.5.4.1. Matching the Physical Properties of the Recycled Binder Blends to that of the Target Binder

Several studies have been conducted to evaluate the dosage of RAs in recycled asphalt binder to restore their penetration point, softening point, and viscosity values to that of the target asphalt binder blend (Forton et al., 2020; Guduru et al., 2021; Sánchez et al., 2020; Zaumanis et al., 2014a). Since European countries still use these empirical tests to characterize their asphalt binder, the European Asphalt Pavement Association (EAPA) suggests conducting at least penetration and softening tests to determine the dosage if this approach is used. According to the EAPA, the dose required to recover the penetration value (flexibility) of the recycled binder blend is determined first; and then checked against the softening value for rutting resistance (EAPA, 2018). Further discussion of other research studies that have used this approach are summarized in the subsequent paragraphs.

Sánchez et al. (2020) conducted a study on three different RAs (crude palm oil, hard stearin, and vegetal oil) to determine the optimum dosage required to restore the properties of the recycled asphalt binder blend prepared at a ratio of 70% virgin asphalt binder and 30% RAP binder to the penetration point (at 25 °C) and softening point of the virgin binder; which was 62 dmm and 48 °C at unaged condition; 27 dmm and 59 °C after RTFO aging; and 11 dmm and 91 °C after RTFO plus 20 hours PAV aging. Based on this study, all RAs were able to reduce the penetration and

softening point of the recycled binder blend to that of the virgin binder in its unaged condition. The dosage rate required to recover the penetration and softening properties in unaged conditions ranged from 3.7% to 4.4% and between 5.2% and 6.0%, respectively. After RTFO aging, the dosage rate required for the penetration value was between 0.9% and 3.0%, the dosage rate could not be determined at the corresponding PAV condition as the recycled blend seemed to be softer than the desired target value (11 dmm) of the virgin asphalt binder. The RAs' dosage rate for the target softening point values at RTFO and RTFO plus 20 hours of PAV aging could not be determined for the same reason. This indicated that rejuvenated asphalt binder blends are less stiff than their counterparts, they are more resistant to fatigue and thermal cracking resistance in the long term. The authors recommended using doses obtained by restoring the penetration properties in unaged conditions as it gave lower dosages than that from the softening values.

Guduru et al. (2021) determined the dosage of two paraffinic oils (lubricating waste engine oil and commercial engineered waste oil), two fatty acids (tallow and waste vegetable oil), and one crude tall oil. The dosages of the RAs were determined to restore the viscosity of the recycled asphalt binder blend with 50 % RAP binder to that of the virgin asphalt binder with a viscosity of 399 Pas at 60 °C and then checked for the 54 °C softening point criteria. In this study, the dosage of the paraffinic oils was the highest (10.8% for the commercial engineered waste oil and 9.6% for lubricating waste engine oil), followed by the crude tall oil (7.9%) and lastly the fatty acids (5.5 % for the waste vegetable oil and 6.0% for the tallow oil). All doses were by weight of the total asphalt binder blend. Fatigue cracking resistance of recycled asphalt mixtures conducted using the indirect tensile strength test showed that fatty acids were the most effective whereas lubricating waste engine oil was the least. In terms of rutting resistance performed using the dry wheel tracking tester, the commercial engineered waste oil was the best, and the crude tall oil was the worst.

Zaumanis et al. (2014a) used a penetration test to determine the dosages of organic-based (waste vegetable grease, organic oil, waste vegetable oil, and distilled tall oil); and petroleum-based (waste engine oil, aromatic extracts) RAs to restore RAP binder with penetration value of 19 dmm to that of the virgin asphalt binder with penetration value of 78 dmm at 25 °C. According to the authors, the RAs' dosage rates and penetration values were exponentially related. Organic-based RAs achieved the target penetration with about 8-11% of dosages, while petroleum-based required between 14-21% of RA dosages to attain the same target. The authors suggested 12% as the optimum dose for all RAs to restore the penetration of the 100 percent RAP binder.

One major drawback of determining the recycling agent dosage rate by using the empirical tests is that they do not provide detailed information on the long-term performance of the rejuvenated asphalt binders. In addition, they do not provide a deeper understanding of the underlying rheological phenomenon (EAPA, 2018).

2.5.4.2. Matching the Rheological Properties of the Recycled Binder Blends to that of the Target Binder

With the development in asphalt mixture design procedures and innovative technologies in the asphalt industry, determining the optimum dosage of RAs by matching the rheological properties of the target asphalt binder seems to be reasonable and trustworthy. This approach involves using blending charts. Many studies have found relationships between rheological properties of recycled asphalt binder and RAs' dosage that include: a linear reduction relationship with HTPG and/or LTPG (Arámbula-Mercado et al., 2018; Karki and Zhou, 2016; Tran et al., 2012; Zaumanis et al., 2014a), decrease in complex modulus ($|G^*|$) and increase in phase angle (δ) from the DSR test (Oliveira et al., 2013; Shen et al., 2007; Yu et al., 2014; Zadshir et al., 2019), and decrease in

stiffness (S) value and increase in slope rate (m) from the BBR test (Shen et al., 2007; Yu et al., 2014).

Martin et al. (2019) explored three rheology-based methods of incorporating RAs in recycled asphalt binders (1) restore the LTPG of the recycled binder blend to that of the target asphalt binder, and verify the HTPG, (2) achieve ΔT_c of -5 °C for the recycled binder blend, and (3) match the continuous HTPG of the recycled asphalt binder blend to that of the target asphalt binder. Descriptions on the procedures of how RA dosages were determined are found in Arámbula-Mercado et al. (2018) and Martin et al. (2019) and it involves three steps. The first step was the preparation of recycled binder blends which first required extracting and recovering reclaimed (aged) asphalt binders from RAP and/ or RAS materials per ASTM D2172 (*Test method A: Centrifuge Extraction*) and ASTM D5404, respectively. Then, recycled asphalt binder blends were formulated at desired proportions using the RAM binder, the base binder, and a recycling agent. Three different recycled binder blends were prepared: the control binder blend (one without recycling agent), a recycled binder blend with low recycling dosage (between 2-5% by weight of total binder), and one with high recycling agent dosage (between 8-10% by weight total binder). The second step consisted of obtaining the HTPG and LTPG of the three recycled asphalt binder blends per AASHTO M320. Lastly, a PG blending chart with the continuous temperature grades of the recycled binder blends and percentages of dosages of the recycling agent was developed to determine the optimum recycling dosage using the methods stated above.

According to Arámbula-Mercado et al. (2018) and Martin et al. (2019), the first method consisted of restoring the LTPG of the recycled binder blend to that of the target asphalt binder and verifying the HTPG yielded insufficient dosages of RAs. After 20 hours and 40 hours of PAV conditioning, the recycled binder blends were in the transition and block cracking zones of the black space

diagram, respectively. This indicated that the rejuvenated recycled binder blends failed to maintain their effectiveness.

The second method which involved achieving a ΔT_c of $-5\text{ }^\circ\text{C}$ or less for the recycled asphalt binder blends yielded high recycling agent dosages compared to method 1 which would be costly and increase their susceptibility to rutting damages. The ΔT_c threshold of $-5\text{ }^\circ\text{C}$ was based on Anderson et al. (2011) study who proposed a maximum ΔT_c of $-5\text{ }^\circ\text{C}$ to minimize the potential of low temperature cracking on asphalt binders after 40 hours of PAV conditioning. However, Arámbula-Mercado et al. (2018) and Martin et al. (2019) conditioned the asphalt binder blends for 20 hours in the PAV before BBR testing instead of the 40 hours used by Anderson et al. (2011), since the latter would significantly increase the recycling agent dosages and was likely to cause poor rutting resistance. To prepare the asphalt binder blends, Arámbula-Mercado et al. (2018) and Martin et al. (2019) used two base binders which had different quality (PG 64-22 from Texas with ΔT_c of $-4.6\text{ }^\circ\text{C}$ and PG 64-22 from Indiana with a ΔT_c of $-1.2\text{ }^\circ\text{C}$ after 20 hours of PAV), and four different recycling agent (tall oil, aromatic extract, vegetable oil, and bio-based oil). In general, the higher quality binder (ΔT_c of $-1.2\text{ }^\circ\text{C}$) required less recycling agent dosage and simultaneously met the $\Delta T_c = -5\text{ }^\circ\text{C}$ criteria (Martin et al., 2019) compared to the lower quality binder (ΔT_c of $-4.6\text{ }^\circ\text{C}$). Based on the black space diagram, all asphalt binder blends that used the lower quality binder as their base binder provided sufficient stiffness reduction and phase angle restoration due to high recycling agent doses (7-12.5% by weight of the total binder). Moreover, after 20 hours of PAV aging, all the blends were in the no block cracking zone, and none was in the block cracking zone after 40 hours of PAV aging. However, the asphalt mixtures prepared using the highest dosage rate (12.5%) obtained with the lower quality binder and tall oil-based recycling agent failed the rutting resistance criteria in the HWTT by reaching a rut depth of 12.5 mm after only 2300 cycles.

As mentioned previously, the higher quality binder required lower dosage rates (1-2% by weight of the total binder) to produce recycled binder blends with a maximum ΔT_c of $-5\text{ }^\circ\text{C}$ after 20 hours PAV. Black space diagram showed that the blends were in the transition zone and block cracking zone after 20 hours and 40 hours PAV, respectively, indicating that the low recycling agent dosages were not effective for long term-performance; despite restoring the phase angle of the recycled blend partially.

The third method of RA dosage determination which targeted matching the continuous HTPG of the recycled asphalt binder blend to that of the target asphalt binder gave dosage values between the first method and second method. Compared to the other two methods, this method used only the DSR test results and improved further the LTPG of the recycled binder blends (Martin et al., 2019). The black space diagram showed low $|G^*|$ and high δ , and all binder blends were within the transition zone after 20 hours of PAV. Besides, only blends with tall oil and aromatic extract-based RAs were within the block cracking zone after 40 hours of PAV. The HWTT conducted on asphalt mixture with 6.5% of aromatic extracts showed improved rutting resistance by reaching a rut depth of 12.5 mm after 10,300 cycles compared to 2300 cycles attained with the 12.5% of tall oil from the second method. However, one should note the potential for moisture damage when the RA dosages of high RAM content mixture are obtained targeting the continuous HTPG of the target binder. According to NCHRP 9-58, while some mixtures passed the dry HWTT, the same mixtures failed the wet HWTT indicating that rutting may not be an issue when mixtures are dosed with RAs to match the continuous HTPG of the target binder, but moisture damages could be of concern (Martin et al., 2019).

Based on the analysis of three methods, Martin et al. (2019) proposed a provisional AASHTO standard for characterizing mixtures with high RAM contents and RAs. They recommend determining the RA dosage to restore the continuous HTPG of the recycled binder blend to that of the target binder. The provisional standard also provides the performance criteria with thresholds for both recycled binder blends and mixtures. However, AASHTO R30 is suggested as a LTOA protocol which as mentioned previously doesn't properly simulate field aging.

2.6. Blending Efficiency of RAM Binder

Different terms such as degree of blending (DoB), blending efficiency, meso-blending, mobilization rate/status, blending ratio, and binder transfer are used to refer to the amount of aged binder activated from RAM during mixture production (Lo Presti et al., 2020). To bring uniformity in the asphalt industry, Lo Presti et al. (2020) proposed the use of DoB. Lo Presti et al. (2020) defined DoB as the percentage of RAM binder that contributes to the performance properties of the asphalt mixtures with or without RAs (RAs). To distinguish DoB from the amount of RAM binder that is usually assumed fully available during asphalt mixture production, Kaseer et al. (2019a) introduced the term binder availability factor [also referred to as the degree of binder availability (DoAv) by Lo Presti et al. (2020)]. According to Lo Presti et al. (2020), DoAv is the maximum percentage of RAM binder that can be assumed will be available during mixture production whereas the minimum percentage of RAM binder that can be assumed will be released during mixture production is known as the degree of binder activity (DoA). DoA is not an inherent property of the RAM, hence affected by the mixture production conditions (Lo Presti et al., 2020). These three indices (DoB, DoAv, and DoA) are referred to as blending efficiency parameters. Based on these definitions, DoAv of the RAM is quantified by either extraction and recovery to

obtain the binder content of the asphalt mixture. In a situation where only RAM is considered, the value of DoA is similar to that of DoAv; unless a recycling agent and/or virgin binder are introduced in the asphalt binder blend/mixture then DoAv will be higher than DoA due to their effect. To what extent DoAv will be higher than DoA will depend on the properties of the RAM and virgin binder, and other factors such as mixing temperature and conditioning time.

DoB is affected by both RAM characteristics and asphalt mixture design and production procedures (Lo Presti et al., 2020). RAM characteristics that affect DoB include aged asphalt binder properties and film thickness, conditioning temperature and time, moisture content, particle size distribution, surface texture, and microgeometry homogeneity of the RAM aggregates (Cavalli et al., 2017; Kaseer et al., 2019a; Lo Presti et al., 2020; Zhang et al., 2015). Asphalt mixture design and production parameters that affect DoB are mixing temperature and time, silo conditioning time, RAM content, properties of RAM and virgin binder, mixture additives such as RAs and anti-stripping agents, virgin aggregates shape, surface texture, aggregate absorption, and amount and type filler particles (Booshehrian et al., 2013; Hettiarachchi et al., 2020; Kadhim and Baaj, 2020; Lo Presti et al., 2020; Shirodkar et al., 2011; Sreeram et al., 2018; Zhang et al., 2015).

Orešković et al. (2020) conducted a literature review and categorized the approaches used to determine/ assess RAM binder blending efficiency parameters into four main groups: mechanical, chemical, visualization, and mechanistic approach.

- *Mechanical approaches* include those that use mechanical blending methods, nanoindentation techniques, physical and/or rheological binder property parameters, or mixture performance property parameters to determine the blending efficiency parameters (Abd et al., 2018; Huang et al., 2005; Kaseer et al., 2019a; Mohajeri et al., 2014; Shirodkar et al., 2011; Yu et al., 2017).

- *Chemical approaches* use solely chemistry-based techniques such as chromatography and spectroscopy to evaluate the blending efficiency of RAM binders (Abdalfattah et al., 2021; Bowers et al., 2014; Castorena et al., 2016; Ding et al., 2018; Hettiarachchi et al., 2020; Orešković et al., 2020; Sreeram et al., 2018). The binder blends used in this approach are obtained through the extraction and recovery process on a blend of RAM and virgin aggregates or artificial aggregates.
- *Visualization approaches* do not involve quantification of the blending efficiency parameters but assess the homogeneity of the asphalt binder blends/mixtures (Abdalfattah et al., 2021; AbuQtaish et al., 2018; Castorena et al., 2016; Orešković et al., 2020; Rinaldini et al., 2014). They are typically used to supplement mechanical and chemical approaches. These approaches involve the usage of microscopy and computed tomography techniques (Orešković et al., 2020).
- *Mechanistic approaches* do not usually involve significant laboratory work (mixing or testing) but use existing data for modeling and simulation techniques to determine the blending efficiency parameters (Bonaquist, 2005; Booshehrian et al., 2013; Orešković et al., 2020; Zhang et al., 2015).

As the asphalt industry moves towards performance-based mixture design practices such as BMD, mechanical-based approaches have the potential of being useful and effective in evaluating the blending efficiency parameters of RAM binder. Therefore, they are the only approaches discussed in detail in this study. The most promising mechanical-based approaches for the determination of the blending efficiency parameters are discussed in the subsequent sub-sections.

2.6.1. Virgin coarse aggregates-Fine RAP mixture

This method employs the use of virgin coarse aggregate materials (retaining on a 9.5 mm sieve or #4 sieve) and fine RAP material (passing #4 sieve); then separating the loose mixture into the coarse aggregate mixture and fine aggregate mixture using sieve #4 (Huang et al., 2005; Shirodkar et al., 2011; Yu et al., 2017). The parameters of properties such as cracking and rutting of the recovered binder from each fraction and that of the virgin binder are used to determine the DoAv. This method assumes that full blending between RAP and virgin binders occurs if the properties parameter values of the recovered binders from the two fractions are the same; otherwise, full blending did not occur (Huang et al., 2005; Shirodkar et al., 2011; Yu et al., 2017).

Huang et al. (2005) introduced this approach using screened RAP material passing the #4 sieve and virgin aggregates retaining on the same sieve. The DoA from this study was around 11% for all three mixtures with RAP content ranging from 10% to 30% RAP by weight of aggregates. Shirodkar et al. (2011) followed this method but used fine RAP passing the #8 sieve and virgin aggregates retaining on the #4 sieve. The blend was separated into fine and coarse fractions using sieve #4. The researchers conducted both coating study and blending study on two mixtures (25% RAP mixture and 35% RAP mixture) using a PG 70-28 binder for the 25% RAP mixture and a PG 58-28 binder for the 35% RAP mixture. The coating study determined the RAP binder transfer (i.e., DoA) whereas the blending study determined the DoAv. The DoA was obtained by computing the percentage of the weight of the aged binder coating the virgin aggregates over the original weight of the binder in RAP. The AASHTO M320 rutting parameter ($|G^*|/\sin \delta$) from the DSR was used to determine the DoAv. Results from the coating study showed that the DoA was 24% and 15% for the 25% RAP mixture and 35% RAP mixture, respectively. The blending study found that DoAv of a mixture with the PG 58-28 binder was higher than that of a mixture with the

PG 70-28 binder. Moreover, the DoAv for the 25% RAP mixture and 35% RAP mixture was 70% and 96%, respectively.

Yu et al. (2017) used RAP material passing through the #4 sieve and washed virgin limestone aggregates retaining on the 3/8" sieve. The study used three RAP mixtures with 20% RAP, 40% RAP, and 60% RAP by weight of the aggregates, and sieve 3/8" was used to separate the mixtures into fine and coarse mixture fractions. The study found a linear relationship between the natural logarithm of the binder properties and RAP content, and therefore Equation 2.2 was developed to calculate the DoAv. However, to account for fine particles stuck on coarse aggregates mix, Equation 2 was employed to account for this impact on the specific binder property parameter. Therefore, in Equation 2.2, R_m was substituted by R'_c from Equation 2.3 for coarse aggregate mixtures' property parameters.

$$DoAv = \frac{\ln(R_m) - \ln(R_v)}{\ln(R_p) - \ln(R_v)} * 100\% \quad \text{Equation 2.2}$$

Where,

R_m = Specific binder property parameter of the mixture (fine or coarse aggregate mixture);

R_v = Specific binder property parameter for the virgin binder; and

R_p = Specific binder property parameter for the proportion binder (mixed RAP binder and virgin binder).

$$R'_c = \exp \frac{\ln(R_c) * P_{bc} - \ln(R_f) * P_{bf} * \alpha}{P_{bc} - P_{bf} * \alpha} \quad \text{Equation 2.3}$$

Where,

R'_c = Corrected specific binder property of the coarse aggregate mix;

R_c = Uncorrected specific binder property of the coarse mix;

P_{bc} = asphalt binder content of the coarse aggregate mix;

R_f = Specific binder property of the fine aggregate mix;

P_{bf} = asphalt binder content of the fine aggregate mix; and

α = Ratio of weight of the fine particle sticking on the coarse aggregate to the weight of the coarse aggregate mix.

The study used both fatigue and rutting resistance parameters. The fatigue resistance parameters used were $|G^*| \sin \delta$ and fracture energy from the DSR and a fatigue monotonic test, respectively, whereas $|G^*|/\sin \delta$ and J_{nr} were used as rutting resistance parameters. The average DoAv from this study ranged from 27.8 to 83.4% (Table 2.4), and they were not sensitive to either fatigue or rutting resistance parameters. Moreover, when a RA was introduced on the 60% RAP mixtures (dosed at 0.5% by weight of the mixture), the DoAv increased impacting both the fatigue and rutting parameters.

Table 2.4: DoAv results from Yu et al. (2017) study

Mix type	$ G^* \sin \delta$ (%)	fracture energy (%)	$ G^* /\sin \delta$ (%)	$J_{nr3.2}$ (%)	Average
20% RAP	21.2	20.9	36.2	32.9	27.8
40% RAP	81.6	84.8	83.0	84.0	83.4
60% RAP	63.6	71.4	73.5	73.7	70.6
60% RAP+RA	68.0	74.9	84.8	91.4	79.8

Besides only being useful in determining DoA and DoAv. This technique involves extraction and recovery of the binder blend for DoAv determination. Studies have found that solvents used for extraction affect the properties of the binder (AbuHassan et al., 2019; Bouraima et al., 2017; Ge et al., 2019; Xu et al., 2018b).

2.6.2. Gap graded mixtures of coarse virgin aggregates and RAP material

As part of the NCHRP 9-58 project, Kaseer et al. (2019a) developed a method to determine DoAv using gap-graded mixtures. This approach involved the preparation of two gap-graded asphalt mixtures: virgin aggregate asphalt mixture and recycled asphalt mixture. The virgin aggregate asphalt mixtures included three different fractions: a coarse fraction (retaining on the 3/8" sieve), an intermediate fraction (passing the 3/8" but retaining on the #4 sieve), and a fine fraction (a combination of material passing the #4 sieve and retaining on #4 8 and passing the #8 and retaining on the #30 sieve). The recycled asphalt mixture in the study was prepared the same way as the virgin aggregate, except that the intermediate fraction was replaced with RAP material. After conditioning both asphalt mixtures at 135 °C for two hours, while still hot the loose asphalt mixtures were separated into three fractions using a 3/8" and #4 sieves (coarse, intermediate, and fine fractions). The asphalt content of each fraction was determined using the ignition oven. The approach assumes that the DoAv will be 100% if the intermediate fractions of both mixtures have the same binder content; otherwise, the intermediate fraction of the recycled mixture will have higher binder content than the virgin aggregate asphalt mixture. If the difference in binder contents between the two fractions is equal to the binder content of the RAP, then RAP is acting as a black rock and no aged binder is activated, otherwise, the aged binder was partially activated.

The DoAv from this study ranged from 50% to 95% depending on the RAP source and mixing temperature. The DoAv was also affected by the HTPG of the RAP, with softer RAP having a higher DoAv. Also, the addition of RAs at low mixing temperature (140 °C) impacted the DoAv significantly whereas no impact was observed at high mixing temperature (150 °C). In addition, no significant effect on the DoAv was observed when RAs were added on the RAP itself or blended with the virgin binder (Kaseer et al., 2019a).

This approach does not account for the RAP binder that gets absorbed by the RAP aggregates; and the intermediate RAP fraction is not a good representative of the entire RAP stockpile as RAP stockpiles mostly consist of a lot of fines and some coarse fractions (Kaseer et al., 2019a). Moreover, the ignition oven requires the computation of correction factors due to loss in aggregate weights which may be cumbersome for unknown RAP sources (Rodezno and Brown, 2017).

2.6.3. Recycled asphalt mixture performance property parameter

With this approach asphalt mixtures with high RAM contents are designed with the assumption that full blending will occur. Then, their performance properties are compared to a control mixture (i.e., one without RAM or with acceptable RAM limits) to obtain the DoA or DoB depending on the experiment design.

Abed et al. (2018) followed this approach to determine the blending efficiency of the 50% RAP (by weight of aggregates) warm asphalt mixture at three different production conditions (mixing for 1, 3, or 5 min. at 95, 115, or 135 °C). The researchers used a blending chart to determine the recycling agent dosage and confirmed it using both physical and rheological parameters. The rejuvenated binder blend was found to have the same viscosity and critical high temperature as the target binder. The DoB was obtained as a ratio of indirect tensile stiffness moduli of the recycled asphalt mixtures and the control mixtures. The DoB ranged from 86 to 96% when mixing for 3 or 5 min at 135 °C. When the mixing temperature was 115 °C and the time was 5 min the DoB was 79%. At other production combinations of temperature and mixing time, the DoB was less than 60%. DoB was found to be a function of mixing time and temperature, and it could be obtained by using stiffness and strength parameters.

Sobieski et al. (2021) conducted a study to determine the DoA using RAP stockpiles representative to three climatic zones of the U.S. (dry no-freeze zone, wet no-freeze zone, and wet freeze zone). The samples were prepared using 100% RAP and conditioned at five different temperatures (70, 100, 140, 170, 190 °C) for four hours. The DoA was determined from the ratio of the indirect tensile strength of the particular RAP stockpile to the global maximum indirect tensile strength of the RAP stockpiles at a specific conditioning temperature. The DoA of the RAP stockpiles was found to range from 10-90% depending on the conditioning temperature.

2.7. Performance Characterization of Asphalt Binder and/or Mixtures with RAs

Characterization of asphalt binders and mixtures is vital to understand their behavior and performance. The complexity/sophistication, automation, and robustness involved in the sample preparation, running the test, analysis of the raw data, and variability of the test results vary depending on the test. This section discusses a few studies which have used different tests and parameters to characterize recycled binder blends and/or mixtures with RAs.

A laboratory study by Tran et al. (2012) evaluated the performance of 50% RAP and 20% RAP + 5% RAS mixtures (with and without RAs) compared to a control virgin mixture. The mixtures were dosed with 12% of the RA by weight of the recycled binder targeting a PG 67-22 binder. The Cracking resistance of the recycled binder blends was assessed with the LAS test conducted at 32.1 °C. The results indicated that the RA was more effective on the 20% RAP + 5% RAS blend on the 50% RAP blend. All mixtures passed the commonly accepted failure criterion of 0.8 on the Tensile Strength Ratio (TSR) test; however, it was found that the RA increased the moisture susceptibility of the mixtures. The APA results for rutting resistance showed that all mixtures were rut resistant (rut depths less than 5.5 mm) based on past research on the NCAT test track. The top-

down cracking resistance, low temperature cracking resistance, and reflective cracking resistance of the mixtures were assessed using the Energy Ratio (ER) test, the Indirect Tensile Test (IDT), and OT respectively. Based on the ER test, mixtures with RAs met the proposed minimum dissipated creep strain energy at failure ($DCSE_f$) and ER thresholds, but the $DCSE_f$ correlated better with the N_f from LAS than the ER. The virgin mixture was found to have better low temperature and reflective cracking resistance than the mixtures with the RA. Moreover, the critical low temperatures from the IDT correlated well with those from the BBR test. Lastly, according to the $|E^*|$ test, mixtures with RA were more susceptible to aging and stiffer than the virgin mixture after both short-term and long-term aging conditions.

Mogawer et al. (2013) conducted a study to evaluate the use of RAs in high RAM content mixtures without sacrificing their rutting performance. Three high RAM content mixtures: 40% RAP, 5% RAS, and 35% RAP + 5% RAS were evaluated against a control virgin mixture. The high RAM content mixtures were dosed with three different RA types at dosages ranging from 0.50 to 1.64% by weight of the RAM. The HWTT conducted at 45 °C showed that the control mixture had worse rutting and moisture damage resistance compared to high RAM content mixtures with or without RAs. However, the 40% RAP and 5% RAS mixtures with RAs were more susceptible to rutting and moisture damage than their corresponding mixtures without RAs. For the 35% RAP + 5% RAS, the addition of the RAs increased their rutting slightly, albeit they did not show any stripping issues due to moisture damage. The N_f from the OT indicated that mixtures with high RAM content were more susceptible to fatigue and reflective cracking failure than the control mixture. Although the incorporation of RAs in the mixtures increased their N_f , the degree of effectiveness was dependent on the RA type. Based on the thermal stress restrained specimen test, the addition of

the RAs on high RAM content mixtures improved their low temperature cracking resistance by almost 2 °C when compared to their corresponding high RAM content mixtures without RAs.

A laboratory study by Podolsky et al. (2021), evaluated the effectiveness of soybean derived RA. The study evaluated a field produced mixture with 30% RAP and 3% of the soybean oil (by weight of the total binder) compared a control mixture with 20% RAP. Based on the DCT results, the 30% RAP mixture met the Iowa DOT criterion for low temperature cracking resistance (minimum fracture energy of 400 J/m² for standard traffic) whereas the control mixture failed. However, the 30% RAP mixture was more susceptible to moisture damage as compared to the control mixture, despite passing the stripping inflection point (SIP) requirement for standard traffic (minimum of 10,000 passes). The |E*| master curves showed that the 30% RAP mixture was softer at intermediate temperatures than the control mixture whereas at low and high temperatures, both mixtures had similar stiffness properties. Lastly, cores extracted from the field sections showed that both mixtures met the density requirements and were entitled to pay incentives of 3.1% and 4.0% for the control and the 30% RAP mixture, respectively.

Santos et al. (2021) reported improvement in the J_{nr} and N_f from the MSCR and LAS tests, respectively when 100% RAP binders were dosed with different soybean-based RAs. However, the FTIR test showed an increase in carbonyl and sulfoxide functional groups in rejuvenated binder blends as compared to virgin binders. Contrary to the prior mentioned findings, Zhu et al. (2017) and Liu et al. (2018) reported a decrease in carbonyl and sulfoxide functional groups after conducting an FTIR test on recycled binder blends dosed with bio-based and waste engine oils, respectively. According to Baqersad and Ali (2019), the carbonyl and sulfoxide functional groups of the RAs alone have an impact on their long term performance.

Using the HWTT, Zhang and Bahia (2021) investigate the rutting and moisture susceptibility resistance of three high RAM content mixtures (30% RAP mixture, 50% RAP mixture, and 30% RAP + 5% RAS mixture) with and without RAs compared to a virgin control mixture. The ABR of the high RAM content mixtures were 27%, 45%, and 47.5% for the 30% RAP mixture, 50% RAP mixture, and 30% + 5% RAS mixture, respectively. Two bio-based RAs and re-refined engine oil bottoms (REOB) were used to restore the properties of the aged RAM. The dosages of the REOB ranged between 5% to 10% while that of the bio-based RAs was between 3% and 5%. High RAM content mixtures were found to have improved rutting and moisture damage resistance than the control mixture; however, the improvement decreased with the addition of RAs, especially the REOB. The authors recommended using a HWTT analysis procedure that separates the rutting phase from the stripping phase to avoid the influence of moisture damage to rutting resistance; and that selection of RAs should include parameters to assess their moisture damage potentials.

Zhang et al. (2021) conducted a study aimed at investigating the feasibility of using blended binder test results to predict the performance of high RAM content mixtures and adjust the dosages of RAs. The authors reported that the $J_{nr3.2}$ from the MSCRR showed a better correlation with the creep slope from the HWTT than the Superpave rutting parameter ($|G^*|/\sin\delta$). Besides, the Superpave cracking parameter ($|G^*|\sin\delta$) showed a better correlation ($R^2 = 0.87$) with the post peak slope parameter from the IDEAL-CT test performed at 25 °C. However, no trend between the $|G^*|\sin\delta$ parameter and fracture energy parameter from the IDEAL-CT was observed which in turn affected the correlation between the CT_{index} and $|G^*|\sin\delta$ parameter. In addition, the N_f at 15% strain correlated well with the CT_{index} ($R^2 = 0.78$). Among the parameters from the BBR test for low temperature cracking resistance evaluation, the m-value showed a better correlation ($R^2 = 0.87$) with the CT_{index} from the IDEAL-CT test conducted at 0 °C than the stiffness value and the

ΔT_c parameter. Since recycled binder blends were found to be “m-controlled” and the m-values were found to correlate well with mixture cracking resistance, the authors suggested dosing RAs to target the m-value to achieve thermal cracking resistance of high RAM content mixtures.

A number of tests have been conducted to evaluate the performance of recycled binder blends and/or mixtures with or without RAs. High RAM content mixtures are affected by several factors including constituent materials, inherent behaviors, and mixture production factors. Therefore, it's expected that highway agencies select tests that simulate the distresses in their pavements as close as practical when evaluating the performance of recycled binder blends and mixtures with RAs.

2.8. Field Performance of high RAM content Asphalt Binders/ Mixtures with RAs

In the most recent NAPA survey, the percentage of RAP mixtures incorporating RAs remained at 4 percent from 2017 to 2019. This percentage was 7 percent and 3 percent in 2016 and 2015, respectively. The percentage of RAS mixtures with RAs was 9 and 11 percent in 2019 and 2018, respectively (Williams et al., 2020). Nevertheless, few documented field projects of high RAM content mixtures with RAs are available in the U.S.

In 2017, NCAT conducted a study for the Alabama DOT to evaluate the performance of high RAM content mixtures (12.5 mm NMAS) with different RAs and a PG 67-22 binder (Xie et al., 2017). The control mixture contained 20% RAP, and it was produced at 149 °C with no RA but included 0.80% of an anti-strip additive by weight of the virgin binder. The high RAM content mixture was produced at 129 °C, and it incorporated 25% RAP and 5% PC RAS with RAs. The RAs used in this study were composed of fatty acids derivatives (Product I), and fast pyrolysis of pine trees (Product II). The dosage of Product I was 7.8% and Product II was 13.8% by weight of the virgin

binder. Moreover, mixtures with Product I and Product II included different anti-stripping additives at a rate of 0.52% and 0.43% by weight of the virgin binder, respectively. After being subjected to traffic loading for two years, the average International Roughness Index (IRI) of the control test section, and test sections with Product I, and Product II were 54.5 in./mi., 59 in./mi., and 45 in./mi, respectively. Furthermore, their rut depth were 0.18 in., 0.19 in., and 0.25 in., respectively. All test sections showed a good ride quality and rutting performance, with IRI and rut depth less than the FHWA's recommended thresholds of 95 in./mi. and 0.5 in., respectively (Xie et al., 2017). However, low-severity level longitudinal cracking was observed on the northbound outside lane of the test section, while no cracking was observed on the inside lane of the southbound. A higher cracking severity level was observed on the test sections with RAs' mixtures. Alligator cracking was observed in the test section with Product I, while the section with Product II showed mostly longitudinal and transverse cracking. Based on these cracking differences, the authors concluded that the RAs used were not effective in improving the cracking resistance of high RAM content mixtures.

A study conducted by Zhou et al. (2019) for the Texas DOT assessed the performance of four test projects which included a total of 17 test sections and constructed with high RAM content mixtures with and without RAs. The HWTT and Overlay Test (OT) were conducted per Tex-242-F and Tex-248-F on plant-produced mixtures after conditioning at 135 °C for 2 and 4 hours, respectively. The subsequent paragraphs describe the mixtures used as well as their performance.

The first test project consisted of five test sections each 2000 ft-long. They were all overlay test sections with 2 in. thick, and they were constructed on the outside of the eastbound lane of SH31 near Tyler, Texas. SH31 is a two-divided highway with annual average daily traffic (AADT) of 9800 and 10% truck traffic, which is estimated to be 3.5 million ESALs after 20 years of traffic.

The control test section's mixture had 29.2 % ABR (10.8% ABR from RAP + 18.4% from MW RAS), produced with a PG 64-22 binder with no RAs. The mixtures for test sections with RAs involved a modification of the control mixture with two bio-based RAs (BR6 and BR8 with a total fatty acid content of 91% and 90%, respectively). The dosages of the BR6 and BR8 RAs were 2.6% and 3.7% by weight of the total binder, respectively. All three mixtures had the same 4.6% total binder. Another test section was paved with a virgin mixture which was modified by removing the RAP and MW RAS in the control mixture with a PG 70-22 virgin binder. The total binder content of this mixture was 4.5%. The last test section was paved with a mixture that was a modification of the control mixture with an emulsion-based recycling agent (R1) dosed at 1.3% by the weight of the total binder, and its total asphalt binder content was 4.7%. Based on the HWTT, none of the mixtures exceeded a rut depth of 12.5 mm after 15,000 passes. The OT showed that there was no improvement in cracking resistance for high RAM content mixtures with RAs (BR6, BR8, or R1). These results were in line with the field survey of test sections after two years in service as no measurable rutting was observed and reflective cracking seemed more pronounced in the test sections with RAs.

The second test project was a major rehabilitation and it consisted of four test sections each about 1500 ft. long. The test project's pavement layers thickness was: 4 in-surface layer, 10 in- granular flexible base, and 6 in-stabilized subgrade. It was constructed on the eastbound lane of FM468 near Cotulla, Texas. The estimated traffic load on FM468 was 11.5 million ESALs after 20 years of in service. The first test section for this project consisted of a virgin mixture which was prepared with a PG70-22 binder without RAM or RAs. The control test section's mixture was prepared using a PG 64-22 base binder, it had 30% ABR from RAP with no RAs. The total binder content of the control mixture was 6.3%. The control mixture was modified to include RAs for test sections

with bio- RAs (BR5 and BR3, both had total fatty acid content greater than 97%). The dosages of BR5 and BR3 were 3% and 2% by weight of the total binder, respectively. The total binder content of the mixtures with the bio-RAs was 6.1%. Results from the HWTT showed that the virgin mixture and the mixture with the BR3 had a rut depth of more than 12.5 mm after 15,000 passes (15.9 mm and 12.6 mm, respectively). The control mixture had the lowest rut depth (10.6mm), followed by the mixture with BR5 (11.7 mm). Based on the OT, the virgin mixture had the highest number of cycles to failure (N_f), about 669, followed by the mixture with the BR3 (377). The control mixture had the lowest N_f (43). The N_f of the mixture with RA BR5 was 100. After 3.8 years in service, none of the test sections showed any cracks. However, rutting was observed, and test sections with RAs had more rutting than the control and the virgin test sections. Hence, caution on potential rutting damages should be practiced when selecting a RA.

The third test project involved milling and inlaying a 1.5 in-thick overlay on the westbound lane of FM1463 near Katy, Texas. FM1463 is two way-highway with an estimated traffic loading of 1.83 million ESALs after 20 years of in service. This project consisted of four test sections each stretching at 1000 ft-long. The mixture for the control test section had a 28.8% ABR (16.3% ABR from RAP + 13.5% ABR from PC RAS). It was produced with a PG 64-22 binder and the total binder content of the mixture was 5.2%. The mixtures of the remaining three test sections were a modification of the control mixture by incorporating RAs. The RAs used were BR5, BR7, and BR8 and they were dosed at 3.5%, 4.0%, and 7.5% by weight of the total binder, respectively. BR7 had a total fatty acid content of about 75%. The total binder contents of the mixtures with RAs were kept the same as the control mixture (5.2%) except for the mixture with BR7 for which the recycling agent was added on top of the total binder content not replaced. Hence, the total binder content of the mixture with BR7 was 5.4%. The HWTT showed that the mixtures containing BR5

and BR8 had high rut depth after 15,000 passes (12.8 mm and 12.5 mm, respectively). The control mixture had the least rut depth (4.3 mm), followed by the mixture containing BR7 (9.4 mm). The N_f from the OT were 29, 83, 110, and 48 for the control, BR5, BR7, and BR8 containing mixtures, respectively. Field survey of the test sections, 17 months after they were opened to traffic showed no measurable rutting. Moreover, no longitudinal reflective cracking was observed on the control test section and the BR5 test section. The test section with the BR7 t showed minimal reflective cracking whereas the test section with BR8 had the longest reflective cracking distress (\approx 200 ft. long). Unfortunately, the test section with BR7 was removed after this period to allow the widening of the roadway. There was still no measurable rutting on the remaining test sections 18 months later. However, the length of the reflective cracks on the BR8 test section had increased to about 1200 ft. long. The control test section had the least reflective cracking length, followed by the BR5 test section. In addition, the lengths of their reflective cracks were below 200 ft. long.

The last test project consisted of four test sections, 1000 ft. long each. The project involved constructing a 2 in. thick overlay on an existing cracked asphalt pavement on SH67 near San Angelo, Texas. SH67 is a two-way highway with estimated 20-year traffic loading of 3.0 million ESALs. The mixture for the control test section contained 30% ABR from RAP without a RA. It was produced using a PG 64-22 binder and the total binder content of the mixture was 5.3%. The same control mixture was used for the test sections with RAs by incorporating two bio-based RAs (BR3 and BR1 both having a total fatty acid content greater than 97%) and an improved RA (R1Pro). The dosages of the RAs by weight of the total binder were 3.0%, 3.0%, and 11.0% for the BR3, BR1, and R1Pro, respectively. The total binder contents of the mixtures with RAs were kept the same as the control mixture (5.3%). After 15,000 passes of the HWTT, the control mixture had the least rut depth (5.8 mm) whereas all the mixtures with the RAs had rut depth exceeding 12.5

mm. However, the control mixture had the lowest N_f from the OT (51) while the mixtures with the R1Pro had the highest N_f (149). Furthermore, the test sections did not show any rutting or cracking 2.3 years after being opened to traffic.

Based on the above observations, Zhou et al. (2019) concluded that the field performance of the RAs differs and that mixtures with bio-based RAs with less than 97% total fatty acid content performed worse (in terms of cracking) than the control mixtures. Moreover, rutting may be an issue for mixtures containing bio-based RAs in hot climate conditions and subjected to heavy traffic.

As part of the NCHRP 9-58 project, Kaseer et al. (2020) evaluated the field performance of high RAM mixtures containing RAs in Texas, Nevada, Indiana, Wisconsin, and Delaware. The Texas test sections included a control section and a rejuvenated section, both with 0.28 RBR. While the control mixture included a WMA additive to aid with compactability during construction, the rejuvenated mixture included 2.7% tall oil-based RAs. For the Nevada project, the control mixture contained 0.15 RBR (all from RAP), while two rejuvenated mixtures contained 0.3 RBR with 2% tall oil and 2% aromatic extract-based RA, respectively. For the Indiana project, the control mixture contained 0.32 RBR (0.25 from RAP + 0.07 from RAS) while the rejuvenated mixture contained 0.42 RBR (0.14 from RAP + 0.28 from RAS) and 3.5% tall oil. For the Wisconsin project, the control and rejuvenated test sections contained 0.22 and 0.31 RBR (all from RAP), respectively. The rejuvenated mixture contained 1.2% modified vegetable oil. Finally, in the Delaware project, the control and the rejuvenated mixtures contained 0.34 RBR (0.17 from RAP + 0.17 from RAS) and 0.41 RBR (0.24 from RAP + 0.17 from RAS), respectively. The rejuvenated mixture was dosed with 0.8% tall oil. The Texas test sections were designed to assess the effectiveness of the RAs on improving the performance of asphalt mixtures with the same RBR

content, while the Nevada, Indiana, Wisconsin, and Delaware test sections were designed to evaluate the performance of rejuvenated mixtures with higher RBR content as compared to those currently used by the DOTs.

Two years after construction, the pavement distress survey indicated a moderate severity level of longitudinal and transverse cracking on the rejuvenated section as compared to the low-severity level observed on the control section. After two years of service, the control mixture in Indiana exhibited minimum visible cracking whereas the rejuvenated mixture showed a significant amount of low-severity transverse and longitudinal cracking and some alligator cracking. The Delaware and Nevada projects showed no or minimal visible cracking on both the control and rejuvenated mixtures after one and two years of service, respectively. Low-severity transverse cracking was observed on both the control and rejuvenated mixtures on the Wisconsin test sections one year after construction.

For all test sections, field cores were obtained soon after construction and tested for resilient modulus and cracking susceptibility (I-FIT test) as per ASTM D7369 and AASHTO TP124, respectively. Statistical analysis of the resilient moduli of the control and rejuvenated mixtures placed in Texas, Wisconsin, and Delaware test sections showed that the mixtures were not statistically significant different. Due to the higher RBR, the rejuvenated mixtures in Nevada and Indiana exhibited higher resilient moduli as compared to the control mixtures. All mixtures with RAs were found to be more susceptible to cracking as compared to the control mixtures since they exhibited a statistically low flexibility index in the I-FIT test. Based on the visual distress survey and laboratory testing of the field cores, they concluded that the addition of RAs did not necessarily improve the cracking resistance of high RAM mixtures.

The recently completed research cycle on the NCAT test track investigated the performance of high RAM content mixtures with RAs. (West et al., 2021a). The first RA was a plant-engineered bio-oil (herein referred to as DS). This experiment began in the 2015 research cycle and continued through the 2018 research cycle. The high RAM content mixture with DS was compared against a control mixture with 20% RAP (0.177 RBR), produced with a PG 64-22 virgin binder with no RA. Initially, the high RAM content mixture incorporated 20% RAP and 5% PC RAS (0.282 RBR) and a PG 67-22 base binder, with 10% DS by weight of the RAM binders. The control mixture and the experimental mixture were paved as surface layers on test sections N1 and N7 at thicknesses of 1.6 and 1.5 inches, respectively. After the application of approximately 1.4 million ESALs, cracks were observed in test section N7. After a detailed forensic test section N7 was milled and repaved with a mixture containing 35% RAP (RBR was kept 0.282) with 5% of DS by weight of the RAP binder. After the N1 and N7 (repaved) test section had been trafficked with 6.2 and 2.1 million ESALs, they showed approximately 0.2 and 0.1% of the lane area had cracks. Near the end of the 2015 research cycle (October 2017), the cracked lane area was 10.2 and 21.3% for the N1 and N7 test sections after 9.7 and 6.6 million ESALs (Figure 2.1). At the end of the 2015 research cycle (December 2017), the test sections showed good ride quality and rutting performance. However, the N7 test sections had a higher cracked surface area than the N1 test section, but they were near-surface cracks with less than 1 mm opening. At the beginning of the 2018 research cycle (October 2018), the cracked lane area on the N1 test section increased slightly from 10.3% to 11.5% after 16.6 million ESALs, then jumped to 37.4% after 16.9 million ESALs, and to 45.8% by the end of the 2018 research cycle (February 2021). As shown in Figure 2.1, the cracked area on test section N7 did not increase until March 2019 (after 8.9 million ESALs) when it was 22.9%, then it increased gradually to 33.1% after about 12.7 million ESALs (December

2019). There was no increase in the cracked area between December 2019 and February 2020 after 13.3 million ESALs. Although the cracks on test section N7 were in low severity level, in some areas the cracks had connected, and fines were visible. Field cores showed that these cracks started from the bottom and propagated to the surface affecting the performance of the N7 test section. Both test sections (N1 and N7) had good ride quality, microtexture, and rutting performance (less than 5.0 mm rut depth). A spray on RA was applied on the distressed surface of the N7 test section with the intention of extending its life and mitigating bottom-up fatigue cracking. However, this increased the cracking significantly from 33.1% (before the application) to 53.1% when week after the application. Based on these results, the following were inferred (1) test section N7 had a higher cracked area than test section N1, (2) increase of the cracked lane area was high in spring (around March/April) and fall (around October), and (3) the spray-on RA should be applied on a pavement with a sound structural integrity as it is intended to rectify near-surface distresses (West et al., 2021a).

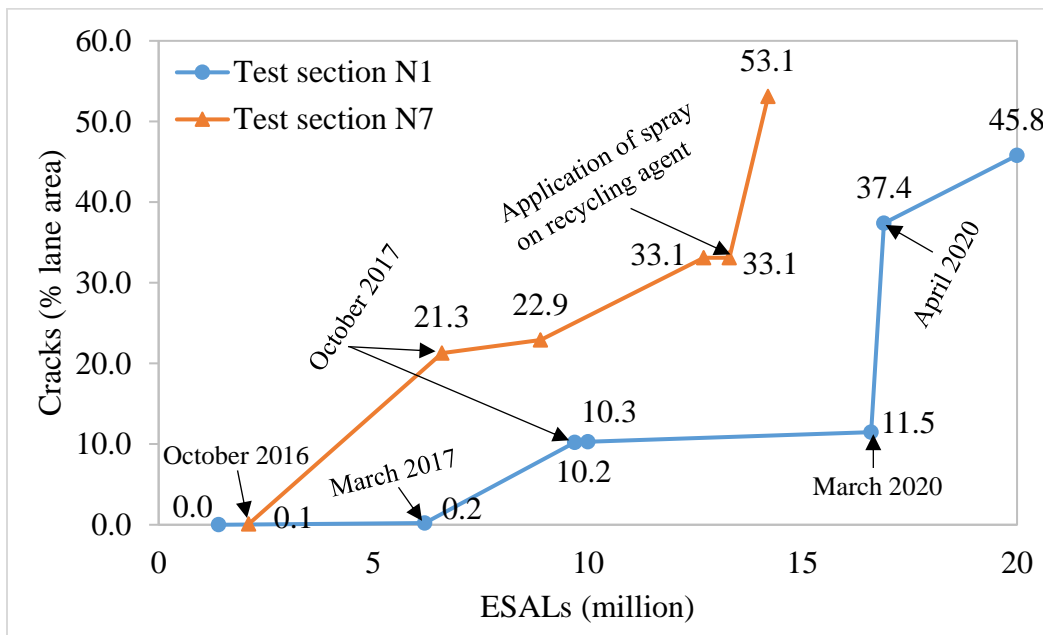


Figure 2.1: Crack growth of the N1 and N7 test sections from 2015 to 2017

The second RA that was evaluated during the 2018 research cycle was a modified vegetable oil (herein referred to as AN). This experiment involved a field comparison of the control mixture with 30% RAP by weight of the aggregates (25% ABR) produced with a PG 64-22 binder, and a high RAM content mixture with 45% RAP by weight of the aggregates (38% ABR) and prepared with a PG 64-22 base binder and the RA. Both mixtures were designed following the provisional 2018 Virginia DOT's BMD specification. The control mixture had no RA, but it incorporated a warm mix additive to improve workability, facilitate compaction at lower temperatures, and enhance asphalt mixture resistance to moisture damage. The control and the high RAM content mixture were placed on test sections N3A and N3B of the test track. After application of 10 million ESALs (end of the 2018 research cycle), the following findings were reported: (1) both test sections had good rutting performance (less than 5 mm rut depth), and they were in agreement with the APA and HWTT conducted on the plant produced mixtures, (2) test section N3B had good ride quality, while that of test section N3A was influenced by the rough transition at the beginning of the section, (3) both test sections had similar microtexture measurements with no sign of raveling despite the Cantabro mass loss on the plant produced mixtures being over the threshold specified by the Virginia DOT; and (4) both test sections exhibited good cracking performance. However, it was recommended that the test sections continue to be monitored as the laboratory cracking tests (I-FIT, OT, and IDEAL-CT) on plant-produced mixtures showed a significant decrease in the test results on the critically aged samples as compared to those reheated to compaction temperature (West et al., 2021a).

The aforementioned studies have shown that the performance of high RAM content mixtures is not only a function of RAs but also the pavement structure thicknesses, traffic loading, existing pavement conditions, and project climate. Moreover, the effectiveness of RAs varies depending

on their chemical formulation. Due to the numerous choices and alternatives of products in the market, a comprehensive study of the effect of the RAs on long-term field performance is necessary to the asphalt industry. Therefore, field studies dedicated to RAs' screening procedures, composition analysis, and performance evaluation of the RAs are in need.

2.9. Summary

RAs include both softeners and rejuvenators. Softeners reduce only the stiffness of the aged binder whereas rejuvenators can partially restore the chemical balance of the aged binder in addition to decreasing their stiffness. RA are classified/categorized based on their origin (i.e., petroleum-based or bio-based), chemical constituents (e.g., aromatic oils, fatty acids, paraffinic oils, etc.), or whether they are originally manufactured/engineered (e.g., modified vegetable oils) or recycled from wastes (e.g., re-refined engine oil bottoms). Based on their mechanism of action, RAs can be regarded as softeners (reduce the viscosity of aged binder), replenishers (reduce viscosity and restore the maltene to asphaltene ratio of the aged binder), and dispersants (reduce viscosity, disrupt asphaltene intermolecular associations, and may restore the maltene to asphaltene ratio if they are petroleum-based).

The effectiveness of RAs was found to be influenced by their type and dosage, properties of virgin and RAM binders, amount of RAM in recycled binder blends and/or mixtures, mixing temperature and conditioning time, and method of addition. Nevertheless, other factors like compatibility, diffusion, and dispersion affect the performance of high RAM content mixtures with RAs. In line blending

Moreover, three methods were identified as the common RAs dose determination: user experience, recommendations from the manufacturer, and use of blending charts of blended asphalt binder's properties. User experience is based on the knowledge of the user on a specific type of RA and asphalt mixture design/production. Dosages recommended by the manufacturer require the contractor to provide the manufactures with the properties of the virgin and RAM binders (or sample of the material) to be used in the project. The use of blending charts involve matching the physical (e.g., penetration, softening point, viscosity, etc.) or rheological (e.g., HTPG, LTPG, and ΔT_c , etc.) properties of the recycled binder blend to that of the target binder.

Laboratory studies showed that RAs improve the cracking resistance and moisture susceptibility of the mixtures with minor effects on their rutting resistance. However, some researchers have reported an increase in aging susceptibility when RAs are incorporated. A limited number of field studies showed mixed results in terms of cracking performance with some experimental sections showing better performance than the control sections, while others showed the opposite Field performance of mixtures with RAs is not only a function of dosage and chemical formulation, but also traffic loading, existing pavement condition, and structural thickness of the pavement.

2.10. Knowledge Gaps Identified from Literature

The following gaps were identified from the literature review:

- i. The different categorization/classification systems and the increasing number of products available in the market indicate that a systematic classification of RAs with consideration of their performance properties is needed for users to easily screen different products.

- ii. In the US, the most common method of incorporating RA at the asphalt plant is in line with the virgin binder. Studies are warranted to investigate other approaches which can be employed at the plant and still yield mixtures with satisfactory performance.
- iii. Lack of a performance-based RA determination approach and application of an aging protocol that is representative to field aging, convenient for routine use, and able to distinguish among mixtures.
- iv. Lack of understanding of the quantity of RAM binder that contributes to mixture performance and therefore a need a common methodology to quantify the RAM binder availability. However, this seems difficult as a very RAM behaves differently. Therefore, research should be focused more on establishing the quality (criteria and thresholds) of RAM to be used in mixture production.

While the above-stated knowledge gaps were identified from the literature review conducted for this study. The main objective of this dissertation was to develop a performance-based methodology to incorporate RAs in mixtures using mixture aging protocol which is representative of field aging and convenient for routine use.

3. METHODOLOGY

3.1. Introduction

This chapter describes the overall experimental testing plans that were followed to achieve the objectives of this study. Since each DOTs (Wisconsin and South Dakota) had requirements of how the project should be conducted (for instance, RA dosage method, tests to be performed, etc.,) two different testing plans as shown in Figure 3.1 and Figure 3.2 were employed. The experimental testing plans included a rheological evaluation of all three base (virgin) asphalt binders, recycled asphalt binder blends, and mixtures with and without RAs. Wisconsin materials included: two virgin binders with performance grade (PG) 58S-28 and polymer modified binder (PMB) PG 58V-28, two different virgin aggregate sources, two RAP stockpiles, one RAS source, and two bio-based RAs (Figure 3.1). The South Dakota experimental plan involved one virgin binder (PG 58S-34 PMB), one virgin aggregate source, one RAP source, and four RAs: three bio-based and one petroleum-based (Figure 3.2).

Recycled asphalt binder blends with and without RAs were graded based on the conventional Superpave performance grading (PG) per AASHTO M320-17 and the Multiple Stress Creep Recovery (MSCR) following AASHTO M332-19. In addition, the recycled asphalt binder blends for Wisconsin were evaluated for (1) fatigue resistance using the Linear Amplitude Sweep (LAS) per AASHTO TP101-12, (2) ductility and block cracking potential using the Glover-Rowe (G-R) parameter, and (3) low-temperature rheological properties taking into consideration the hardening process using the extended Bending Beam Rheometer (BBR) test per AASHTO TP122-16. The Fourier-Transform Infrared Spectroscopy using the Attenuated Total Reflectance (FTIR-ATR)

technique was conducted on all asphalt binder blends to assess the evolution of asphalt binder blends chemical structure due to oxidative aging.

Wisconsin mixtures were assessed for rutting resistance and moisture susceptibility using the HWTT whilst South Dakota mixtures were evaluated for rutting resistance using the APA test. Both Wisconsin and South Dakota mixtures were evaluated for intermediate temperature cracking and low temperature cracking resistance using the Indirect Tensile Asphalt Cracking Test (IDEAL-CT) and Disc-shaped Compact Tension (DCT) test, respectively. The dynamic modulus ($|E^*|$) test was conducted only on the Wisconsin mixtures to evaluate their stiffness and aging characteristics. One should note that except for IDEAL-CT tests which were performed on control mixtures and high RAM content mixtures with and without RAs, all the other tests conducted on Wisconsin mixtures were conducted on control and high RAM content mixtures with RAs only. For South Dakota tests were conducted on the control mixtures and high RAM content mixtures with and without RAs

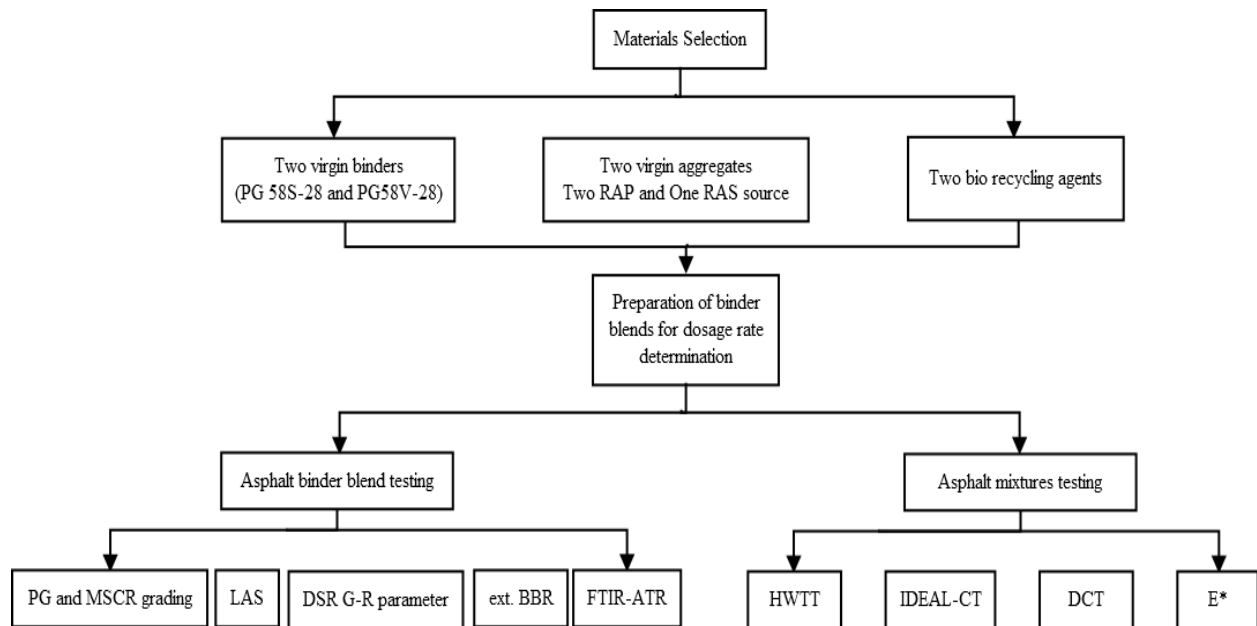


Figure 3.1: Experimental testing plan for Wisconsin material

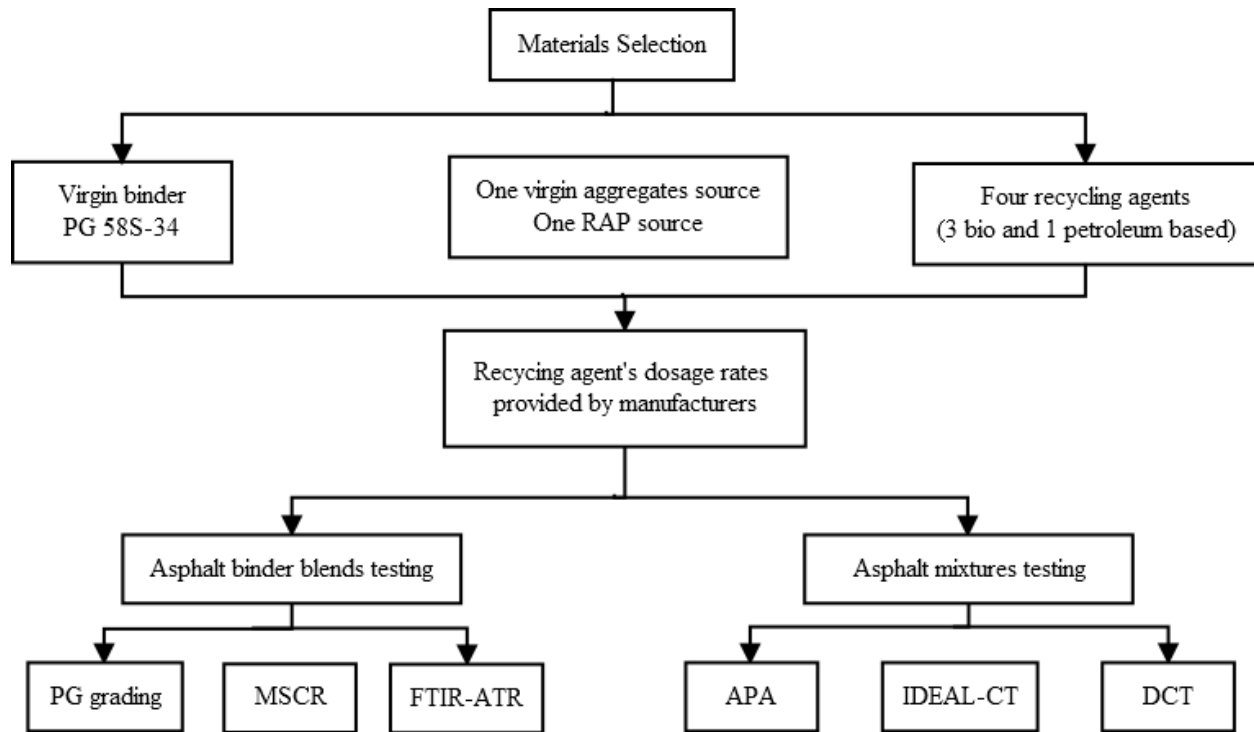


Figure 3.2: Experimental testing plan for South Dakota material

3.2. Material Selection

3.2.1. Base Binders and Recycling Agents

As mentioned previously binder blends and mixtures for Wisconsin were prepared using a virgin asphalt binder (PG 58S-28) and a polymer-modified binder (PMB) (PG 58V-28). For South Dakota, one PMB (PG 58S-34) was included in the evaluation. A total of five different proprietary RAs were evaluated. They are referred to as RA1, RA2, RA3, RA4, and RA5 in this study. RA1 and RA2 were used with the Wisconsin materials. The RAs used with the South Dakota materials were RA1, RA3, RA4, and RA5. Both RA1 and RA3 are obtained from modified vegetable oils. RA2 originates from engineered plant oil, whereas RA4 is obtained from derivatives of fatty acids. RA5 is an asphalt flux; also known as a softener produced from vacuum distillation of petroleum

crude oil. Table 3.1 shows the physical properties of the RAs as extracted from their respective material safety data sheets.

Table 3.1: Physical properties of the RAs

Property	RA1	RA2	RA3	RA4	RA5
Origin	Modified vegetable oil	Plant-engineered oil	Modified vegetable oil	Fatty acids derivatives	Distilled crude oil
Appearance	Black liquid	Yellow liquid	Light reddish-orange liquid	Brown/dark liquid	Black-brown viscous semi-solid
Odor	-	Mild	-	Smokey/Pungent	Tar-like
pH	7.4	-	-	-	-
Flash Point (°C)	>250	>260	>250	>190	>232
Spec. gravity @ 25°C	0.936	0.931	0.980	0.943	0.950-1.130
NFPA* 704 rating	0-1-0	2-1-0	0-1-0	0-1-0	2-1-0

*Stands for National Fire Protection Association

3.2.2. Virgin Aggregates and RAM Materials

Virgin aggregates along with recycled asphalt materials (RAP and RAS) were provided by contractors from each state. For Wisconsin, two different contractors supplied the material: virgin aggregate and RAP from the first contractor will be referred to as Aggregate 1 and those from the second contractor as Aggregate 2. Aggregate 1 and Aggregate 2 used RA1 and RA2, respectively. Along with the aggregate and RAM materials, the contractors provided the initial job mixture formula (JMFs) which were used as baselines to design mixtures with asphalt binder replacement (ABR) ratios specific for this study. The initial mixture design provided by the contractors had 28.0 % RAP by weight of the aggregates for Aggregate: and 10.1% RAP and 3.4 % RAS by weight of the aggregates for Aggregate 2. These proportions correspond to 21.7% ABR for Aggregate 1 while for Aggregate 2 it is 23.1% ABR (8.2% from RAP and 14.9 % from RAS). Moreover, the JMF provided for Aggregate 1 had a 0.20% dose requirement of Evotherm P75 as an antistripping

agent which was not added in asphalt mixtures used for this study so that the effectiveness of RAS could be evaluated without any confounding effects from the antistripping agent. Table 3.2 and Table 3.3 show the particle size distribution and properties of Aggregate 1, whereas Table 3.4 and Table 3.5 are for Aggregate 2. Both asphalt mixtures used the same RAS material.

Table 3.2: Particle size distribution of Aggregate 1 material

Sieve size	5/8" x 3/8"	3/8" Bit	1/8" MS	5/8" Sand	RAP1	RAS
3/4" (19 mm)	100.0	100.0	100.0	100.0	100.0	100.0
1/2" (12.5 mm)	85.0	100.0	100.0	99.0	95.0	100.0
3/8" (9.5 mm)	48.0	100.0	100.0	93.0	87.0	100.0
#4 (4.75 mm)	7.0	76.0	100.0	78.0	68.0	95.7
#8 (2.36 mm)	2.8	50.0	89.0	67.0	54.0	94.3
#16 (1.18 mm)	2.1	35.0	58.0	58.0	44.0	77.2
#30 (0.60 mm)	1.8	25.0	34.0	43.0	35.0	54.6
#50 (0.30 mm)	1.5	18.0	18.0	13.0	19.0	46.8
#100 (0.15 mm)	1.1	12.0	7.0	2.6	10.0	37.9
#200 (0.075 mm)	1.0	7.8	1.9	1.3	6.7	27.8

Table 3.3: Properties of Aggregate 1 material

Property	5/8"x3/8"	3/8" Bit	1/8" MS	5/8" Sand	RAP1	RAS	WisDOT Specs.
Bulk specific gravity	2.732	2.714	2.597	2.667	2.666	2.550	-
Absorption	0.7	0.8	0.6	0.4	0.7	2.0	-
Coarse aggregate angularity (1)	99.3	100	100	58.7	87.8	-	75 min.
Coarse aggregate angularity (2+)	95.4	99.5	100	45.9	81.5	-	60 min.
Fine aggregate angularity	-	48.2	48.2	38.1	41.4	50.3	43 min.
Flat and elongated particles (5:1)	0.7	2.3	-	0.2	0.6	-	5 max.

Table 3.4: Particle size distribution of Aggregate 2 material

Sieve size	5/8" Chip	3/8" Chip	Mfrd. Dry	Mfrd. Wash	Torp. Sand	RAP2
3/4" (19 mm)	100.0	100.0	100.0	100.0	100.0	100.0
1/2" (12.5 mm)	84.3	100.0	100.0	100.0	100.0	100.0
3/8" (9.5 mm)	20.1	83.9	100.0	100.0	100.0	93.3
#4 (4.75 mm)	2.5	2.8	100.0	100.0	97.5	76.4
#8 (2.36 mm)	2.0	1.8	79.2	85.1	82.0	58.7
#16 (1.18 mm)	1.9	1.7	41.6	44.7	67.1	41.2
#30 (0.60 mm)	1.8	1.6	21.8	23.2	48.0	33.5
#50 (0.30 mm)	1.8	1.6	8.5	11.6	17.2	20.9
#100 (0.15 mm)	1.8	1.6	6.4	6.8	5.7	14.4
#200 (0.075 mm)	1.6	1.5	3.8	5.0	3.0	10.8

Table 3.5: Properties of Aggregate 2 material

Property	5/8" Chip	3/8" Chip	Mfrd Dry	Mfrd Wash	Torp Sand	RAP2	WisDOT Specs.
Bulk specific gravity	2.675	2.744	2.708	2.701	2.678	2.681	-
Absorption	2.0	1.0	1.9	2.0	1.0	1.3	-
Coarse aggregate angularity (1)	100	100	-	-	-	97.3	75 min.
Coarse aggregate angularity (2+)	98	97.9	-	-	-	94.7	60 min.
Fine aggregate angularity	-	-	48.1	47	41.5	43.6	43 min.
Flat and elongated particles (5:1)	1.8	2.1	-	-	-	-	5 max.

South Dakota's virgin aggregates were supplied by a contractor from South Dakota, and the RAP was provided by the South Dakota DOT. Table 3.6 presents the particle size distribution of the aggregates along with their physical properties (Table 3.7) as extracted from the baseline JMF that was provided by the contractor. The RAP gradation was conducted at NCAT. However, one should note that the JMF from the contractor did not contain RAP; therefore, asphalt mixtures were redesigned to attain desired ABRs ratio for this study.

Table 3.6: Particle size distribution of South Dakota material

Sieve size	3/4"x5/8"	5/8"x3/8"	3/8" minus	#4x#20	Man. Sand	RAP
3/4" (19.0 mm)	100.0	100.0	100.0	100.0	100.0	100.0
5/8" (16.0 mm)	91.0	100.0	100.0	100.0	100.0	99.0
1/2" (12.5 mm)	42.0	95.0	100.0	100.0	100.0	96.0
3/8" (9.5 mm)	9.0	70.0	100.0	100.0	100.0	90.0
#4 (4.75 mm)	4.2	10.0	75.0	99.0	100.0	73.0
#8 (2.36 mm)	4.0	7.8	54.0	28.0	97.0	58.0
#16 (1.18 mm)	3.9	7.3	39.0	4.0	73.0	45.0
#40 (0.420 mm)	3.8	6.9	27.0	1.4	45.0	31.0
#200 (0.075 mm)	1.8	3.0	8.8	0.3	5.0	9.0

Table 3.7: Properties of South Dakota aggregates

Property	3/4"x5/8"	5/8"x3/8"	3/8" minus	#4x#20	Man. Sand
Flat and elongation (3:1)	31	42	27	-	-
Flat and elongation (5:1)	5	10	8	-	-
Sand Equivalency	-	-	76	100	86
Fine aggregate angularity	-	-	48	48	48

3.3. Preparation of Recycled Asphalt Binder Blends

Preparation of the recycled binder blends started with extraction and recovery of the aged asphalt binders from RAM (RAP and RAS) per AASHTO T164-14 and ASTM D5404-12, respectively. The solvent used for the extraction of the aged asphalt binders from RAM was trichloroethylene. Both virgin and recovered asphalt binders were preheated at 150 °C for two hours, then mixed at the required proportions, and blended using a low shear mixer (200 rpm) for 15 minutes. Recycled asphalt binder blends were sampled at this point and stored for further testing. To prepare rejuvenated binder blends RAs were added to the binder blends and blended for an extra 15 minutes, then sampled for further testing. (Figure 3.3). Tables 3.8 and 3.9 show a matrix of combinations of the asphalt binder blends prepared for this study.



Figure 3.3: Preparation of recycled binder blends (a) Addition of RAs (b) checking temperature

Table 3.8: Wisconsin's asphalt binder blends combinations

Material/Blending Ratios	Factor	Description
Virgin binder	2	PG 58S-28 and PG58V-28 PMB
RAM aged binder	3	RAP ₁ , RAP ₂ , and RAS
Blending ratio Virgin binder/aged RAM binder and Virgin binder/aged RAM binder/RA	15	PG 58S-28+20% RAP1 or RAP2 PG 58S-28 + 25% RAS PG 58S-28+30% RAP1 or RAP2+5% RAS PG 58S-28+40% RAP1 or RAP2 PG 58V-28 +20% RAP1 PG 58S-28+25% RAS+RA1 or RA2 PG 58S-28+30% RAP1 or RAP2+5% RAS +RA1 or RA2 PG 58S-28+40% RAP1 or RAP2+RA1 or RA2 PG 58V-28+40% RAP1+RA1

Table 3.9: South Dakota’s asphalt binder blends combination

Material/Blending Ratios	Factor	Description
Virgin binder	1	PG 58S-34 with polymer modification
RAM aged binder	1	One RAP source
Blending ratio Virgin binder/aged RAM binder and Virgin binder/aged RAM binder/RA	10	PG 58S-34+20% RAP PG 58S-34+35% RAP PG 58S-34+50% RAP PG 58S-34+35% ABR+RA (either RA1, RA3, RA4, or RA5) PG 58S-34+50% ABR+RA (either RA1, RA3, or RA4)

3.4. Asphalt Binder Testing

Table 3.10 presents detailed information about the asphalt binder testing conducted on the base (virgin) binders and both recycled binder blends and rejuvenated recycled binder blends. The performance of the asphalt binders was evaluated against rutting resistance, intermediate temperature cracking resistance, low temperature cracking resistance, and growth of oxidative aging products. Asphalt binders were conditioned in the Rolling Thin-Film Oven (RTFO) and Pressure Aging Vessel (PAV) per AASHTO T240 and AAHTO R28, respectively to simulate short and long-term aging of the binders. All RTFO samples were conditioned at 163 °C for 85 minutes. PAV samples were conditioned after RTFO at a temperature of 100 °C for 40 hours and 60 hours for Wisconsin and South Dakota samples, respectively to assess the effect of extended PAV aging. The subsequent sub-sections summarize the binder performance tests.

Table 3.10: Asphalt binders performance properties and parameters

Performance Property	Test	Protocol	Testing		Parameter
			Aging level	Conditions	
Rutting resistance	DSR	AASHTO T320	Unaged and RTFO	@ High PG temp.	$ G^* /\sin \delta$
		AASHTO M332	RTFO	@ High PG temp	$J_{nr3.2}$ and %R
Intermediate temperature cracking resistance	DSR	AASHTO T320	40-or 60 hours PAV	@ Interm. PG temp.	$ G^* /\sin \delta$
	LAS	*AASHTO T391	40 hours PAV	@ Interm. PG temp.	# of cycles to failure (N_f)
	DSR master curve	AASHTO T315	Unaged and 40-or 60 hours PAV	Frequency sweep (0.1-30 Hz) @ temp range of 10-70 °C	G-R
Low temperature cracking resistance	BBR	AASHTO T313	40- or 60-hours PAV	@ Low PG temp.	Stiffness and m-values, and ΔT_c
		*AASHTO TP 122-16	40 hours PAV	24 hours at binder T_g temp.	
Products of oxidative aging	FTIR-ATR	N/A	Unaged and 40- or 60-hours PAV	Scan range of 4000-650 cm^{-1} @ resolution of 4 cm^{-1}	Carbonyl and sulfoxide areas

Note: * indicates tests conducted only on Wisconsin asphalt binder blends

3.4.1. Performance Grading and ΔT_c Parameter

The DSR was used to characterize the rheological characteristics of the asphalt binder blends by measuring the complex modulus (G^*) and phase angle (δ) at specific temperatures and frequencies per AASHTO T315. ASTM D7643 was followed to determine the continuous performance grade of the asphalt binder blends, then graded per AASHTO M320 and M332, respectively. Furthermore, the ΔT_c parameter was computed from the BBR results of 40-hours and 60-hours PAV aged residues. The ΔT_c is a numerical difference between the stiffness criterion at 300 MPa and the m-value criterion at 0.300. The parameter is used to assess the loss of relaxation properties in the asphalt binders. For asphalt binders with better ductility and block cracking resistance a higher (less negative) ΔT_c is desirable.

3.4.2. Multiple Stress Creep Recovery (MSCR) Test

The MSCR was conducted per AASHTO T350 and M332 to characterize and grade elastic responses and rutting resistance of asphalt binder blends. The test was performed using the DSR's 25 mm parallel plate geometry with a 1 mm gap at 64 °C and 58 °C on Wisconsin and South Dakota RTFO aged binder blends, respectively. Ten loading cycles were applied at low-stress level (0.1 kPa) and high-stress level (3.2 kPa). Each stress level consisted of 1 sec of creep and 9 sec of recovery. The strain responses were utilized to calculate the non-recoverable creep compliance (J_{nr}) at 3.2 kPa, percent recovery (%R), and percent difference in nonrecoverable creep compliance between the 0.1 kPa and 3.2 kPa stress level. Lower J_{nr} and higher %R values indicate better rutting resistance and elastic characteristics in the binder.

3.4.3. G-R parameter

To compute the G-R parameter, a frequency sweep test was performed using the DSR at multiple test temperatures and frequency ranges of 0.1 to 10 rad/sec. During testing, the maximum strain was controlled at one percent to endure the behavior of the asphalt binder blends remained in the linear viscoelastic range. The G-R parameter was computed from Equation 3.1 using the $|G^*|$ and δ at 15 °C and 0.005 rad/sec. The G-R parameter considers both stiffness and embrittlement and it is useful in indicating the ductility and cracking potential of asphalt binders. The G-R parameter damage zone of 180 kPa and 600 kPa were proposed for unmodified asphalt binder and they indicate the onset block cracking and significant cracking, respectively (Glover et al., 2005; Rowe, 2011). Moreover, the aging index in terms of the G-R parameter was evaluated to assess the effect of RAs on the aging resistance of the recycled binder blends. The aging index was calculated as a

ratio of the G-R value of the recycled binder blend after RTFO plus 40 or 60 PAV conditioning to the G-R value of the same recycled binder blend at unaged conditions.

$$G - R = \frac{|G^*|(\cos\delta)^2}{\sin\delta} \text{ at } 15 \text{ }^\circ\text{C and } 0.005 \text{ rad/sec} \quad \text{Equation 3.1}$$

3.4.4. Linear Amplitude Sweep (LAS) Test

The LAS test was conducted per AASHTO T391 to evaluate the fatigue resistance of the asphalt binder blends. The test was conducted at the intermediate PG temperature on 40 hours PAV aged asphalt binder residues. The asphalt binder blends were first tested to determine the undamaged linear viscoelastic properties by applying small strains of 0.1% (frequency sweep test), then the strain amplitude was increased (up to 30% applied strain) at 10 Hz loading frequency to cause accelerated fatigue damage (amplitude sweep test). The viscoelastic continuum damage theory is used resulting in the fatigue power-law damage model. The test relates the fatigue parameter (N_f) normalized to 1 million ESALs and the applied shear strain as a pavement structure indicator. A higher N_f is desirable for asphalt binder blends with better fatigue resistance.

3.4.5. Extended Bending Beam Rheometer (BBR) Test

The extended BBR test was conducted to characterize the low-temperature rheological properties of the asphalt binder blends while taking into consideration the physical hardening process per AASHTO TP 122-16. For this study, the asphalt binder blends were conditioned at the glass transition temperature (T_g) for 1 hour and 24 hours, before running the BBR. The T_g of the recycled binder blends was obtained using the Differential Scanning Calorimetry (DSC) after RTFO plus 40 hours PAV aging. The stiffness value and m value were used to assess the performance of the binder blends.

3.4.6. Oxidative Aging Products

The products of oxidation aging in asphalt binder blends (i.e., carbonyl and sulfoxide functional groups) were assessed using the Fourier-Transform Infrared Spectroscopy with the application of the Attenuated Total Reflectance (FTIR-ATR) technique. To conduct the tests, the crystal area was cleaned, and the background was collected. Samples were heated at 150 °C and 175 °C for RTFO and PAV aged samples, respectively for 5 minutes or until the sample reached a workable viscosity, without exceeding 10 minutes of preheating. The workable sample was then placed onto the crystal area and the pressure arm was released to enable adequate contact between the sample and the crystal. The sample was scanned after making sure that the contact exists. For this study, 64 scans were attained at the region of 4000-650 cm^{-1} with a resolution of 4 cm^{-1} . To quantify the growth of oxidation products in the asphalt binder blends both carbonyl and sulfoxide areas were computed. The carbonyl area was calculated by integrating the area of the spectrum between the wavenumbers of 1660 and 1753 cm^{-1} , using the magnitude of the absorption at 1753 cm^{-1} as the baseline. The sulfoxide area was calculated by integrating the area of the spectrum between the wavenumbers of 995 and 1047 cm^{-1} , the magnitude of the absorption at 1047 cm^{-1} was used as a baseline.

3.5. Determination of Optimum RA Dosage for Asphalt Mixtures

The optimum RAs' dosages for the Wisconsin mixtures were determined using blending charts of the recycled asphalt binder blends (RAM binder + virgin binder). To determine the optimum dosage, extracted and recovered binders from RAM were blended with the base binder at the desired proportions to prepare the recycled binder blends. Weighed portions of the recycled binder blends were dosed with 5% of RAs by weight of the total binder. Then, both recycled binder blends

(with and without RAs) were RTFO plus 40 hours PAV conditioned. The DSR and BBR tests were conducted on unaged/ RTFO and RTFO plus 40 hours PAV aged samples to determine the true HTPG and LTPG of the samples, respectively. Several researchers have established that the continuous HTPG and LTPG of the recycled asphalt binder blends and the percentage of ABR in the blends have a linear relationship (Arámbula-Mercado et al., 2018; Tran et al., 2012; Zaumanis et al., 2014a). Therefore, linear interpolation of the true HTPG and LTPG of the recycled binder blends without RA and that with RAs (dosed at 5% by weight of total binder) was utilized to determine the optimum RA dosage. Figure 3.4 and Figure 3.5 are presented as examples for RA dosage determination using RA1 for the 25% ABR blend and targeting the LTPG of the virgin binder. In addition to targeting the LTPG of the base binders, the dosages of RAs targeting their HTPG (58 °C for the PG 58S-28 binder and 64 °C for the PG 58V-28), and the dosage of RAs targeting the true HTPG and LTPG of the 20% ABR blend (control) were determined. This was important to understand how dosages varied depending on the selected target. As presented in Table 3.11, the dosages determined to match the HTPG resulted in the highest RA dosage among the three approaches. Although this approach was recommended in NCHRP 9-58, the researchers warned of a potential increase in moisture susceptibility of asphalt mixtures when this approach is used. NCHRP Project 09-58 also reported that targeting the LTPG of the 20% ABR control blend was insufficient to yield acceptable cracking resistance of the resultant mixture. Targeting the HTPG of the 20% ABR blend, and the LTPG of the base binder yielded RA dosages between the other two approaches. From these two approaches that yielded mid-range dosages. Targeting the LTPG of the base binder was selected as the optimum dosage that was used for the performance evaluation of Wisconsin mixtures since it was in general the more conservative of the two approaches.

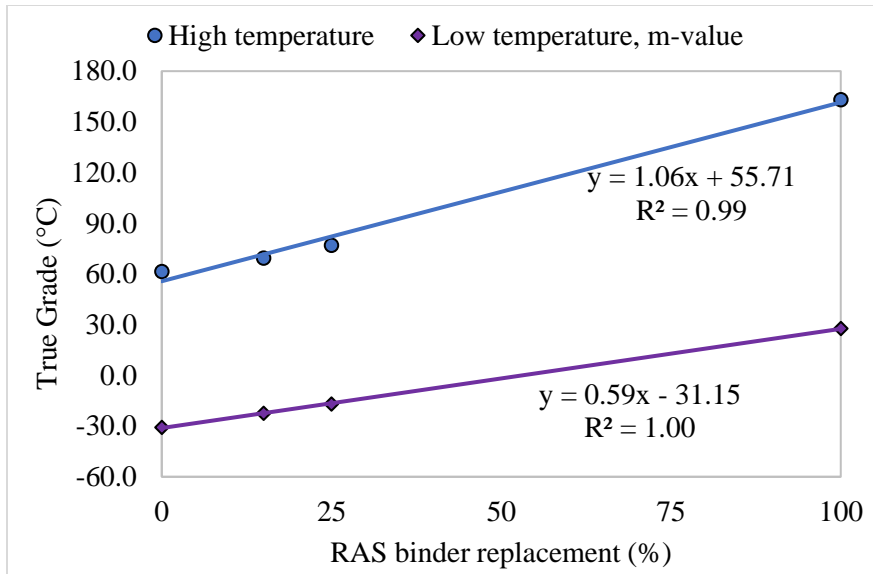


Figure 3.4: Effect of RAS binder increase on true grade

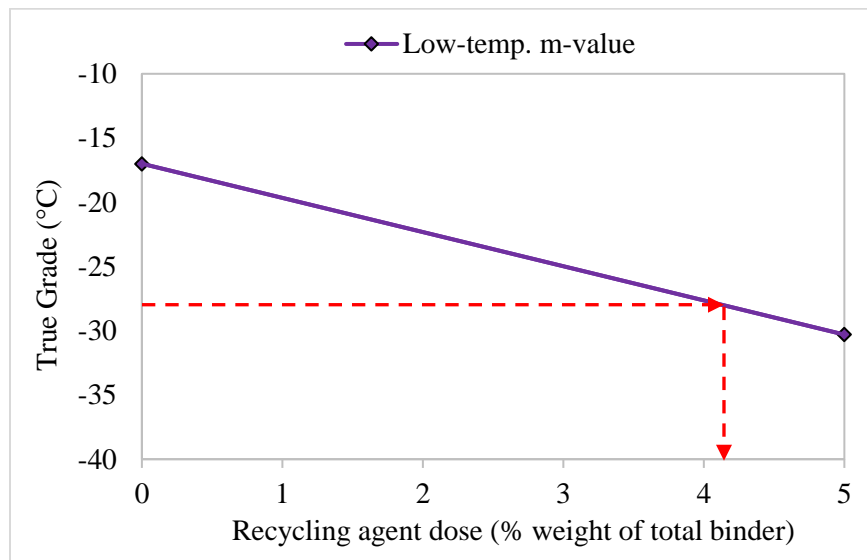


Figure 3.5: Example of RA dosage determination

Table 3.11: Recycling agents' dosage for Wisconsin Mixtures

Base Binder	Recycled Binder Blend	Recycling Agent	Target 20% ABR blend True Grade		Target PG of Base Binders	
			HT	LT	HT	LT
PG 58S-28	25% ABR	RA ₁	7.1	3.3	11.0	4.1
		RA ₂	6.3	4.0	9.8	5.0
	35% ABR	RA ₁	3.5	0.8	11.4	2.1
		RA ₂	2.9	0.9	9.6	2.5
	40 % ABR	RA ₁	3.3	1.3	8.0	2.4
		RA ₂	2.8	1.5	6.9	2.8
PG 58V-28	40% ABR	RA ₁	1.3	1.8	8.4	3.0

As mentioned previously, the RAs' dosages for South Dakota mixtures were provided by the manufacturers except that of RA5 (asphalt flux) which was determined at NCAT. The recycling agent's dosages provided by the manufacturers ranged from 1.8 to 4.0%; with the 35% ABR blend having the lowest and the 50% ABR blend the highest (Table 3.12). The manufacturers were asked to target the true LTPG of the control blend (i.e., 20% ABR blend) after RTFO plus 60 hours of PAV conditioning at 100 °C. The final dosages provided by the suppliers are presented in Table 3.12.

Table 3.12: Recycling agents' dosages for South Dakota mixtures

Recycled Binder Blend	RA Type	RA dosages by Weight of the Total Binder
35% ABR	RA1	1.8
	RA3	2.8
	RA4	2.1
	RA5	45
50% ABR	RA1	3.1
	RA3	4.0
	RA4	3.8

3.6. Design of Asphalt Mixtures

All asphalt mixtures for this project were designed following the Superpave volumetric mixture design (AASHTO R35) to meet either the 2020 Wisconsin DOT Specifications for Highway and Structures Construction Manual or the 2015 South Dakota DOT Standard Specifications for Roads and Bridges Manual. The Wisconsin asphalt mixtures were designed to meet the requirements of medium traffic, which is one to eight million equivalent standard axle loads (ESALs) whereas South Dakota mixtures met class Q2 traffic (maximum daily truck traffic count of less than 249 trucks per day) requirements. All asphalt mixtures had a nominal maximum aggregate size (NMAS) of 12.5 mm. Table 3.13 shows the specifications of 12.5 mm-NMAS mixtures for medium traffic and class Q2 traffic requirements for Wisconsin DOT and South Dakota DOT, respectively.

Table 3.13: Specifications requirements for 12.5 mm-NMAS mixtures for both Wisconsin and South Dakota DOTs

Criteria	WisDOT Specs	SDDOT Specs
Ndesign gyrations	75	50
Air voids content (Va), %	4.0	4.0
Voids in mineral aggregates (VMA), %	>14.5	>14.5
Voids filled with asphalt (VFA), %	70-76	65-80
Dust to binder (D/B) ratio	0.6-1.2	0.6-1.4

A total of eight asphalt mixtures were designed with the Wisconsin aggregates and RAM using the unmodified binder (PG 58S-28) (four asphalt mixtures per aggregate type) and two mixtures with the PG 58V-28 using Aggregate 1 materials (Table 3.14). For South Dakota, 10 different mixtures were prepared as shown in Table 3.15. Mixtures with 20% ABR were selected as the control mixtures for both Wisconsin and South Dakota mixtures since 20% ABR (from RAP only) is currently a typical RAM content in new mixture designs. In addition, 20% ABR (from RAP only) is currently the percentage allowed in South Dakota asphalt mixtures.

High RAMs combinations for Wisconsin materials included 25% ABR, 35% ABR, and 40% ABR with the PG 58S-28 binder as these are the current maximum allowable binder replacement in asphalt mixtures as indicated in Table 3.14. For the 25% ABR, the recycled binder came from RAS only while the 35% ABR mixtures had 30% from the RAP and 5% from RAS. With PG 58V-28, only 20% ABR (control) and 40% ABR mixtures were prepared using Aggregate 1 materials and recycling agent RA1. The PG 58V-28 mixtures used the same aggregate blends as the PG 58S-28 binder. As mentioned in the previous section, the RAs' dosage by weight of total asphalt binder shown in Table 3.17 were obtained by targeting the LTPG of -28°C after 40 hours of PAV aging to satisfy both climate and traffic conditions in Wisconsin.

For South Dakota, high RAM content mixtures were 35% ABR and 50% ABR and they were specifically selected by the South Dakota DOT. As mentioned previously these mixtures used a PG 58S-34 and one RAP source. Rejuvenated 35% ABR mixtures incorporated either RA1, RA3, RA4, or RA5 whereas rejuvenated 50% ABR mixtures used either RA1, RA3, or RA4. As presented in the previous section, the dosages of the bio-based RAs were selected based on the recommendation of the respective RA manufacturer to target the LTPG of the 20% ABR binder blend, as requested by South Dakota DOT. The manufacturer was provided with a virgin binder and extracted RAP binder PG characterization results conducted at NCAT. The final dosage rates recommended by the suppliers ranged from 1.8 to 4.0%, with higher dosages for the 50% ABR mixtures. The flux dosage of the 35% ABR mixture was optimized at NCAT to match the low PG grade of the 20% ABR binder blend after 60 hours of PAV aging. Although this dosage rate is not practically feasible, it was included in the evaluation to assess the performance of the mixture. Only the 35% ABR mixture was evaluated with the asphalt flux since the dosage rate required for the 35% ABR mixture was extremely high and closer to the maximum limit allowable.

Table 3.14: Wisconsin's asphalt mixtures combinations

Base Binder	Asphalt Binder Replacement	Combinations
PG 58S-28	20 % ABR	Aggregate 1 + PG 58S-28 + RAP ₁
		Aggregate 2 + PG 58S-28 + RAP ₂
	25% ABR	Aggregate 1 + PG 58S-28 + RAS + RA ₁
		Aggregate 2 + PG 58S-28 + RAS + RA ₂
	35% ABR	Aggregate 1 + PG 58S-28 + RAP ₁ + RAS + RA ₁
		Aggregate 2 + PG 58S-28 + RAP ₂ + RAS + RA ₂
40 % ABR	Aggregate 1 + PG 58S-28 + RAP ₁ + RA ₁	
	Aggregate 2 + PG 58S-28 + RAP ₂ + RA ₂	
PG 58V-28	20% ABR	Aggregate 1 + PG 58V-28 + RAP ₁
	40% ABR	Aggregate 2 + PG 58V-28 + RAP ₂ + RA ₂

Table 3.15: South Dakota's asphalt mixtures combinations

Asphalt Binder Replacement	Combinations
20% ABR	Aggregates + RAP + PG 58S-34 PMB
35% ABR	Aggregates + RAP + PG 58S-34 PMB + No RA
	Aggregates + RAP + PG 58S-34 PMB + RA ₁
	Aggregates + RAP + PG 58S-34 PMB + RA ₃
	Aggregates + RAP + PG 58S-34 PMB + RA ₄
	Aggregates + RAP + PG 58S-34 PMB + RA ₅
50 % ABR	Aggregates + RAP + PG 58S-34 PMB + No RA
	Aggregates + RAP + PG 58S-34 PMB + RA ₁
	Aggregates + RAP + PG 58S-34 PMB + RA ₃
	Aggregates + RAP + PG 58S-34 PMB + RA ₄

Table 3.16: Maximum allowable percent asphalt binder replacement (WisDOT, 2021)

RAM	Lower layers	Upper layers
RAP and FRAP in any combination	40	25
RAS alone	25	20
RAP, FRAP, and RAS combination	35	25

Table 3.17: Recycling agent dosages for Wisconsin mixtures

Base Binder	Asphalt Binder Replacement	Recycling Agent	Dosage by Weight of Total Binder (%)
PG 58S-28	25% ABR	RA ₁	4.1
		RA ₂	5.0
	35% ABR	RA ₁	2.1
		RA ₂	2.5
	40% ABR	RA ₁	2.4
		RA ₂	2.8
PG 58V-28	40% ABR	RA ₁	3.0

Table 3.18 and Table 3.19 show the cold feed percentages for Wisconsin aggregate blends. To control the amount of fines in the mixtures aggregates stockpile 5/8" x 3/8" (from Aggregate 1 source) was fractionated on a 3/8" sieve. During batching, the appropriate proportions in the blends were weighed separately and combined. All Wisconsin's RAP materials were fractionated on a #4 sieve. For all Aggregate 1 blends and Aggregate 2 control (20% ABR), the respective fractions were weighed separately at the appropriate proportions and combined during batching. For Aggregate 2 blends (35% ABR and 40% ABR) only one fraction of the RAP was used. The 35% ABR blend used the coarse fraction (+#4 sieve RAP only) and the 40% ABR used the fine fraction (-#4 sieve RAP only). This was necessary to meet some of the volumetrics criteria as will be discussed later in this section. The cold feed percentages of South Dakota's blends are presented in Table 3.20. For the South Dakota blends, RAP was fractionated on a #8 sieve, the two fractions were weighted at appropriate proportions and combined during batching.

Table 3.18: Wisconsin's Aggregate 1 blends

Aggregate I Blend	5/8" x 3/8"	3/8" Bit	1/8" MS	5/8" Sand	RAP1	RAS
20% ABR	20.0%	16.0%	17.0%	22.0%	25.0%	-
25% ABR	27.0%	27.0%	10.0%	30.0%	-	6.0%
35% ABR	20.0%	10.8%	17.0%	14.0%	37.0%	1.2%
40% ABR	18.0%	7.0%	18.0%	7.0%	50.0%	-

Table 3.19: Wisconsin's Aggregate 2 blends

Aggregate 2 Blend	5/8" Chip	3/8" Chip	Mfrd Dry	Mfrd Wash	Torp Sand	Dust	RAP2	RAS
20% ABR	7.0%	20.0%	-	32.0%	16.0%	-	25.0%	-
25% ABR	7.5%	28.0%	29.0%	-	28.0%	1.0%	-	6.5%
35% ABR	10.0%	-	27.0%	-	22.0%	-	39.5%	1.5%
40% ABR	10.0%	20.0%	-	23.0%	14.0%	-	33.0%	-

Table 3.20: South Dakota's aggregate blends

Aggregate Blend	3/4"x5/8"	5/8"x3/8"	3/8" minus	#4x#20	Man. Sand	RAP
20% ABR	10.0%	15.0%	11.0%	20.0%	24.0%	20.0%
35% ABR	9.0%	15.0%	-	11.0%	31.0%	34.0%
50% ABR	9.0%	11.0%	-	11.0%	27.0%	42.0%

It is worth noting that, Wisconsin DOT specifies the total binder contents for HMAs to be determined at the regressed air void contents of 3%. With this procedure, a typical Superpave volumetrics mixture design is followed, and all volumetrics should be met at a target air void content of 4%. Then, the total binder content of the mixture at 3% air void contents is determined. Both optimum and total binder contents at 4% and 3% air void contents, respectively must be reported on the final JMF. Studies have shown that the regressed air void contents approach increases the total binder content of the mixture by 0.3% to 0.4%, hence increasing the effective asphalt binder content by approximately 1% (Tran et al., 2019a; West et al., 2018a).

The JMFs of the Wisconsin asphalt mixtures used in this study are depicted in Table 3.21 and Table 3.22. The ABRs of Wisconsin's mixtures were within the $\pm 2.5\%$ thresholds set for this part of the study. All but two asphalt mixtures met all the 2020 Wisconsin DOT requirements for a 12.5 mm-NMAS mixture and medium traffic. These mixtures were the 35% ABR and 40% ABR with Aggregate 2 material, and they did not meet the D/B ratio requirement of 0.6-1.2. Moreover, as stated previously, these mixtures used fractioned RAP2; mixture 35% ABR used + #4 RAP2 whereas the 40% ABR mixture used - #4 RAP2. The binder content of the RAP2 fractions as determined using the ignition oven were 4.53% and 6.99% for the + #4 RAP2 and - #4RAP2, respectively. Furthermore, the mixture designs were developed using aggregate stockpiles originally selected for mixtures with lower ABR provided by Wisconsin contractors. As the ABR increases the amount of fines increases, causing the D/B ratio to increase. Several blends were tested, but it was not possible to meet the D/B with the stockpiles available without sacrificing other requirements such as VMA. The trial mixtures closer to meeting the D/B ratio and all the other volumetric requirements were selected for further testing and evaluation. Although the original mixture design provided by the contractor using Aggregate 1 included Evotherm P75 as an anti-strip agent, it was decided to exclude the anti-strip agent, as it could potentially alter the effect of the RAs in the mixtures.

Table 3.21: Wisconsin's JMF for Aggregate 1 mixtures

Mixture Type	20%ABR	25%ABR	35%ABR	40%ABR
% Passing Sieve Size				
3/4"	100.0	100.0	100.0	100.0
1/2"	95.5	95.7	95.0	94.7
3/8"	84.8	83.9	83.8	83.7
#4	64.7	61.5	63.8	64.0
#8	51.9	48.9	51.6	51.7
#16	39.6	37.8	39.4	39.3
#30	28.4	26.8	28.5	28.7
#50	13.9	13.8	14.7	15.2
#100	6.4	7.3	7.2	7.5
#200	3.7	4.6	4.4	4.5
Mix Design Information				
N _{design} , gyrations	75	75	75	75
NMAS (mm)	12.5	12.5	12.5	12.5
Optimum AC% @ 4% Va	5.5	5.5	5.3	5.1
% VMA @ 4% Va	15.3	15.6	15.0	14.7
% VFA @ 4% Va	74.1	74.5	73.5	73.0
D/B Ratio @ 4% Va	0.67	0.83	0.84	0.90
% VMA @ 3% Va	15.3	15.2	14.9	14.6
Regressed AC% @ 3% Va	5.9	5.7	5.6	5.4
% Vbe @ 3% Va	12.3	12.2	11.9	11.6
%ABR Information @ 3% Va				
% RAP Content (by weight of aggregates)	25	-	37	50
% RAS Content (by weight of aggregates)	-	6	1.2	-
% ABR from RAP	19.1	-	29.7	41.7
% ABR from RAS	-	26.2	5.3	-
% Total ABR	19.1	26.2	35.0	41.7

Table 3.22: Wisconsin's JMF for Aggregate 2 mixtures

Mixture Type	20%ABR	25%ABR	35%ABR	40%ABR
% Passing Sieve Size				
3/4"	100.0	100.0	100.0	100.0
1/2"	98.9	98.8	98.0	98.4
3/8"	89.5	89.5	88.4	88.8
#4	67.4	64.5	68.6	70.1
#8	55.5	53.7	54.2	54.9
#16	35.8	37.5	37.6	36.6
#30	23.9	24.9	25.4	24.4
#50	12.1	11.9	12.6	13.3
#100	7.1	7.5	8.1	8.4
#200	5.2	5.3	5.7	6.3
Mix Design Information				
N _{design} , gyrations	75	75	75	75
NMAS (mm)	12.5	12.5	12.5	12.5
Optimum AC% @ 4% Va	5.8	6.2	5.8	5.8
% VMA @ 4% Va	15.4	15.6	14.8	14.7
% VFA @ 4% Va	74.1	74.7	73.0	72.7
D/B Ratio @ 4% Va	1.08	1.07	1.28	1.41
% VMA @ 3% Va	15.5	15.4	14.5	14.6
Regressed AC% @ 3% Va	6.1	6.5	6.1	6.1
% Vbe @ 3% Va	12.5	12.4	11.5	11.6
%ABR Information @ 3% Va				
% RAP Content (by weight of aggregates)	25	-	39.5	33
% RAS Content (by weight of aggregates)	-	6.5	1.5	-
% ABR from RAP	19.3	-	29.3	37.8
% ABR from RAS	-	24.9	6.1	-
% Total ABR	19.3	24.9	35.4	37.8

Table 3.23 shows the JMF of the asphalt mixtures developed with the South Dakota materials. Different from Wisconsin DOT on 3% air void content requirement, South Dakota DOT follows the typical Superpave procedure, and the total asphalt binder content is determined at 4% air void contents. Only the control mixture (20% ABR) met the South Dakota DOT specifications for Q2

traffic. Both the 35% ABR and 50% ABR mixtures failed the VMA criteria of 14.5% by 0.1% and 0.5%, respectively. As mentioned previously, these mixtures were redesigned from a baseline JMF provided by the contractor that did not contain RAP. Several blends were tried, but it was not possible to meet the VMA criteria with the materials provided and still keep the gradations within the primary control points of a 12.5-mm NMAS mix. The trial mixtures closer to meeting the VMA criteria and all the other volumetric requirements were selected for further testing.

Table 3.23: South Dakota’s JMFs

Mixture type	20% ABR	35% ABR	50% ABR
% Passing sieve size			
3/4"	100.0	100.0	100.0
5/8"	98.9	98.9	98.8
1/2"	92.7	92.7	92.6
3/8"	84.4	83.9	84.3
#4	68.6	68.6	70.0
#8	48.0	54.4	54.8
#16	33.1	39.8	40.2
#40	21.7	26.0	26.4
#200	4.7		5.7
Mix Design Information			
N _{design} , gyrations	50	50	50
NMAS (mm)	12.5	12.5	12.5
Optimum AC @ 4% V _a	5.7	5.4	5.2
Virgin AC (%)	4.60	3.53	2.89
% VMA @ 4% V _a	15.5	14.4	14.0
% VFA @ 4% V _a	74.1	72.6	71.4
D/B ratio @ 4% V _a	0.92	1.15	1.31
% V _{be}	11.5	10.4	10.0
%ABR Information			
% RAP Content (by weight of aggregates)	20.0	34.0	42.0
% ABR	19.3	34.6	44.4

3.7. Asphalt Mixtures Mixing Procedure

Before mixing, all three asphalt binders were preheated in an oven for three to four hours. Asphalt binders PG 58S-28 and PG 58S-34 PMB were preheated at 152 °C; the PG 58V-28 was preheated in the oven at 163 °C. The RAPs were preheated at 135 °C for at least an hour and a half but not more than three hours whilst RAS was added without any preheating for asphalt mixtures that incorporated it. The virgin aggregates were preheated overnight at 177 °C for all DOT control mixtures (i.e., 20% ABRs), whereas for high RAM content mixtures they were preheated overnight at 188 °C.

For all asphalt mixtures with RAs, a low-speed shear mixer (200 rpm) was used to blend the RAs with the base binders for 30 ±5 minutes before mixing with the aggregates and RAM. The RAs were added to the mixture as a replacement of the base binders. During mixing preheated virgin aggregates were added in the bucket followed by preheated RAP/or cold RAS, they were thoroughly mixed for at most two minutes before adding a heated asphalt binder. The blends were moved to the rotary mixer and mixed until all the aggregates were coated with asphalt. For asphalt mixtures that used RAP and RAS together, RAS was added to the hot aggregates first followed by the preheated RAP. During the mixing process, the temperature was checked to make sure that the mixtures had the desired mixing temperature of 152 °C and 163 °C or if any adjustments were necessary. After the mixing process was complete, the mixtures were poured into pans to uniform thickness of about 1” to 2” depending on the size of the sample it was spread for short term oven aging (STOA).

3.8. Short and Long-Term Aging of Asphalt Mixtures

AASHTO R30 section 7.1 (*Mixture conditioning for Volumetric Mixture Design*) was followed for mixture design and volumetric computations. After the mixing process was complete, the loose mixtures were placed in pans at an even thickness of 1” to 2” and stirred every hour for two hours. Wisconsin asphalt mixtures prepared for volumetrics design purposes were conditioned at 138 °C, whereas South Dakota mixtures were conditioned at 135 °C. Specimens for bulk specific gravity (G_{mb}) were compacted at these temperatures as well; whereas samples for theoretical maximum specific gravity (G_{mm}) were reduced into two testing sizes using the mechanical splitter per AASHTO R47-19 and were spread on sheet pans which measures 17” long x 25” wide x 1” deep each. The G_{mm} samples were left to cool at room temperature at the same time spatulas were used to separate aggregate particles from bonding taking care not to fracture them.

To simulate short-term field aging for performance evaluation, the loose mixtures were subjected to short-term oven aging (STOA) per AASHTO R30 section 7.2 (*Short-Term Conditioning for Mixture Mechanical Property Testing*) for four hours at 135 °C. The loose mixture was placed in pans at an even thickness of 1” to 2” and stirred every hour for four hours.

The long-term performance of asphalt mixtures in the field is typically simulated using an accelerated laboratory aging protocol. Generally, there are two commonly used laboratory-based long term oven aging (LTOA) protocols: (1) conditioning of compacted specimen in an oven (Bell et al., 1994), which is the current AASHTO R30, and (2) aging of loose asphalt mixture prior to compaction (Chen, 2020; Chen et al., 2018b; Kim et al., 2018). As mentioned previously, the AASHTO R30 procedures for LTOA has been found to underestimate the field aging level as it simulates 1-2 years rather than 7-10 years of field performance and only one time-temperature combination is prescribed regardless of the climate (Newcomb et al., 2015), in addition, it causes

both radial and vertical oxidation gradient in the specimen (Houston et al., 2005), and may lead to deformation of the geometry of the specimen due to softening and slumping (Reed, 2010). Due to the mentioned limitations of the AASHTO R30 procedure, conditioning of loose mixtures to simulate LTOA has been gaining interest over the past few years. Recently, work conducted by (Kim et al., 2018) as part of project NCHRP 9-54 recommended a procedure which calls for conditioning loose mixtures at 95 °C for a period that depends on the climate of the project location, rheology properties of the asphalt binder, pavement layer depth, and years of field aging. To simplify the complications involved with aging duration computation, Kim et al. (2018) provided aging duration maps for different combinations of pavement depths and years of field aging. While this procedure could have been accelerated by increasing the temperature to 135 °C, researchers were concerned of the disruption of polar molecular association and decomposition of sulfoxides to sulfones through secondary oxidation which may occur when the temperature exceeds 100 °C (Petersen, 2009). This characteristic is asphalt chemistry and rheology dependent when mixtures are specially intended for the prediction of field aging. A study by Chen et al. (2018b) for the NCAT top-down fatigue cracking experiment found that loose mixtures aged at 95 °C for 5 days and 135 °C for eight hours were equivalent and expected to simulate 4 to 5 years of field aging in Alabama based on the high-temperature performance, Glover-Rowe parameter, and carbonyl area results. Moreover, Hall et al. (2019) found the 135 °C for 8 hours loose mixture aging protocol more effective in discriminating mixtures and consistent with field performance compared to the 95 °C for 5 days.

Since in this study asphalt mixtures with different RAs and RAM contents are evaluated, the desired LTOA will be one with the ability to distinguish their performance but also representative of field aging. Therefore, the loose mixture aging protocol at 135 °C for 6 hours recommended for

discriminating asphalt mixtures based on their performance in Wisconsin by Bahia et al. (2018) was used. Moreover, the same procedure is being used for the National Road Research Alliance (NRRA) mixture Rejuvenator Test Sections (Phase II) study (Jo Sias, 2020). To condition the loose mixture for LTOA, about 2400 to 2700 g of the samples were uniformly spread on half sheet pans measuring 17” long x 25” wide x 1” deep at a uniform thickness of ¾” to 1” to allow air flow for accelerated oxidation, then placed in an oven set at 135 °C for 6 hours. Table 3.24 summarizes the aging conditions, along with temperatures, aging durations, and the aging process used in this study. It is worth noting that, all samples compacted at their respective conditioning temperature per AASHTO T312-19.

Table 3.24: Summary of mixture aging conditions used in this study

Aging Condition	Conditioning Time (hrs.)	Conditioning Temp. (°C)	Conditioning Process
Mix design and Volumetric computations	2	138 for Wisconsin mixtures 135 for South Dakota mixtures	Loose mixtures were spread in pans at an even thickness of 1” to 2” and stirred every hour
Short-Term Oven (STOA)	4	135	Loose mixtures were spread in pans at an even thickness of 1” to 2” and stirred every hour
Long-Term Oven Aging (LTOA)	6	135	After STOA, 2400 to 2700 g of loose samples were placed on half sheet pans, each pan measures 17” x 25” x 1” deep. Each sample was evenly spread on a pan at thickness of ¾” to 1” to promote airflow.

3.9. Asphalt Mixture Performance Testing

Table 3.25 summarizes the tests along with the parameters used to assess the asphalt mixtures. The test conducted to evaluate the performance of the asphalt mixtures included: Hamburg wheel tracking test (HWTT), Asphalt Pavement Analyzer (APA) test, Indirect Tensile Asphalt Cracking Test (IDEAL-CT), Disc-shaped Compact Tension (DCT) test, and dynamic modulus ($|E^*|$) test. The HWTT was conducted on specimens after STOA to evaluate rutting resistance and moisture susceptibility of the Wisconsin mixtures; whilst the APA test was conducted on STOA specimens to evaluate the rutting resistance for South Dakota mixtures. The IDEAL-CT and DCT tests were performed on LTOA mixtures to assess the intermediate and low-temperature cracking resistance of all mixtures, respectively. The $|E^*|$ was performed on both STOA and LTOA asphalt mixtures to evaluate the stiffness and aging characteristics of the Wisconsin mixtures. All specimens for performance testing were prepared to meet a target air void content of 7.0 ± 0.5 %; except for APA specimens, which were compacted to heights of 115 ± 2.0 mm at the design gyrations (i.e., 50 gyrations).

Table 3.25: Asphalt mixtures performance properties and parameters

Property	Test	Protocol	Aging Condition	Parameter
Rutting resistance	HWTT/APA	AASHTO T324/T340	STOA	# of passes to 12.5 mm and corrected rut depth (CRD)/rut depth
Moisture susceptibility	HWTT	AASHTO T324	STOA	Stripping inflection point (SIP) and stripping number (SN)
Intermediate temp. cracking resistance	IDEAL-CT	ASTM D8225-19	LTOA	Cracking tolerance index (CT_{index})
Thermal cracking resistance	DCT	ASTM D7313-13	LTOA	Fracture energy (G_f)
Viscoelasticity	$ E^* $	AASHTO TP132-19	STOA	$ E^* $ and phase angle master curves and black space diagrams
Aging resistance			LTOA	

3.9.1. Hamburg Wheel Tracking Test (HWTT)

The HWTT was conducted to assess the rutting resistance and moisture susceptibility of the asphalt mixtures per AASHTO T324. To conduct the test, HWTT specimens were loaded with two steel wheels each 158 ± 1 lb. for 20,000 passes while submerged in a water bath maintained at a temperature of $46 \text{ }^\circ\text{C}$ (Figure 1). Four HWTT replicates were prepared, two for each side. Two linear variable differential transformers (LVDTs) each on the side of the HWTT machine were continuously recording the relative vertical positions of the steel wheels which are then translated into rut depth measurements.

Two rutting test parameters were used for HWTT data analysis: the traditional total rut depth (TRD) specified in AASHTO T 324 and the corrected rut depth (CRD), both at 20,000-wheel passes. The CRD is a simplified version of the viscoplastic strain increment parameter ($\Delta\varepsilon^{vp}$) proposed by Yin et al. (2014) and represents the projected rut depth at 20,000 passes due to permanent deformation of the mixture only. Stripping inflection point (SIP) and stripping number (SN) were used to evaluate the moisture damage potential of the mixtures. SIP is obtained by interpolating the intersection of two tangential lines that best fits the creep and stripping phase of the HWTT curve. SN was proposed by Yin et al. (2014), and it refers to the number of wheel passes at the onset of stripping. SN is an objective approach as it's determined from curve fitting of the entire rut depth curve as opposed to SIP which is more subjective (Yin et al., 2020). According to Kvasnak et al. (2010), SIP of greater than 10,000-wheel passes to be a good indicator of moisture damage resistant mix. Yin et al. (2020) found SIP and SN of 9,000- and 2,000-wheel passes, respectively to be the best criterion of a moisture damage-resistant asphalt mixture.

The HWTT setup and illustration for the determination of both TRD and CRD @20,000 using the HWTT rut depth curve are shown in Figure 3.6. For both TRD and CRD @20,000 a lower value

is desired for asphalt mixtures with better rutting resistance; the opposite applies to SIP and SN for moisture damage potential.

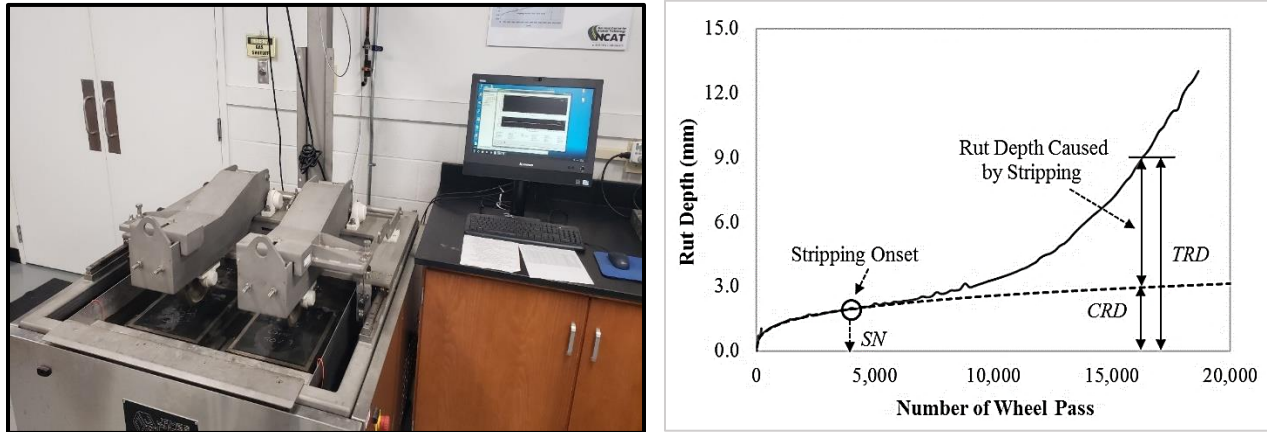


Figure 3.6: HWTT (a) Experimental setup (b) Data analysis

3.9.2. Asphalt Pavement Analyzer (APA) Test

The APA was conducted per AASHTO T340-10 to evaluate the rutting resistance of the mixtures. Specimens for APA were compacted to Ndesign (i.e., 50 gyrations) and height of 115 ± 2.0 mm tall. A total of six specimens were prepared per asphalt mix, and they were randomly divided into three pairs to reflect the testing positions (left, center, and right) in the APA setup [Figure 3.7 (a)]. After compaction, specimens were left to cool at room temperature overnight; then air void contents were determined to check whether they are within the 3.0 to 5.0 % air voids range as the mixtures were designed to meet a requirement of 4.0% air void contents. They were left to dry under a fan for at most a week. Before testing, specimens were conditioned at 58 °C (high-temperature PG of the base binder) for a minimum of 6 hours. During testing, wheels (100 lbs.) are loaded onto pressurized linear hoses (100 psi.) and tracked back and forth over testing specimens for about 8000 cycles to induce rutting. The APA was run in automatic mode; the 25 initial seating cycles were first applied then the software was restarted for the actual test. Rut

depths are accumulated at an interval of 100 cycles and the final value after all the cycles are complete is taken as a rut depth for that mixture [Figure 3.7 (b)]. A lower rut depth is desired for a mixture resistant to rutting.

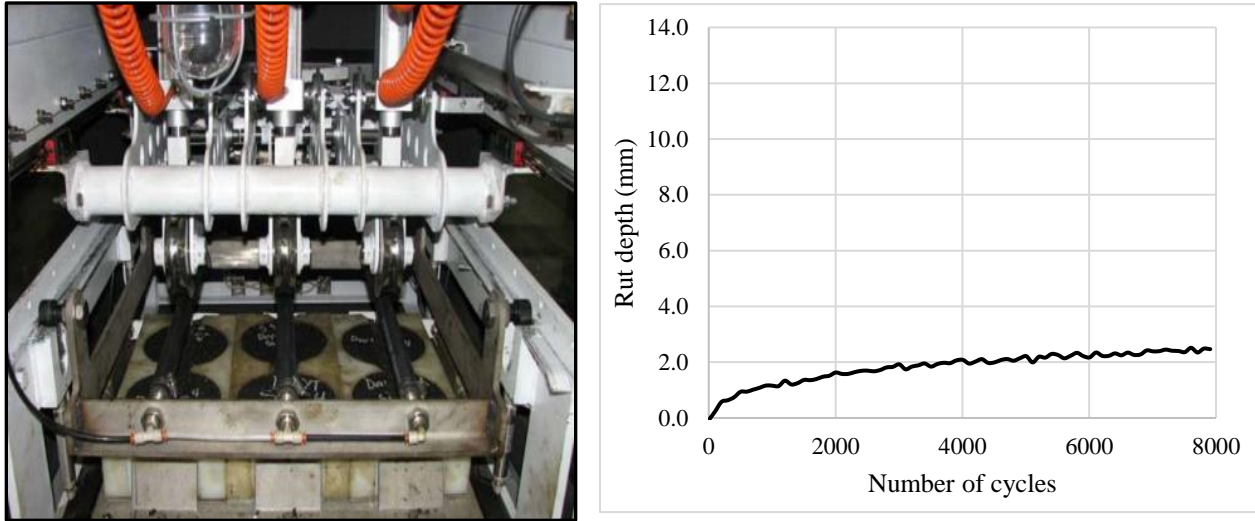


Figure 3.7: APA (a) Experimental setup (b) Data analysis

3.9.3. Indirect Tensile Asphalt Cracking Test (IDEAL-CT)

The IDEAL-CT was used to evaluate the intermediate-temperature cracking resistance of the asphalt mixtures. The test was conducted per ASTM D8225-19; the number of replicates per mixture ranged from four to six specimens. Before testing, specimens were conditioned in an environmental chamber at 25 ± 1.0 °C for 2 hours \pm 10 minutes. During the test, a monotonic load was applied on a gyratory specimen at a constant displacement rate of 50 mm/min as shown in Figure 3.8 (a). Once the testing was complete, the load-displacement curve was analyzed to determine the work of fracture, which refers to the total area under the curve, and the slope of the curve at a 25 percent reduction from the peak load [Figure 3.8 (b)]. The final test parameter, the

cracking tolerance index (CT_{index}), was then calculated using Equation 3.2. A higher CT_{index} value is desired for asphalt mixtures with better cracking resistance.

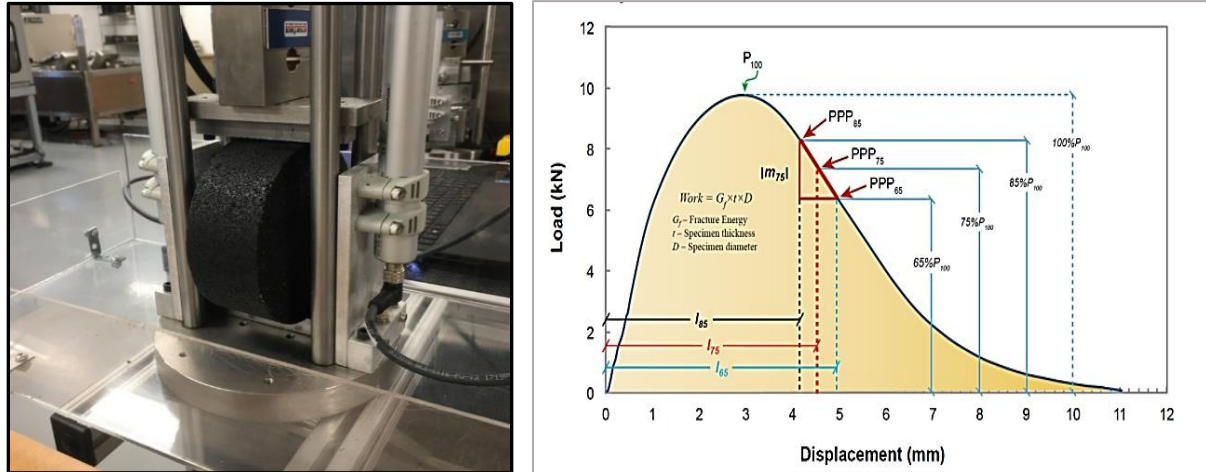


Figure 3.8: IDEAL-CT (a) Experimental setup (b) Data analysis

$$CT_{index} = \frac{t}{62} * \frac{l_{75}}{D} * \frac{G_f}{|m_{75}|} * 10^6 \quad \text{Equation 3.2}$$

Where,

t = specimen thickness;

l_{75} = displacement at 75% of peak load;

D = specimen diameter;

G_f = fracture energy; and

$|m_{75}|$ = slope at 75% peak load.

3.9.4. Disk-shaped Compact Tension (DCT) Test

The DCT test was conducted following ASTM D7313-13 to assess the low-temperature cracking resistance of the mixtures. The test specimens were prepared by saw-cutting a 160 mm-high by 150 mm-diameter, compacted to 7.5 % air void contents into two halves of 50 ± 5 mm thick. The halved specimens were then trimmed to attain a flat edge on one side of the specimen for studs. Then, a notch 62.5 ± 2.5 mm long was saw-cut at the center of the flat edge, followed by coring two 1-inch diameter holes on each side of the notch. The final testing specimen had a target air void content of 7.0 ± 0.5 %; the number of replicates ranged from four to six specimens. Since the asphalt binders had a LTPG of -28 °C and -34 °C, the test was conducted at -18 °C and -24 °C respectively, as ASTM D7313-13 recommends running the test at 10 °C above the LTPG of the asphalt binder. Before testing, the specimens were conditioned in an environmental chamber for eight to sixteen hours. The test began by loading a DCT specimen in tension using metal rods that were inserted through core holes as shown in Figure 3.9 (a). A clip gage was then installed over the crack mouth before the start of the experiment to control and record the crack mouth opening displacement (CMOD). The test was conducted in CMOD control mode with the clip gage opening at a constant rate of 0.017 mm/sec. The test was terminated when the load dropped below 0.1 kN. Figure 3.9 (b) presents an example of the load versus CMOD behavior in the DCT test. For data analysis, the fracture energy (G_f) was calculated using Equation 3.3, where the area under the load-CMOD curve was determined through numerical integration using the trapezoidal rule. A higher G_f value is desired for asphalt mixtures with better resistance to low-temperature cracking.

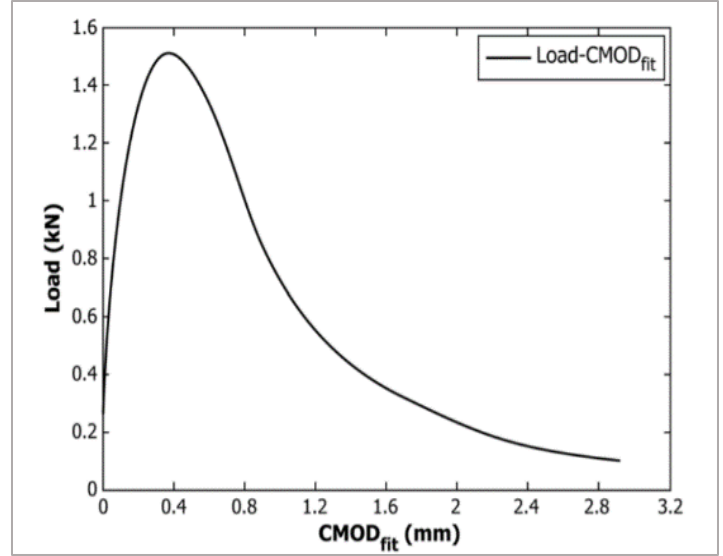


Figure 3.9: DCT (a) Experimental setup (b) Data analysis

$$G_f = \frac{Area}{B * (W - a)}$$

Equation 3.3

Where,

G_f = fracture energy (J/m^2);

$Area$ = area under load-CMOD curve;

B = specimen thickness (m); and

$W-a$ = initial ligament length (m).

3.9.5. Dynamic Modulus ($|E^*|$) Test

Dynamic modulus testing was performed following AASHTO TP132-19 using the IPC global[®] AMPTPRO equipment to evaluate the stiffness of the asphalt mixtures [Figure 3.10 (a)]. This test was conducted on both STOA and LTOA asphalt mixtures. Larger specimens were compacted to 180 mm tall and 150 mm diameter with air void contents of 8.0 %. From these larger specimens, four 38 mm diameter by 110 mm tall specimens were cored and saw-cut per AASHTO PP99-19. Three replicates of small specimens for every asphalt mixture for each conditioning type (STOA and LTOA) that met the air void criteria ($7.0 \pm 0.5\%$) were selected for testing. Specimens were tested at three temperatures (4, 20, and 35 °C) and three loading frequencies (10, 1, and 0.1 Hz) at each testing temperature. As shown in Figure 3.10 (b), the data collected facilitated the construction of the $|E^*|$ master curves for the asphalt mixtures using the time-temperature superposition principle so that the relative stiffness of the asphalt mixtures could be examined across a wide range of frequencies. AASHTO R84-17 was followed to construct the dynamic master curves at the 20°C reference temperature by using the generalized sigmoidal function as shown in Equation 3.4.

$$\log|E^*| = \delta + \frac{\alpha}{1 + e^{\beta + \gamma \log(\omega)}} \quad \text{Equation 3.4}$$

Where,

$|E^*|$ = dynamic modulus;

α , β , δ , and γ = fitting parameters; and

ω = reduced frequency.

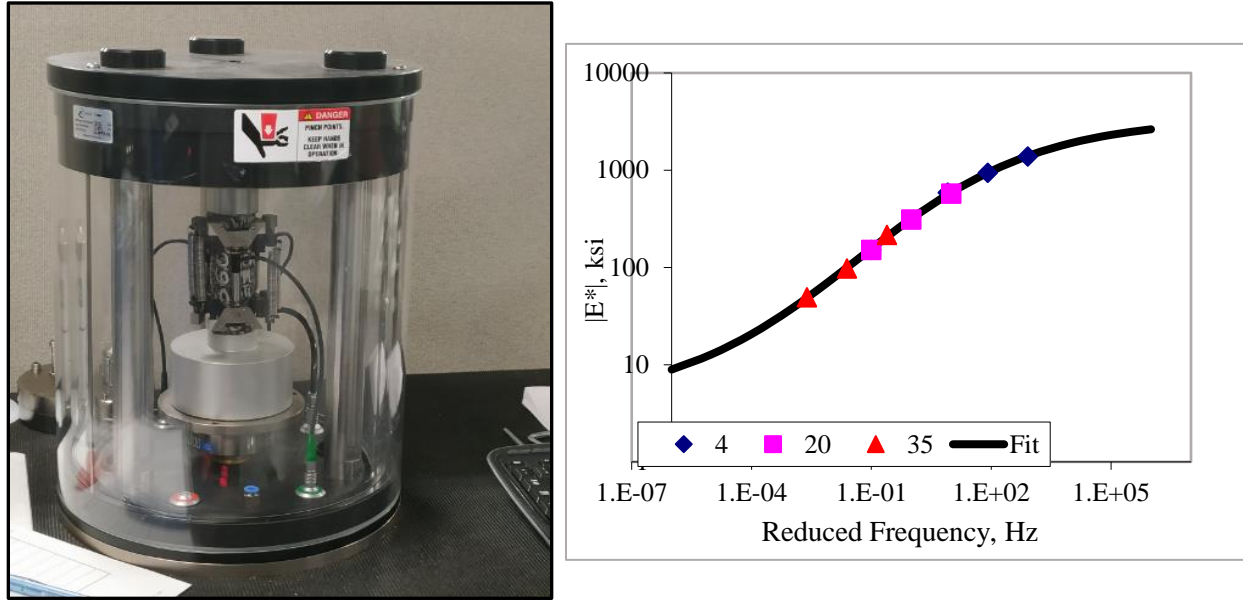


Figure 3.10: Dynamic modulus (a) Experimental setup (b) Data analysis

The Glover-Rowe mixture parameter ($G-R_m$) originally proposed by Mensching et al. (2015) will be used to evaluate the block cracking potential of the mixtures. Mensching et al. (2015) proposed to use $|E^*|$ and phase angle (δ) values at frequencies closer to the inflection point (representing the peak of δ master curve) for mixture Black space diagram analysis as the differentiation between aggregates and binder dominance on the properties of the mixture is observed at this point. However, research has shown that the frequency at which the inflection point occurs is distinct for each mixture and it tends towards the low-frequency side (left side of the inflection point) of the δ master curve plot with an increase in aging level and RAM contents in the mixtures (Ogbo et al., 2019). Alternatively, Oshone et al. (2019) and Ogbo et al. (2019) suggested the $G-R_m$ be determined at a frequency of 5 Hz and reference temperature of 20 °C since the 5 Hz point consistently fall on the high-frequency end (right side of the inflection point) of the δ master curve plot and can be directly measured during the $|E^*|$ testing. As shown in Equation 3.5, the $G-R_m$ for this study was calculated using $|E^*|$ and δ values at 20 °C and 5 Hz.

$$G - R_m = \frac{|E^*|(\cos\delta)^2}{\sin\delta} \text{ at } 20 \text{ }^\circ\text{C and } 5 \text{ Hz}$$

Equation 3.5

4. ASPHALT BINDER TESTING RESULTS

4.1. Introduction

In this chapter, the testing results of the recycled binder blends with and without RAs are described. For Wisconsin materials, the recycled binder blends were prepared with the PG 58S-28 and PG 58V-28 base binders, two RAP binders (RAP1 and RAP2), and one RAS binder. The RAs used with these materials were RA1 and RA2. The rejuvenated recycled binder blends were prepared with a dosage of 5% (by weight of the total binder) of RAs. For South Dakota recycled binder blends, the materials used were a PG 58S-34 base binder, one RAP binder (also referred to as SD RAP in this study), and four different RA products (RA1, RA3, RA4, and RA5). As stated in Section 3.5, for South Dakota blends, the dosages of the RAs RA1, RA3, and RA4 were determined by the manufactures. The dosage of RA5 was determined at NCAT, and it was found to be 45% by weight of the total binder, and it should be noted that it's presented in this study for evaluation purposes only as this rate is impractical for field application. The overall objective of this chapter was to evaluate the effect of high RAP and/or RAS contents in the recycled binder blend properties and assess the effectiveness of the RAs in improving these properties.

4.2. Performance Grading and ΔT_c Parameter

Table 4.1 shows the Superpave performance grade that was determined following AASHTO M320. Based on the AASHTO M320 classification, the PG 58S-28 binder remained PG 58-28 whereas the PG 58V-28 was PG 64-28. For the RAM materials: RAP1 was PG 82-22, RAP2 was PG 82-16, and RAS was PG 160+26. As expected, the RAS binder was heavily aged compared to

the RAP binders. The addition of RAMs into the PG 58S-28 improved the rutting resistance of the resultant recycled blends as the HTPG increased by one grade in comparison to the base binder for all combinations, except for the blend with 25% RAS which its HTPG was two grades higher than the base binder. For the PG 58V-28 recycled binder blends, the PG grade increase when compared to the base binder PG grade was: one for 20% RAP2 and 40% RAP2 blends, two for 15% RAS, 15% RAP2 + 5% RAS, and 30% RAP2 + 5% RAS blends, and three for the 25% blend. However, after RTFO plus 40 hours of PAV, the fatigue resistance, thermal cracking resistance, and stress relaxation properties were negatively affected since the true intermediate and low-temperature PG increased, and the ΔT_c value decreased due to the impact of RAMs.

The addition of the RAs (RA1 and RA2) decreased the true high PG to the original grade of the base binders, except for the recycled binder blends with 25% RAS. Moreover, the true intermediate temperature and the ΔT_c improved; and the low-temperature PG was restored to that of the base binders (-28 °C) after RTFO plus 40 hours of PAV.

Table 4.1: Performance grading of the recycled binder blends with the PG 58S-28 and PG 58V-28 binders

Temperature (°C)	True High	True Interm.	True Low	ΔT_c	High PG	Low PG
Materials						
PG 58S-28	60.3	16.8	-30.7	-0.2	58	-28
RAP1	83.1	26.2	-22.9	-3.0	82	-22
PG 58V-28	66.1	17.4	-30.6	1.0	64	-28
RAP2	86.4	27.1	-21.1	-1.6	82	-16
RAS	163.2	38.2	27.7	-52.6	160	26
Recycled binder blends prepared with PG 58S-28						
80% PG 58S-28 + 20% RAP1	64.8	22.1	-25.8	-3.2	64	-22
60% PG 58S-28 + 40% RAP1	69.5	24.3	-23.2	-4.8	64	-22
85% PG 58S-28 + 15% RAS	67.8	23.3	-22.5	-7.0	64	-22
75% PG 58S-28 + 25% RAS	77.0	25.1	-17.0	-11.2	76	-16
80% PG 58S-28 + 15% RAP1 + 5% RAS	64.2	20.4	-26.2	-3.3	64	-22
65% PG 58S-28 + 30% RAP1 + 5% RAS	67.8	23.6	-24.5	-3.9	64	-22
Recycled binder blends prepared with PG 58V-28						
80% PG 58V-28 + 20% RAP2	74.0	21.5	-26.3	-1.9	70	-22
60% PG 58V-28 + 40% RAP2	75.8	24.3	-23.8	-3.7	70	-22
85% PG 58V-28 + 15% RAS	81.1	21.5	-21.8	-9.4	76	-16
75% PG 58V-28 + 25% RAS	86.1	25.1	-19.1	-10.9	82	-16
80% PG 58V-28 + 15% RAP2 + 5% RAS	76.1	21.3	-24.6	-3.6	76	-22
65% PG 58V-28 + 30% RAP2 + 5% RAS	76.4	24.6	-22.9	-4.6	76	-22
Recycled binder blends prepared with PG 58S-28/ PG 58V-28 and RA1/RA2						
55% PG 58S-28 + 40% RAP1 + 5% RA1	62.3	16.5	-33.3	-1.1	58	-28
70% PG 58S-28 + 25% RAS + 5% RA1	68.4	17.8	-30.3	-4.9	64	-28
60% PG 58S-28 + 30% RAP1 + 5% RAS + 5% RA1	63.5	15.5	-33.0	-1.6	58	-28
55% PG 58S-28 + 40% RAP1 + 5% RA2	61.2	15.9	-31.7	-1.9	58	-28
70% PG 58S-28 + 25% RAS + 5% RA2	67.3	19.2	-28.0	-5.8	64	-28
60% PG 58S-28 + 30% RAP1 + 5% RAS + 5% RA2	62.7	14.5	-31.5	-2.3	58	-28
55% PG 58V-28 + 40% RAP2 + 5% RA1	68.8	17.1	-30.9	-3.9	64	-28

Further analysis of the effect of increased RAM in recycled binder blend properties was conducted to evaluate the linear blending relationship between the percentage of RAM (by weight) in the blend and the temperature properties. From Figure 4.1 to Figure 4.6, the true temperature properties of both PG 58S-28 and PG 58V-28 increased linearly with an increase in RAM contents at both high and intermediate temperatures, whereas at low temperatures (stiffness and m-value) they were decreasing. However, the rate (slope) of increase/ decrease of the temperature properties were high for recycled binder blends with RAS binder only, followed by those with RAP and RAS binder, and finally, those with RAP binder only, indicating high stiffness and low relaxation properties the RAS had compared to the RAPs. The relationship of RAM binder increase with the ΔT_c parameter was polynomial for both PG 58S-28 and PG 58V-28 blends with RAP only, but linear for blends with RAS only or a combination of RAP and RAS binder.

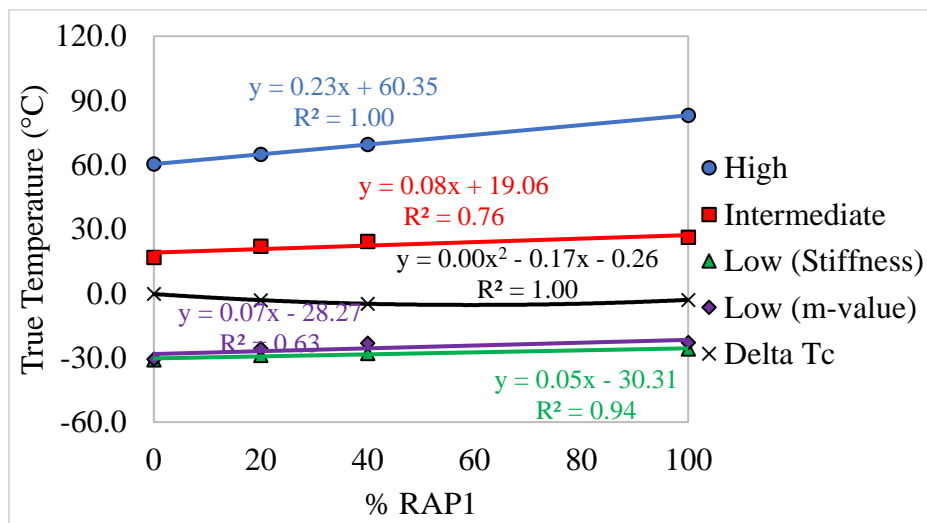


Figure 4.1: Relationship between temperature properties and RAP1 binder increase for the recycled binder blends with the PG 58S-28 binder

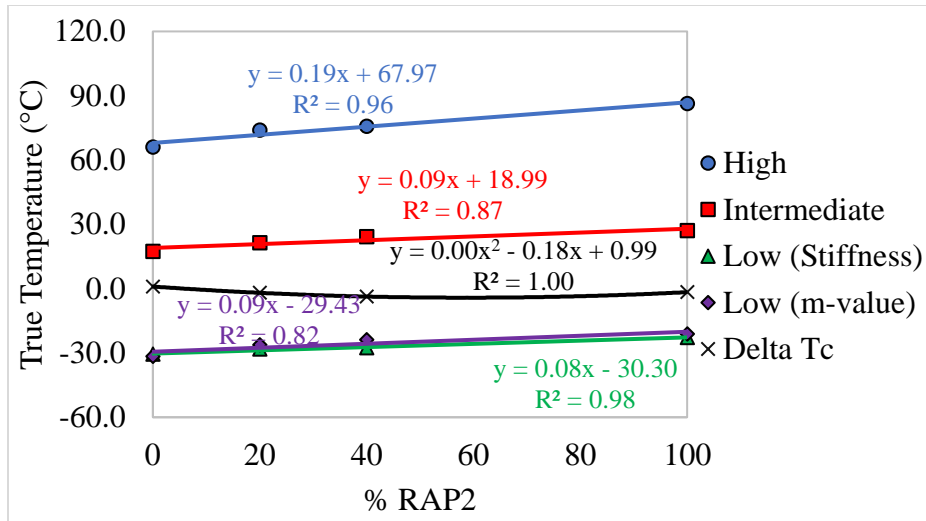


Figure 4.2: Relationship between temperature properties and RAP2 binder increase for the recycled binder blends with the PG 58V-28 binder

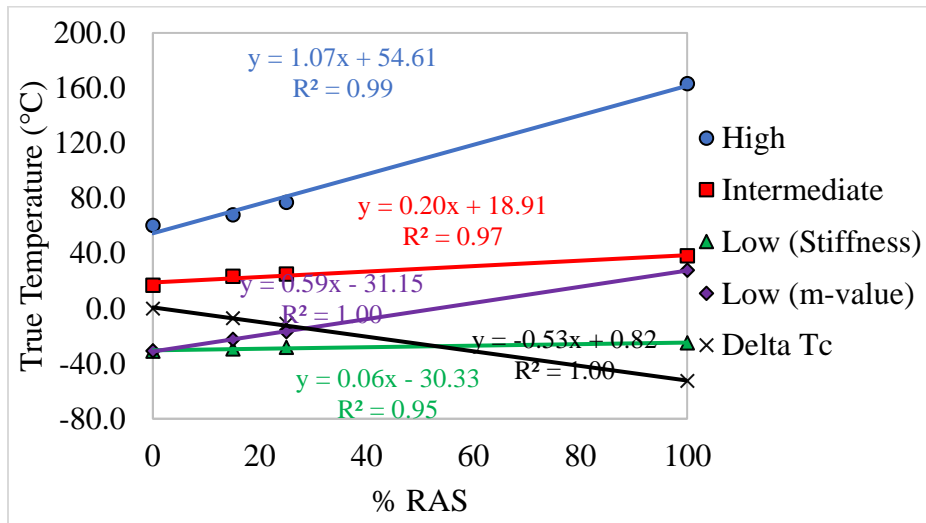


Figure 4.3: Relationship between temperature properties and RAS binder increase for the recycled binder blends with the PG 58S-28 binder

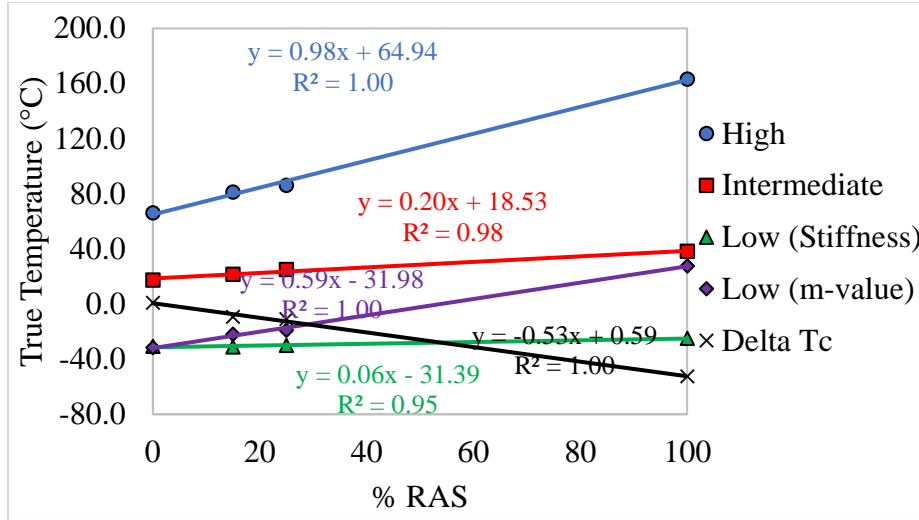


Figure 4.4: Relationship between temperature properties and the RAS binder increase for the recycled binder blends with the PG 58V-28 binder

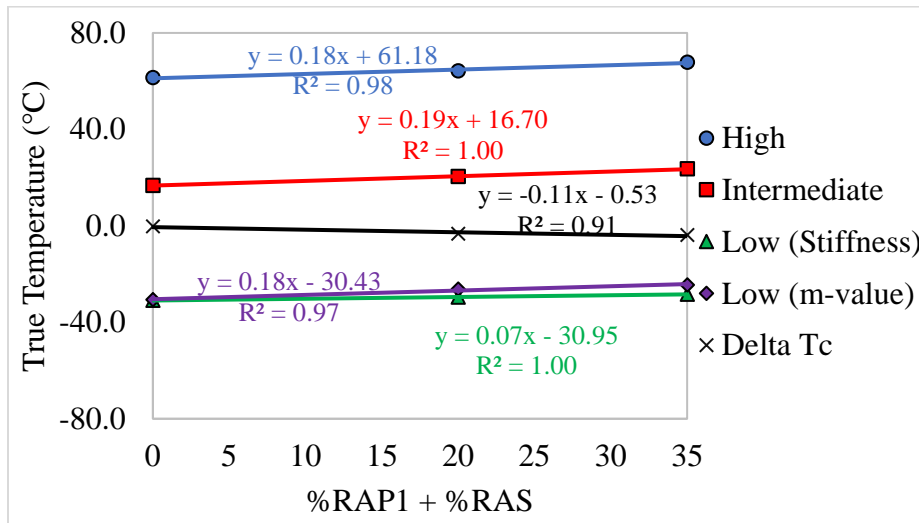


Figure 4.5: Relationship between temperature properties and RAP1 + RAS binder increase for the recycled binder blends with the PG 58S-28 binder

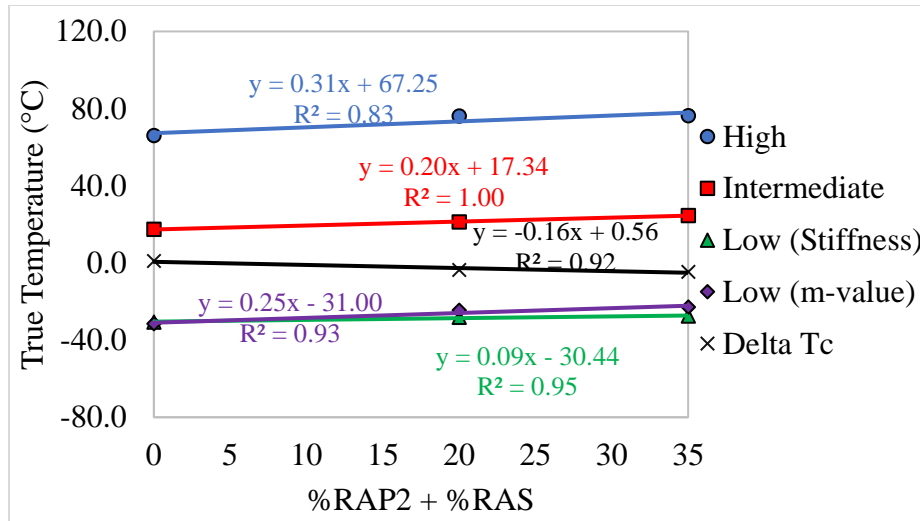


Figure 4.6: Relationship between temperature properties and the RAP1 + RAS binder increase for the recycled binder blends with the PG 58V-28 binder

The impact of RAs in improving the temperature properties of high RAM content recycled binder blends was assessed using the relative change (difference) in temperature properties between the high RAM content blends (with and without RAs) and the control blend (20% ABR). Figure 4.7 to Figure 4.10 show the difference in temperature properties. One should note that only the recycled binder with 40% ABR from RAP1 and RA1 was used for the PG 58V-28 binder. For the true high temperature, a positive change indicates an increase in high-temperature properties compared to the control blend whereas vice versa is true for a negative change. For true intermediate and low temperature (both stiffness and m-value) properties a negative change indicated improvement in the properties as compared to the control blend. For the ΔT_c parameter, a less negative (more positive) value was desirable. The effectiveness of the RAs seemed not to be consistent throughout the temperature properties. For instance, for the 25% ABR blend with the PG 58S-28, RA2 was more effective in improving the high-temperature properties than RA1. RA1 seemed effective in improving the intermediate and low-temperature properties and the ΔT_c than

RA2. For the 35% ABR and 40% ABR blends with the PG 58S-28 binder, both RAs had detrimental effects on the true high temperature (negative change values); but for both 35% ABR and 40% ABR blends, RA2 was more detrimental than RA1. RA2 was more effective in improving the intermediate temperature properties of these blends as compared to RA1. When considering the low-temperature properties and the ΔT_c , RA1 was more effective than RA2. Moreover, the RAs were more effective in blends with RAP only (i.e., 40% ABR) than those with RAS only (25% ABR). For the 40% ABR blend with the PG 58V-28 binder, the addition of RA1 had negative impacts on the high-temperature properties when compared to the control blend and the 40% ABR blend without RA1. The intermediate and low-temperature properties improved; however, the ΔT_c of the blend without RA1 was slightly higher than that with RA1.

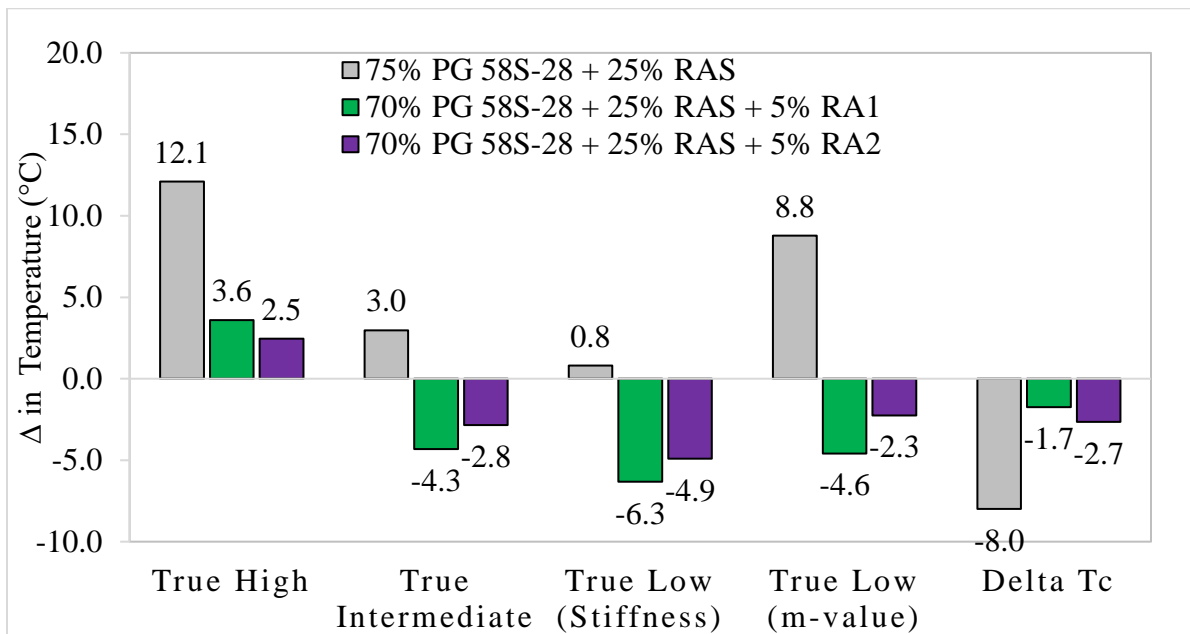


Figure 4.7: Change in true temperature properties of the 25% ABR blends with the PG 58S-28 binder

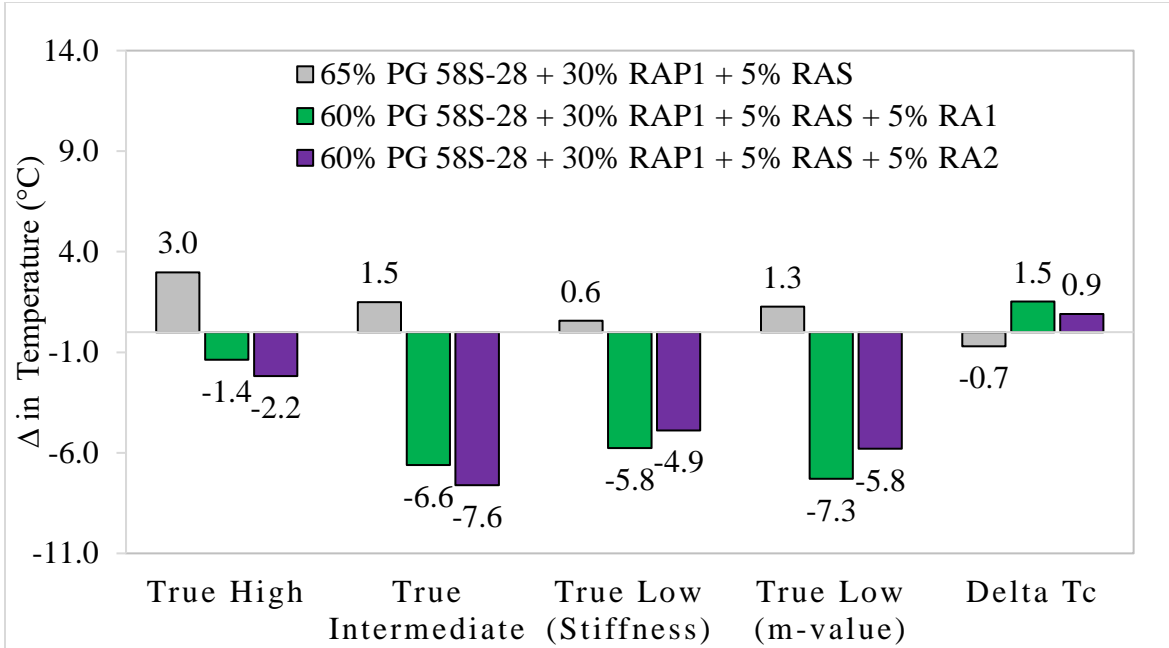


Figure 4.8: Change in true temperature properties of the 35% ABR blends with the PG 58S-28 binder

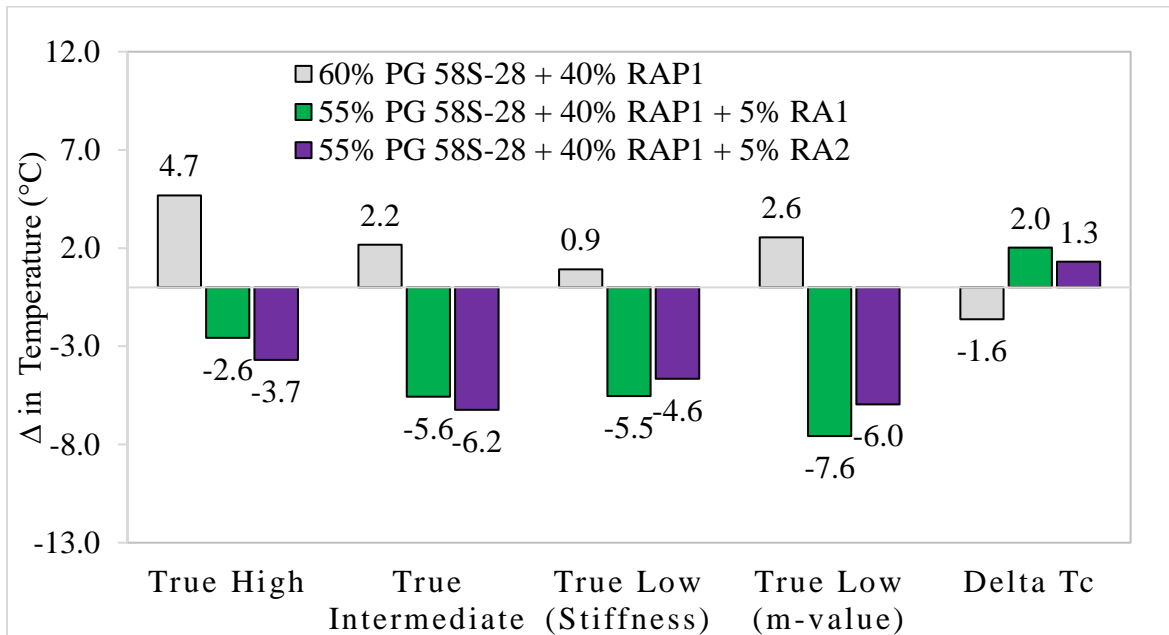


Figure 4.9: Change in true temperature properties of the 40% ABR blends with the PG 58S-28 binder

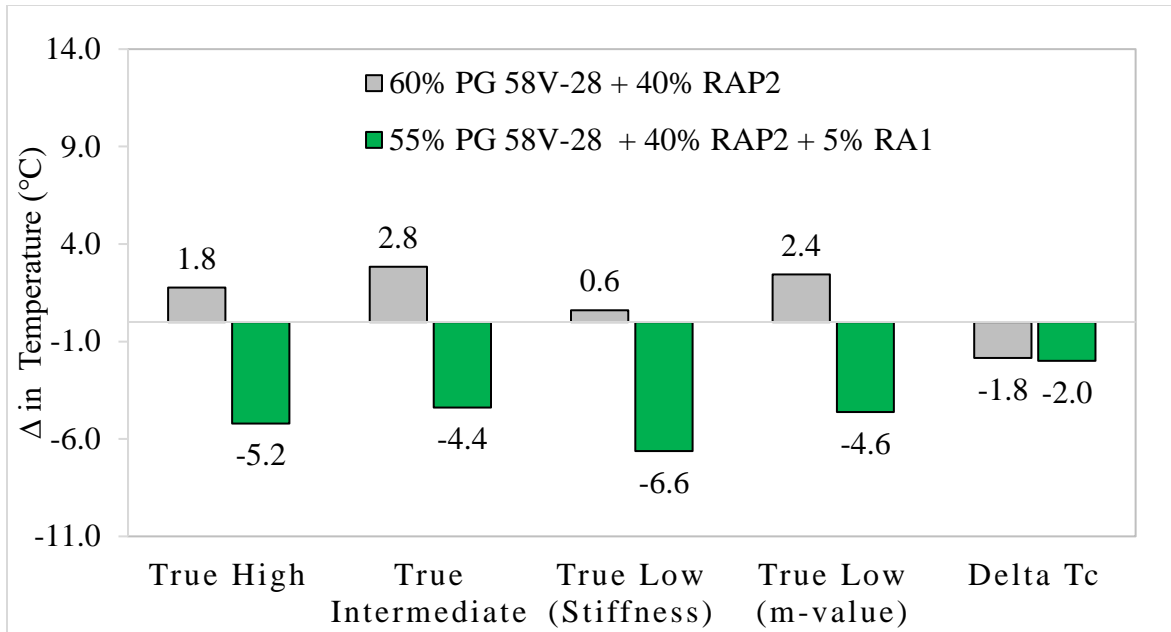


Figure 4.10: Change in true temperature properties of the 40% ABR blends with the PG 58V-28 binder

Table 4.2 summarizes the performance grading of the recycled binder blends prepared with the PG 58S-34 base and the SD RAP binders. Unless otherwise specified, all the recycled blends were RTFO plus 60 hours PAV aged. As previously described, the dosages of the bio-based RAs were determined by the manufacturer targeting the true LTPG of the control blend (20% ABR blend). The increase in RAP binder content (i.e., 20% RAP, 30% RAP, and 50% RAP) increased the high temperature, potentially improving the rutting performance, where potential adverse effects were observed in the fatigue and thermal cracking properties.

The addition of RAs to high RAP content recycled binder blends (35% RAP and 50% RAP) decreased the high-temperature properties and resulted in a HTPG of 64 °C, which was the same as the control (20% RAP blend) except for the 35% RAP blend with RA5 which had a HTPG of 52 °C (12 °C lower than the control). This substantial reduction in HTPG of RA5 is associated with the high dosages used (45% by weight of the total binder). The intermediate and low-

temperature properties were improved with the addition of the RAs. For instance, the true intermediate temperature of the 35% RAP and 50% RAP blends before the addition of the RAs were 22.8 °C and 21.4 °C, respectively. After the addition of the RAs, the true intermediate temperature of the blends ranged between 12.8 °C and 20.9 °C, the 35% ABR with RA5 had the highest value and the 50% ABR with RA4 had the lowest value. The LTPG of the 35% RAP and 50% RAP blends with RAs were 6 °C lower than the control blend whereas those of ones without RA were 6 °C and 12 °C higher.

Table 4.2: Performance grading of the recycled binder blends with the PG 58S-34 binder

Temperature °C	True High	True Interm.	True Low	ΔT_c	HTPG	LTPG
Material and Control blend (20% ABR)						
PG 58S-34 @RTFO plus 20-hour PAV	63.2	8.6	-36.4	0.4	58	-34
PG 58S-34 @RTFO plus 60-hour PAV	63.2	11.5	-28.2	-5.7	58	-28
RAP @RTFO	85.0	26.7	-22.4	-2.3	82	-22
RAP @RTFO plus 60-hour PAV	85.0	36.3	-9.1	-9.4	82	-4
PG 58S-34 + 20% RAP	66.8	15.8	-27.2	-4.1	64	-22
35% ABR blends with and without RAs						
PG 58S-34 + 35% RAP	68.6	22.8	-23.4	-6.5	70	-22
PG 58S-34 + 35% RAP + 1.8% RA1	67.6	19.9	-28.6	-3.5	64	-28
PG 58S-34 + 35% RAP + 2.8% RA3	67.6	18.1	-28.5	-5.1	64	-28
PG 58S-34 + 35% RAP + 2.1% RA4	64.9	20.1	-29.4	-3.0	64	-28
PG 58S-34 + 35% RAP + 45% RA5	54.3	12.8	-31.1	-4.5	52	-28
50% ABR blends with and without RAs						
PG 58S-34 + 50% RAP	74.4	21.4	-21.6	-7.4	70	-16
PG 58S-34 + 50% RAP + 3.1% RA1	69.1	18.3	-28.0	-5.6	64	-28
PG 58S-34 + 50% RAP + 4.0% RA3	68.4	19.5	-28.0	-5.3	64	-28
PG 58S-34 + 50% RAP + 3.8% RA4	66.0	20.9	-28.4	-2.9	64	-28

Figure 4.11 presents the relationship of RAP content with temperature properties of the PG 58S-34 recycled binder blends. As expected, the increase in RAP content and the temperature properties were linearly related, with coefficient of determination (R^2) ranging from 0.96 (at true high temperature) to 0.78 (for ΔT_c parameter).

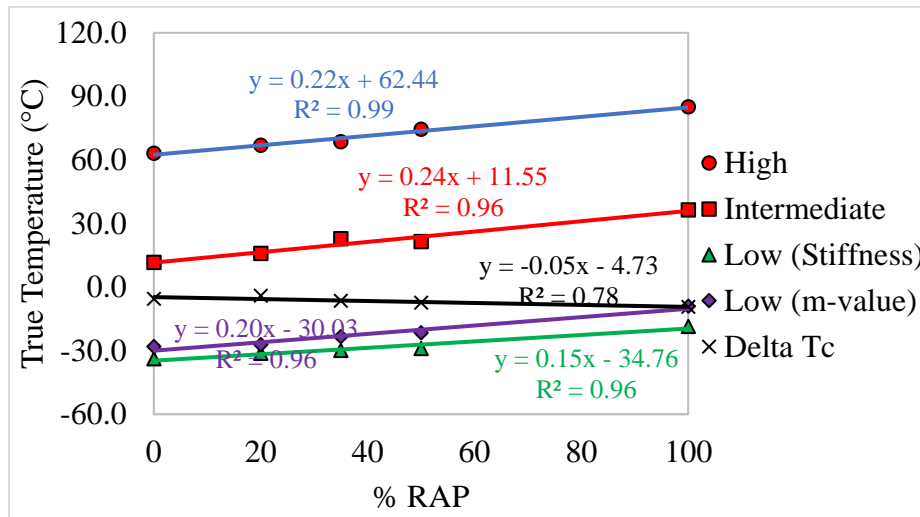


Figure 4.11: Relationship between temperature properties and the RAP binder increase for the recycled binder blends with the PG 58S-34 binder

The effectiveness of RAs in reducing the negative impact of high RAP content in the blends was evaluated by calculating the change in true temperature properties relative to the control blend (20% ABR). As stated previously, a positive change indicates an increase in true high-temperature properties whereas vice versa is true for a negative change. For true intermediate temperature, and low temperature (both stiffness and m-value) properties a negative change indicated improvement in the properties. For the ΔT_c parameter, a less negative (more positive) value indicates the effectiveness of the RAs towards restoring block cracking properties of the blend.

Figure 4.12 shows the change in temperature properties of the 35% ABR blend with the PG 58S-34 binder after the addition of the RAs. As expected, the blend without RA had a higher true high temperature than the control (20% ABR blend) because of RAP stiffness. However, the addition of RAs decreased the true high temperature at different effectiveness. For instance, the decrease in the true high temperature for blends with RA1 and RA3 had a positive change indicating that it was higher compared to the control blend. Blends with RA4 and RA5 had a negative change indicating that they had lower true high temperature than the control blend. The asphalt flux (RA5) had a more negative impact to the true high temperature of all the RAs due to its high softening effect when compared to others. Increased RAP content had a negative impact on the true intermediate and low (both at stiffness and m-value) temperatures due to the observed positive changes in Figure 4.12. The addition of the RAs decreased this effect as can be seen at the true intermediate temperature the change was lesser positive for blends with bio-based RAs (RA1, RA3, and RA4); and negative for the blend with RA5. For the true low temperature, the change was negative for all RAs indicating that they were all able to reduce the true low temperature, however, RA5 had more impact than the remaining. The ΔT_c decreased with an increase in RAP content (negative change); however, with the addition of the RAs, the ΔT_c improved, blends with RA3 and RA5 had a lesser negative change whereas those with RA1 and RA4 had a negative change in ΔT_c .

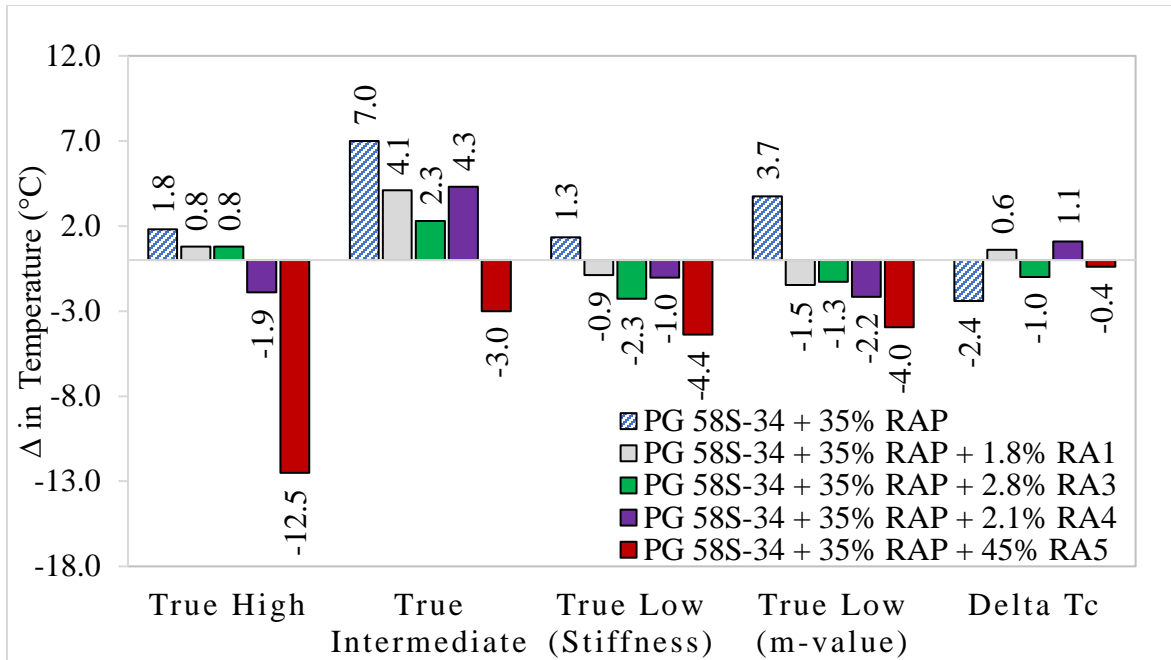


Figure 4.12: Change in true temperature properties of the 35% ABR blends with the PG 58S-34 binder

The changes in the continuous performance grade of the 50% RAP blends with the PG 58S-28 base binder are shown in Figure 4.13. Only bio-based RA was used with the 50% RAP blend since it was impractical to determine the dosage of the asphalt flux (RA5). As stated previously, the differences between the high RAP content blends (with and without RAs) and the control blend were used to assess the effectiveness of RAs. The 50% RAP blend without RA had a higher true high temperature compared to the control and other recycled binder blends with RAs. The blend with RA4 had a slightly lower high true temperature than the control while RA1 seemed to have a high true high temperature among all blends with RAs. For intermediate temperature properties, all 50% RAP blends had higher true intermediate temperatures than the control blend, with the blend without RA having the highest. Among the 50% RAP blends with RAs, one with RA4 showed the highest while that with RA1 was the lowest. For true low-temperature properties, the 50% blend without RA had decreased (a positive change) true low-temperature value (at both creep

stiffness and m-value) than the control blend. The addition of the RAs increased/improved the true low temperature. At the true low temperature (at stiffness), RA1 seemed more effective, followed by RA3; RA4 had the same value as the control blend. For the true low temperature (at m-value), RA4 was more effective whereas RA1 and RA3 had a similar impact. Lastly, the 50% RAP blend without RAs showed decreased ΔT_c value than the control. Among the blends with RA, RA4 had improved/higher ΔT_c value of all.

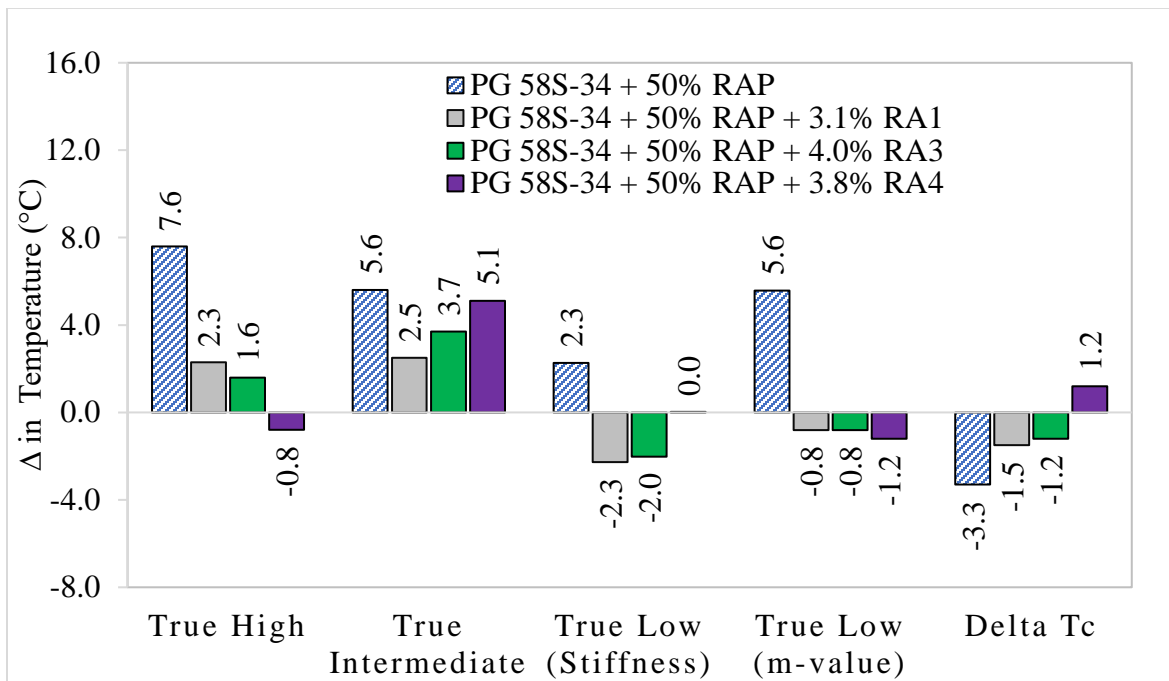


Figure 4.13: Change in the true temperature properties of the 50% ABR blends with the PG 58S-34 binder

4.3. Multiple Stress Creep Recovery (MSCR)

The multiple stress creep recovery (MSCR) test was conducted at 64 °C and 58 °C for Wisconsin and South Dakota recycled binder blends per AASHTO T350 and M332 to characterize and grade elastic response and rutting resistance of the recycled binder blends after RTFO conditioning. The non-recoverable creep compliance (Jnr) and percent recovery at 3.2 kPa stress level were used for

rutting resistance and elastic response evaluation, respectively. Figure 4.14 and Figure 4.15 show the changes in J_{nr} and percent recovery at 3.2 kPa with an increase in ABR for blends prepared with the PG 58S-28 binder. As can be seen in Figure 4.14, the J_{nr} value decreased with the increase in ABR content, indicating the stiffening effect introduced by the RAMs. Moreover, except for the 20% RAP1 and 15% RAP1+5% RAS blends, the percent recovery seemed to increase as well (Figure 4.15). The J_{nr} of the RAMs at the stress level of 3.2 kPa was: 0.1936 kPa-1 for RAP1, 7.995×10^{-5} kPa-1 for RAS, and 0.07143 kPa-1 for RAP2.

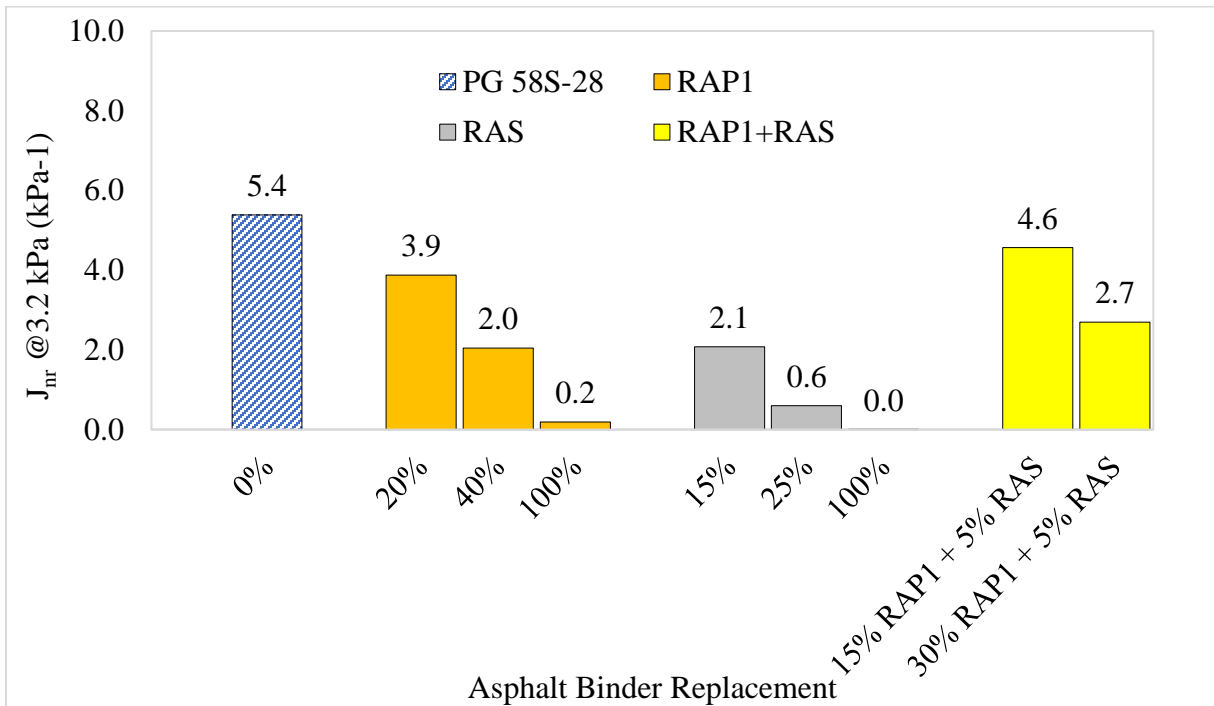


Figure 4.14: Effect of increase in ABR on J_{nr} @ 3.2 kPa and 64 °C for recycled binder blends with the PG 58S-28 binder

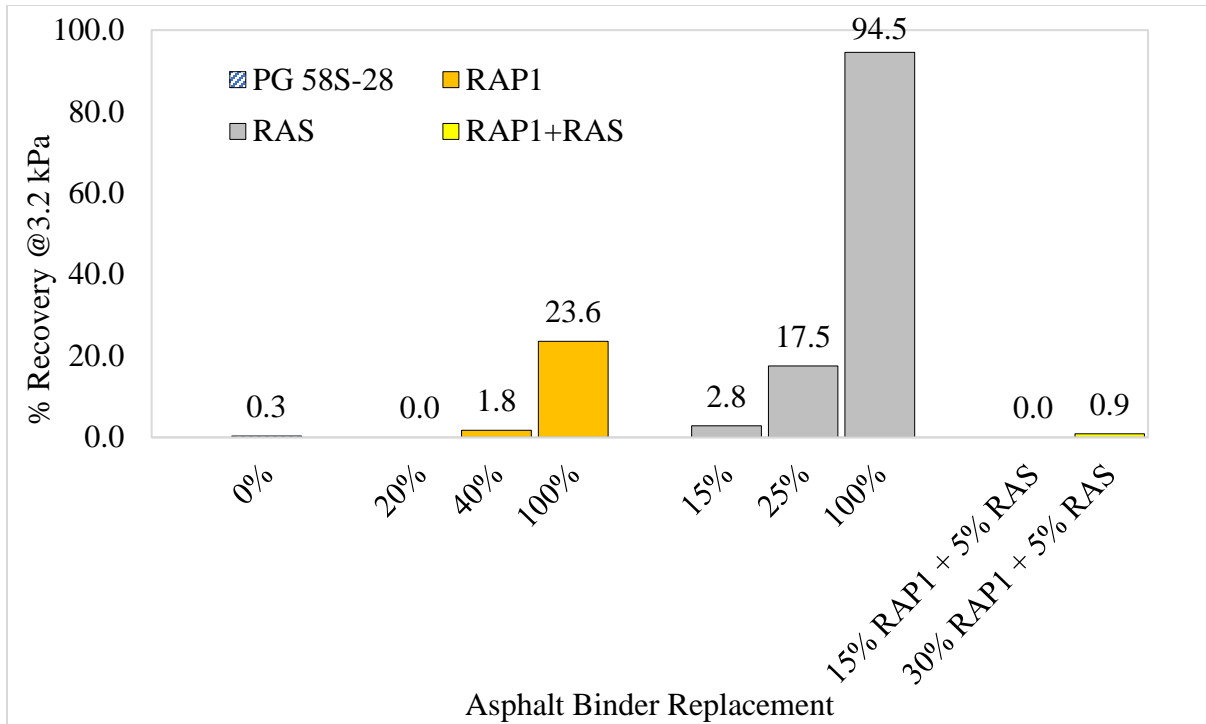


Figure 4.15: Effect of increase in ABR on % recovery @3.2 kPa and 64 °C for recycled binder blends with the PG 58S-28 binder

The changes in Jnr and percent recovery at 3.2 kPa with the increase in ABR contents for blends prepared with the PG 58V-28 binder are shown in Figure 4.16 and Figure 4.17. The recycled binder blends with RAS only showed a decrease in Jnr as the RAS content increases, whereas those with RAP2 only or RAP2 + RAS showed an increase in Jnr values as the RAM content increases. Contrary to the Jnr, the percent recovery decreases with an increase in ABR contents for blends with RAP2 only and RAP2 + RAS and an increase for RAS blends.

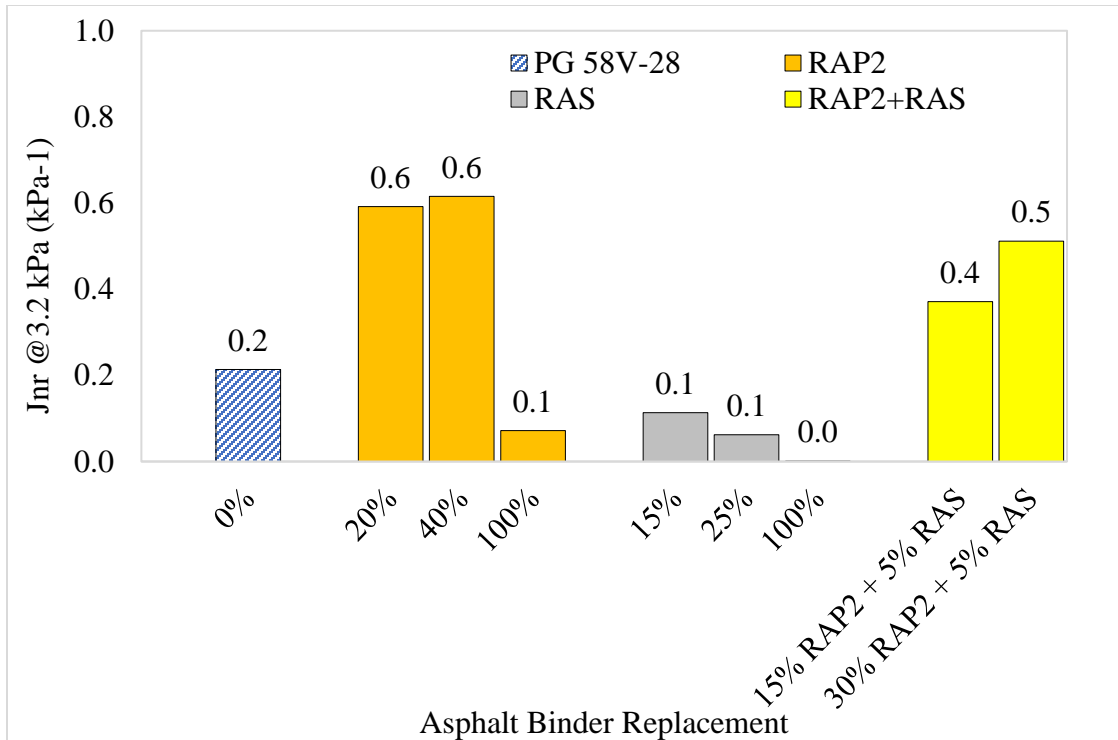


Figure 4.16: Effect of increase in ABR on J_{nr} @ 3.2 kPa and 64 °C for recycled binder blends with the PG 58V-28 binder

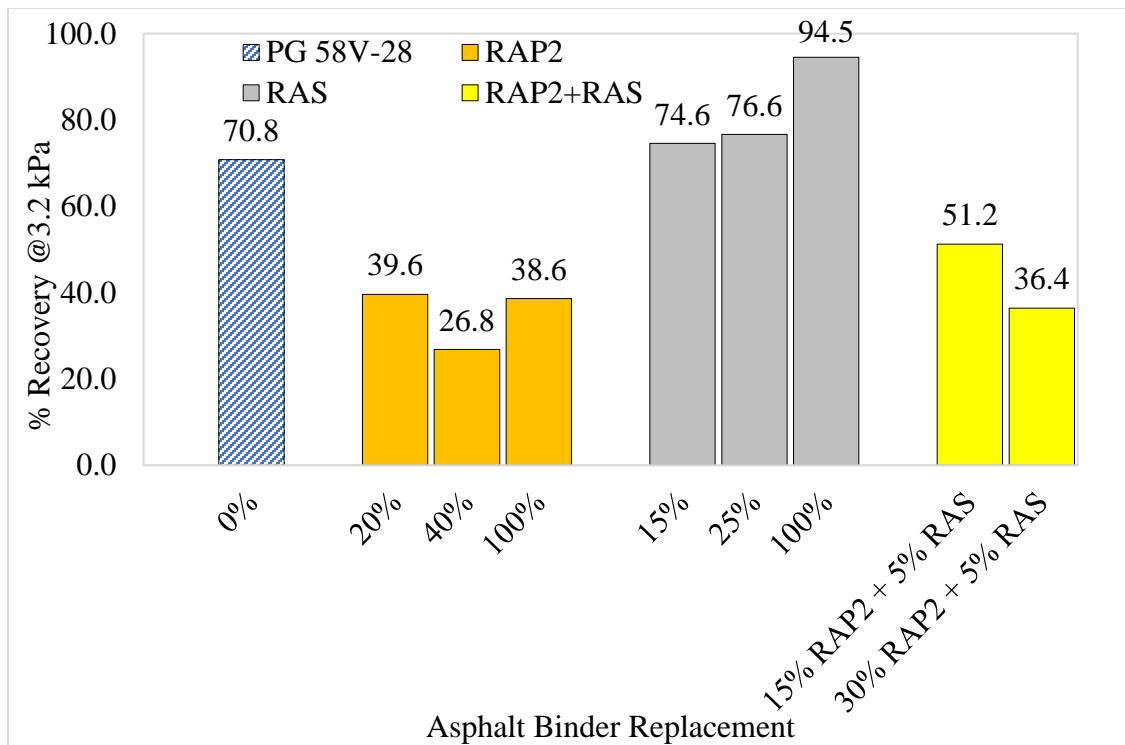


Figure 4.17: Effect of increase in ABR on % recovery @ 3.2 kPa and 64 °C for recycled binder blends with the PG 58V-28 binder

Figure 4.18 and Figure 4.19 present the changes in J_{nr} and percent recovery values at 3.2 kPa after the addition of RAs in the recycled asphalt blends with high ABR. The recycled asphalt binder blends with RAs had high J_{nr} values than those without RAs and the control blend except for the RAS blends which had higher J_{nr} values than the corresponding blend without RAs but lower than the control (Figure 4.18). This indicates that the RAM type had a higher impact on the J_{nr} than the ABR content of the recycled blend. Furthermore, the J_{nr} values of recycled asphalt binder blends with RA2 seemed to be consistently higher than those with RA1 regardless of the RAM type or content. For recycled asphalt binder blends prepared with the PG 58V-28 binder, blend with 40% RAP2 was the only one evaluated with RAs, using RA1. As expected, the J_{nr} of the blend with RA1 was higher than that without a RA.

The percent recovery at the stress level of 3.2 kPa of the recycled asphalt binder blends decreased with the addition of the RAs (Figure 4.19). The recycled asphalt binder blends with RA1 had higher percent recovery values than those with RA2, regardless of the RAM type or content. Comparing the two controls of the blends (i.e., 20% RAP1 with PG 58S-28 and 20% RAP2 PG 58V-28), it was clear that the PG 58V-28 had polymer modification as it shows the highest percent recovery (39.6%) whilst the PG 58S-28 blend doesn't show any. The effect of polymer modification is reflected after the addition of RAs to high ABR blends as well. The 40% RAP2 recycled binder blend prepared with PG 58V-28 and dosed with RA1 had a higher percent recovery than the corresponding blend prepared with PG 58S-28 and RA1. Moreover, this blend had the highest percent recovery among all recycled asphalt binder blends with RAs.

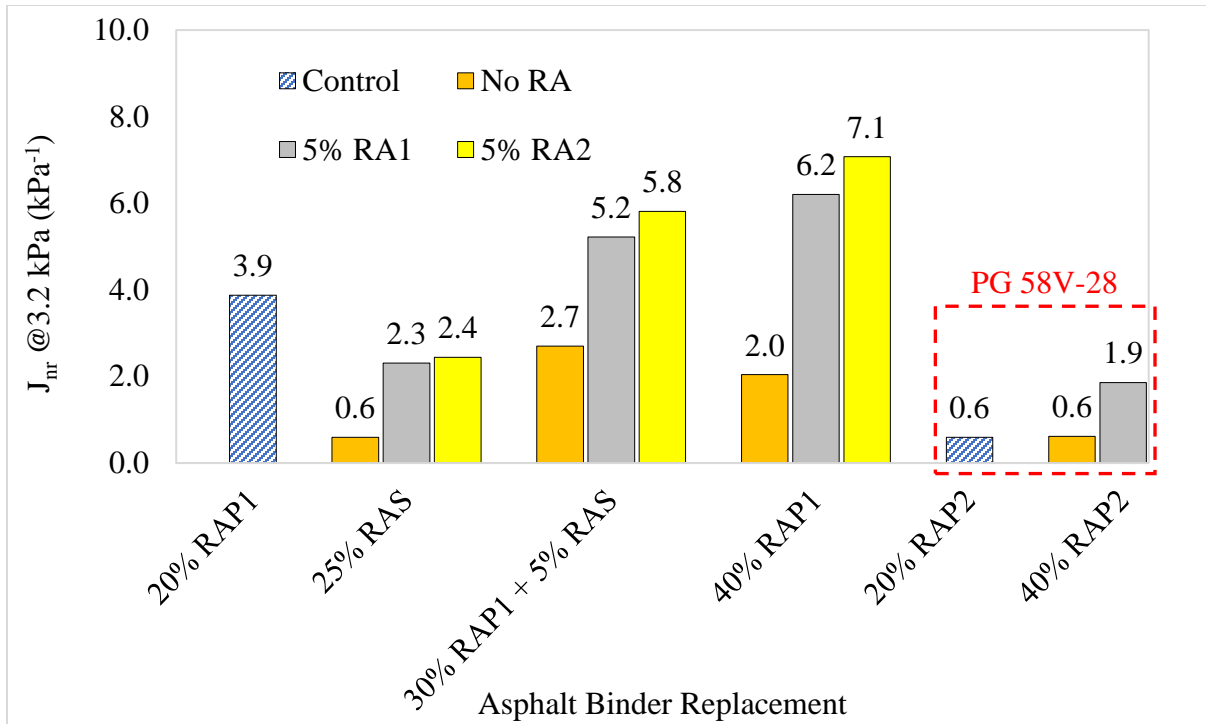


Figure 4.18: Effect of addition of RAs on J_{nr} @ 3.2 kPa and 64 °C

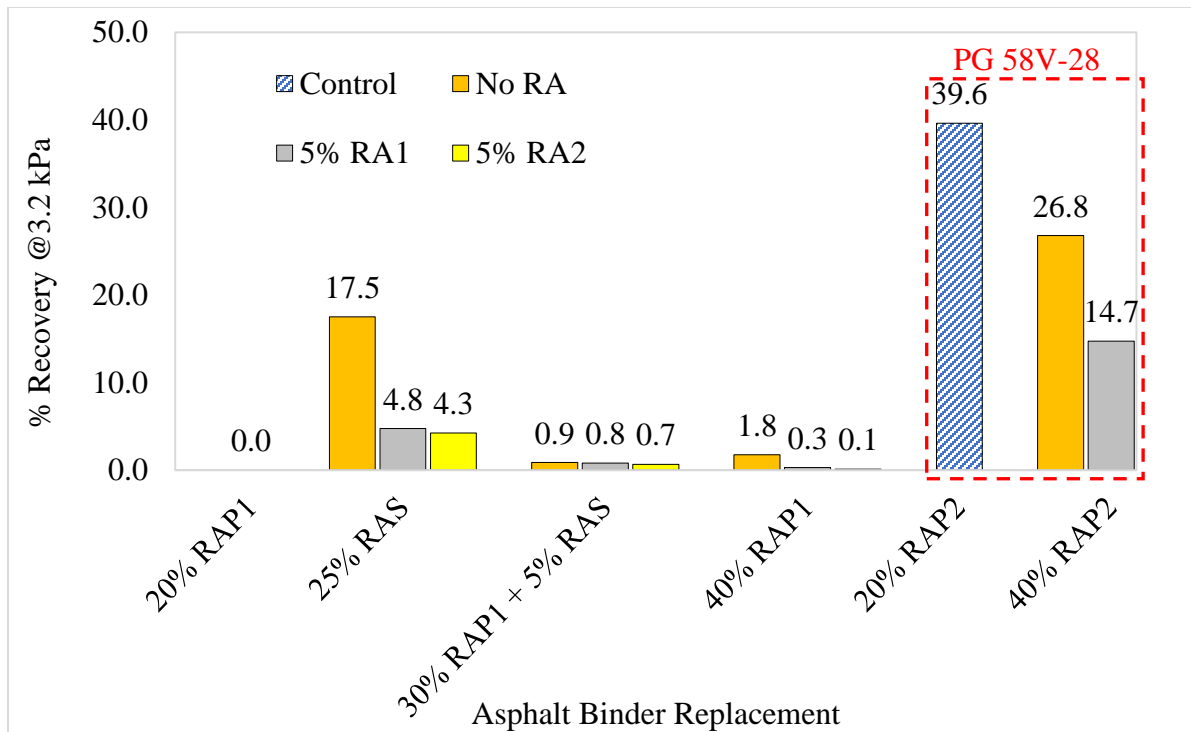


Figure 4.19: Effect of addition of RAs on % recovery @ 3.2 kPa and 64 °C

The MSCR tests for South Dakota recycled binder blends were performed at 58 °C after RTFO conditioning. Figure 4.20 and Figure 4.21 present the J_{nr} and percent recovery at the stress level of 3.2 kPa of the recycled binder blends prepared with the PG 58S-34 and SD RAP, after adding 20%, 35%, and 50% RAP. As shown in Figure 4.20, the J_{nr} values decrease with an increase in ABR from RAP indicating the stiffening properties introduced by RAP in the blends. The percent recovery of these blends was found to be influenced by the J_{nr} values as well. For instance, the percent recovery of the PG 58S-34 base binder (53.14%) was almost similar to that of the RAP (49.28%); hence indicating that the high percent recovery of the RAP was influenced by the low J_{nr} value (0.021 kPa⁻¹).

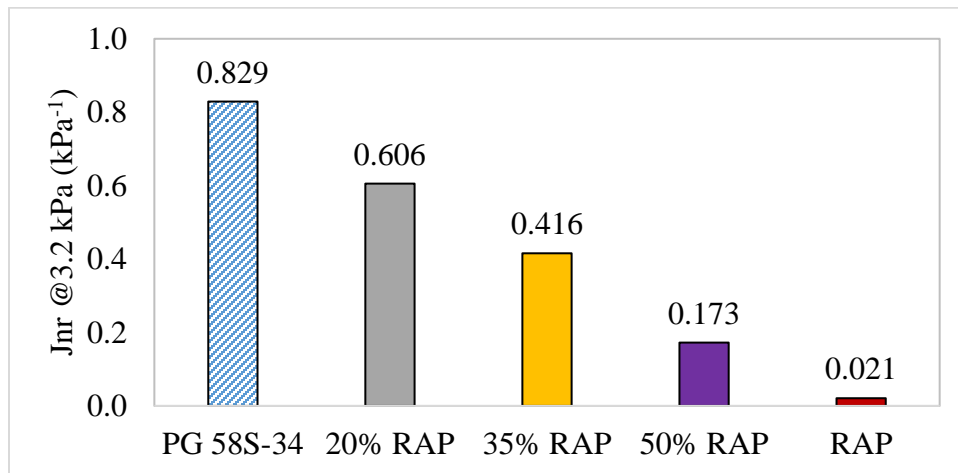


Figure 4.20: Effect of increase in ABR on J_{nr} @ 3.2 kPa and 58 °C for recycled binder blends with the PG 58S-34 binder

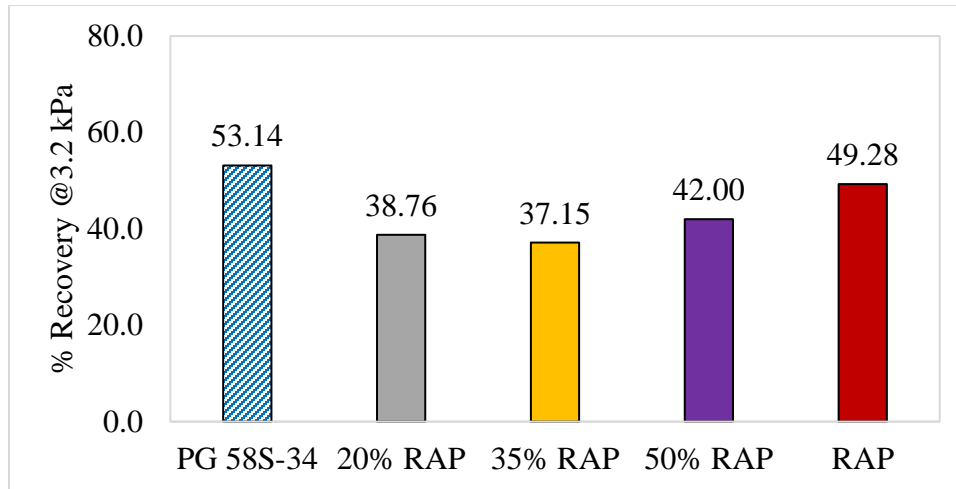


Figure 4.21: Effect of increase in ABR on % recovery @3.2 kPa and 58 °C for recycled binder blends with the PG 58S-34 binder

After adding the RAs into the recycled asphalt binder blends, the Jnr value was higher compared to the control blend (20% RAP) and the recycled binder blends (35% RAP and 50% RAP) without RAs as shown in Figure 4.22. The effectiveness of the RAs on the Jnr value was dependent on its type and the quantity of the ABR in the blend. For instance, the 35% RAP blend with RA5 had the highest Jnr value because RA5 was a petroleum-based (asphalt flux) RA and acted as a softener; thus, a higher RA dosage (45% by weight of total binder) was required for its LTPG to match that of the 20% RAP. When the Jnr values of the recycled binder blends with rejuvenators were compared based on the ABR contents of the blend, the 35% RAP seemed to have higher values than the corresponding 50% RAP. For recycled binder blends with RAs, RA3 and RA4 had higher Jnr values for the 35% RAP and 50% RAP blend, respectively. As expected, the incorporation of RAs into the blend decreased their percent recovery (Figure 4.23). Among the recycled binder blends with RAs, those with RA1 had an almost similar recovery, and they were the highest of all. No recovery was observed in the recycled binder blend with RA5.

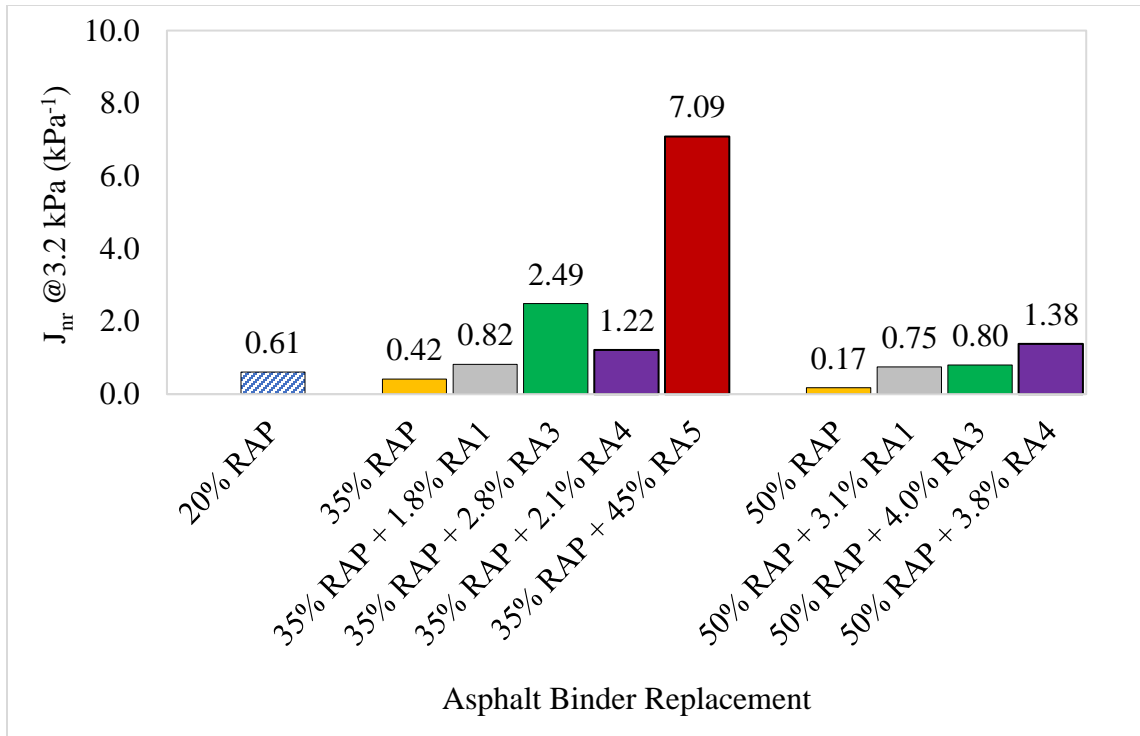


Figure 4.22: Effect of addition of RAs on J_{nr} @ 3.2 kPa and 58 °C for recycled binder blends with the PG 58S-34 binder

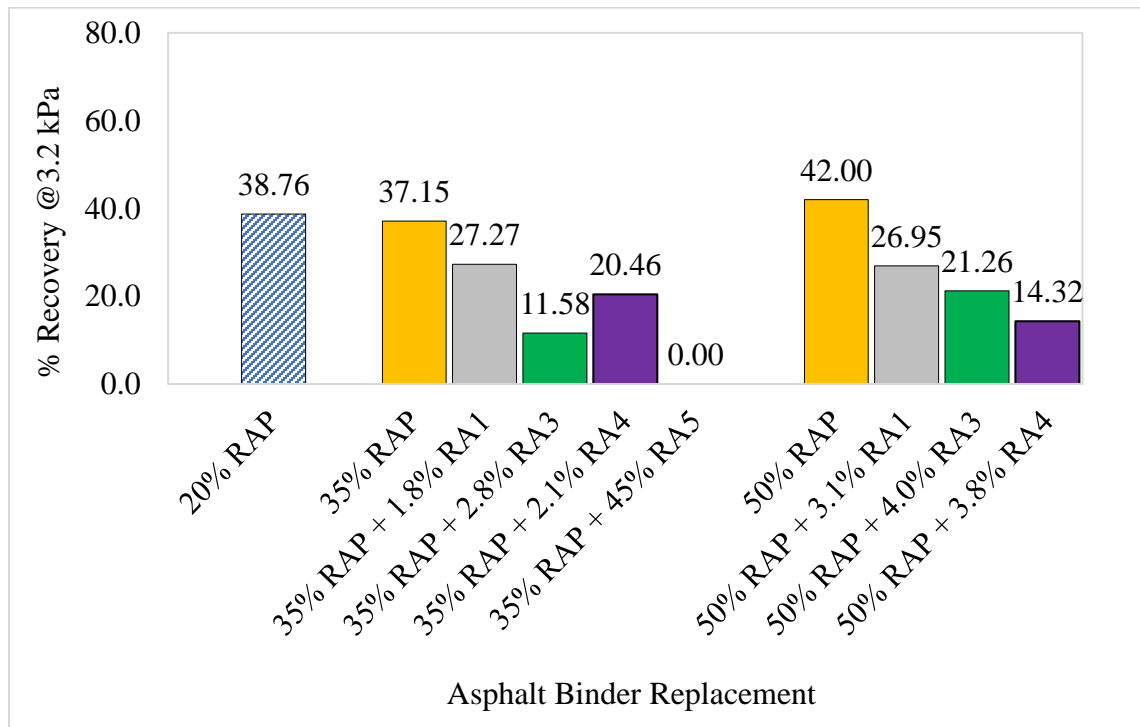


Figure 4.23: Effect of addition of RAs on % recovery @ 3.2 kPa and 58 °C for recycled binder blends with the PG 58S-34 binder

As can be seen in Figure 4.24, the percent recovery was influenced by both the RAM type and base binder type. When tested by themselves, RAMs (specifically RAS) had higher percent recovery and lower J_{nr} values. Base binder with polymer modification (PG 58V-28 and PG 58S-34) had reasonable both percent recovery and J_{nr} values depending on the extent of modification. As expected, the base binder without polymer modification (PG 58S-28) shows low percent recovery and high J_{nr} values. Hence, the rate of decrease of percent recovery due to RAs was dependent on the base binder type, RAM type, as well as their contents.

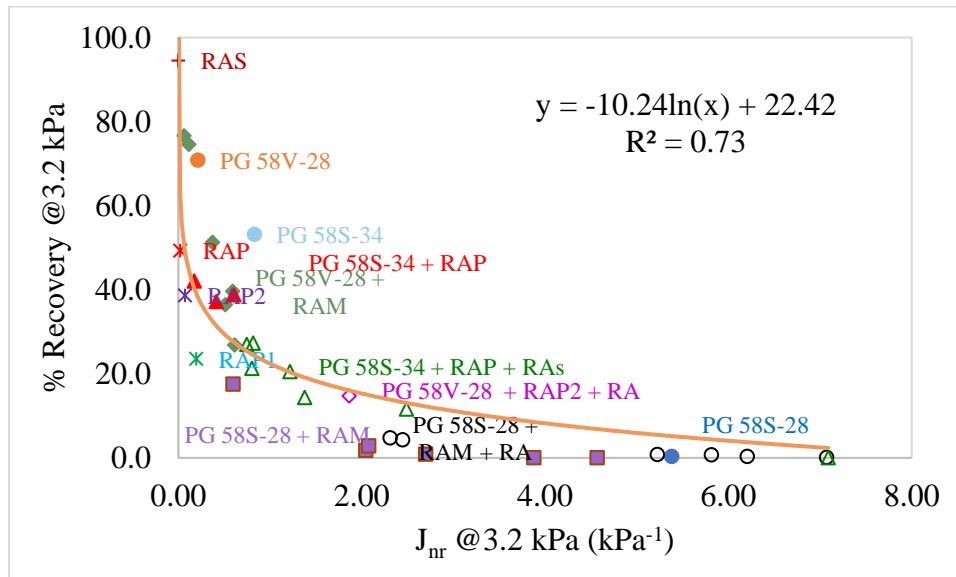


Figure 4.24: Relationship of J_{nr} and % recovery for all recycled binder blends

4.4. Viscoelasticity and Aging Properties

The viscoelastic and aging properties of the recycled binder blends were evaluated using the black space diagram and the G-R parameter. The black space diagrams show the change (shift) in recycled binder viscoelastic properties because of the aging or rejuvenation effect. The black space diagram is a plot of $|G^*|$ versus δ at 15 °C and 0.005 rad/sec. The G-R thresholds (180 kPa and 600 kPa) proposed by Rowe (2011) during a discussion on paper by Anderson et al. (2011) are

used to demarcate initiation (onset) of block cracking and significant cracking, respectively. The binders with $|G^*|$ and δ values falling between the onset cracking zone and significant cracking zone are said to be in the damage zone. The G-R parameter considers both stiffness and embrittlement properties of the binder and it indicates the block cracking potential at intermediate temperature.

Figure 4.25 and Figure 4.26 show the black space diagrams of the RAM binders, PG 58S-28 virgin binder, and the recycled binder blends with and without RA1 at unaged (original) and after RTFO plus 40 hours-PAV conditions, respectively. As can be seen from Figure 4.25, the binder from RAS is in the block cracking zone whereas the remaining samples were in the no cracking zone. For samples that were in the no cracking zone, the binder from RAP1 has the highest $|G^*|$ and lowest δ whereas vice versa is true for the virgin binder (PG 58S-28). When the recycled binder blends were compared against the control (20% ABR), the recycled binder blends without the RA had higher $|G^*|$ values but lower δ values indicating poor relaxation properties. The recycled binder blend with RAS only (25% ABR) had the worst relaxation properties with stiffness values close to the recycled binder blend with RAP1 only (40% ABR). After, the addition of the RA (5% of RA1), the relaxation properties of the recycled binder blends improved (shifting to the right-bottom corner) compared to the control except for the blend with RAS only (25% ABR+5% RA1).

After RTFO plus 40 hours-of PAV conditioning, the data points of all the samples shifted to the left-top corner of the black space diagram (Figure 4.26). One should note that the binder from RAS was too stiff to be tested after RTFO plus 40 hours-PAV aging. The virgin binder and the recycled binder blend with RAS only and without RA1 (25% ABR) moved to the cracking zone. The binder from RAP1 and the recycled binder blend with RAP only and without RA1 (40% ABR) were in the damage zone. The recycled binder blend with 30% RAP and 5% RAS (35% ABR) had similar

properties as the control, and they are both failing on the cracking initiation boundary. For recycled binder blends with RA1, the 25% ABR recycled binder blend was on the boundary as the control but with lower δ values. The 35% ABR and 40% ABR recycled binder blends remained in the no cracking zone, with almost similar values.

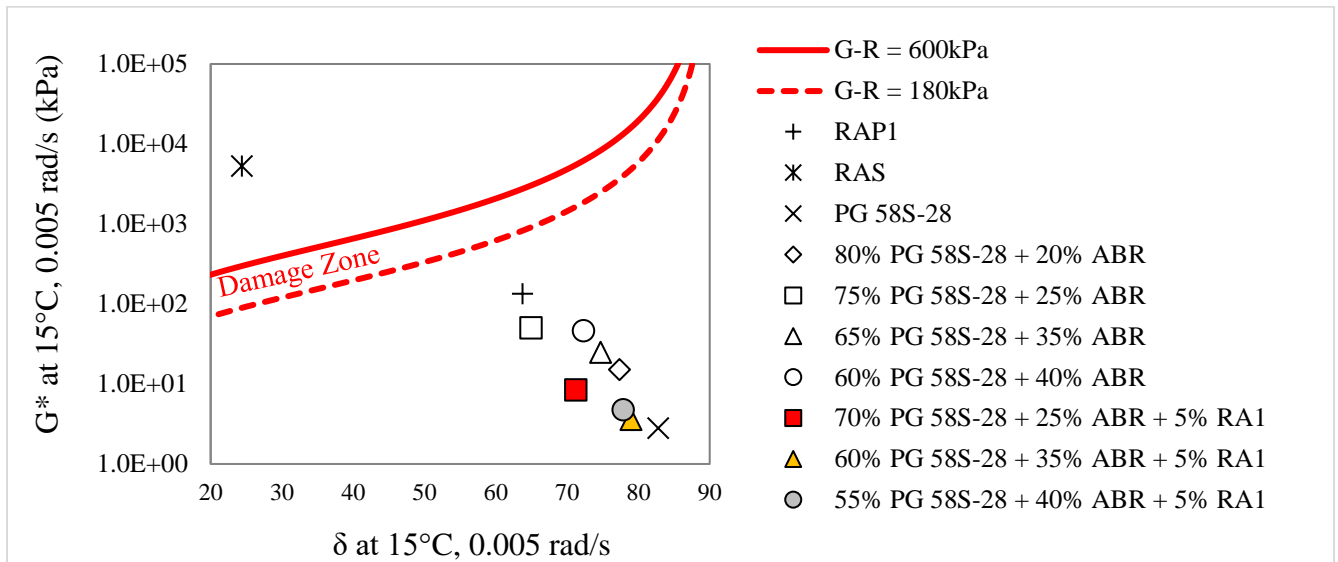


Figure 4.25: Black space diagram of the recycled binder blends prepared with the PG 58S-28 binder and with or without RA1 at the unaged condition

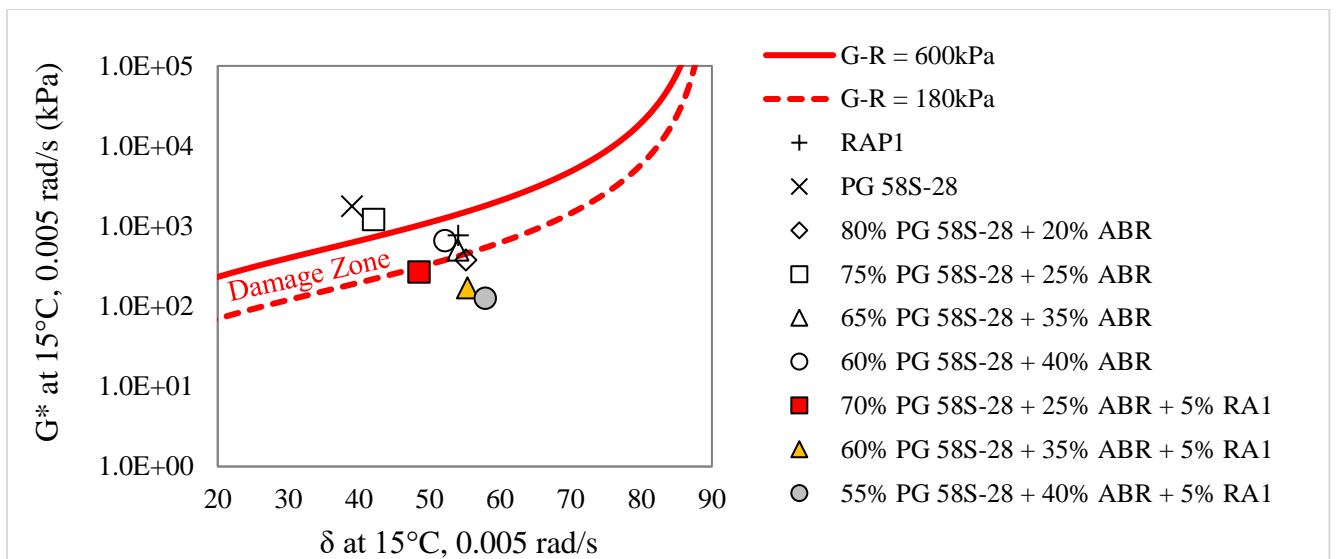


Figure 4.26: Black space diagram of the recycled binder blends prepared with the PG 58S-28 binder and with or without after RTFO plus 40 hours PAV

The black space diagrams of recycled binder blends with and without RA2 at the unaged condition and after RTFO plus 40 hours PAV conditioning are shown in Figure 4.27 and Figure 4.28, respectively. At unaged condition, after the addition of RA2 the recycled binder blends shifted to the lower-right corner. In addition, they showed similar properties as with RA1 (Figure 1) but with stiffness properties like that of the virgin binder (PG 58S-28). After RTFO plus 40 hours of PAV conditioning, the recycled binder blends moved to the upper-left corner of the black space diagram as expected. The recycled binder blend with RAS only and RA2 (25% ABR + 5% RA2) moved into the damage zone. The other recycled binder blends with RA2 (35% ABR+5% RA1 and 40 % ABR + 5% RA2) remained in the no cracking zone with almost similar viscoelastic properties.

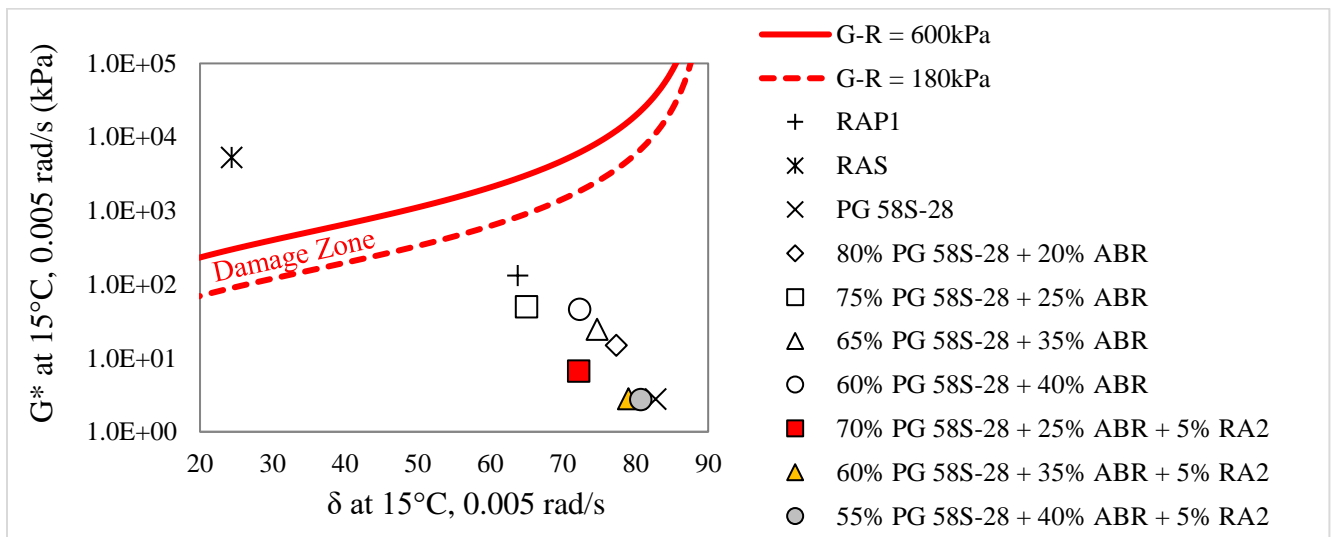


Figure 4.27: Black space diagram of the recycled binder blends prepared with the PG 58S-28 binder and with or without RA2 at the unaged condition

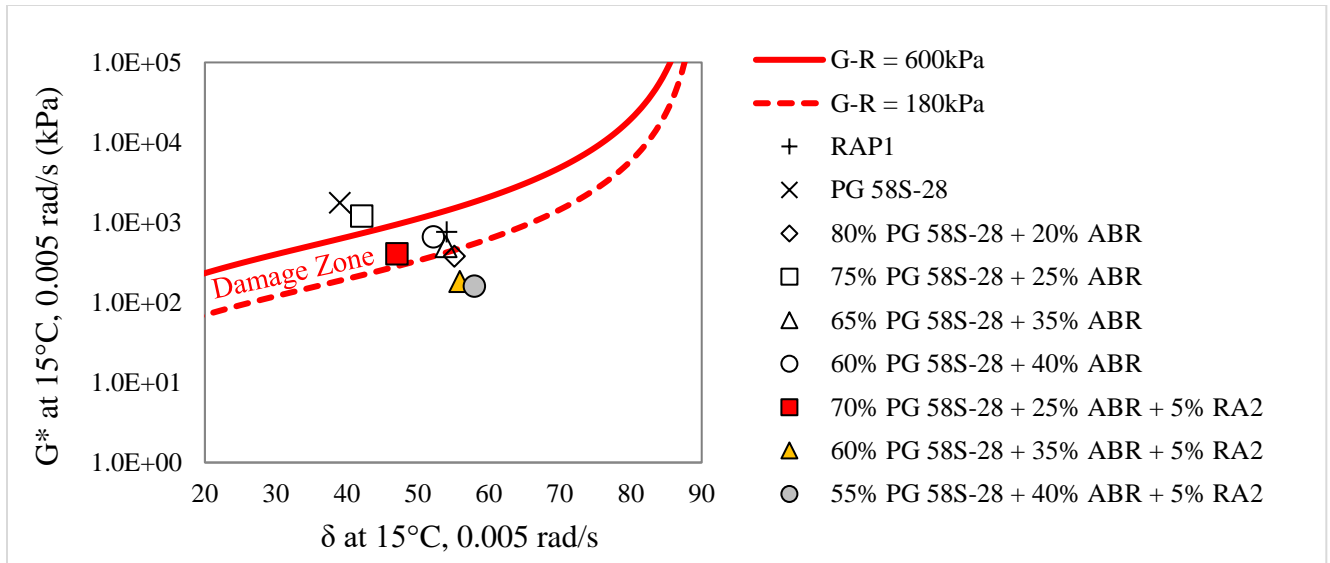


Figure 4.28: Black space diagram of the recycled binder blends prepared with the PG 58S-28 binder and with or without RA2 after RTFO plus 40 hours PAV

Figure 4.29 and Figure 4.30 present the black space diagrams of the binder from RAP2, the virgin binder PG 58V-20, and the recycled binder blends with and without RA1. At the unaged condition, the binder from RAP2 had values close to the onset of cracking boundary whilst the remaining samples were in the no cracking zone. When the recycled binder blends without RA1 were compared to the control, the 25% ABR had the highest $|G^*|$ and lowest δ indicating poor relaxation properties. The 35% ABR and 40% ABR recycled binder blends had almost $|G^*|$ and δ values as the control. Adding RA1 on the 40% ABR recycled binder blend (40% ABR+5% RA1) lowered the $|G^*|$ value but the δ value did not change.

As expected after RTFO plus 40 hours PAV, the data points shifted to the upper-left corner of the black space diagram indicating loss of relaxation properties due to aging. The binder from RAP2 and the recycled binder blend with RAS only (25% ABR) crossed into the cracking zone, the remaining were in the damage zone; except the 40% ABR recycled binder blend with RA1 which was on the boundary of the onset of cracking. It is worth noting that, the proposed G-R thresholds

(180 kPa and 600 kPa) were developed using limited data of unmodified binder, thus their application into PMB blends may be questionable.

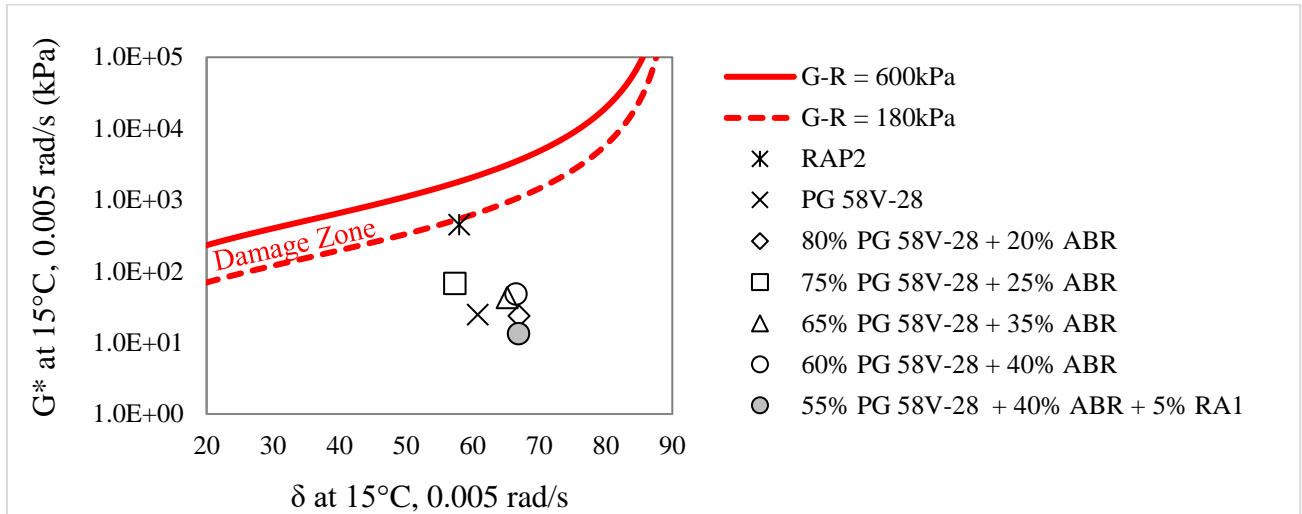


Figure 4.29: Black space diagram of the recycled binder blends prepared with the PG 58V-28 binder and with or without RA1 at the unaged condition

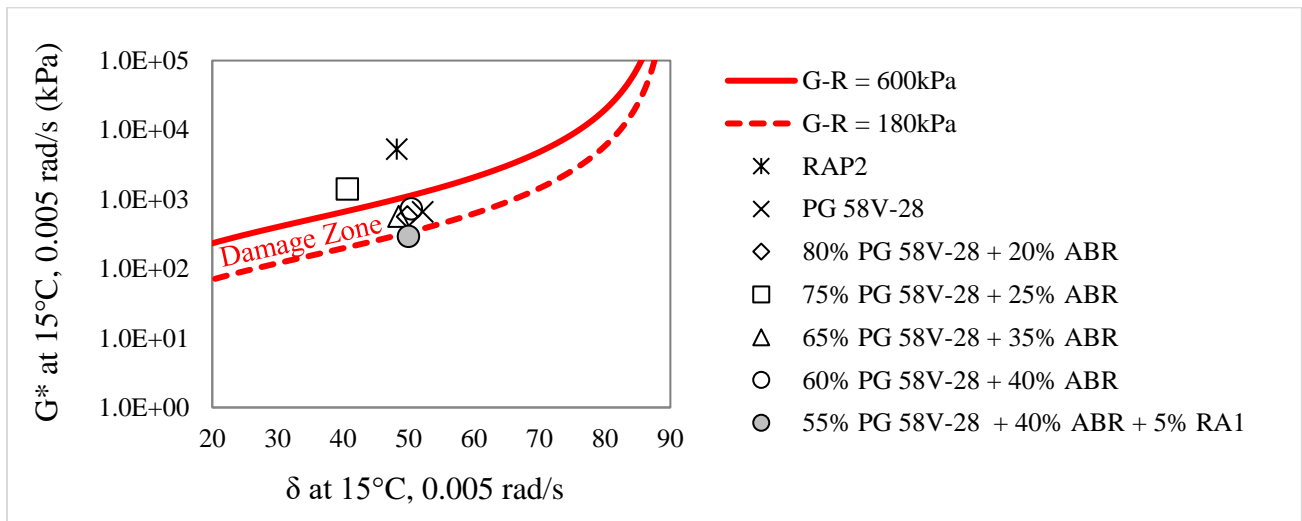


Figure 4.30: Black space diagram of the recycled binder blends prepared with the PG 58V-28 binder and with or without RA1 after RTFO plus 40 hours PAV

The aging resistance of the recycled binder blends was assessed using the G-R aging index. Figure 4.31 shows the G-R aging index of the recycled binder blends prepared from the PG 58S-28 binder and RAP1 and/or RAS binders with and without RA1. When the recycled binder blends with and without RA1 were compared against each other, the recycled binder blends with the RA had a higher aging index than those without the RA, indicating increased oxidative aging susceptibility due to the addition of RA1. However, except for the 35% ABR with RA1; none of the recycled binder blends exceeded the aging index of the control blend.

For the recycled binder blends prepared from the PG 58S-28 and RAP1 and/or RAS binders, their G-R aging index values increased after the addition of RA2 as expected but exceeded the control blend (20% ABR) as shown in Figure 4.32. For the recycled binder blends with RA2, the 25% ABR had the lowest aging index whilst the 40% had the highest aging index value.

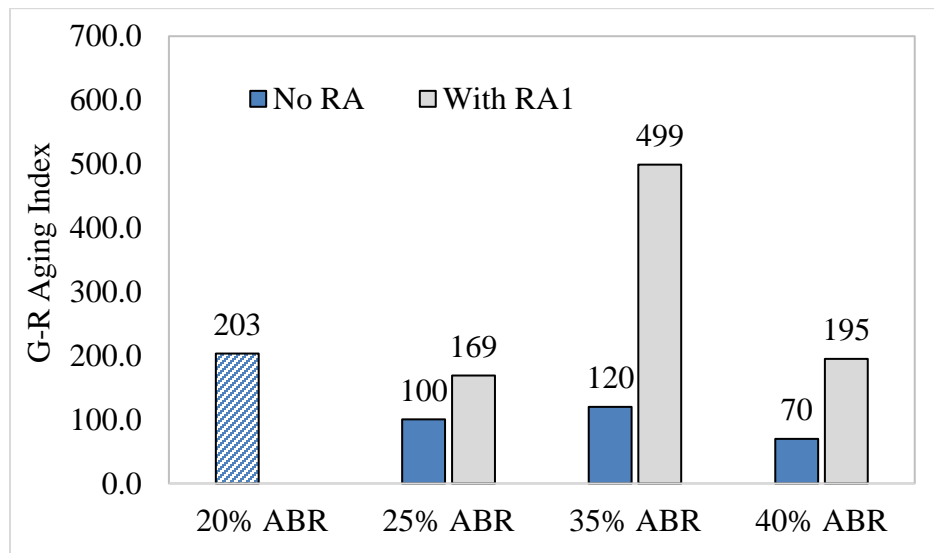


Figure 4.31: G-R aging index of the recycled binder blends prepared with the PG 58S-28 binder and with or without RA1

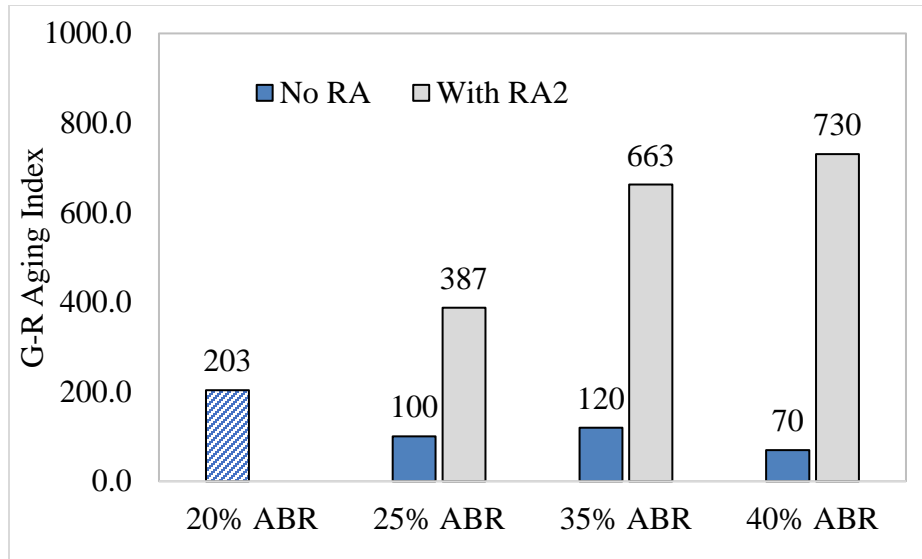


Figure 4.32: G-R aging index of the recycled binder blends prepared with the PG 58S-28 binder and with or without RA2

The G-R aging index of the recycled binder blends prepared from the PG 58V-28 binder and RAP2 and/or RAS binders is shown in Figure 4.33. As can be seen, the control had the highest G-R index of all the recycled binder blends. The effect of RAM in the blend seemed to be dependent on the blend itself, with the 25% ABR having the highest value. Moreover, adding RA1 on the 40% ABR increased its aging index.

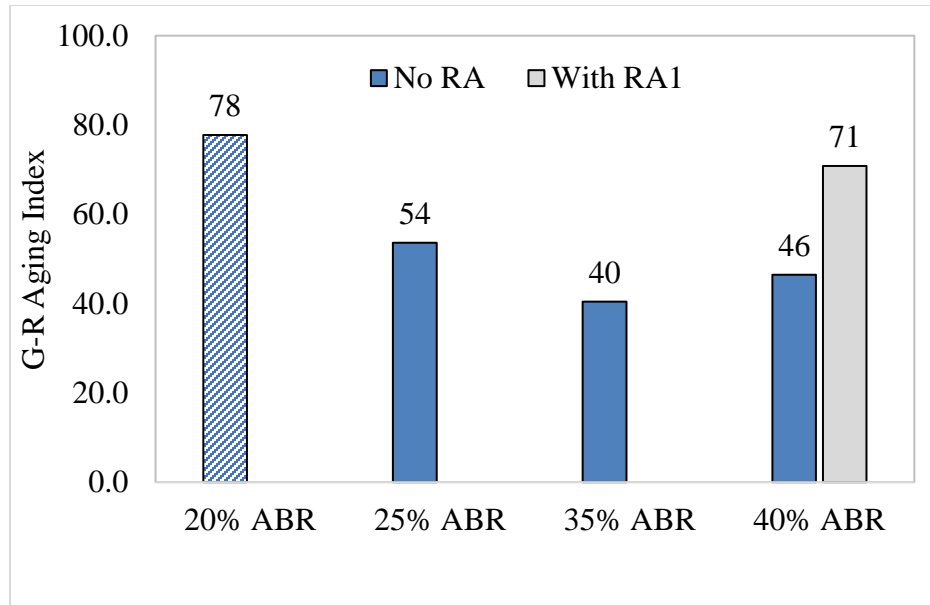


Figure 4.33: G-R aging index of the recycled binder blends prepared with the PG 58V-28 binder and with or without RA1

Figure 4.34 and Figure 4.35 present the black space diagrams of the recycled binder blends prepared from PG 58S-24 and SD RAP binder at the unaged condition and after RTFO plus 60 hours PAV conditioning. From Figure 4.34, it can be noted that at unaged conditions, the virgin binder PG 58S-34 and the recycled binder blends with and without RAs were in the no cracking zone (i.e., below the 180 kPa threshold). The SD RAP binder was in the damage zone. The 35% ABR recycled asphalt binder blend without RA had a lower $|G^*|$ value than the corresponding 50% ABR, indicating the stiffening effect of increased RAP. However, their δ values were approximately equal. Moreover, incorporating the RAs to the recycled binder blends dropped the $|G^*|$ to almost the same value as that of the control blend (20% ABR) but with slightly different δ values regardless of the RAP content of the recycled blend. One should note that the 35% ABR recycled binder blend with RA5 (petroleum flux) was too soft, making it impossible to be tested at the unaged state.

After RTFO plus 60 hours of PAV conditioning, the data points shifted from the lower-right corner to the upper-left corner of the black space diagram indicating increased stiffness and brittleness in the sample due to the aging effect (Figure 4.35). At this state, the SD RAP binder and the 50% blend without RA were in the significant cracking zone (i.e., above the 600 kPa threshold). The virgin binder (PG 58S-34), the 35% ABR blend without recycling, and the 35% ABR and 50% ABR blends with RA3 were in the damage zone. Moreover, the control blend (20% ABR), the 35% ABR and 50% ABR recycled binder blends with RA1, RA4, and RA5 (for the 35% ABR only) remained in the significant cracking zone despite the shifting due to aging. Furthermore, after RTFO plus 60 hours of PAV aging, the 50% ABR blend without RA had a higher $|G^*|$ value than the corresponding 30% ABR and the control (20% ABR) blend. The control had a higher δ value than the 35% ABR and 50% ABR without RAs. With RAs, the $|G^*|$ decreased but the recycled binder blends (both 35% ABR and 50% ABR) with RA3 had slightly higher values than the control. The recycled binder blends with RA1 (only the 35% ABR blend), RA4 (both the 35% ABR and 50% ABR), and RA5 had approximately $|G^*|$ as the control blend. The 50% ABR blend with RA1 had the lowest $|G^*|$ value. Except for the 35% ABR with RA3, all recycled binder blends with RAs had higher δ values than the control and their corresponding blends without RAs.

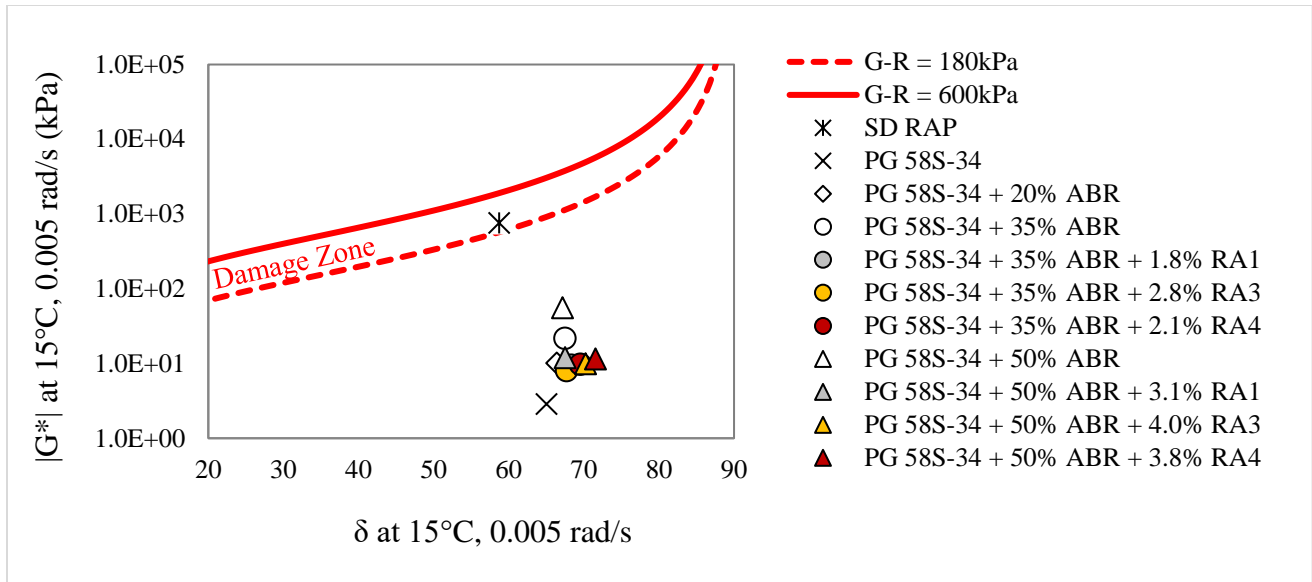


Figure 4.34: Black space diagram of the recycled binder blends prepared with the PG 58S-34 binder and with or without RAs at the unaged state

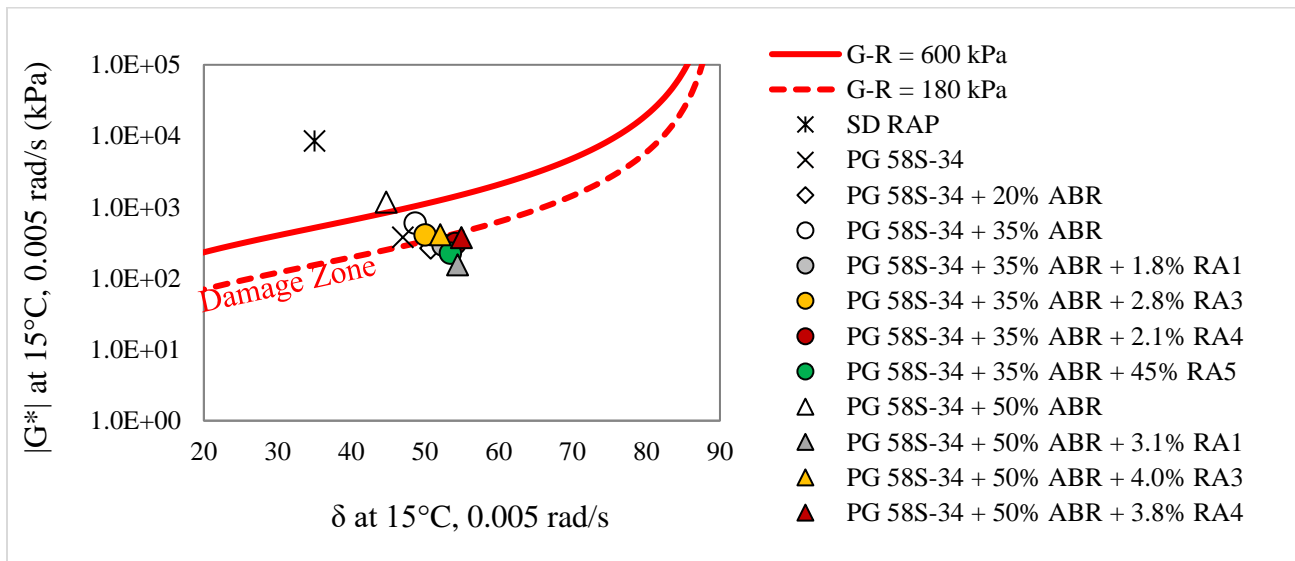


Figure 4.35: Black space diagram of the recycled binder blends with the PG 58S-34 binder and with or without RAs after RTFO plus 60 hours PAV

The G-R aging index results of the recycled binder blends prepared from the PG 58S-34 and the SD RAP binders with and without RAs are shown in Figure 4.36. The control blend (20% ABR) had a lower aging index than all the recycled binder blends with or without RAs, except the 50% ABR blend with RA1, which had the lowest value of all. When the 35% ABR blends were compared among themselves, the aging index of the blends without RA and those with RA1 and RA4 were approximately in the same range whilst that with RA3 had the highest aging index value. For the 50% ABR blends, the blend with RA1 had a lower aging index than that without RA, whereas the RA3 and RA4 had a higher aging index than that without RA with the blend with RA3 having the highest value. Based on the aging index values, RA1 maintained or decreased the oxidative aging susceptibility regardless of the ABR in the blend. RA3 and RA4 seemed to increase the oxidative aging susceptibility of the 30% and 50% ABR blends.

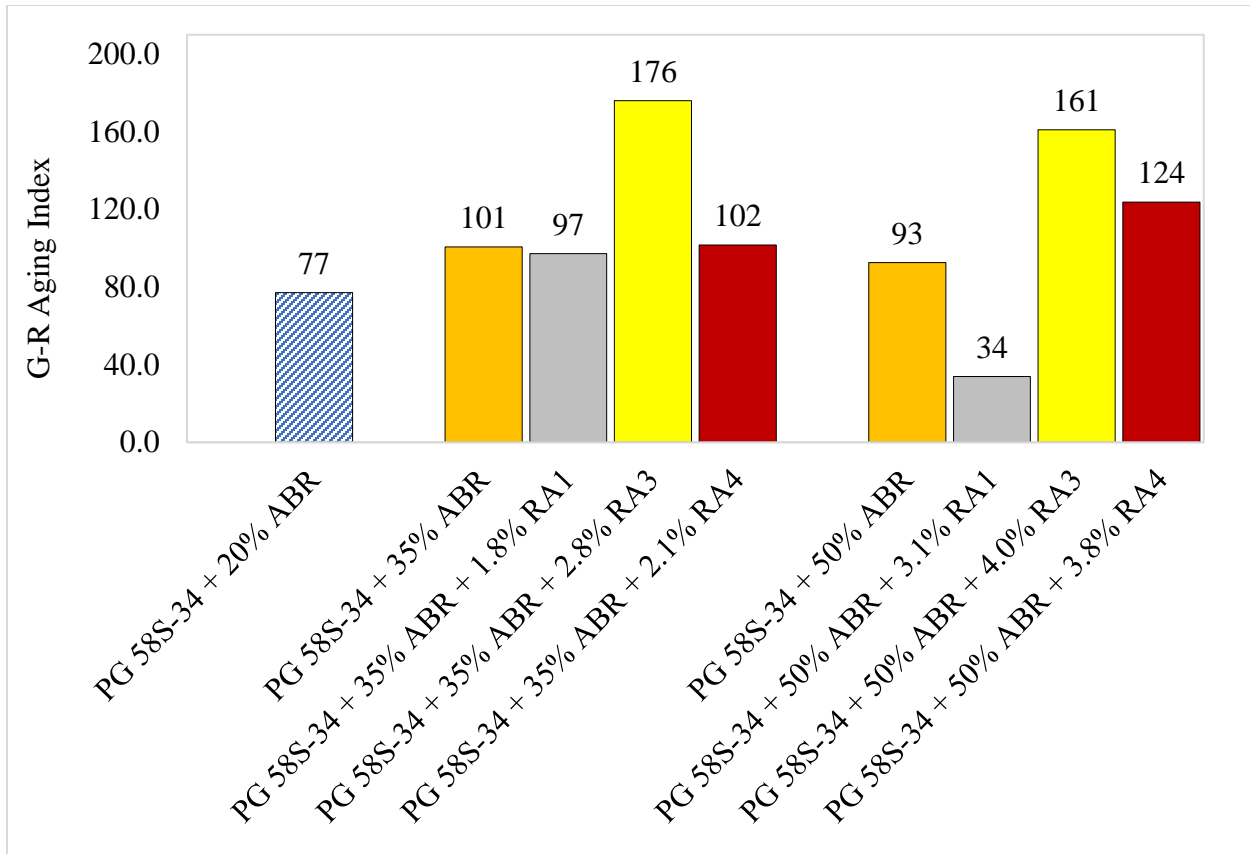


Figure 4.36: G-R aging index of the recycled binder blends prepared with the PG 58S-34 binder and with or without RAs

4.5. Linear Amplitude Sweep (LAS) Test

The linear amplitude sweep (LAS) test was conducted at 28 °C on RTFO plus 40 hours PAV residues of the recycled binder blends. Figure 4.37 and Figure 4.38 presents the number of cycles to failure (N_f) at 2.5% strain of the recycled binder blends prepared with the PG 58S-28 and PG 58V-28 binders without RAs, respectively. As presented in Figure 4.37, adding RAM decreased the N_f of the recycled binder blends; however, the decrease in N_f was not consistent with the increase in RAM contents except for the RAP1+RAS blends. The same trend was observed in recycled binder blends prepared with the PG 58V-28 (Figure 4.38), except the inconsistency was observed in the RAS blends. One should note that when the N_f of the PG 58V-28 binder was higher

than that of the PG 58S-28 binder, so their recycled binder blends. Moreover, the RAS blends for both PG 58S-28 and PG 58V-28 had high N_f than the RAP or RAP + RAS blends, indicating that analysis of heavily oxidized binder with LAS may lead to erroneous interpretations as the cracks may not be homogeneously distributed in the continuum (Karki and Zhou, 2018).

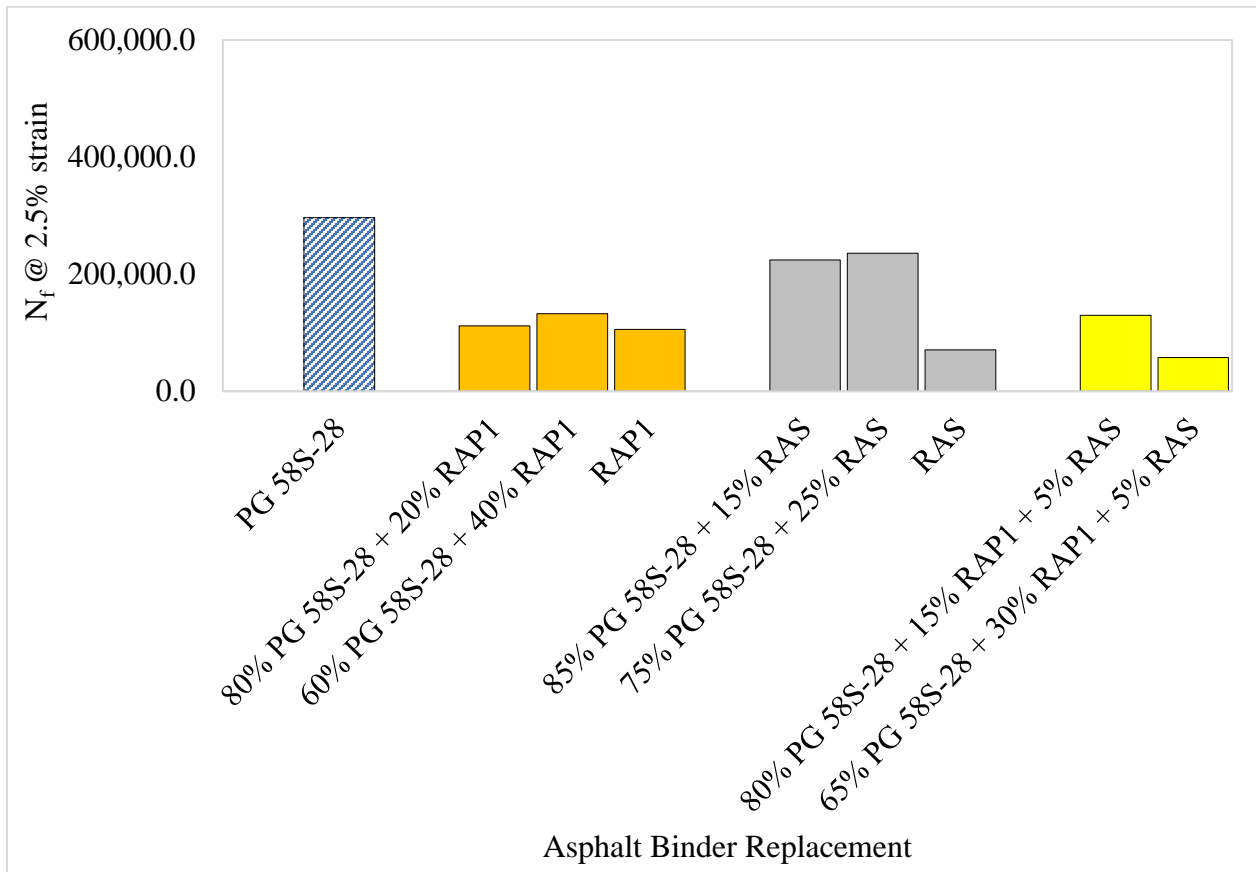


Figure 4.37: N_f at 2.5% strain of the recycled binder blends prepared with the PG 58S-28 binder

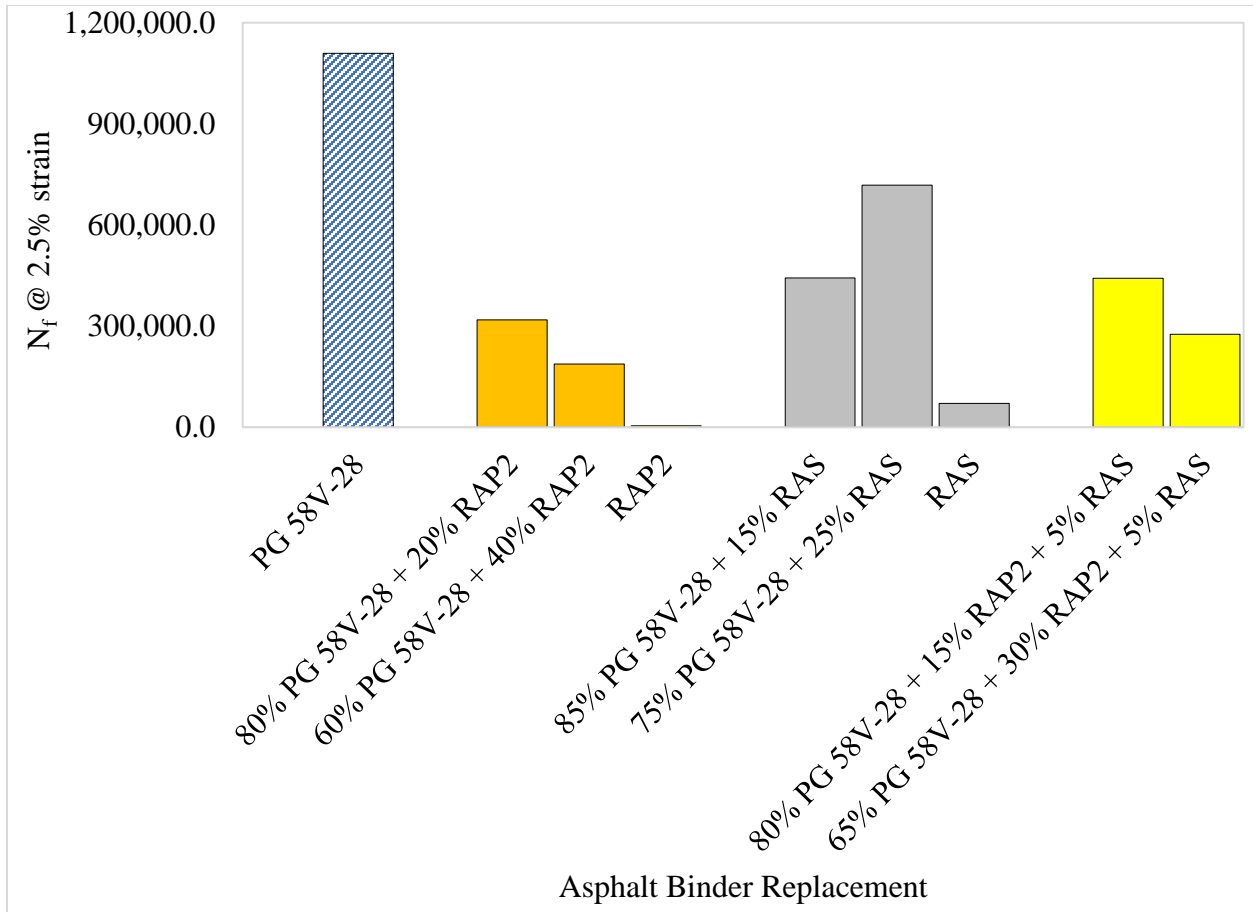


Figure 4.38: N_f at 2.5% strain of the recycled binder blends prepared with the PG 58V-28

Figure 4.39 shows the N_f at 2.5% strain of the recycled binder blends with RAs for both the PG 58S-28 (without the dotted box) and the PG 58V-28 binders. In general, an increase in N_f is observed with the addition of the RAs except for the 40% RAP1 blend with the PG 58S-28. As stated earlier on the influence of RAS binder on N_f results, the blends with RAS had higher N_f even after adding the RAs compared to RAP1+RAS and RAP1 blends. Moreover, the effect of RAs on N_f was not consistent since RA1 was more effective than RA2 for the RAS blends but less effective for the RAP1+RAS and RAP1 blends. In addition, when the effect of RA1 on the N_f of the 40% RAP blend prepared with the PG 58S-28 and PG 58V-28 binders were compared, the blend with the PG 58V-28 binder had a higher N_f than one with the PG 58S-28 despite the dosage

amount of RA1 being the same (5% by weight of total binder) and the two RAPs (RAP1 and RAP2) having almost similar high true temperature grade (86.4 °C) and true intermediate temperature grades (26.2 °C and 27.1 °C). Based on this analysis, it can be inferred that the effect of RAs on the N_f of the recycled binder blends is influenced by the type of the RA itself, RAM type, and content in the recycled binder blend, and the type and content of the base binder.

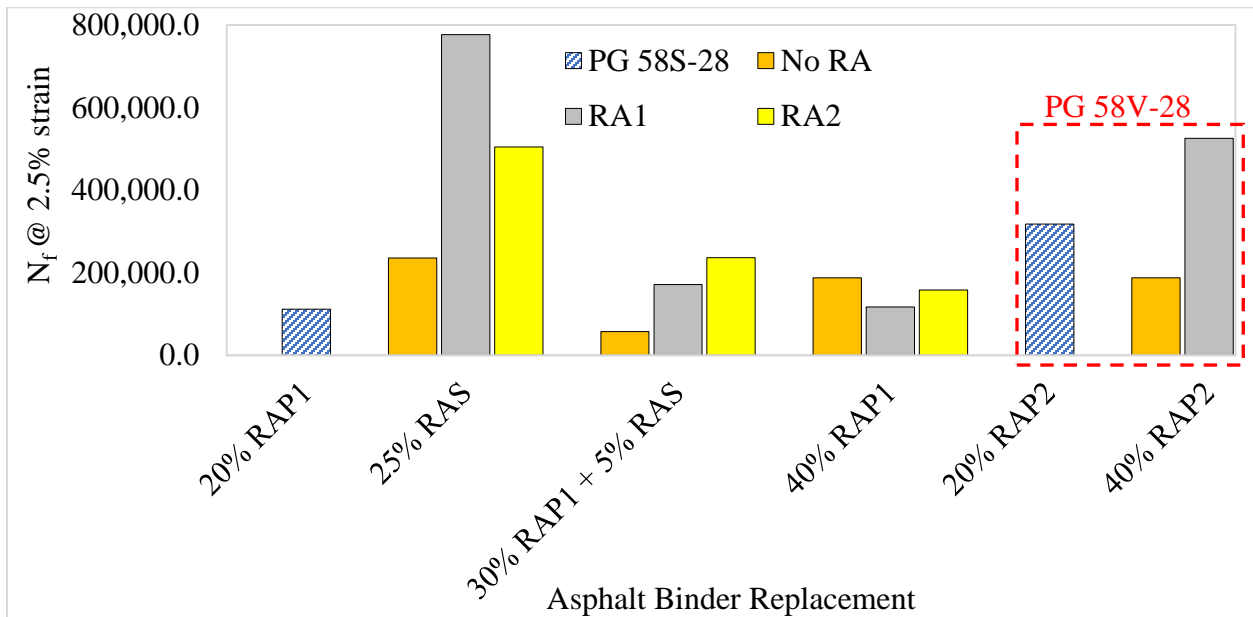


Figure 4.39: N_f at 2.5% strain of the recycled binder blends with RAs

Further analysis of the LAS results using the $|B|$ parameter is presented in Figure 4.40. The $|B|$ parameter is inherently a negative value and indicates a reduction of fatigue life per unit increase in strain, therefore a lower $|B|$ is desired for asphalt binder with better resistance to fatigue resistance. As expected, the high RAM contents recycled binder blends without RAs had higher $|B|$ parameter values than the control blend for the PG 58S-28 blends; with the 25% RAS blend having the highest (4.8). For the PG 58V-28 blend, the control (20% RAP2) and the high RAM content recycled binder blend without RA (40% RAP2) had similar $|B|$ parameter value (3.9).

When RAs were added to the recycled binder blends, the values of the $|B|$ parameter decreased indicating an improvement in fatigue life. For the 35% RAP1+5% RAS and 40% RAP1 blends, the $|B|$ parameter value of the blends with RA1 was higher by one unit compared to that with RA2. Moreover, they were both lower than that of the control blend. The $|B|$ parameter of the 25% RAS recycled binder blends were the same for both RA1 and RA2 RAs (4.1), and it was the highest among the recycled binder blends with RAs. For the PG 58V-28 blend, the $|B|$ parameter value decreased by one unit after the addition of RA1 compared to the control and the 40% RAP2 recycled binder blend without a RA. Based on this analysis, the reduction in fatigue life of the recycled binder blends was dependent on the RAM and base binder (type and contents) and the type of RAs.

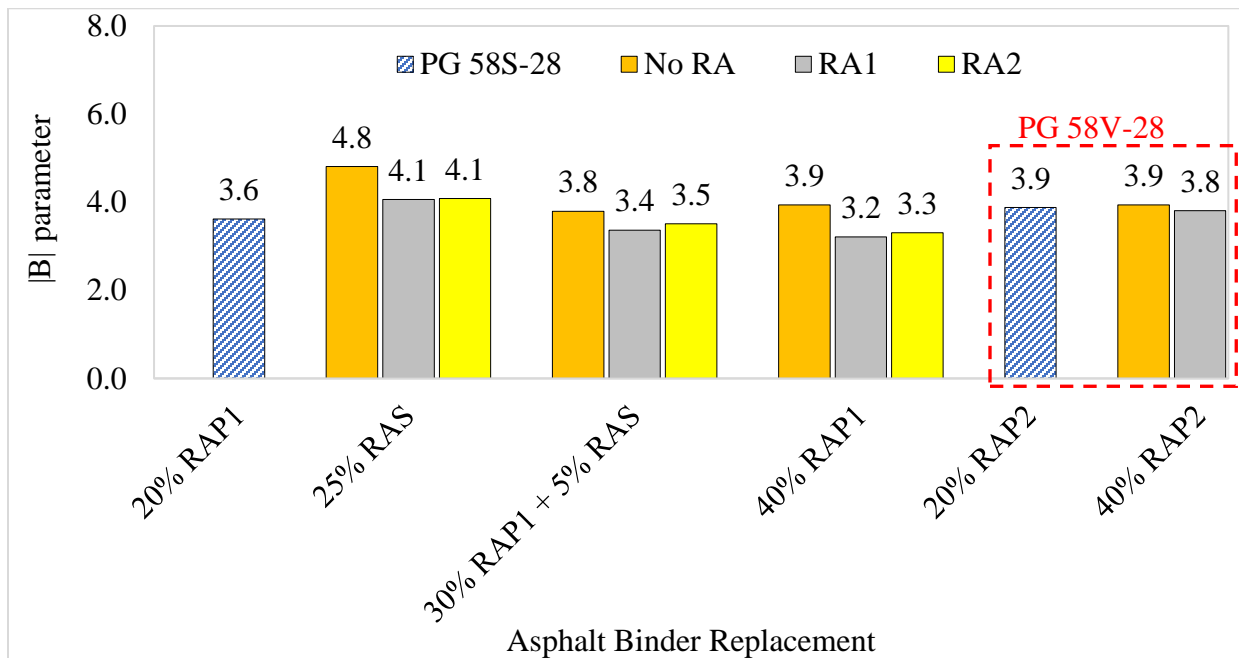


Figure 4.40: $|B|$ parameter of the recycled binder blends with and without RAs

4.6. Extended Bending Beam Rheometer (BBR) Test

The extended bending beam rheometer (BBR) test was conducted per AASHTO TP 122-16 to evaluate the thermal properties of the recycled binder blends while considering their physical hardening characteristics. Physical hardening is a phenomenon that leads to an increase in asphalt binder stiffness when it is stored at a temperature below room temperature. Tabatabaee et al. (2012) showed that the rate of physical hardening in asphalt binder is high at the glass transition temperature (T_g) and insignificant beyond the T_g limits. Therefore, for this study, the recycled binder blends were conditioned at the glass transition temperature. The T_g of the recycled binder blends was obtained using the Differential Scanning Calorimetry (DSC) after RTFO plus 40 hours of PAV aging. One should note that only recycled binder blends prepared with the PG 58S-28 binder as a base binder, with RAs were evaluated with this test and their results are presented in Table 3. According to Tabatabaee et al. (2012), among others, the T_g influences the low-temperature properties of asphalt binders. Moreover, Moraes and Bahia (2015) found that oxidative aging and increase in asphaltene fractions in the asphalt binder decrease the T_g , thus increasing their cracking susceptibility and durability-related issues. As can be seen in Table 4.3, the T_g of the 25% RAS and 30% RAP1+5% RAS blends with RA1 were higher (more negative) compared to the corresponding with RA2, meaning that RA1 improved the thermal properties of the recycled binder blend. However, for the 40% RAP1, RA2 is more effective than RA1 since T_g was slightly higher. As expected, when the stiffness and m-values after one- and 24-hours conditioning were compared, the transition to glassy behavior increased the brittleness of the recycled binder blends (increase in stiffness) and decreased the stress relation properties (decrease in m values).

Table 4.3: Results of the extended BBR test at T_g conditioning

Recycled Binder Blend	T_g , °C	After One hour of BBR Conditioning		After 24 hours of BBR conditioning	
		S, MPa	m-value	S, MPa	m-value
25% RAS + 5% RA1	-14.5	69	0.340	120	0.289
25% RAS + 5% RA2	-11.1	86	0.313	90	0.288
30% RAP1 + 5% RAS + 5% RA1	-9.4	46	0.389	55	0.358
30% RAP1 + 5% RAS + 5% RA2	-5.2	34	0.403	35	0.382
40% RAP1 + 5% RA1	-18.2	145	0.338	184	0.295
40% RAP1 + 5% RA2	-19.3	183	0.315	195	0.281

Using the stiffness value after one hour and 24 hours of conditioning at T_g of the recycled binder blends, the hardening (stiffness) rate was computed to further understand the effectiveness of the RAs. As shown by Tabatabaee et al. (2012), the hardening rate is the difference of the stiffness values (i.e., $S(60)$ after 24 hours and one hour of conditioning) normalized to the initial stiffness value (i.e., $S(60)$ after one-hour conditioning). In this study, the hardening rates of the recycled binder blend with RA1 were consistently higher than those with RA2 (Figure 4.41), with the 25% RAS having the highest value.

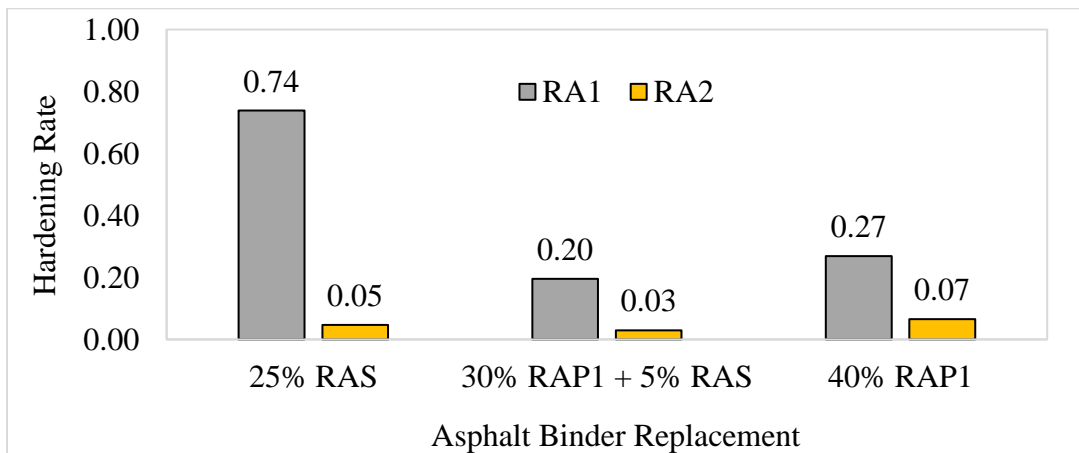


Figure 4.41: Hardening rate of the recycled binder blends with RAs

4.7. Products of Oxidative Aging

Oxidative aging of binders involves a change in their chemical composition and structures. The FTIR-ATR technique was used to assess the increase in the absorbance bands of the carbonyl (C=O) and sulfoxide (S=O) functional groups due to aging. As mentioned in Section 3.4.6, to quantify the increase in absorption, band areas rather than the peak values were used. Figure 4.42 shows the C=O + S=O area of RAs by themselves at an unaged state. From Figure 4.42, the petroleum-based RA (RA5) had the lowest C=O + S=O area than all the bio-based RAs (RA1, RA2, RA3, and RA4). Among the bio-based RAs, RA4 had the highest C=O + S=O area whereas RA2 had the lowest.

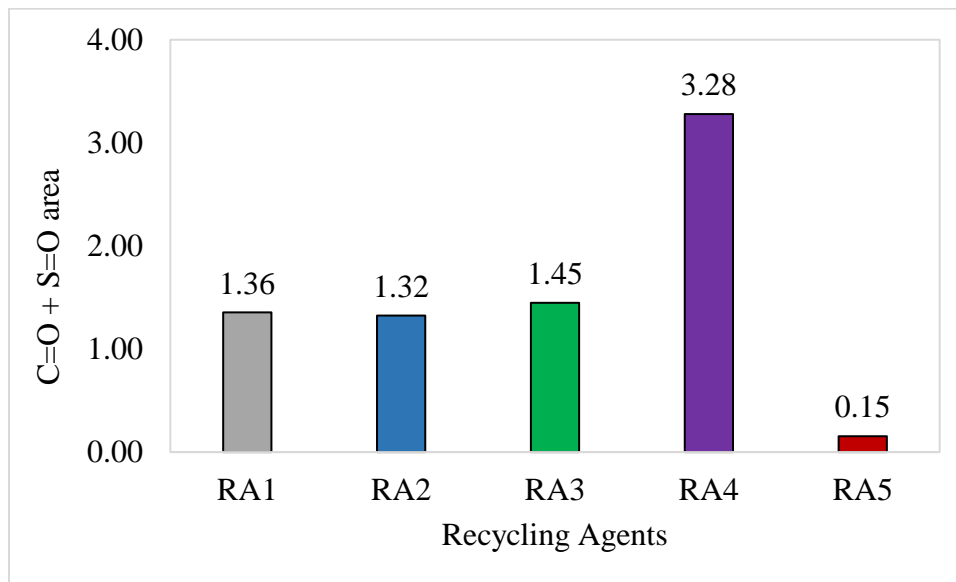


Figure 4.42: C=O + S=O areas of the RAs at unaged state

Figure 4.43 shows the sum of the C=O and the S=O areas of the recycled binder blends (with and without RAs) prepared with the PG 58S-28 binder after RTFO plus 40 hours of PAV conditioning. As can be seen, before the incorporation of RAs, the sum of the C=O and S=O area of the recycled asphalt binder blends with high ABR was higher than that of the control (20% RAP1), and it varied

depending on both the type and content of RAM in the blend. After adding the RAs, the C=O + S=O area decreased depending on the RA type and the RAM type as well. For example, additional of RA1 had lower C=O + S=O area than RA2 on the 25% RAS and 40% RAP1 blends, whereas on the 30% RAP1 + 5% RAS blend, RA2 had less C=O + S=O area than RA1.

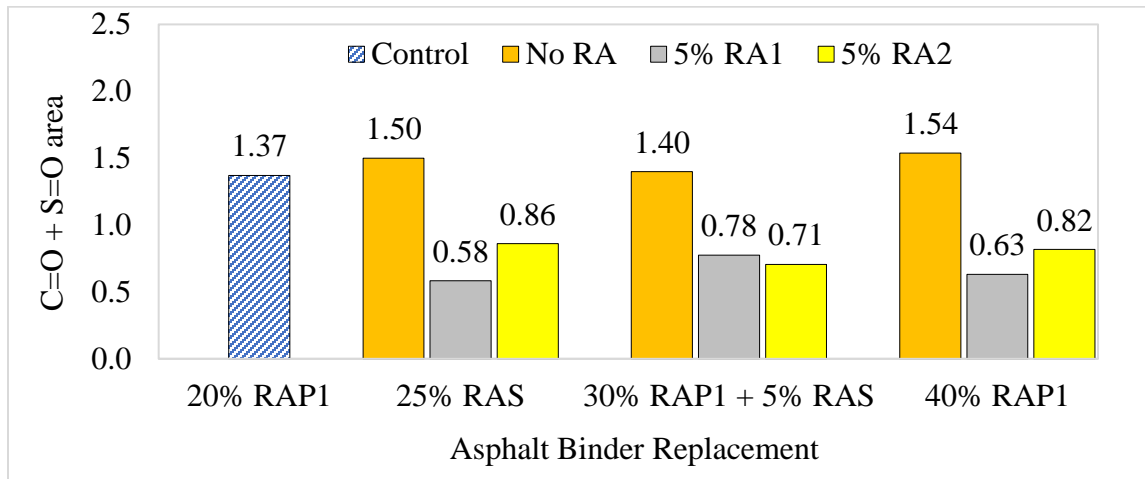


Figure 4.43: C=O + S=O areas of the recycled binder blends prepared with the PG 58S-28 binder after RTFO plus 40 hours PAV.

Figure 4.44 presents the C=O + S=O area of the recycled binder blends prepared with the PG 58S-34 binder after RTFO plus 60 hours PAV conditioning. As expected, the high RAP content blends (35% RAP and 50% RAP) without RAs had higher C=O + S=O areas than the control blend (20% RAP). After the addition of the RAs, the C=O + S=O area decreased for all blends except for the blend with RA4. The recycled binder blends with RA4 had the highest C=O + S=O area, which was 1.77 and 1.99 for the 35% RAP and 50% RAP, respectively. The 35% RAP blend with RA5 had the lowest C=O + S=O area, followed by blends with RA1, and then RA3. When the C=O + S=O area of the recycled binder blends after RTFO plus 60 hours PAV compared to that of the RAs, they correspond to each other. Therefore, the effectiveness of the RAs in decreasing the C=O + S=O area can be in the following order: RA5>RA1>RA3>RA4.

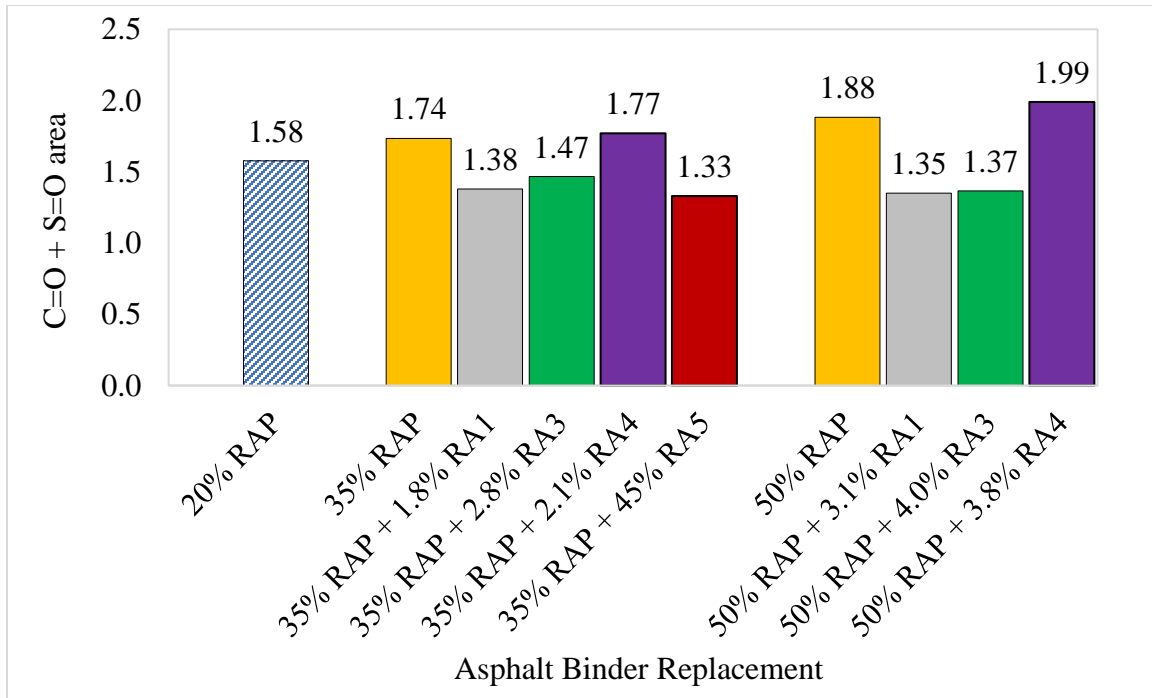


Figure 4.44: C=O + S=O areas of the recycled binder blends prepared with the PG 58S-34 binder after RTFO plus 60 hours PAV

4.8. Summary

The objective of this chapter was to evaluate the effect of high RAP and/or RAS contents in the recycled binder blend properties and assess the effectiveness of the RAs in restoring these properties. To accomplish this objective, three base binders (PG 58S-28, PG 58V-28, and PG 58S-34 PMB) were used along with four RAM binders (RAP1, RAP2, RAS, and SD RAP). Recycled binders from RAP1, RAP2, and RAS were used with the PG 58S-28 and PG 58V-28; along with two bio-based RAs (RA1 and RA2). The SD RAP binder was used with the PG 58S-34 binder, along with three bio-based RAs (RA1, RA3, and RA4) and one petroleum-based RA (RA5). Based on the analysis conducted, the following was found:

- i. The increase in RAM contents on the base binders improved the high-temperature properties of the recycled binder blends but it had detrimental effects on their intermediate

and low-temperature properties after RTFO plus 40- or 60-hours PAV. The addition of the RAs improved the high, intermediate, and low-temperature properties to that of the base binders (PG 58S-28 and PG 58V-28) and the control blend (20% ABR) for the PG 58S-34 blends after RTFO plus 40 hours and RTFO plus 60 hours conditioning, respectively.

- ii. The increase in RAM binders in the recycled binder blends increased their J_{nr} indicating the stiffening effects introduced by the RAM in the base binders. The addition of RAs decreased the J_{nr} , and their effectiveness varied depending on their type. Moreover, the RAM type had a significant impact on the J_{nr} values rather than their contents. The percent recovery of the recycled binder blends was influenced by the J_{nr} parameter, and they were both dependent on the constituents' contents and type in the blend.
- iii. The addition of RAM binder into base binders (PG 58S-28 and PG 58V-28) decreased their N_f after RTFO plus 40 hours PAV, indicating loss of fatigue resistance; however, the decrease was dependent on the RAM type. Recycled binder blends with RAS binder only had higher N_f than those with RAP only binder or RAP+RAS binder. The addition of the RAs improved the fatigue resistance of the recycled binder blends; however, their effectiveness was a function of their type, base binder, and RAM binder type and content. Similar findings were shown using the $|B|$ parameter, as the $|B|$ parameter increased when RAM was added, with the RAS blends having the highest value. However, the addition of recycling agents decreased the $|B|$ parameter indicating improvement in intermediate temperature cracking resistance of the recycled binder blends.
- iv. The addition of RAM binder into the base binders increased the C=O + S=O area, but it was dependent on the RAM type. The addition of the RAs decreased the C=O + S=O area, but the effectiveness was a function of RA type and RAM type and content.

5. ASPHALT MIXTURES PERFORMANCE RESULTS

5.1. Introduction

Both descriptive and inferential statistics were used to analyze the raw data from the mixture performance tests. For the results presented graphically, the bars represent the mean values, and the whiskers denote the mean plus/minus one standard deviation of the test replicates. The normality of the data sets was checked using the Anderson-Darling test. Bartlett's test was used to check the homogeneity of the data set variances. Analysis of variance (ANOVA) and Tukey-Kramer post hoc test was used to assess the statistically significant differences in the values of the performance testing parameters (multiple groups). While ANOVA shows whether the differences in the values of the groups are statistically significant, the Tukey-Kramer test indicates the exact groups that their values are statistically significantly different (if any). For two groups data set, a paired t-test was used to assess the statistical significance difference among the mean values of the groups. All statistical analyses were conducted at a significance level of 0.05.

Since highway agencies are transitioning towards balanced mixture design (BMD) practice, Wisconsin's mixtures are compared to the preliminary BMD threshold criteria in Table 5.1 developed under project WHRP 0092-20-04 (West et al., 2021b) for mixtures produced in Wisconsin. Only the criteria at a traffic level of 2 – 8 million ESALs (medium traffic) will be used since the mixtures in this study were designed to meet the specifications of this traffic level.

Table 5.1: Preliminary BMD thresholds for Wisconsin mixtures by West et al. (2021b)

Traffic Level (ESALs)	HWTT @STOA				IDEAL-CT Min. CT _{index} @ LTOA	DCT Min. Fracture Energy (J/m ²) @LTOA
	Min. # of passes to 12.5 mm rut depth	Min. SIP (passes)	Max. CRD @ 20,000 passes	Min. SN (passes)		
>8 million	15,000	9,000	6.0	2,000	40	300
2 – 8 million	15,000		7.0			
<2 million	10,000		8.0			

5.2. Rutting Resistance and Moisture Susceptibility

Figure 5.1 and 5.2 present the HWTT rut depth curves for Wisconsin’s mixtures prepared with Aggregate 1 and Aggregate 2, respectively. In general, all high RAM content mixtures with RAs and produced with the PG 58S-28 binder and the PG 58V-28 performed better compared to the control mixtures (20% ABRs) due to the stiffness added by the high RAM contents. All the Aggregate 1 mixtures with the PG 58S-28 binder exhibited a stripping phase while the (PG 58V-28) PMB mixtures showed no stripping potential. Moreover, the control mixture exhibited stripping earlier compared to the high RAM content mixtures with RA1. For Aggregate 2 mixtures, all mixtures showed stripping potential following a similar trend. When Aggregate 1 mixtures with RA1 and the PG 58S-28 binder were compared among themselves, the mixture with RAS only (25% ABR) and with RAP+RAS (35% ABR) showed better performance than the RAP only (40% ABR) mixture. Also, as expected mixtures with the PG 58V-28, both the control and the 40% ABR performed better compared to those with the PG 58S-28 binder. In addition, no stripping potential was observed on Aggregate 1 mixtures with PG 58V-28. For Aggregate 2, all mixtures exhibited stripping potential following a similar trend.

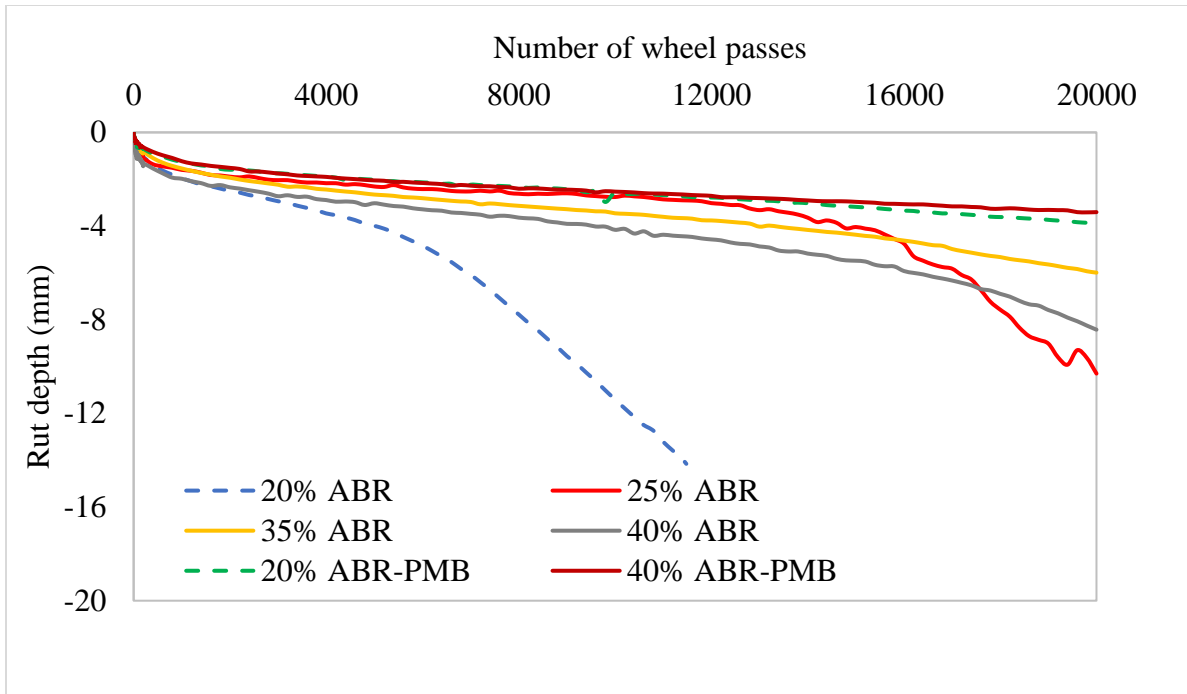


Figure 5.1: HWTT rut depth curves for Aggregate 1 mixtures

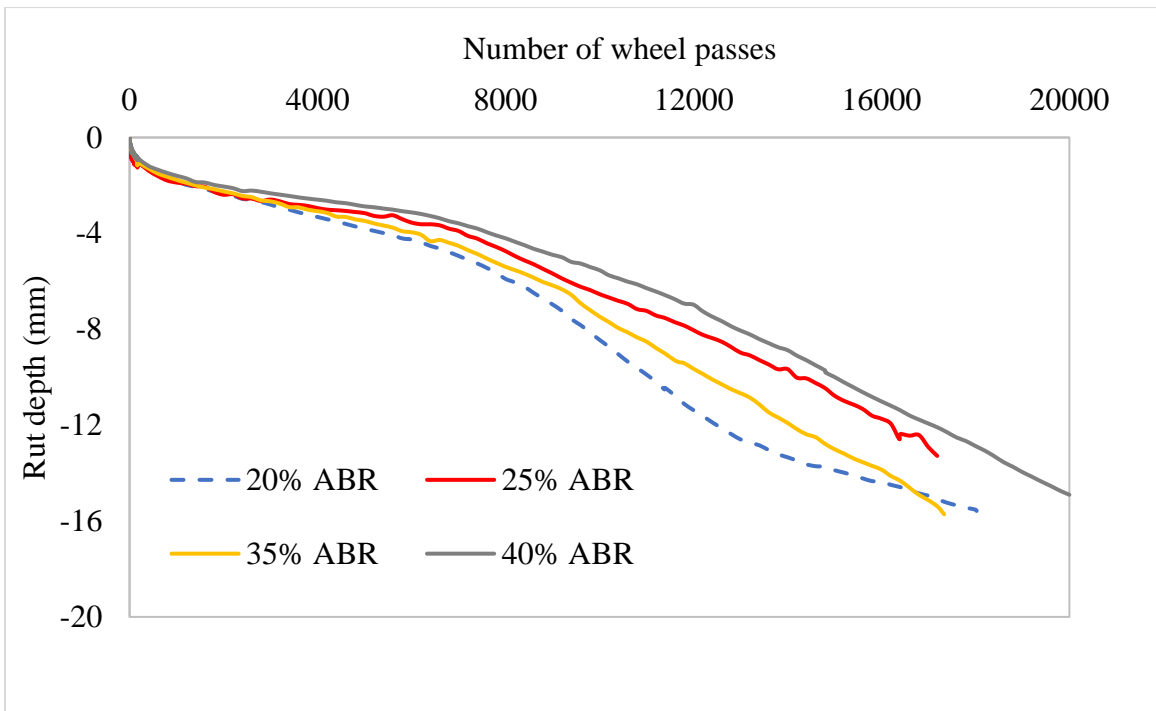


Figure 5.2: HWTT rut depth curves for Aggregate 2 mixtures

Table 5.2 presents the results of the HWTT of Aggregate 1 mixture. As shown in Table 5.2, the control mixture with Aggregate 1 and PG 58S-28 (20 % ABR) had the highest TRD and CRD at 20,000-wheel passes (>12.5 mm and 5.8 mm, respectively). The control mixture had the least number of passes to 12.5 mm rut depth (i.e., 10,600) while all high RAM content mixtures of Aggregates 1 with RA1 and the PG 58S-28 had number of wheel passes greater than 20,000 passes. When high RAM content mixtures with RA1 and the PG 58S-28 binder were compared among themselves, the 35% ABR mixture had the lowest TRD at 20,000 passes (6.0 mm) but the highest CRD (4.6 mm); and the 25% ABR mixture had the lowest CRD (3.0 mm) but highest TRD (10.3 mm) which further corroborates the ability of CRD to exclude rutting potential associated with stripping of the mixture. All mixtures with Aggregate 1 and the PG 58V-28, had significantly low TRD and CRD at 20,000 passes. The control mixture (20% ABR-PMB) had a TRD and CRD of 3.9 mm and 3.5 mm, respectively whereas the 40% ABR-PMB mixture had a TRD of 3.4 mm and a CRD of 3.3 mm. In addition, the number of passes to 12.5 mm rut depths was greater than 20,000 passes for both the 20% ABR-PMB and 40% ABR-PMB mixtures. When comparing these results to the preliminary BMD threshold criteria for medium traffic (2 – 8 million ESALs); only the 20% ABR mixtures failed the 15,000-minimum number of passes to 12.5 mm rut depth. None of the mixtures failed the CRD threshold criteria of 7 mm max CRD at 20,000 passes.

The moisture susceptibility results in terms of SIP and SN are also presented in Table 5.2. For mixtures with Aggregate 1 and the PG 58S-28, the results indicated that the control (20% ABR) mixture had both lower SIP and SN values (i.e., 6,000 and 1,957 passes respectively) than all the high RAM content mixtures, indicating that it is more susceptible to moisture damage. The control mixture with the PG 58V-28 had higher SIP and SN than mixtures with the PG 58S-28 binder. Based on these results, it was inferred that high RAM content mixtures with either the PG 58S-28

binder or the PG 58V-28, and RA1 at the selected dosage had better rutting resistance and were less susceptible to moisture damage than the control mixtures (20% ABR and 20% ABR-PMB). In addition, only the 20% ABR mixture failed both the SIP and SN preliminary BMD threshold criteria, while the remaining mixtures all passed the minimum criteria.

Table 5.2: Aggregate 1 HWTT results

Binder Type	Mixture Type	TRD @ 20,000 (mm)	# of passes to 12.5 mm	CRD @ 20,000 (mm)	SIP (passes)	SN (passes)
PG 58S-28	20% ABR	>12.5	10,600	5.8	6,000	1,957
	25% ABR	10.3	>20,000	3.0	14,800	4,384
	35% ABR	6.0	>20,000	4.6	15,600	15,000
	40% ABR	8.4	>20,000	4.3	15,700	5,708
PG 58V-28	20% ABR-PMB	3.9	>20,000	3.5	17,400	>20,000
	40% ABR-PMB	3.4	>20,000	3.3	>20,000	>20,000

The HWTT results for Aggregate 2 mixtures are presented in Table 5.3. Both the control (20% ABR) and the high RAM content mixtures with RA2 had TRD greater than 12.5 mm at 20,000-passes. Moreover, the number of wheel passes to 12.5 mm rut depth for the 20% ABR mixture was 12,900, which was the lowest when compared to the rejuvenated mixtures. The 40% ABR mixture had the highest number of passes to the 12.5 mm rut depth of all the mixtures. The CRD ranged from 5.3 mm to 4.2 mm, with the 20% ABR mixture having the highest value; and among the rejuvenated mixtures, the 35% ABR mixture had the highest CRD value. Based on the number of passes to 12.5 mm rut depth and the CRD parameter, rejuvenated mixtures had better rutting resistance than the control at the selected dosage of RA2. Only the 20% ABR and 35% ABR mixtures failed the preliminary BMD threshold criteria of 15,000 minimum number of passes to 12.5 mm rut depth whereas none of the mixtures failed the 7 mm CRD threshold.

Moisture susceptibility results showed that except for the 25% ABR mixture which had the lowest SIP (7,150 passes) the 35% ABR and 40% ABR mixtures had higher SIP passes (9,200 and 9,800 passes, respectively) than the 20% ABR mixture (Table 5.3). However, the SN showed that the 20% ABR mixture had higher SN passes than the 35 % ABR and 40% ABR mixtures. The 25% ABR mixture has the highest SN passes of all. When the moisture susceptibility values were compared against the preliminary BMD threshold criteria, none of the mixtures failed the SN while mixture 20% ABR and 25% ABR failed the SIP threshold of a minimum number of passes of 9,000.

Table 5.3: Aggregate 2 HWTT results

Mixture Type	TRD @ 20,000 (mm)	# of passes to 12.5 mm	CRD (mm) @ 20,000	SIP (passes)	SN (passes)
20% ABR	>12.5	12,900	5.3	8,700	3,297
25% ABR	>12.5	16,900	4.2	7,150	3,411
35% ABR	>12.5	14,600	4.8	9,200	2,904
40% ABR	>12.5	17,600	4.3	9,800	3,273

For the South Dakota mixtures, the rutting resistance was evaluated using the APA test at 58 °C. In this experiment, six replicates were prepared per mixture type to get three pairs, one per wheel path. Figure 5.3 presents the APA rut depth results for both the 35% ABR and 50% ABR mixtures along with the control mixture (20% ABR). As shown in Figure 5.3, all mixtures but the 35% ABR with RA5 have less rut depth compared to the control mixture (20% ABR). None of the mixtures exceeded a 7 mm rut depth threshold required by South Dakota DOT for Q2 roadways. Therefore, these high RAP mixtures with or without RAs are expected to perform equivalent to the control mixture as long as they are subjected to similar conditions.

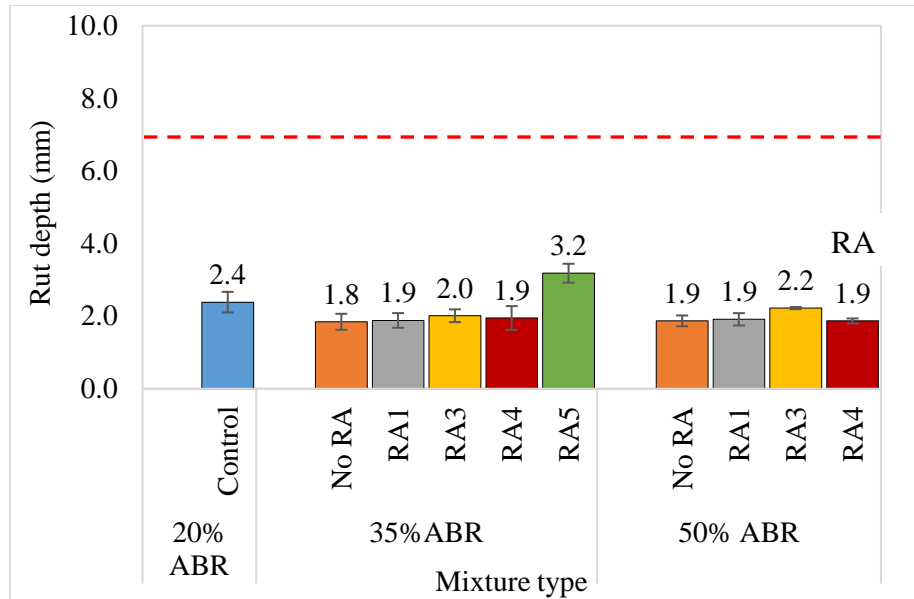


Figure 5.3: APA rut depth results for South Dakota mixtures

5.3. Intermediate Temperature Cracking Resistance

The intermediate temperature cracking resistance of all the mixtures was evaluated using the IDEAL-CT per ASTM D8225-19. The result from the test was evaluated using the CT_{index} which is the primary output of the test. Figure 5.4 shows the CT_{index} results of Aggregate 1 mixtures with and without RA1. The bars indicate the mean values whereas the whiskers represent a plus and minus one standard deviation. The coefficient of variation (COV) of Aggregate 1 mixtures produced with the PG 58S-28 binder was between 7.1% and 22.6% whereas those with the PG 58V-28 binder had a COV ranging from 6.3% to 22.0%.

As can be seen from Figure 5.4, the control mixtures (20% ABR and 20% ABR-PMB) had higher mean CT_{index} values compared to high RAM content mixtures with and without RA1. However, high RAM content mixtures with RA1 had higher mean CT_{index} values compared to their corresponding mixtures without RA1. For instance, the differences in mean CT_{index} units between the high RAM content mixtures with and without RA1 were 11, 7, and 20 for the 25% ABR, 35%

ABR, 40% ABR mixtures. For the 40% ABR-PMB mixtures, the difference was approximately 4 CT_{index} units. Moreover, when the control mixtures were compared, the 20% ABR (with PG 58S-28) had higher mean CT_{index} values than the 20% ABR-PMB (with PG 58V-28) despite having the same total binder content. This indicated that the polymer modification had a negative effect on the intermediate temperature cracking resistance of the mixture in terms of CT_{index} . However, this may not be the case as the computation of the CT_{index} involves, among others two contradicting parameters, the post peak slope and fracture energy (Bahia et al., 2020). In addition, the current testing procedure of the test (single temperature and loading rate of 25 ± 1 °C and 50 ± 2 mm/min, respectively) may not be able to fully capture the benefit of polymer modification on intermediate temperature cracking resistance. This drawback in the test is recognized by the asphalt industry. NCAT is collaborating with NRRA to investigate the impact of polymer modification on both IDEAL-CT and I-FIT tests (Yin et al., 2021).

The statistical significance differences among the CT_{index} values of the asphalt mixtures were evaluated and results are denoted using capital letters. Mixtures with different letters indicate that they were statistically significant different. Based on ANOVA, the CT_{index} of Aggregate 1 mixtures produced with the PG 58S-28 binder were statistically significant different. The Tukey-Kramer test showed that the CT_{index} values of the control mixture (20% ABR) were statistically significant different from the high RAM content mixtures regardless of whether they have RA1 or not. For high RAM content mixtures, the CT_{index} values of the 25% ABR and 40% ABR mixtures (with and without RAs) were statistically significant different from each other. However, the CT_{index} values of the 35% ABR mixtures (with and without RA1) were not statistically significant different. For mixtures with the PMB, the control mixture (20% ABR-PMB) was statistically significant different from the 40% ABR-PMB mixtures (with and without RA). However, the 40%

ABR-PMB mixtures with and without RA1 were not statistically significant different. When compared to the proposed minimum CT_{index} criterion of 40, all high RAM content mixtures without RA1 failed the criterion. Among the high RAM content mixtures with RA1, only the 40% ABR mixture passed the criterion but two of these mixtures barely failed it.

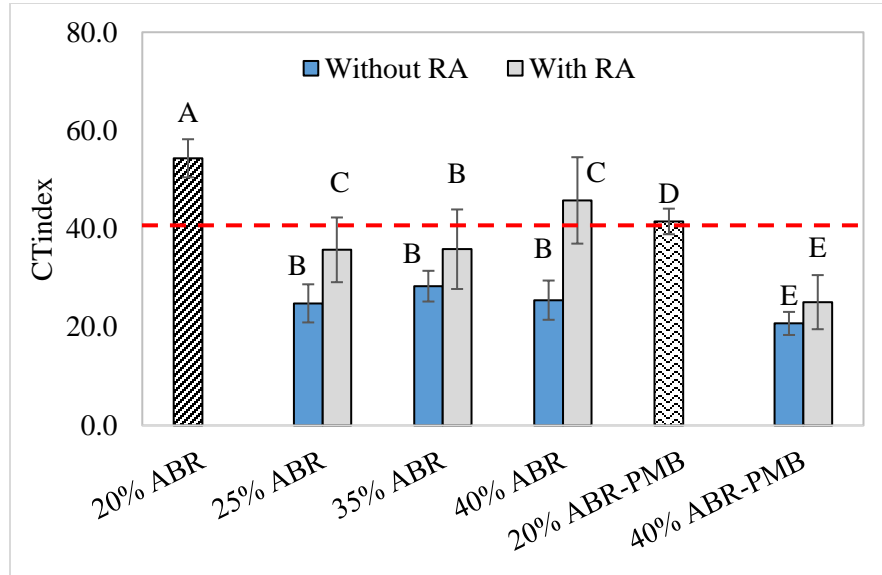


Figure 5.4: CT_{index} results of Aggregate 1 mixtures

The CT_{index} results of Aggregate 2 mixtures are presented in Figure 5.5. As observed previously with Aggregate 1 mixtures, the control mixture (20% ABR) had a higher mean CT_{index} value than the high RAM content mixtures (with and without RA2). High RAM content mixtures with RA2 had higher mean CT_{index} values than their corresponding mixtures without RA2. The differences in mean CT_{index} values between high RAM content mixtures with and without RA2 were about 15, 10, and 4 CT_{index} units for the 25% ABR, 35% ABR, 40% ABR mixtures. The COV of Aggregate 2 mixtures ranged from 11.4% to 24.6%.

ANOVA indicated that statistical significance difference exists among the CT_{index} values of Aggregate 2 mixtures. Moreover, the control mixture was statistically significant different from the high RAM content mixtures (with or without RA2). When high RAM content mixtures with and without RA2 were compared against each other, the 25% ABR and 35% ABR mixtures were statistically significant different whereas the 40% ABR mixtures were not. Based on these results it can be inferred that RA2 did not yield mixtures with similar/ better intermediate temperature cracking resistance as the control at the selected dosages. Nevertheless, all Aggregate 2 mixtures met the minimum CT_{index} criterion of 40.

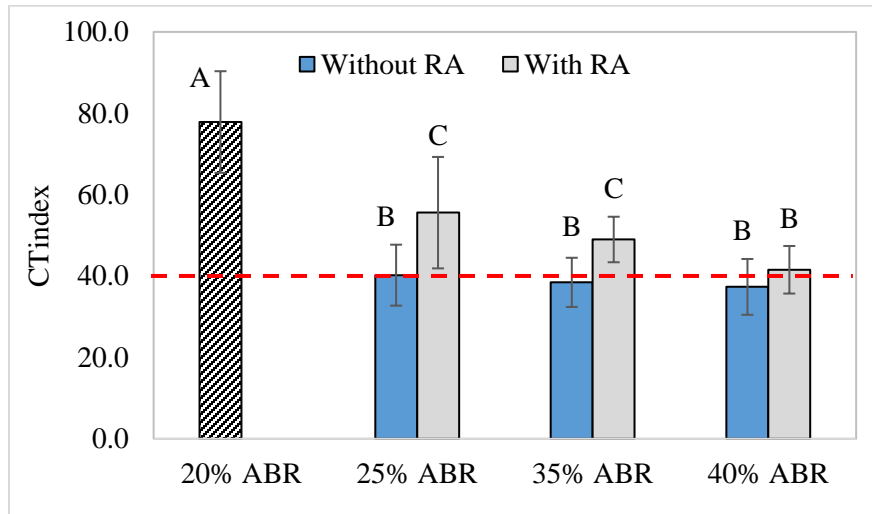


Figure 5.5: CT_{index} results of Aggregate 2 mixtures

The CT_{index} results of South Dakota mixtures are presented in Figure 5.6. The COV of the CT_{index} values ranged between 8.7% to 23.0%. As shown in Figure 5.6, the control mixture (20% ABR) had a higher CT_{index} compared to all high RAP content mixtures (35% ABR and 50% ABR mixtures). However, high RAP content mixtures without RAs had a lower mean CT_{index} value than those with RAs. When the 35% ABR mixtures with RA were compared, the mixture with RA3 had the highest mean CT_{index} value, followed by that with RA5 and RA1, the mixture with RA4

had the lowest mean CT_{index} value. For the 50% ABR mixtures with RA, the mixture with RA4 had the highest mean CT_{index} value, followed by that with RA1, and finally one with RA3.

According to ANOVA, the CT_{index} values of the South Dakota mixtures were statistically significant different (Figure 5.6). The Tukey-Kramer test showed that the CT_{index} values of the control mixture were statistically significant different from all high RAP content mixtures with and without RAs, indicating that regardless of whether the mixture was rejuvenated or not, their intermediate temperature cracking resistance was less compared to the control mixture. Of all the high RAP content mixtures, only the CT_{index} values of the 35% ABR and the 50% ABR mixtures with RA3 and RA4, respectively were statistically significant different from their corresponding mixtures without RAs. Lastly, the 35% ABR and 50% ABR mixtures without RA were not statistically significant different from each other.

While the analysis of rejuvenated recycled binder blends showed improvement in terms of intermediate temperature cracking resistance, this improvement was not evident at the mixture level. This may be due to the fact that recycled binder blends use extracted RAM binder at the exact design proportions, whereas in mixtures although 100% of RAM binder availability is assumed, in reality, less than 100% contribution occurs.

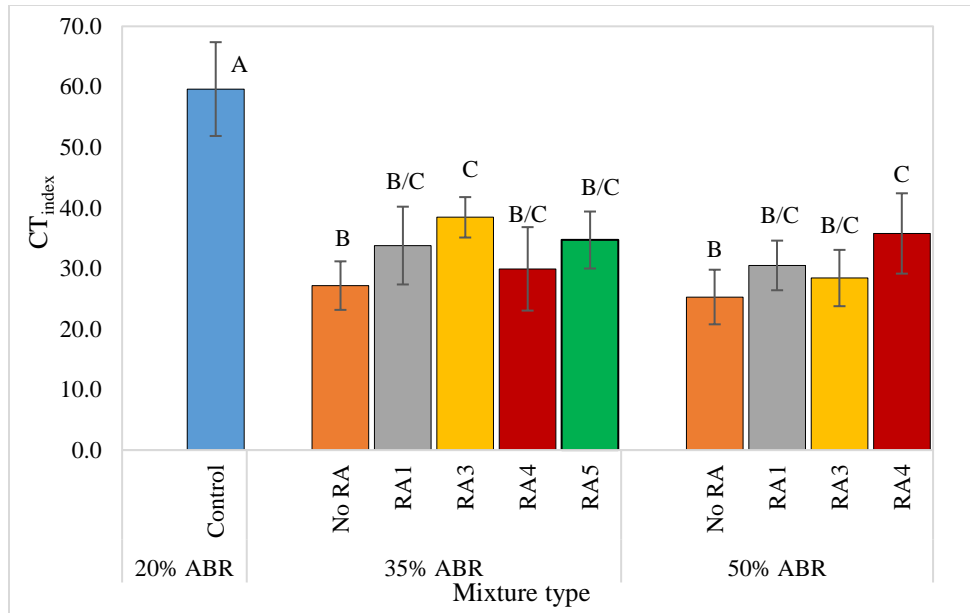


Figure 5.6: CT_{index} results of the South Dakota mixtures

As mentioned previously, among the parameters used in the computation of the CT_{index}; the post peak slope and fracture energy are contradicting. The post peak slope is obtained at 75% of the peak load and it is inherently a negative value. However, an absolute value is usually applied, and therefore whenever post peak is mentioned in this study it should be considered as an absolute value. The post peak slope indicates the resistance of the mixture to crack propagation. The higher the post peak slope, the more brittle the mixture, hence a worse crack propagation resistance (Zhou et al., 2017). The fracture energy indicates the resistance of the mixture to crack initiation, and it is computed from the area of the load-displacement curve divided by the cross-sectional area of the specimen (thickness*diameter).

Figure 5.7 and Figure 5.8 show the relationship between the CT_{index} and the post peak slope and fracture energy for Wisconsin mixtures, respectively. Only mixtures produced with the PG 58S-28 binder were used in the analysis. Aggregate 1 mixtures with the PMB (PG 58V-28) were not used to avoid the confounding effect of the PMB on the correlations. As shown in Figure 5.7 and

Figure 5.8, the CT_{index} shows moderate and very poor correlation with the post peak slope ($R^2 = 0.56$) and fracture energy ($R^2 = 0.06$), respectively. These findings were in line with those reported by Bahia et al. (2020).

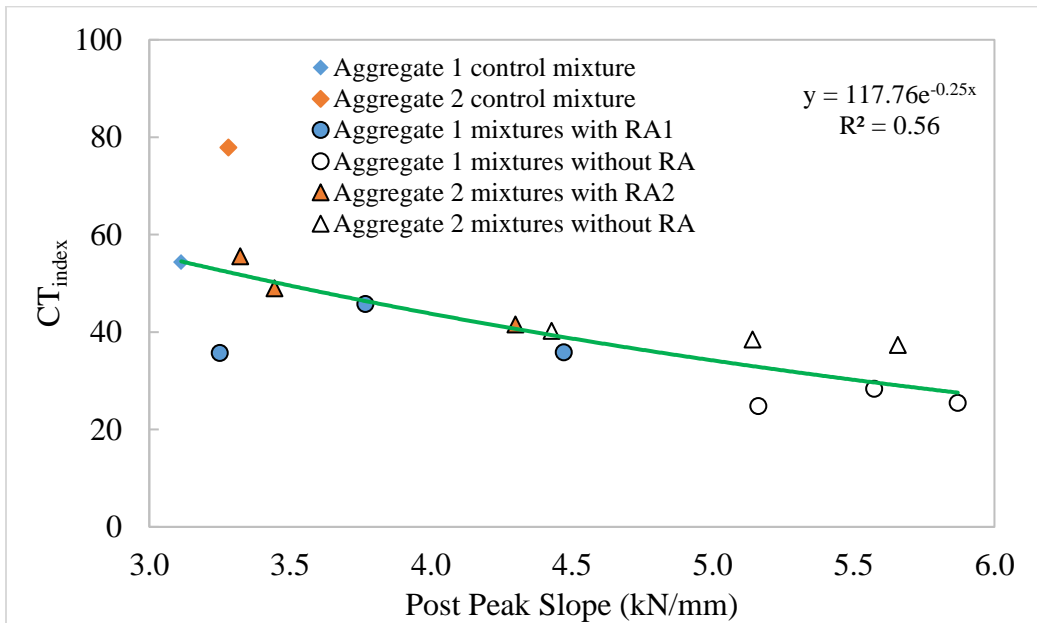


Figure 5.7: Relationship between CT_{index} and post peak slope for Wisconsin mixtures

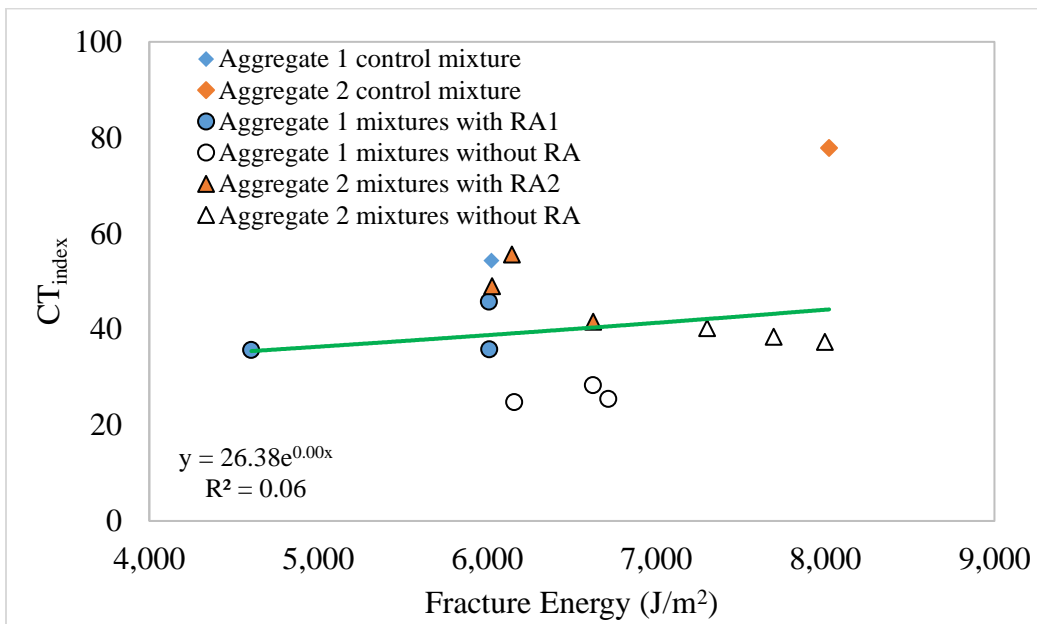


Figure 5.8: Relationship between CT_{index} and fracture energy for Wisconsin mixtures

The relationships between the CT_{index} and the post peak slope and fracture energy for the South Dakota mixtures is shown in Figure 5.9 and Figure 5.10, respectively. Based on Figure 5.9, a moderate correlation ($R^2 = 0.46$) exists between the CT_{index} and the post peak slope whereas there was no correlation with the fracture energy. While these results are in line with those found with the Wisconsin mixtures, it is worth noting that, the binder (PG 58S-34) used to produce South Dakota mixtures was polymer modified, and therefore it might had an influence on the relationships.

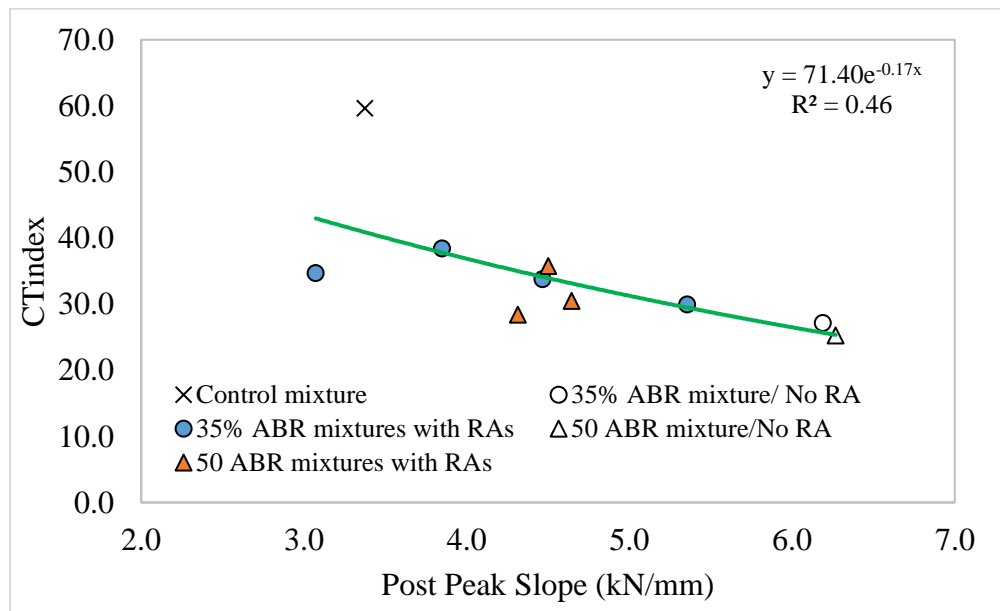


Figure 5.9: Relationship between CT_{index} and post peak slope for South Dakota mixtures

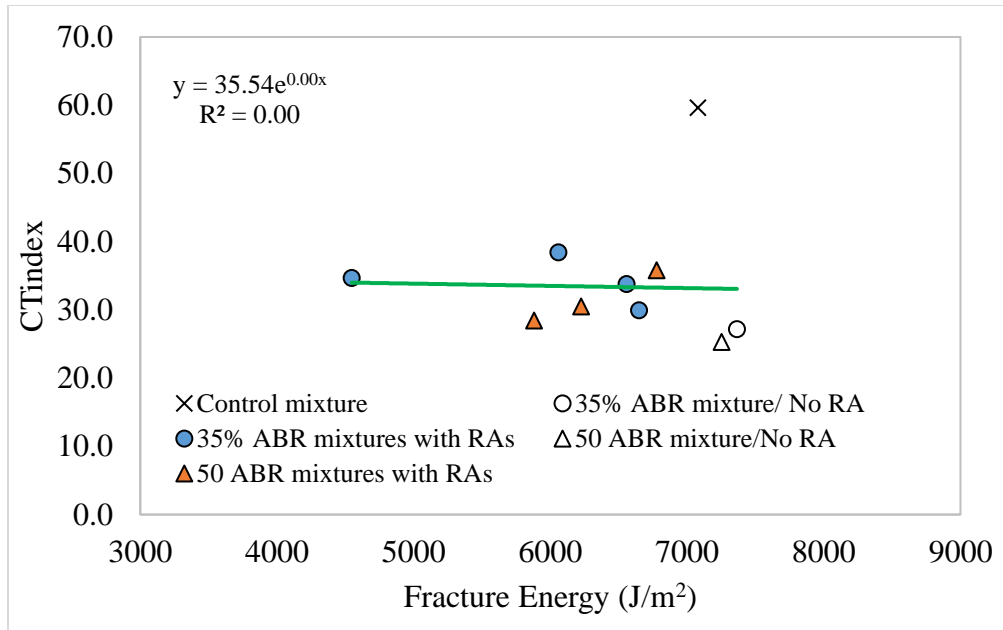


Figure 5.10: Relationship between CT_{index} and fracture energy for South Dakota mixtures

Since both post peak slope and fracture energy parameter are of importance to the overall mixture cracking resistance parameter (CT_{index}), thresholds on the post peak slope and fracture energy must be established to avoid a risk of using softer mixtures that will have better-cracking propagation resistance (low post peak slope) but poor crack initiation resistance (low fracture energy) (Bahia et al., 2020). Using Aggregate 1 and 2 mixtures produced with the PG 58S-28 binder, a space diagram of the post peak slope and fracture energy was developed as shown in Figure 5.11. Assuming that the preliminary BMD's CT_{index} limit of 40 is sufficient to produce mixtures with acceptable intermediate temperature cracking resistance, therefore the post peak slope value must be limited to about 4.4 whereas the minimum value of the fracture energy is 6000 J/m².

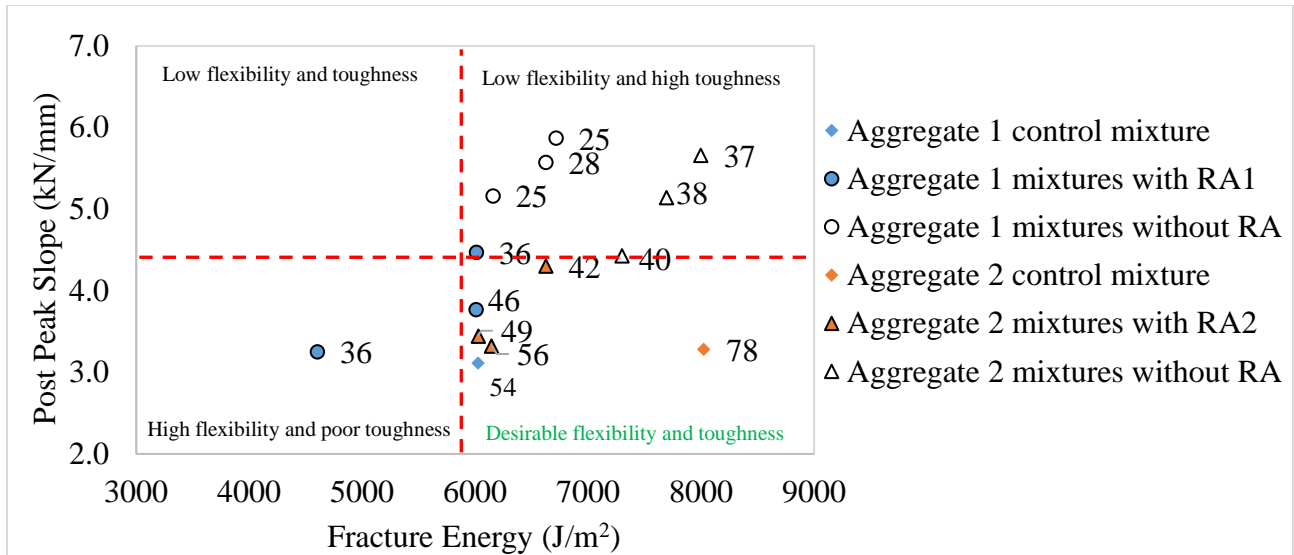


Figure 5.11: Space diagram of IDEAL-CT parameters for Wisconsin mixtures

A limited evaluation was also conducted to explore alternatives to improve the CT_{index} of Aggregate 1 mixtures with RA1 (25% ABR and 35% ABR) that barely failed the preliminary BMD threshold (40 CT_{index}). Since the optimum dosages of RAs were determined based on recycled binder testing, it was hypothesized that these dosages might have been low at the mixtures' level since the extent of interaction between RA and RAM binder is dependent on the active RAM binder and the diffusion of RA into RAM binder. Therefore, a slight increase in RA dosage was expected to improve the results. Therefore, the original RA dosages were increased by 1%. The RA of the 25% ABR increased from 4.1% to 5.1% whereas that of the 35% ABR from 2.1% to 3.1% (by weight of the total binder). As presented in Figure 5.12, both mixtures still failed the preliminary BMD criteria. When mixtures with the different RA1 dosages were compared, the CT_{index} value of the 25% ABR mixture increased by 2 CT_{index} whereas that of the 35% ABR mixture decreased by 4 CT_{index} units. The CT_{index} of the 25% ABR mixture without RA was statistically significant different from both the one with the original RA dosage and one with the original RA dosage + 1%. However, the 25% mixtures with RA (i.e., original RA dosage and

original RA dosage + 1%) were not statistically significant different. The CT_{index} of the 35% ABR mixtures (with and without RA) were not statistically significant different. Thus, this finding suggests that increasing the RA dosage may not necessarily improve the CT_{index} (intermediate temperature cracking resistance) of the mixtures.

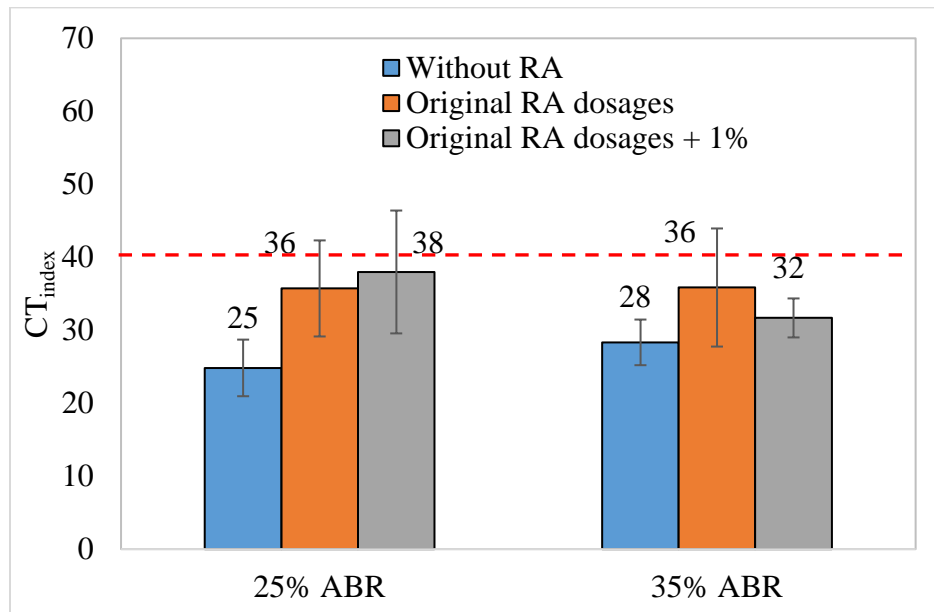


Figure 5.12: Mean CT_{index} values after an increase of RA dosage

The CT_{index} results obtained from the South Dakota mixtures were not expected as the RAs did not show statistical significant changes in the CT_{index} values except for the 35% ABR and 50% ABR mixtures with RA3 and RA4, respectively. In addition, IDEAL-CT tests were conducted to attempt to understand the cause of these results. Three possible reasons were hypothesized:

- i. The RAs' dosages recommended by the manufacturer were low as they were selected targeting the true LTPG of the 20% ABR blend (after RTFO plus 60-hour PAV). Therefore, the RAs' dosages were determined targeting the LTPG of the base binder (-34 °C) which will increase the dosage and could improve the CT_{index} of the mixtures.

- ii. The LTOA used (loose mixture aging at 135 °C for 6 hours after STOA) was too aggressive. However, as stated previously, the LTOA used is expected to better simulate the field aging compared to the AASHTO R30. Moreover, the procedure is effective in distinguishing high RAM content mixtures with RAs as these additives introduce different aging characteristics on both binders and mixtures. Therefore, to understand the effectiveness of RA with aging, the IDEAL-CT was conducted on STOA (loose mixture aging at 135 °C for four hours) and loose mixtures aged for 6 hours at 135 °C, and 3 days at 95 °C (based on NCHRP 9-54 recommendation) in addition of the STOA.
- iii. RAs alone may not be effective to significantly improve the cracking resistance of high RAP mixtures when a 100% blending between aged binder and virgin asphalt is assumed. A combination of RA and additional binder content to account for the inactive RAM binder may be a more effective approach. Therefore, a 75% discount factor (DF) was assumed, and the optimum binder content of the mixtures was adjusted to reflect it. DOTs like Georgia and Iowa have implemented this approach.

Due to time constraints and a limited number of materials, only the 35 % ABR mixtures and RA1 were used to understand the above-mentioned hypotheses. Figure 5.13 shows the mean CT_{index} values of the 35% ABR mixtures with different dosages of RA1. The dosage of RA1 to target the LTPG of the base binder was 3.6% (by weight of the total binder), doubled the original dosage (1.8%) which targeted the true LTPG of the 20% ABR blend. The statistical analysis showed a significant difference between the 35 % ABR mixture without RA and with 3.6% RA1. This indicated that, at a higher dosage (i.e., 3.6%), RA1 was improved the intermediate temperature cracking resistance of the 35% ABR mixture. However, the difference in CT_{index} values between the mixtures with 1.8% and 3.6% RA1 was not statistically significant.

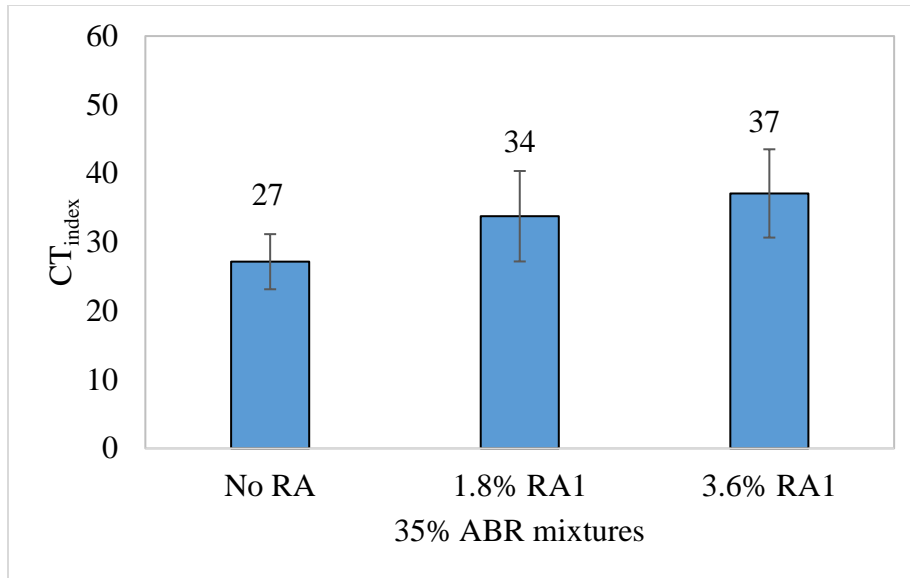


Figure 5.13: Mean CT_{index} values of the 35% ABR mixture after an increase in the dosage of RA1

Figure 5.14 summarizes the mean CT_{index} of the 35% ABR mixtures at three different aging levels. As stated previously, the three different aging levels were conducted to evaluate the effectiveness of the 35% ABR with RA1 with aging using dosages recommended by the manufacturer (i.e., 1.8% by weight of the total binder). Based on the statistical analysis, the CT_{index} values of the 35% ABR mixtures with and without RA1 were statistically significant after STOA. However, after STOA plus 6 hours at 135 °C, and STOA plus 3 days at 95 °C, the CT_{index} values of the 35 % ABR mixtures with and without RA1 were not statistically significant different. This result suggests that the effectiveness of RA may be decreasing with aging.

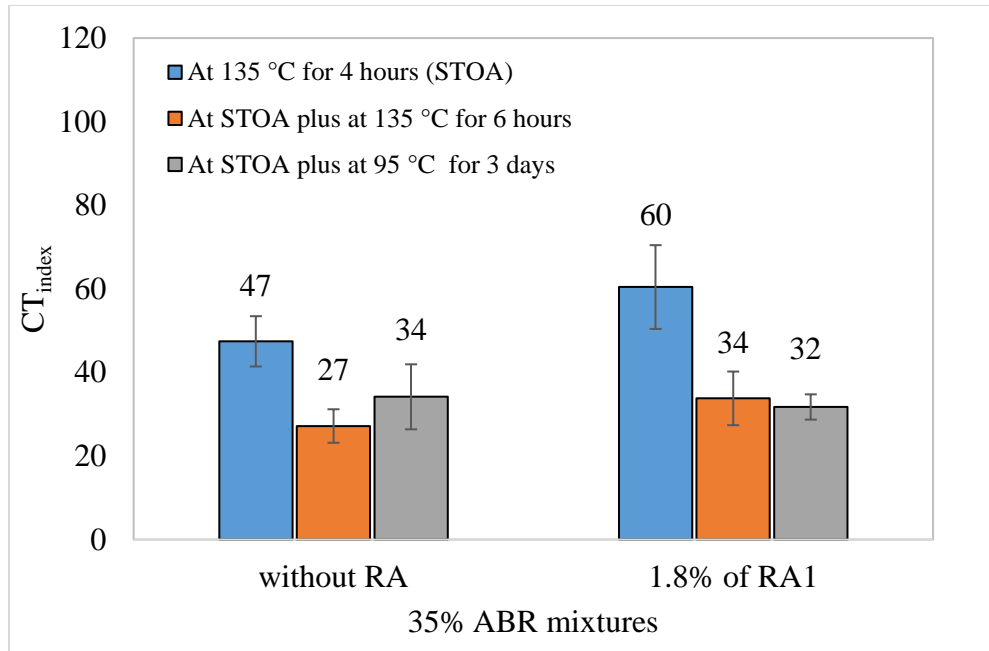


Figure 5.14: Mean CT_{index} values of the 35% ABR mixture at different aging levels

Lastly, the CT_{index} values were evaluated on 35% ABR mixtures with and without RA1 after LTOA. The 35% ABR mixtures with RA1 at the dosage recommended by the manufacturer (i.e., 1.8%) used a 75% DF applied on the total binder content of the mixture to account for the inactive RAP binder and therefore, increasing the effective binder content of the mixture (Figure 5.15). Based on the statistical analysis, the CT_{index} values of the 35% ABR mixture with RA1 and 75% DF were statistically significant higher than that of the 35% ABR mixture without RA. These results suggest that when a 75% DF was used, the intermediate temperature cracking resistance of the 35% ABR mixture improved indicating the impact of increased virgin binder and RA.

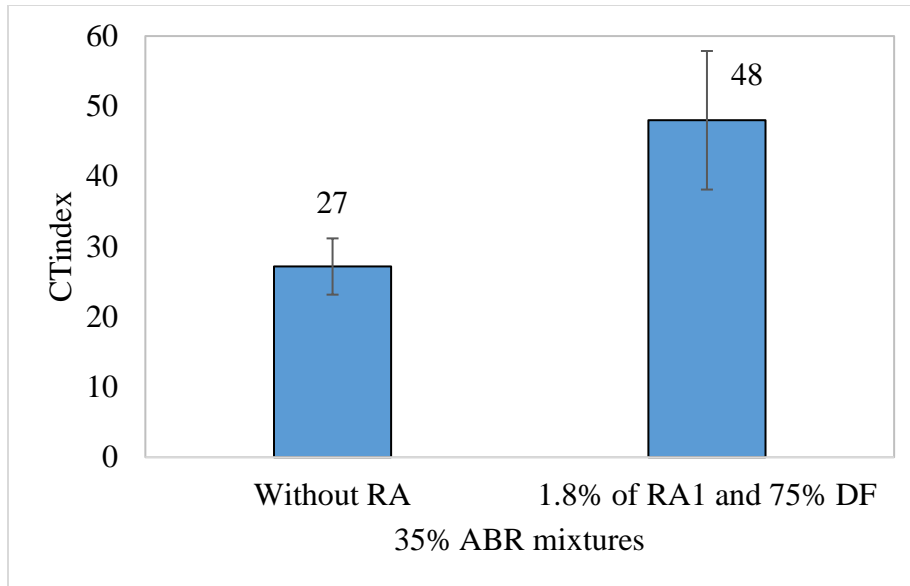


Figure 5.15: Mean CT_{index} values of the 35% ABR mixture with a discount factor

5.4. Low-Temperature Cracking Resistance

As discussed in the previous section, a higher fracture energy (G_f) value of the asphalt mixture is indicative of better resistance to thermal cracking. The number of DCT replicates for all mixtures ranged from 4 to 6 specimens. The fracture energy results along with the statistics grouping for the Wisconsin mixtures are shown in Figure 5.16. From Figure 5.16, the mean fracture energy values of the asphalt mixtures with RAs were higher than the control mixtures. In addition, the 20% ABR-PMB mixture had a higher mean fracture energy than the 20% ABR mixture. ANOVA conducted on Aggregate 1 mixtures with PG 58S-28 binder showed that the values of the fracture energy values are statistically significant different. However, as shown in Figure 3.7 the Tukey-Kramer test could not detect mixtures with significant different fracture energy values. This is attributed to the small sample size (replicates ranged from five to six) and the ANOVA p-value (0.0333) being close to the significance level limit (0.05) For Aggregate 1 mixtures with the PMB, the t-test showed that the fracture energy values were not statistically significant different. These

results indicate that mixtures with RA1 at the selected RA dosage rates are expected to have equivalent thermal cracking resistance as the control mixtures. In addition, all Aggregate 1 mixtures met the preliminary minimum fracture energy criterion of 300 J/m² recommended for Wisconsin's BMD evaluation.

Like Aggregate 1, the control mixture (20% ABR) of Aggregate 2 mixtures had lower fracture energy than the rejuvenated as well, except the 40% ABR mixture. ANOVA showed that the differences among the fracture energy values are statistically significant different. As shown in Figure 5.16, the statistical differences of the fracture energy values exist between the 20% ABR and 25% ABR mixtures; and the 25% ABR and 40% ABR mixtures. Therefore, mixtures with RA2 at the selected dosages are expected to have better/similar thermal cracking resistance as the control. Lastly, all Aggregate 2 mixtures also met the preliminary BMD minimum fracture energy criterion.

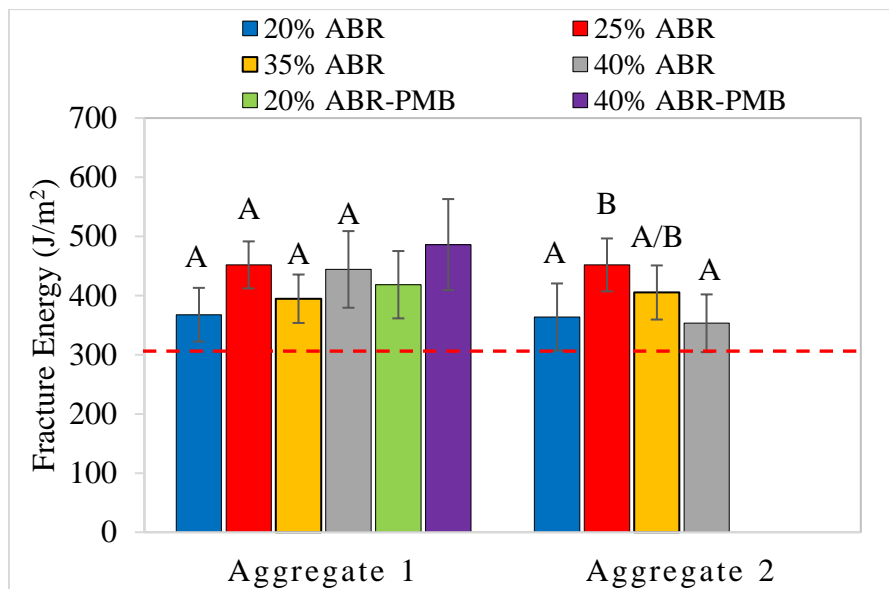


Figure 5.16: DCT's fracture energy results for the Wisconsin mixtures

Figure 5.17 presents the DCT fracture energy results of the South Dakota mixtures. For the 35% ABR mixtures, all mixtures except the one without RA and the one with RA4 had higher mean fracture energy values than the control mixture (20% ABR). The 35% ABR mixture without RA had the lowest mean fracture energy of all. When 35% ABR mixtures with RAs were compared among themselves, the 35% ABR mixture with RA5 had the highest mean fracture energy. ANOVA conducted on the fracture energy values of the 35% ABR mixtures (the 20% ABR mixture was also included) showed that the fracture energy values were statistically significant different. According to Tukey-Kramer, statistical significant difference exist between the control and the mixture without RA. The mixture with RA3 was statistically significant different from that without the RA. Lastly, the mixtures with RAs were not statistically significant from each other. This result indicates that, at the selected dosage rate, the 35% ABR mixtures are expected to have better or equivalent thermal cracking as the control.

For the 50% ABR mixtures, the control mixture (20% ABR) had high fracture energy than all the 50% ABR mixtures. Moreover, the mixture without RAs had a higher mean fracture energy than the mixture with RA4, but less than those with RA1 and RA3. ANOVA performed on the combined fracture energy of the 20% ABR mixture and the 50% ABR mixtures, showed that all the mixtures were not statistically significant different from each other. Therefore, regardless of whether the 50% mixture had RAs or not, they were expected to have equivalent resistance against thermal cracking resistance as the control mixture.

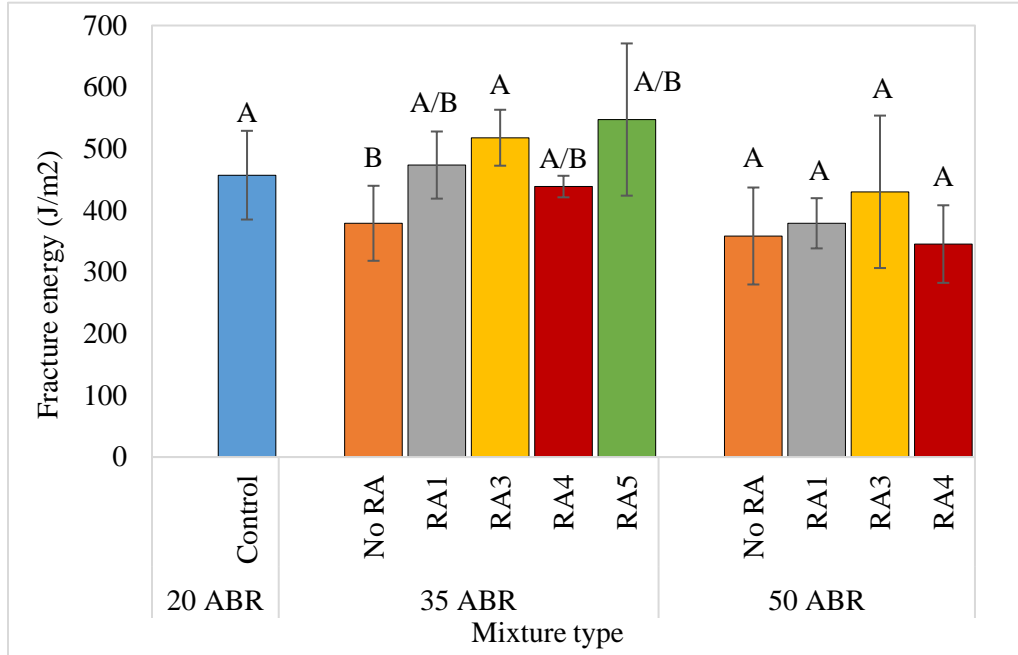


Figure 5.17: DCT's fracture energy results of South Dakota mixtures

5.5. Viscoelasticity and Aging Properties

To assess the stiffness properties of the asphalt mixtures over a wide range, the dynamic modulus master curves were constructed at a reference temperature of 20 °C. Moreover, statistical significance differences among the stiffness values were evaluated on the three critical testing conditions, which are: low temperature and high frequency (4 °C and 10 Hz), intermediate temperature and frequency (20 °C and 1 Hz), and high temperature and low frequency (35 °C and 0.1 Hz). The Tukey-Kramer groupings are shown in letters; mixtures with different letters are statistically significant different.

Figure 5.18 and Figure 5.19 present the dynamic modulus master curves of Aggregate 1 mixtures with the PG 58S-28 binder after STOA and LTOA, respectively. For the STOA condition, the 25% ABR mixture has the lowest $|E^*|$ values at high frequency/low temperatures (right-hand side of the curve) while the remaining three mixtures curves overlap each other. The 35% ABR mixture has

the highest stiffness values at intermediate frequency/temperatures while at low frequency/high temperatures (left-hand side of the curve) the 20% ABR mixture had the lowest stiffness with the 40% ABR mixtures being close to it. For LTOA condition, the 25% ABR and 20% ABR mixtures had the lowest $|E^*|$ values at high and low frequencies, respectively. In both cases, the master curves of the remaining three mixtures were close to each other.

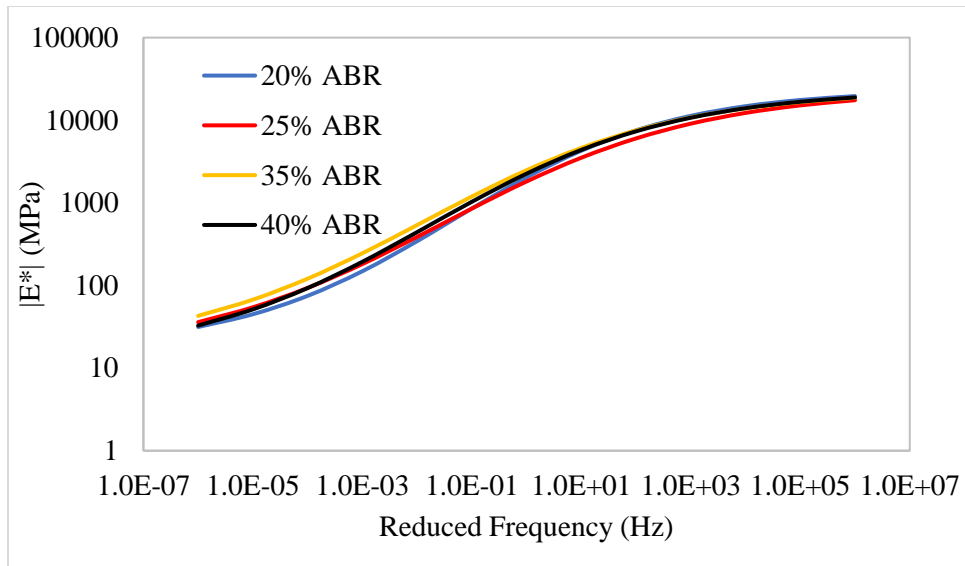


Figure 5.18: Dynamic modulus master curves of Aggregate 1 mixtures with the PG 58S-28 binder after STOA

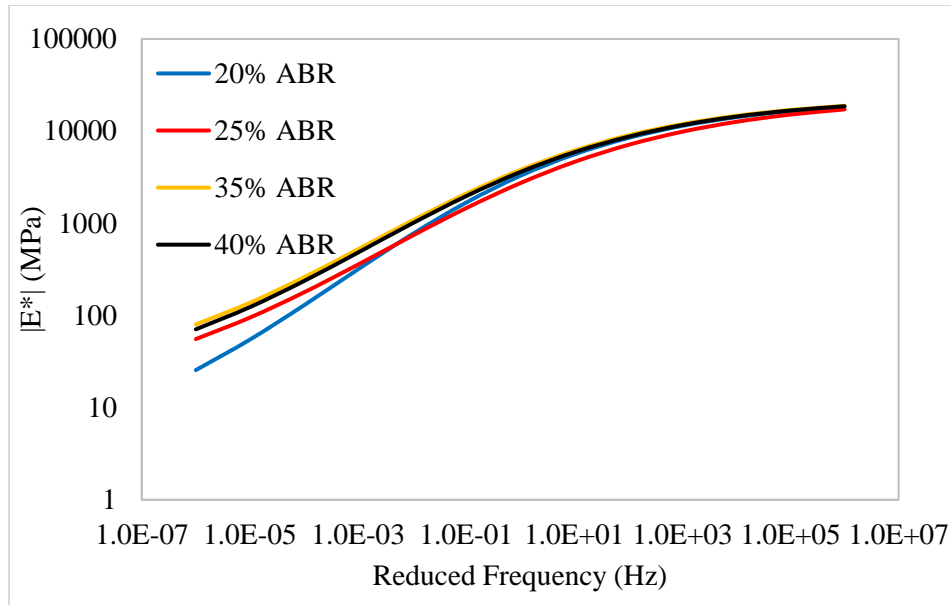


Figure 5.19: Dynamic modulus master curves of Aggregate 1 mixtures with the PG 58S-28 binder after LTOA

For Aggregate 1 mixtures with PG 58S-28 binder, ANOVA showed that the $|E^*|$ values were statistically significant different after both STOA and LTOA regardless of the testing conditions. Further statistical analysis of Aggregate 1 mixtures after STOA by the Tukey-Kramer showed that the difference in $|E^*|$ values are statistically significant different between the 20% ABR and 25% ABR mixtures, but the results were not statistically different between the 20% ABR and 35% ABR and 40% ABR mixtures at low temperature and high-frequency testing conditions (Table 5.4). At intermediate temperature and frequency testing conditions, statistical significance difference exists between the 20% ABR and the 35% ABR mixtures, but the results showed no statistical difference between the control and the 25% ABR and 40% ABR mixtures. At the high temperature and low-frequency test conditions the difference in stiffness values was statistically insignificant for all but the 20% ABR and 35% ABR mixtures (Table 5.4). After LTOA, statistical significance differences exist between the 20% ABR and the 25% ABR mixtures at both low temperature and high

frequency and intermediate temperature and frequency testing conditions. At high temperature and low frequency test condition, the 20% ABR mixture were statistically significant different from the 35% ABR and 40% ABR mixtures (Table 5.4).

Table 5.4: Tukey-Kramer grouping of Aggregate 1 mixtures with the PG 58S-28 binder

Testing conditions	STOA			LTOA		
	4 °C & 10 Hz	20 °C & 1 Hz	35 °C & 0.1 Hz	4 °C & 10 Hz	20 °C & 1 Hz	35 °C & 0.1 Hz
20% ABR	A	A/B	A	A	A	A
25% ABR	B	B	A/B	B	B	A
35% ABR	A	C	B	A	A	B
40% ABR	A	A/C	A/B	A	A	B

The dynamic modulus master curves of Aggregate 1 mixtures with the PG 58V-28 binder are shown in Figure 5.20 after both STOA and LTOA. In both cases, the control mixture (20% ABR-PMB) had high $|E^*|$ values than the rejuvenated mixture at low frequencies whereas at intermediate and high frequencies the curves are overlapping. Also, as expected the LTOA conditioned specimens had higher stiffness values than STOA specimens. A t-test on the stiffness values showed that their $|E^*|$ values were not statistically significant except for LTOA run at intermediate temperature and frequency test conditions.

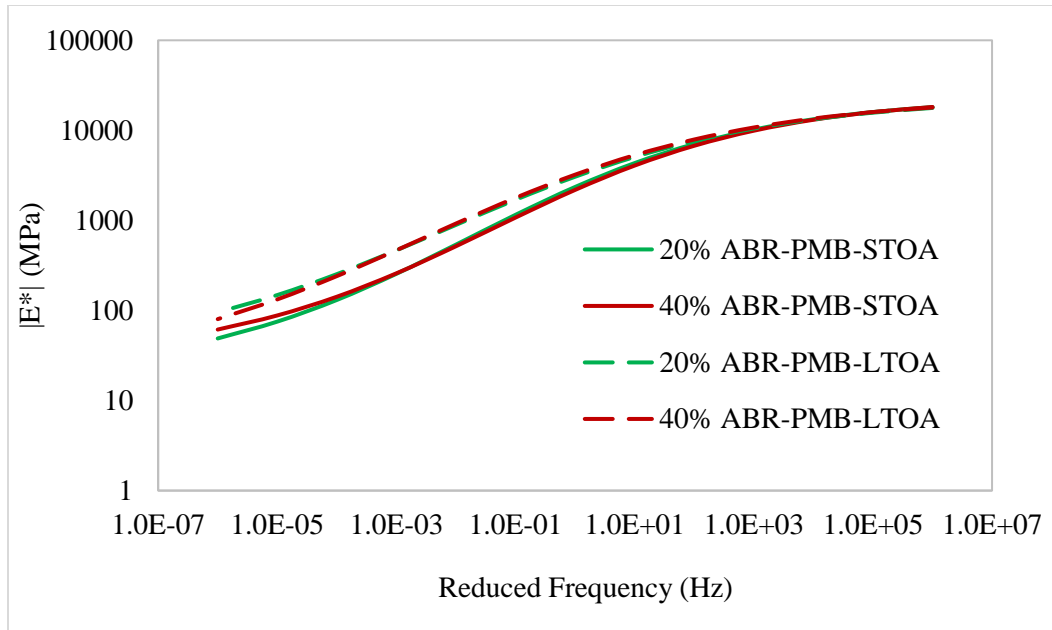


Figure 5.20: Dynamic modulus master curves of Aggregate 1 mixtures with the PMB after STOA and LTOA

The dynamic modulus master curves of Aggregate 2 mixtures after STOA and LTOA are shown in Figure 5.21 and Figure 5.22, respectively. From Figure 5.21, $|E^*|$ values of all Aggregate 2 mixtures are close to each other at high frequencies after STOA. While the other three remain close to each other, the $|E^*|$ values of the 25% ABR mixture decrease as the curves extend to intermediate frequencies. At low frequencies, the 20% ABR mixture has the lowest stiffness followed by the 40% ABR mix; the 25% ABR and 35% ABR mixtures overlap each other. After LTOA, the 20% ABR mixture has equivalent $|E^*|$ values as the 35% ABR and 40% ABR mixtures at high frequencies, whereas the 25% ABR mixture has the lowest $|E^*|$ values (Figure 5.22). In addition, at intermediate frequencies the $|E^*|$ values are on top of each other, whilst at low frequencies, the 20% ABR and 40% ABR mixtures has the lowest $|E^*|$ values, and the 25% ABR and 35% ABR are close to each other with the highest stiffness values.

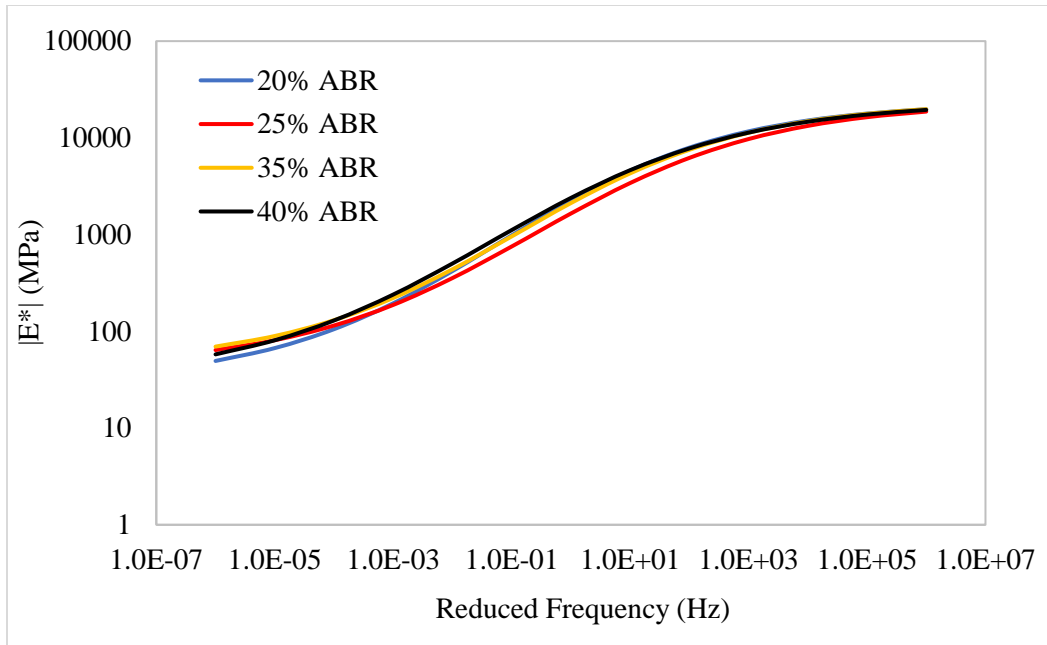


Figure 5.21: Dynamic modulus master curves of Aggregate 2 mixtures after STOA

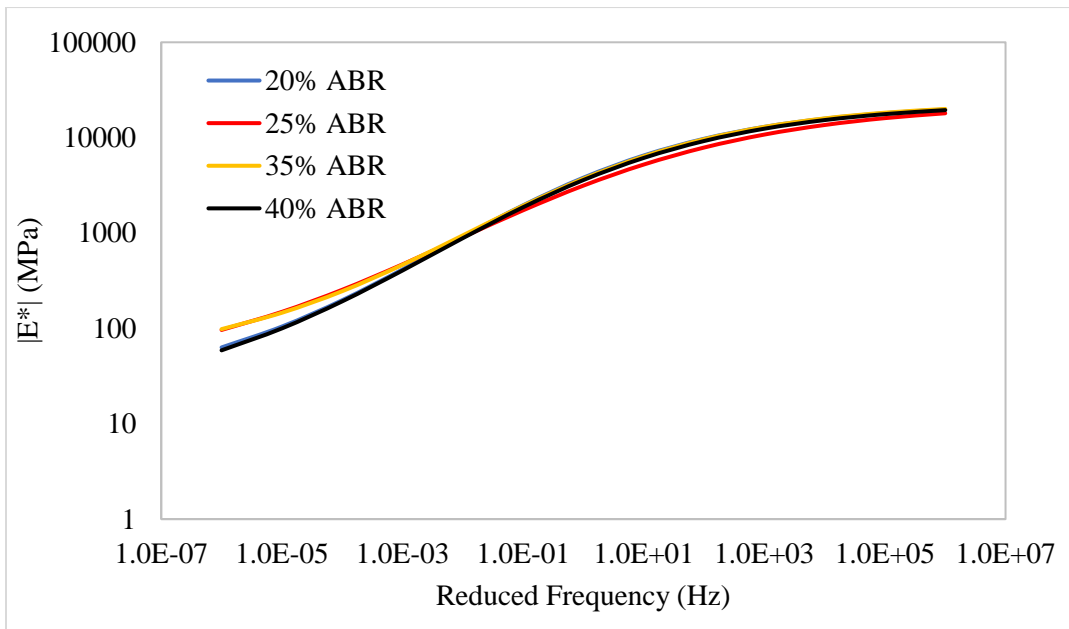


Figure 5.22: Dynamic modulus master curves of Aggregate 2 mixtures after LTOA

According to ANOVA, the stiffness values for Aggregate 2 mixtures were statistically significant different except for mixtures run at high temperature and low-frequency testing conditions after both STOA and LTOA. Based on Tukey-Kramer grouping (Table 5.5), the statistical significant different exists between the 20% ABR and 25% ABR mixtures after both STOA and LTOA and at low temperature and high frequency and intermediate temperature and frequency testing conditions.

Table 5.5: Tukey-Kramer groupings of Aggregate 2 mixtures

Testing conditions	STOA			LTOA		
	4 °C & 10 Hz	20 °C & 1 Hz	35 °C & 0.1 Hz	4 °C & 10 Hz	20 °C & 1 Hz	35 °C & 0.1 Hz
20% ABR	A	A	A	A	A	A
25% ABR	B	B	A	B	B	A
35% ABR	A	A/C	A	A	A	A
40% ABR	A	A/D	A	A	A	A

In summary, the 25% ABR mixture had the lowest $|E^*|$ value at low and intermediate frequencies after both STOA and LTOA for Aggregate 1 and Aggregate 2 mixtures with the PG 58S-28 binder. For Aggregate 1 mixtures with the PG 58V-28, the 20% ABR mixture had the highest $|E^*|$ value at a low frequency than the rejuvenated mixture, whereas at intermediate and high frequency the curves overlap. Moreover, the $|E^*|$ values of the control mixtures were statistically significant different from the 25% ABR at low temperature and high frequency and intermediate temperature and frequency testing conditions after both STOA and LTOA, indicating that the RAs were less effective in activating the RAS binder. At high temperature and low-frequency testing conditions, the $|E^*|$ values of the control mixture were statistically significant different when compared to the 35% ABR mixture of Aggregate 1 after STOA; after LTOA the statistical insignificance difference existed between the 20% ABR and 35% ABR. For Aggregate 2, the 20% ABR mixture was

statistically significant different from the 25% ABR mixture only, after either STOA or LTOA at low temperature and high frequency and intermediate temperature and frequency testing conditions. No statistical significant differences existed between the control and the rejuvenated mixtures at high temperature and low-frequency testing conditions after either STOA or LTOA.

The aging characteristics of the asphalt mixtures were evaluated using black space diagrams, constructed using $|E^*|$ and δ values at 20 °C and 5 Hz. Figure 5.23 and Figure 5.24 presents the black space diagrams of Aggregate 1 and Aggregate 2 mixtures, respectively. In both Figures, the mixtures are located more towards the bottom right corner after STOA, but with the increase in aging level (i.e., after LTOA) the points shifted to the upper right corner, which indicates an increase $|E^*|$ and reduction of relaxation properties (decrease in δ) of the mixtures.

Analysis of Aggregate 1 mixtures with the PG 58S-28 binder after STOA as presented in Figure 5.23 shows that the control mixture (20% ABR) was more on the right-top side compared to other rejuvenated mixtures. Moreover, the 35% ABR and 40% ABR mixtures fall in the same region of $|E^*|$ but have lower δ values than the 20% ABR mix. The 25% ABR mixture showed both lower $|E^*|$ and δ than the control mixture. The 35% ABR mixture has the lowest δ value than all other rejuvenated mixtures after STOA. After LTOA, Aggregate 1 mixtures with the PG 58S-28 binder showed a similar trend as observed after STOA. For mixtures with PG 58V-28, the control mixture (20% ABR-PMB) had slightly higher $|E^*|$ values than the 40% ABR-PMB mixture. Different from mixtures with the PG 58S-28 binder that showed similar trends when observed after STOA and LTOA; for mixtures with the PG 58-28, the 20% ABR-PMB mixture has a lower $|E^*|$ value than the 40% ABR-PMB after LTOA. In addition, mixtures 20% ABR-PMB and 40% ABR-PMB have similar δ values after LTOA.

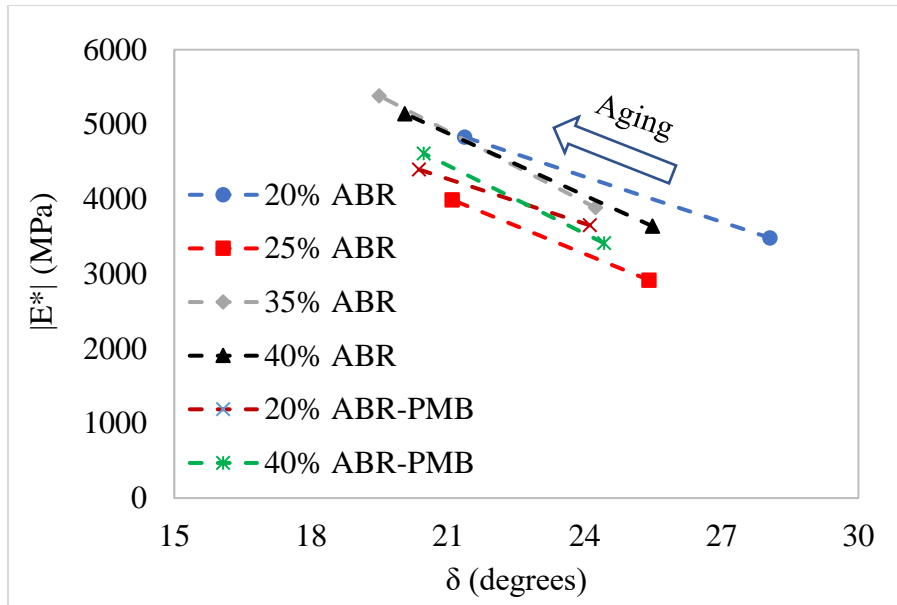


Figure 5.23: Black space diagram of Aggregate 1 mixtures

The black space diagram of the Aggregate 2 mixtures are shown in Figure 5.24. As stated previously, the points shift from the bottom-right corner to the top-left corner when the aging level is increased from STOA to LTOA, leading to increased stiffness and loss of relaxation properties. After STOA, the control mixture (20% ABR) and 35% ABR mixture fall in a similar region, while the 40% ABR has similar $|E^*|$ as the control but lower δ value. The 25% ABR mixture is on the most right corner with the lowest $|E^*|$ and highest δ values after STOA. After LTOA, the control mixture had the highest $|E^*|$ value. The 35% ABR and 40% ABR mixtures are in a similar region with lower $|E^*|$ and higher δ than the control mix; whereas mixture 25% ABR had both lower $|E^*|$ and δ values than both the control and other rejuvenated mixtures (35% ABR and 40% ABR).

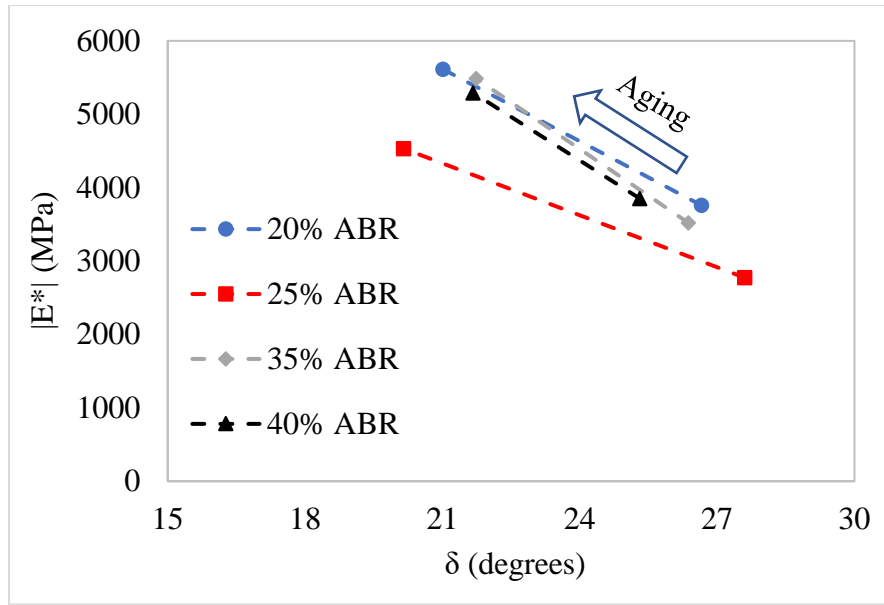


Figure 5.24: Black space diagram of Aggregate 2 mixtures

Furthermore, the Glover-Rowe mixture ($G-R_m$) parameter was used to evaluate the cracking potential of the asphalt mixtures. The $G-R_m$ parameter was obtained using $|E^*|$ and δ values at 20 °C and 5 Hz (Martin et al., 2019; Ogbo et al., 2019; Oshone et al., 2019; Zhang et al., 2020). The $G-R_m$ results of Aggregate 1 mixtures after STOA and LTOA with the PG 58S-28 binder and PG 58V-28 are depicted in Figure 5.25. For mixtures with PG 58S-28 binder, the control mixture (20% ABR) showed higher $G-R_m$ values than the 25% ABR mixture, but lower than the 35% ABR and 40% ABR mixtures after both STOA and LTOA. For mixtures with PG 58V-28, the control mixture (20% ABR-PMB) had a slightly higher $G-R_m$ value than the 40% ABR-PMB mixtures after STOA, an opposite trend is observed after LTOA. Both 20% ABR-PMB and 40% ABR-PMB are expected to have similar block cracking resistance after LTOA. The $G-R_m$ results of Aggregate 2 mixtures after both STOA and LTOA conditions are presented in Figure 5.26. For Aggregate 2 mixtures, the 20% ABR mixture had $G-R_m$ higher values than all rejuvenated mixtures after both STOA and LTOA (except for the 40% ABR mixture after STOA).

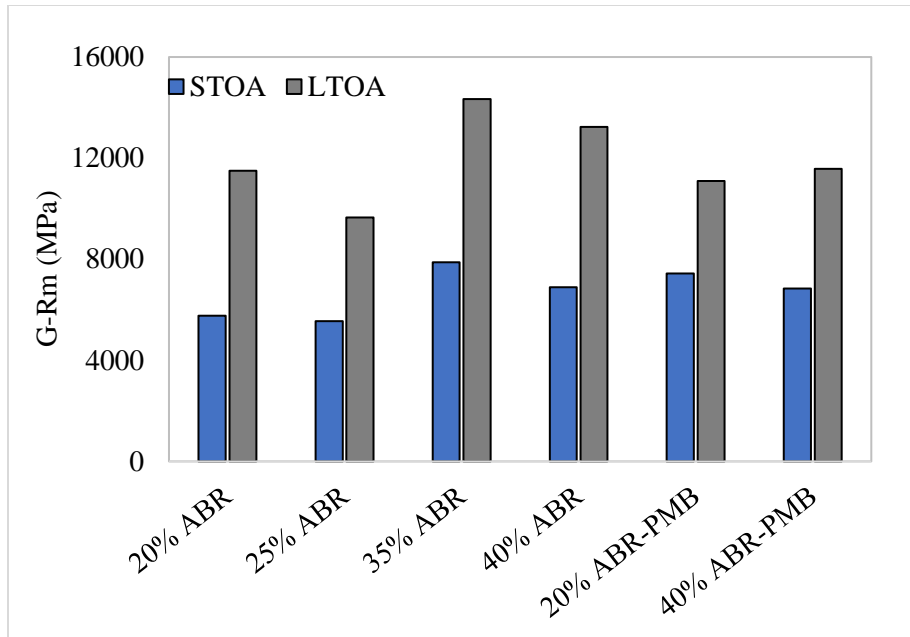


Figure 5.25: G-R_m of Aggregate 1 mixtures

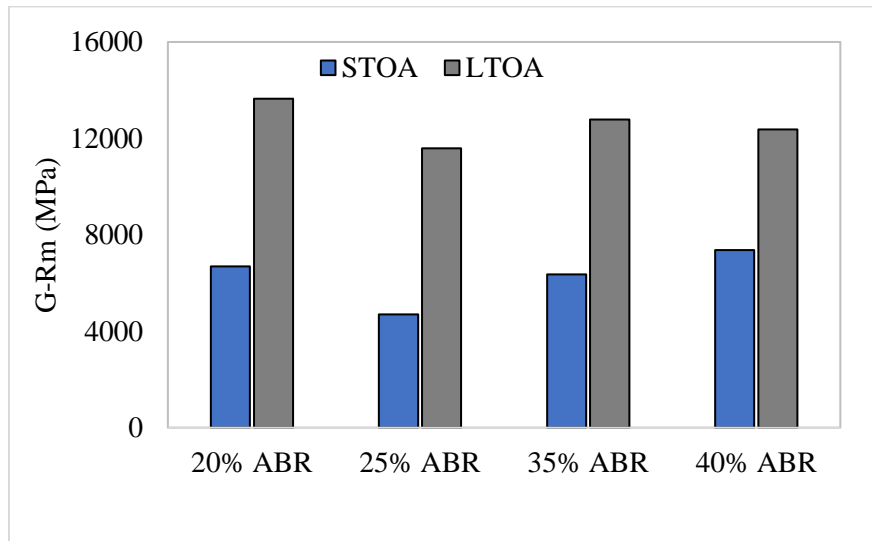


Figure 5.26: G-R_m of Aggregate 2 mixtures

Besides the black space diagrams, the $G-R_m$ aging index (aging ratio) was used to evaluate the aging susceptibility of the mixtures. The index is a ratio of $G-R_m$ values after LTOA and STOA of the respective mixture. A lower value is desirable for mixtures with lower aging susceptibility potential. Figure 5.27 shows the $G-R_m$ aging index of both Aggregate 1 and Aggregate 2 mixtures. For Aggregate 1 mixtures with the PG 58S-28 binder, the control mixture (20% ABR mixture) had a higher $G-R_m$ index than all the rejuvenated mixtures. Among the rejuvenated mixtures, the 25% ABR mixture had the lowest $G-R_m$ index and the 40% ABR had the highest. For Aggregate 1 mixtures with the PG 58V-28, the control mixture (20% ABR-PMB) had a lower $G-R_m$ index than the 40% ABR-PMB mix. For Aggregate 2 mixtures, the control mixture (20% ABR mixture) had an equivalent $G-R_m$ index as the 35% ABR mixture, but lower than the 25% ABR mix. Of all Aggregate 2 mixtures, the 40% ABR mixture had the lowest $G-R_m$ index value. Based on the above analysis of the $G-R_m$ index, the following can be inferred:

- The control mixture was more susceptible to aging than the rejuvenated mixtures for Aggregate 1 mixtures with PG 58S-28. For mixtures with PG 58V-28, the control was less susceptible to aging than the rejuvenated mixture.
- Comparison of the control mixtures of Aggregate 1 (20% ABR and 20% ABR-PMB) showed that the 20% ABR-PMB was less susceptible to aging than the 20% ABR mixture, which indicates an improved aging resistance due to polymer modification as expected.
- For Aggregate 2 mixtures, the aging susceptibility potential of the control mixture was expected to be equivalent to that of the 35% ABR mix, less than that of the 25% ABR, but higher than that of the 40% ABR mixture. In addition, the 25% ABR mixture showed the highest susceptibility to aging of all the mixtures.

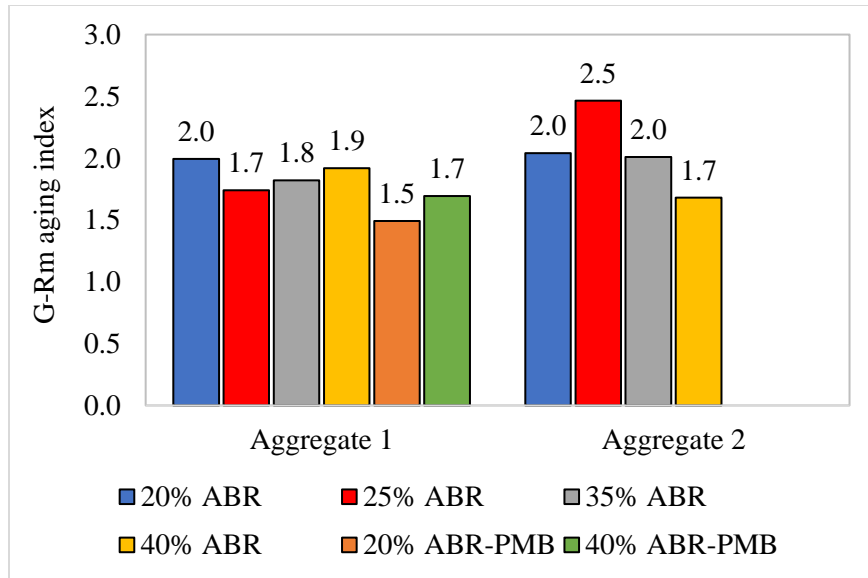


Figure 5.27: G-R_m aging index of Wisconsin mixtures

5.6. Summary

In this chapter, the results of high RAM content mixtures (with and without RAs) were presented and discussed. The high RAM content mixtures were prepared using materials from Wisconsin and South Dakota. Wisconsin materials included two base binders (PG 58S-28 and PG 58V-28), two bio-based RAs (RA1 and RA2), two RAP sources (RAP1 and RAP2), one RAS source, and two aggregate sources (Aggregate 1 and Aggregate 2). Mixtures for Aggregate 1 were prepared along with RAP1 and RA1 whereas Aggregate 2 mixtures used RAP1 and RA2. With this material, the high RAM content mixtures [25% ABR (from RAS only), 35% ABR (30% from RAP + 5% from RAS), and 40% ABR (from RAP only)] were compared to the control mixtures with 20% ABR (from RAP only). The PG 58S-28 binder was used to produce all the mixtures. The PG 58V-28 was used only with Aggregate 1 mixtures to produce a 40% ABR-PMB mixture which was compared to the control (20% ABR-PMB). The RAs dosages for Wisconsin mixtures were determined targeting the LTPG of the base binders (i.e., -28 °C) after RTFO plus 40 hours PAV.

The South Dakota materials included a PG 58S-34 base binder with one RAP and aggregate source. The high RAM contents mixtures were 35% ABR and 50% ABR and they were compared to the control mixture (20% ABR). Three bio-based RAs (RA1, RA3, and RA4) and one-petroleum-based (RA5) were used. The bio-based RAs' dosages were determined by the manufacturers targeting the continuous LTPG of the 20% ABR blend after RTFO plus 60 hours PAV. The dosage of RA5 was determined at NCAT and it was presented in this study for evaluation purposes only as the dosage was too high to be practical. All mixtures were conditioned for STOA and LTOA at 135 °C for four and six hours, respectively. The findings are summarized as follows.

- i. For Wisconsin mixtures, high RAM content mixtures with Aggregate 1 and 2 with RAs had improved rutting resistance and moisture susceptibility potential compared to the control mixtures based on the HWTT. Moreover, all but the 20% ABR mixture with Aggregate 1 and the PG 58S-28 binder and Aggregate 2 mixtures with 20% ABR and 35% ABR passed the preliminary BMD requirement of the minimum number of wheels passes of 15,000 to 12.5 mm rut depth. Furthermore, all the mixtures passed the preliminary BMD threshold of a maximum 7 mm CRD. In addition, all mixtures except Aggregate 1 mixture 20% ABR met the SN criterion of 2,000 passes whereas only the 20% ABR with PG 58S-28 and the 25% ABR failed the 9,000 passes SIP criterion.
- ii. As for South Dakota mixtures, the APA showed that high RAM content mixtures with or without RAs had lower rut depth than the control mixtures (except the 35% ABR mixture with RA5). However, none of the mixtures exceed a 7 mm rut depth threshold required by South Dakota DOT for class Q2 roadways.
- iii. IDEAL-CT results of the Wisconsin mixtures showed that the control mixtures of Aggregate 1 and Aggregate 2 mixtures had better intermediate temperature cracking

resistance than the high RAM content mixtures (with or without RAs). For high RAM content mixtures with Aggregate 1 and the PG 58S-28 binder, although mixtures with RAs had higher average CT_{index} values than their corresponding mixtures without RAs. The CT_{index} values of the 35% ABR mixtures (with and without RAs) were not statistically significant different, and therefore expected to have similar intermediate temperature cracking resistance. The 20% ABR-PMB mixture had better intermediate temperature cracking resistance than the 40 % ABR-PMB mixtures (with and without RA1). However, the 40% ABR-PMB mixtures with and without RA1 were not statistically significant different. Only the control mixtures and the 40% ABR mixture with RA1 met the preliminary BMD requirement of a minimum CT_{index} of 40. The increase of RA1 dosage by 1% to improve the CT_{index} of the 25% ABR and 35% ABR mixtures did not show any significant change. For Aggregate 2 mixtures, high RAM content mixtures with RAs had higher average CT_{index} values than their corresponding mixtures without RA. However, only the CT_{index} values of the 25% ABR and 35% ABR mixtures (with and without RA2) were statistically significant different. Nevertheless, the control and all high RAM content mixtures with RA2 met the minimum CT_{index} criterion of 40.

- iv. IDEAL-CT results of the South Dakota mixtures showed that high RAP content mixtures with or without RAs had a lower intermediate temperature cracking resistance than the control mixture. Nevertheless, high RAP content mixtures with RAs had high mean CT_{index} values than those without RAs. However, only the 35% ABR mixture with RA3 and the 50% ABR mixture with RA4 were statistically significant different from their corresponding mixtures without RAs.

- v. The correlations between results of CT_{index} and the post peak slope and fracture energy of Aggregate 1 and 2 mixtures were used to propose preliminary thresholds for the post peak slope and fracture energy to ensure compliance with CT_{Index} criterion.
- vi. Further investigation conducted using a limited material sets to understand why RAs did not show significant impact on the CT_{index} of the high RAP content mixtures except for two cases suggested the following:
- The RAs dosages recommended by the manufacturer targeting the true LTPG of the 20% ABR blend (after RTFO plus 60-hour PAV) were not sufficient to improve the CT_{index} of the higher RAP content mixtures; instead, the approach targeting the LTPG of the base binder could be employed as it showed significant improvement in the CT_{index} values.
 - IDEAL-CT tests conducted on sample subjected to three aging levels showed that the effectiveness of RA decreases with aging.
 - The application of the 75% discount factor (to account for the inactive RAM binder) on the 35% ABR mixture with RA1 showed improved CT_{index} results, indicating that a combination of RA and increased total binder content could produce mixtures with improved intermediate temperature cracking resistance.
- vii. DCT results of Wisconsin mixtures showed that high RAM content mixtures with RAs had equivalent low temperature cracking resistance as the control mixture. However, all the mixtures exceeded the minimum preliminary BMD fracture energy criterion of 300 J/m^2 .
- viii. DCT results of South Dakota mixtures showed that all high RAP content mixtures had equivalent low temperature cracking resistance as the control mixture except the 35% ABR mixture without RA.

- ix. Based on the $|E^*|$ test, mixed results were found when the rejuvenated mixtures were compared to the control after STOA and LTOA at the three testing conditions evaluated. For instance, the control mixture of Aggregate 1 with the PG 58S-28 binder had significantly higher stiffness value than the 25% ABR mixture after either STOA or LTOA at low temperature and high frequency testing conditions while none was observed at high temperature and low frequency testing conditions after both aging levels. For Aggregate 2 mixture with the PG 58S-28 binder, the control mixture had significantly higher stiffness value than the 25% ABR mixture after either STOA or LTOA at low temperature and high frequency and intermediate temperature and frequency testing conditions.
- x. The control mixture of Aggregate 1 mixtures with the PG 58S-28 binder, had higher $G-R_m$ value than the 25% ABR mixture, but lower than the 35% ABR and 40% after both STOA and LTOA. For mixtures with PG 58V-28, the control mixture (20% ABR-PMB) had a slightly higher $G-R_m$ value than the 40% ABR-PMB mixes after STOA, an opposite trend is observed after LTOA. The control mixture of Aggregate 2 mixtures had higher $G-R_m$ values than all rejuvenated mixes after both STOA and LTOA (except for the 40% ABR mixture after STOA).
- xi. The control mixture was more susceptible to aging than the rejuvenated mixtures of Aggregate 1 with the PG 58S-28 binder. For mixtures with the PG 58V-28, the control mixture was less susceptible to aging than the rejuvenated mixture. Moreover, the 20% ABR-PMB mixture was less susceptible to aging than the 20% ABR mixture, indicating improved aging resistance due to polymer modification. For Aggregate 2 mixes, the aging susceptibility potential of the control is expected to be equivalent to that of the 35% ABR

mix, less than that of the 25% ABR, but higher than that of the 40% ABR. In addition, the 25% ABR mixture is the least susceptible to aging of all rejuvenated mixes.

6. CONCLUSIONS

In this study, a comprehensive experimental test matrix was completed to develop a fundamental understanding of the effect of high RAM on the performance of asphalt binders and mixtures. The results were used to evaluate the effectiveness of RAs in restoring the properties of RAM binder and improving the performance of mixtures; and to recommend a methodology to guide the usage of RAs to produce high RAM content mixtures with satisfactory performance. The following points summarize the major findings of this study.

Rutting and Moisture Susceptibility

- The HTPG of the recycled binder blends increased with the addition of RAM, indicating potential improvement in rutting resistance. The addition of RAs softened the recycled binder blends and decreased the HTPG of the recycled binder blends, restoring the HTPG to that of the base binder. Exception occurred for recycled binder blends with 25% RAS binder, which had HTPG higher than the base binder, and for the recycled binder blends with 35% RAP binder and petroleum-based RA (asphalt flux), which presented an HTPG lower than the base binder.
- J_{nr} and %Recovery MSCR testing parameters were dependent on the constituents of the recycled binder blends (i.e., base binder type, RAM binder content, and RA type and dosage). Moreover, the %Recovery parameter was highly influenced by the J_{nr} of the binders, regardless of the presence and dosage of RAs. RA increased the magnitude of J_{nr} ,

where this increase varied depending on the chemical composition and dosage of the additives as well as the RAM type and content.

- For Wisconsin mixtures, the HWTT results showed that all mixtures with RAs had improved rutting resistance and were less prone to moisture damage when compared to the control mixtures. Exception occurred for Aggregate 2 mixture with 25% ABR which failed the preliminary BMD's SIP criteria of 9,000 passes. For South Dakota mixtures, the APA results showed that the incorporation of RAs into high RAP content mixtures did not have a significant impact on the rutting resistance of the mixtures.

Intermediate Temperature Cracking Resistance

- Increasing the RAM binder content decreased the fatigue resistance behavior of the recycled binder blends. However, when RAs were added to the recycled asphalt blends, the fatigue resistance of recycled binder blends improved. The improvement was influenced by the type and content of both the RAM binder and RA.
- G-R parameter results highlighted the binder stiffening effect due to the use of recycled asphalt materials, where the blends containing high RAM binder consistently showed higher G-R parameters than the base binders, as expected. The addition of RAs to the recycled binder blends decreased the stiffness of all blends, before and after aging. For the bio-based RAs, the decrease in stiffness was followed by an increase in the phase angle (δ).
- The control mixtures had better intermediate temperature cracking resistance than all high RAM contents mixtures (with or without RAs). Only four high RAM content mixtures with RAs had better intermediate temperature cracking resistance than their corresponding mixtures without RAs. The difference in the intermediate temperature cracking

performance between recycled binder blends and mixtures may be due to the fact that mixture design assumed 100% availability of RAM binder even though binder is only partially available. On the other hand, for recycled binder blends the actual RAM binder proportion is blended with the base binder contributing to the performance of the blend. Additional IDEAL-CT tests conducted to explore alternatives to improve the CT_{index} of high RAM content with RAs that did not show significant improvement when compared to their corresponding mixtures without RAs showed that the use of a discount factor which increased virgin binder and RA content improves the intermediate temperature cracking resistance of high RAM content mixtures with RAs.

Low Temperature (Thermal) Cracking Resistance

- ΔT_c parameter results after RTFO plus 40 hours of PAV aging indicated that recycled binder blends with up to 40% RAP binder met the threshold of -5°C . Contrary, the addition of RAS binder between 15 and 25% significantly increased the block cracking susceptibility of the resultant recycled binder blends. When considering the aging protocol of RTFO plus 60-hour PAV, the addition of bio-based RAs to recycled binder blends containing RAP binder by 35% and 50% improved their low temperature cracking resistance.
- At the mixtures level, the control mixtures were not statistically significant different from the high RAM content mixtures with RAs. Therefore, high RAM content mixtures with RAs were expected to have equivalent/better low temperature cracking resistance as the control mixture.

Viscoelasticity Properties and Aging Susceptibility

- $|E^*|$ test results in terms of $G-R_m$ and $G-R_m$ aging index showed mixed results. After STOA, the $G-R_m$ of rejuvenated mixtures was higher than that of the control mixtures. However, after LTOA only the $G-R_m$ of the 35% ABR and 40% ABR of Aggregate 1 mixture were higher than the control mixtures.

The $G-R_m$ aging index of the asphalt mixtures showed high RAM content mixtures with RAs had low or similar oxidative aging susceptibility as the control mixture, except Aggregate 2 mixtures with the 25% ABR which had a higher $G-R_m$ aging index than the control mixture.

Products of Oxidative Aging

- The oxygen containing functionalities (carbonyl and sulfoxide) increased with the increase of the RAM content; while being influenced by the RAM type (RAP, RAS, or RAP + RAS).
- The addition of the RA to the recycled binder blends reduced the carbonyl and sulfoxide area; the effectiveness was dependent on the type and dosage of RA.

7. RECOMMENDATIONS

The results of this study were used to develop a methodology for incorporating RAs into asphalt mixtures with high RAP and/or RAS content. The methodology was divided into two stages: RA's dosage determination and evaluation of asphalt mixture properties:

Stage 1: Determination of the RA's dosage

The RA dosage determination is of utmost importance since its aimed at balancing the cracking and rutting properties of the resultant recycled asphalt blend/mixtures. The following procedures can be followed to determine the RA dosage:

- i. Extract and recover the RAP and/or RAS binder.
- ii. Determine the HTPG and LTPG of the components materials ((i.e., virgin binder, RAP, RAS) to be used for blending.
- iii. Prepare the recycled asphalt binder blend (virgin binder + recovered binder from RAM) at the desired proportion of ABR with an initial RA dosage.
- iv. Age the recycled binder blends in the PAV following an established protocol.
- v. Perform the BBR test on the aged recycled binder blends from (iv).
- vi. Determine the optimum RA dosage using blending charts targeting the LTPG based on the climatic and traffic requirements of the project.

Stage 2: Evaluate the properties of the high RAM content mixtures

At this stage, asphalt mixtures are prepared using the optimum RA dosage obtained in (vi) to conduct mixture performance tests and assess compliance with performance tests criteria.

- vii. Prepare mixture samples for performance testing evaluation. Mixture for rutting resistance should be evaluated after STOA whereas those for intermediate and low temperature cracking resistance must be assessed after LTOA in addition to STOA.
- viii. Test the compacted specimens following the respective protocols for each test and assess if they meet the corresponding performance criteria.
- ix. If any of the threshold is not met, adjust the RA dosage and/or binder content of the mixture and verify performance tests.

To understand the aforementioned steps, materials from Wisconsin were used to illustrate how the methodology can be applied.

- i. The RAM binder was extracted and recovered per AASHTO T164-14 and ASTM D5404-12, respectively.
- ii. The HTPG and LTPG of the component materials were determined following AASHTO M320. The requirements of the component materials are shown in Table 7.1.

Table 7.1: Requirements of the constituent binders

Constituent Material	HTPG		ΔT_c	
	Aging	Threshold	Aging	Threshold
Base binder	Unaged and RTFO	≤ 64 °C	RTFO plus 40	≥ 0.0 °C
RAP binder	RTFO	≤ 82 °C	RTFO	≥ -3.0 °C
RAS binder (if used)	As extracted	≤ 160 °C	As extracted	N/A

- iii. The recycled asphalt binder blends (virgin binder + recycled binder from RAM) were prepared at the desired proportion of ABR with and without RA.
- iv. For those prepared with an RA, an initial dosage of 5% and 20% by weight of the total asphalt binder was used for bio-based and petroleum-based (asphalt flux), respectively.
- v. The recycled binder blends were aged at RTFO plus 40 hours of PAV.
- vi. The standard BBR test on the aged blends from (iv) following AASHTO T313.
- vii. The optimum RA dosage was determined using blending charts targeting the LTPG (i.e., -28 °C for Wisconsin).
 - With the blending chart, the optimum RA dosage is interpolated using the data points with zero RA and with the initial RA dosage (i.e., 5% for bio-based).

It should be noted that asphalt mixtures in this study were developed following the volumetric mixture design approach. However, mixtures with high RAM contents and RAs can be better optimized with a BMD approach, since slight adjustments to the dosage of RAs and/or the mixture total binder content could provide high RAM content mixtures with balanced rutting and cracking performance. The preliminary BMD thresholds developed using mixtures from Wisconsin during the WHRP 0092-20-14 project were adopted to assess the performance of the asphalt mixtures (Table 7.2).

Table 7.2: Preliminary BMD thresholds for Wisconsin mixtures by West et al. (2021b)

Traffic Level (ESALs)	HWTT @STOA				IDEAL-CT Min. CT _{index} @ LTOA	DCT Min. Fracture Energy (J/m ²) @LTOA
	Min. # of passes to 12.5 mm rut depth	Min. SIP (passes)	Max. CRD @ 20,000 passes	Min. SN (passes)		
>8 million	15,000	9,000	6.0	2,000	40	300
2 – 8 million	15,000		7.0			
<2 million	10,000		8.0			

- viii. Asphalt mixture samples for HWTT, DCT, and IDEAL-CT with the RA’s dosage obtained in step (vi) were prepared.
- For HWTT, samples were compacted after aging loose mixtures for four hours at 135°C (STOA).
 - For IDEAL-CT and DCT, samples were compacted after aging the loose mixtures for six hours at 135°C (LTOA) in addition to STOA.
- ix. The compacted specimens were tested following the respective protocols for each test and the results were compared to the thresholds in Table 7.2. In this study, HWTT and DCT results exceeded the required thresholds, while IDEAL-CT results showed that some of the recycled mixtures with RAs barely failed their corresponding performance requirement. Two approaches to improve the IDEAL-CT results (1) increasing the RA’s dosage (2) increasing the virgin binder content were explored. In this study, the use of a discount factor for RAM materials to increase the virgin binder content was found to be more effective than just increasing the RA dosage. However, additional research is needed to better understand binder availability for different RAM materials and mix design variables.

- x. If the IDEAL-CT is not satisfied, increase the RA dosage or increase the asphalt binder content and verify IDEAL-CT and HWTT.

REFERENCES

- Abd, D. M., Al-Khalid, H., & Akhtar, R. (2018). Novel methodology to Investigate and obtain a complete blend between RAP and virgin materials. *Journal of Materials in Civil Engineering*, 30(5).
- Abdalfattah, I. A., Mogawer, W. S., & Stuart, K. (2021). Quantification of the degree of blending in hot-mix asphalt (HMA) with reclaimed asphalt pavement (RAP) using Energy Dispersive X-Ray Spectroscopy (EDX) analysis. *Journal of cleaner production*, 294, 126261.
- Abdelaziz, A., Epps Martin, A., Masad, E., Arámbula Mercado, E., & Kaseer, F. (2020). Effects of ageing and recycling agents on the multiscale properties of binders with high RAP contents. *International Journal of Pavement Engineering*, 1-23.
doi:10.1080/10298436.2020.1797736
- Abed, A., Thom, N., & Presti, D. L. (2018). Design considerations of high RAP-content asphalt produced at reduced temperatures. *Materials and Structures*, 51(4), 1-16.
- AbuHassan, Y., Alin, M., Iqbal, T., Nazzal, M., & Abbas, A. R. (2019). Effect of extraction solvents on rheological properties of recovered asphalt binders. *Journal of Transportation Engineering, Part B: Pavements*, 145(1), 04018064.
- AbuQtaish, L., Nazzal, M. D., Kaya, S., Kim, S.-S., Abbas, A., & Abu Hassan, Y. (2018). AFM-based approach to study blending between RAP and virgin asphalt binders. *Journal of Materials in Civil Engineering*, 30(3), 04017300.
- Al-Saffar, Z. H., Yaacob, H., Mohd Satar, M. K. I., Putra Jaya, R., Ismael, C. R., Mohamed, A., & Rogo, K. U. (2021). Physical, rheological and chemical features of recycled asphalt embraced with a hybrid rejuvenating agent. *International Journal of Pavement Engineering*, 1-19. doi:10.1080/10298436.2021.1878517
- Ali, A. W., Mehta, Y. A., Nolan, A., Purdy, C., & Bennert, T. (2016). Investigation of the impacts of aging and RAP percentages on effectiveness of asphalt binder rejuvenators. *Construction and Building Materials*, 110, 211-217.
- Ameri, M., Mansourkhaki, A., & Daryaei, D. (2018). Evaluation of fatigue behavior of high reclaimed asphalt binder mixes modified with rejuvenator and softer bitumen. *Construction and Building Materials*, 191, 702-712.
doi:<https://doi.org/10.1016/j.conbuildmat.2018.09.182>
- Anderson, R. M., King, G. N., Hanson, D. I., & Blankenship, P. B. (2011). Evaluation of the relationship between asphalt binder properties and non-load related cracking. *Journal of the Association of Asphalt Paving Technologists*, 80.

- Arámbula-Mercado, E., Kaseer, F., Epps Martin, A., Yin, F., & Garcia Cucalon, L. (2018). Evaluation of recycling agent dosage selection and incorporation methods for asphalt mixtures with high RAP and RAS contents. *Construction and Building Materials*, 158, 432-442. doi:10.1016/j.conbuildmat.2017.10.024
- Aschenbrener, T. (2018). *FHWA Division Office Survey on State Highway Agency Usage of Reclaimed Asphalt Shingles: Quantities, Trends, Requirements, and Direction-Results from May 2017*
- Aske, N., Kallevik, H., Johnsen, E. E., & Sjöblom, J. (2002). Asphaltene Aggregation from Crude Oils and Model Systems Studied by High-Pressure NIR Spectroscopy. *Energy & Fuels*, 16(5), 1287-1295. doi:10.1021/ef020065i
- ASTM. (2020). *Standard Classification for Hot-Mix Recycling Agents (D4552/D4552M-20)*
- Bahia, H., Zhang, Y., Swiertz, D., & Soleimanbeigi, A. (2020). Long-term performance of asphalt concrete mixed with RAP and RAS.
- Bahia, H. U. (1995). Critical evaluation of asphalt modification using strategic highway research program concepts. *Transportation research record*(1488).
- Bahia, H. U., Sadek, H., Rahaman, M. Z., Lemke, Z., Swiertz, D., Reichelt, S., & Bitumix Solutions, L. (2018). *Field aging and oil modification study*
- Bajaj, A., Epps Martin, A., King, G., Glover, C., Kaseer, F., & Arámbula-Mercado, E. (2020). Evaluation and classification of recycling agents for asphalt binders. *Construction and Building Materials*, 260, 119864. doi:10.1016/j.conbuildmat.2020.119864
- Baqersad, M., & Ali, H. (2019). Rheological and chemical characteristics of asphalt binders recycled using different recycling agents. *Construction and Building Materials*, 228, 116738. doi:<https://doi.org/10.1016/j.conbuildmat.2019.116738>
- Behnood, A. (2019). Application of rejuvenators to improve the rheological and mechanical properties of asphalt binders and mixtures: A review. *Journal of cleaner production*, 231, 171-182.
- Bell, C. A., Sosnovske, D., & Wieder, J. (1994). *Aging: binder validation: Strategic Highway Research Program*, National Research Council Washington, DC.
- Bennert, T., Ericson, C., & Pezeshki, D. (2015). *Rejuvenating Agents with RAP in Hot Mix Asphalt (HMA)*
- Bonaquist, R. (2005). *Laboratory evaluation of hot mix asphalt (HMA) mixtures containing recycled or waste product materials using performance testing*
- Bonaquist, R. (2014). Impact of mix design on asphalt pavement durability. *Transportation Research Circular*(E-C186).

- Bonicelli, A., Calvi, P., Martinez-Arguelles, G., Fuentes, L., & Giustozzi, F. (2017). Experimental study on the use of rejuvenators and plastomeric polymers for improving durability of high RAP content asphalt mixtures. *Construction and Building Materials*, 155, 37-44. doi:<https://doi.org/10.1016/j.conbuildmat.2017.08.013>
- Booshehrian, A., Mogawer, W. S., & Bonaquist, R. (2013). How to construct an asphalt binder master curve and assess the degree of blending between RAP and virgin binders. *Journal of Materials in Civil Engineering*, 25(12), 1813-1821.
- Bouraima, M. B., Zhang, X.-h., Zhou, S.-w., & Qiu, Y. (2017). Effect of Extraction Residue on the Properties of Asphalt Binders. *Global Journal of Research In Engineering*.
- Bowers, B. F., Huang, B., Shu, X., & Miller, B. C. (2014). Investigation of reclaimed asphalt pavement blending efficiency through GPC and FTIR. *Construction and Building Materials*, 50, 517-523.
- Buchanan, S. (2018). Optimized Mix Design Approach: Contractors Perspective. *Innovations in Asphalt Mixture Design Procedures*, 1.
- Cai, X., Zhang, J., Xu, G., Gong, M., Chen, X., & Yang, J. (2019). Internal aging indexes to characterize the aging behavior of two bio-rejuvenated asphalts. *Journal of Cleaner Production*, 220, 1231-1238. doi:10.1016/j.jclepro.2019.02.203
- Carpenter, S. H., & Wolosick, J. R. (1980). Modifier influence in the characterization of hot-mix recycled material. *Transportation research record*(777).
- Castorena, C., Pape, S., & Mooney, C. (2016). Blending measurements in mixtures with reclaimed asphalt: use of scanning electron microscopy with X-ray analysis. *Transportation Research Record*, 2574(1), 57-63.
- Cavalli, M. C., Partl, M. N., & Poulikakos, L. D. (2017). Measuring the binder film residues on black rock in mixtures with high amounts of reclaimed asphalt. *Journal of cleaner production*, 149, 665-672.
- Chen, A., Liu, G., Zhao, Y., Li, J., Pan, Y., & Zhou, J. (2018a). Research on the aging and rejuvenation mechanisms of asphalt using atomic force microscopy. *Construction and Building Materials*, 167, 177-184. doi:10.1016/j.conbuildmat.2018.02.008
- Chen, C. (2020). *Validation of Laboratory Cracking Tests for Field Top-down Cracking Performance*. Auburn University. Retrieved from <https://etd.auburn.edu/bitstream/handle/10415/7135/Chen%20Chen%27s%20Dissertation%20Final%20Version.pdf?sequence=2&isAllowed=y>
- Chen, C., Yin, F., Turner, P., West, R. C., & Tran, N. (2018b). Selecting a Laboratory Loose Mix Aging Protocol for the NCAT Top-Down Cracking Experiment. *Transportation Research Record: Journal of the Transportation Research Board*, 2672(28), 359-371. doi:10.1177/0361198118790639

- Chesner, W. H., Collins, R. J., MacKay, M. H., & Emery, J. (2002). *User guidelines for waste and by-product materials in pavement construction*
- De Bock, L., Piérard, N., Vansteenkiste, S., & Vanelstraete, A. (2020). *Categorisation and analysis of rejuvenators for asphalt recycling*.
- Ding, Y., Huang, B., & Shu, X. (2018). Blending efficiency evaluation of plant asphalt mixtures using fluorescence microscopy. *Construction and Building Materials*, *161*, 461-467.
- Ding, Y., Huang, B., Shu, X., Zhang, Y., & Woods, M. E. (2016). Use of molecular dynamics to investigate diffusion between virgin and aged asphalt binders. *Fuel*, *174*, 267-273.
- EAPA. (2018). *Recommendations for the Use of Rejuvenators in Hot and Warm Asphalt Production*
- Elkashaf, M., Williams, R. C., & Cochran, E. (2018). Thermal stability and evolved gas analysis of rejuvenated reclaimed asphalt pavement (RAP) bitumen using thermogravimetric analysis–Fourier transform infrared (TG–FTIR). *Journal of Thermal Analysis and Calorimetry*, *131*(2), 865-871. doi:10.1007/s10973-017-6674-9
- Forton, A., Mangiafico, S., Sauzéat, C., Di Benedetto, H., & Marc, P. (2020). Properties of blends of fresh and RAP binders with rejuvenator: Experimental and estimated results. *Construction and Building Materials*, *236*, 117555. doi:10.1016/j.conbuildmat.2019.117555
- Garcia Cucalon, L., Kaseer, F., Arámbula-Mercado, E., Epps Martin, A., Morian, N., Pournoman, S., & Hajj, E. (2019). The crossover temperature: significance and application towards engineering balanced recycled binder blends. *Road Materials and Pavement Design*, *20*(6), 1391-1412. doi:10.1080/14680629.2018.1447504
- GDOT. (2019). Appendix D: Method of Calculating Credited Asphalt Cement Content for Corrected Optimum AC Content for Asphaltic Concrete Mixtures Incorporating Reclaimed Asphalt Pavement (RAP) or Pre- or Post-Consumer Recycled Asphalt Shingle (RAS). *Standard Operating Procedure (SOP) 2: Control of Superpave Bituminous Mixture Designs*.
- Ge, D., You, Z., Chen, S., Liu, C., Gao, J., & Lv, S. (2019). The performance of asphalt binder with trichloroethylene: Improving the efficiency of using reclaimed asphalt pavement. *Journal of cleaner production*, *232*, 205-212.
- Glover, C. J., Davison, R. R., Domke, C. H., Ruan, Y., Juristyarini, P., Knorr, D. B., & Jung, S. H. (2005). Development of a new method for assessing asphalt binder durability with field validation. *Texas Dept Transport*, *1872*, 1-334.
- Guduru, G., Kumara, C., Gottumukkala, B., & Kuna, K. K. (2021). Effectiveness of different categories of rejuvenators in recycled asphalt mixtures. *Journal of Transportation Engineering, Part B: Pavements*, *147*(2), 04021006.

- Haghshenas, H. F., Rea, R., Reinke, G., & Haghshenas, D. F. (2020). Chemical Characterization of Recycling Agents. *Journal of Materials in Civil Engineering*, 32(5), 06020005. doi:10.1061/(asce)mt.1943-5533.0003167
- Hajj, E. Y., Souliman, M. I., Alavi, M. Z., & Salazar, L. G. L. (2013). Influence of hydrogreen bioasphalt on viscoelastic properties of reclaimed asphalt mixtures. *Transportation research record*, 2371(1), 13-22.
- Hall, K. D., Castillo-Camarena, E. A., & Parnell, N. (2019). Effects of Aging Protocols on the Discrimination Potential of a Cracking Test in Asphalt Mixtures *Airfield and Highway Pavements 2019: Testing and Characterization of Pavement Materials* (pp. 51-61): American Society of Civil Engineers Reston, VA.
- Hand, A. J., & Martin, A. E. (2020). *Practical Guide for Using Recycling Agents in Asphalt Mixtures*
- Hettiarachchi, C., Hou, X., Xiang, Q., Yong, D., & Xiao, F. (2020). A blending efficiency model for virgin and aged binders in recycled asphalt mixtures based on blending temperature and duration. *Resources, Conservation and Recycling*, 161, 104957.
- Houston, W. N., Mirza, M., Zapata, C. E., & Raghavendra, S. (2005). *Environmental effects in pavement mix and structural design systems*:NCHRP, Project.
- Huang, B., Li, G., Vukosavljevic, D., Shu, X., & Egan, B. K. (2005). Laboratory investigation of mixing hot-mix asphalt with reclaimed asphalt pavement. *Transportation Research Record*, 1929(1), 37-45.
- Hunter, R. N., Self, A., Read, J., & Hobson, E. (2015). *The shell bitumen handbook*: ICE Publishing London, UK:.
- Im, S., Karki, P., & Zhou, F. (2016). Development of new mix design method for asphalt mixtures containing RAP and rejuvenators. *Construction and Building Materials*, 115, 727-734. doi:10.1016/j.conbuildmat.2016.04.081
- Im, S., & Zhou, F. (2014). *Field performance of RAS test sections and laboratory investigation of impact of rejuvenators on engineering properties of RAP/RAS mixes*
- Jo Sias, D. (2020) *Long-term Testing and Analysis on Asphalt Mix Rejuvenator Field Sections*.
- Johnson, K.-A. N., & Hesp, S. A. M. (2014). Effect of Waste Engine Oil Residue on Quality and Durability of SHRP Materials Reference Library Binders. *Transportation research record*, 2444(1), 102-109. doi:10.3141/2444-12
- Kadhim, H., & Baaj, H. (2020). Evaluating the Performance of the Asphalt Mixes Containing Reclaimed Asphalt Pavement by Considering the Effect of Silo Storage Time. *Journal of Testing and Evaluation*, 48(1), 18-34.

- Karki, P., & Zhou, F. (2016). Effect of rejuvenators on rheological, chemical, and aging properties of asphalt binders containing recycled binders. *Transportation research record*, 2574(1), 74-82.
- Karki, P., & Zhou, F. (2018). *Evaluation of Asphalt Binder Performance with Laboratory and Field Test Sections*
- Karlsson, R., & Isacsson, U. (2003). Application of FTIR-ATR to characterization of bitumen rejuvenator diffusion. *Journal of Materials in Civil Engineering*, 15(2), 157-165.
- Kaseer, F., Arámbula-Mercado, E., Cucalon, L. G., & Martin, A. E. (2020). Performance of asphalt mixtures with high recycled materials content and recycling agents. *International Journal of Pavement Engineering*, 21(7), 863-877. doi:10.1080/10298436.2018.1511990
- Kaseer, F., Arámbula-Mercado, E., & Martin, A. E. (2019a). A method to quantify reclaimed asphalt pavement binder availability (effective RAP binder) in recycled asphalt mixes. *Transportation Research Record*, 2673(1), 205-216.
- Kaseer, F., Martin, A. E., & Arámbula-Mercado, E. (2019b). Use of recycling agents in asphalt mixtures with high recycled materials contents in the United States: A literature review. *Construction and Building Materials*, 211, 974-987. doi:10.1016/j.conbuildmat.2019.03.286
- Kaseer, F., Yin, F., Arámbula-Mercado, E., & Epps Martin, A. (2017). Stiffness Characterization of Asphalt Mixtures with High Recycled Material Content and Recycling Agents. *Transportation research record*, 2633(1), 58-68. doi:10.3141/2633-08
- Kim, S., Sholar, G. A., Byron, T., & Kim, J. (2009). Performance of Polymer-Modified Asphalt Mixture with Reclaimed Asphalt Pavement. *Transportation Research Record: Journal of the Transportation Research Board*, 2126(1), 109-114. doi:10.3141/2126-13
- Kim, Y. R., Castorena, C., Elwardany, M. D., Rad, F. Y., Underwood, S., Akshay, G., . . . Glaser, R. R. (2018). Long-term aging of asphalt mixtures for performance testing and prediction.
- Kvasnak, A., Moore, J., Taylor, A., & Prowell, B. (2010). Preliminary evaluation of warm mix asphalt field demonstration: Franklin, Tennessee. *National Center for Asphalt Technology, Auburn, AL*.
- Lei, Z., Yi-Qiu, T., & Bahia, H. (2016). Relationship between glass transition temperature and low temperature properties of oil modified binders. *Construction and Building Materials*, 104, 92-98. doi:10.1016/j.conbuildmat.2015.12.048
- Lesueur, D. (2009). The colloidal structure of bitumen: Consequences on the rheology and on the mechanisms of bitumen modification. *Advances in Colloid and Interface Science*, 145(1-2), 42-82. doi:10.1016/j.cis.2008.08.011

- Liu, S., Peng, A., Wu, J., & Zhou, S. B. (2018). Waste engine oil influences on chemical and rheological properties of different asphalt binders. *Construction and Building Materials*, *191*, 1210-1220.
- Lo Presti, D., Vasconcelos, K., Orešković, M., Pires, G. M., & Bressi, S. (2020). On the degree of binder activity of reclaimed asphalt and degree of blending with recycling agents. *Road Materials and Pavement Design*, *21*(8), 2071-2090. doi:10.1080/14680629.2019.1607537
- Lu, D. X., Saleh, M., & Nguyen, N. H. T. (2019). Effect of rejuvenator and mixing methods on behaviour of warm mix asphalt containing high RAP content. *Construction and Building Materials*, *197*, 792-802. doi:<https://doi.org/10.1016/j.conbuildmat.2018.11.205>
- Ma, T., Huang, X., Zhao, Y., & Zhang, Y. (2015). Evaluation of the diffusion and distribution of the rejuvenator for hot asphalt recycling. *Construction and Building Materials*, *98*, 530-536.
- Mangiafico, S., Di Benedetto, H., Sauzéat, C., Olard, F., Pouget, S., & Planque, L. (2016). Effect of colloidal structure of bituminous binder blends on linear viscoelastic behaviour of mixtures containing Reclaimed Asphalt Pavement. *Materials & Design*, *111*, 126-139. doi:10.1016/j.matdes.2016.07.124
- Martin, A. E., Kaseer, F., Arambula-Mercado, E., Bajaj, A., Cucalon, L. G., Yin, F., . . . Hajj, E. Y. (2019). Evaluating the effects of recycling agents on asphalt mixtures with high RAS and RAP binder ratios. *NCHRP Research Report*(927).
- Martin, A. E., Mercado, E. A., & Abdelaziz, A. (2021). Binder Availability in Recycled Materials: Review of Literature and Available Quantification Methods.
- Mensching, D. J., Rowe, G. M., Daniel, J. S., & Bennert, T. (2015). Exploring low-temperature performance in Black Space. *Road Materials and Pavement Design*, *16*(sup2), 230-253. doi:10.1080/14680629.2015.1077015
- Mogawer, W., Bennert, T., Daniel, J. S., Bonaquist, R., Austerman, A., & Booshehrian, A. (2012). Performance characteristics of plant produced high RAP mixtures. *Road Materials and Pavement Design*, *13*(sup1), 183-208. doi:10.1080/14680629.2012.657070
- Mogawer, W. S., Austerman, A., Al-Qadi, I. L., Buttlar, W., Ozer, H., & Hill, B. (2017). Using binder and mixture space diagrams to evaluate the effect of re-refined engine oil bottoms on binders and mixtures after ageing. *Road Materials and Pavement Design*, *18*(sup1), 154-182. doi:10.1080/14680629.2016.1266756
- Mogawer, W. S., Austerman, A. J., Kluttz, R., & Puchalski, S. (2016). Using Polymer Modification and Rejuvenators to Improve the Performance of High Reclaimed Asphalt Pavement Mixtures. *Transportation research record*, *2575*(1), 10-18. doi:10.3141/2575-02

- Mogawer, W. S., Booshehrian, A., Vahidi, S., & Austerman, A. J. (2013). Evaluating the effect of rejuvenators on the degree of blending and performance of high RAP, RAS, and RAP/RAS mixtures. *Road Materials and Pavement Design*, 14(sup2), 193-213. doi:10.1080/14680629.2013.812836
- Mohajeri, M., Molenaar, A., & Van de Ven, M. (2014). Experimental study into the fundamental understanding of blending between reclaimed asphalt binder and virgin bitumen using nanoindentation and nano-computed tomography. *Road Materials and Pavement Design*, 15(2), 372-384.
- Moraes, R., & Bahia, H. (2015). Effect of Mineral Fillers on the Oxidative Aging of Asphalt Binders: Laboratory Study with Mastics. *Transportation research record*, 2506(1), 19-31. doi:10.3141/2506-03
- NCAT. (2014). NCAT Researchers Explore Multiple Uses of Rejuvenators. *NCAT Newsletter*. Retrieved from <http://eng.auburn.edu/research/centers/ncat/research/newsletters/atnspring2014.pdf>
- Newcomb, D., Epps, J., & Zhou, F. (2016). Use of RAP & RAS in High Binder Replacement Asphalt Mixtures: A Synthesis. *National Asphalt Pavement Association, Special Report*, 213.
- Newcomb, D., Martin, A. E., Yin, F., Arambula, E., Park, E. S., Chowdhury, A., . . . Coleri, E. (2015). *Short-term laboratory conditioning of asphalt mixtures*.
- Norouzi, A., Sabouri, M., & Kim, Y. R. (2014). Evaluation of the fatigue performance of asphalt mixtures with high RAP content. *Journal of Tylor and Francis Group*, 1069-1077.
- Nsengiyumva, G., Haghshenas, H. F., Kim, Y.-R., & Kommidi, S. R. (2020). Mechanical-Chemical Characterization of the Effects of Type, Dosage, and Treatment Methods of Rejuvenators in Aged Bituminous Materials. *Transportation research record*, 2674(3), 126-138. doi:10.1177/0361198120909110
- Ogbo, C., Kaseer, F., Oshone, M., Sias, J. E., & Martin, A. E. (2019). Mixture-based rheological evaluation tool for cracking in asphalt pavements. *Road Materials and Pavement Design*, 20(sup1), S299-S314. doi:10.1080/14680629.2019.1592010
- Oliveira, J. R., Silva, H. M., Jesus, C. M., Abreu, L. P., & Fernandes, S. R. (2013). Pushing the Asphalt Recycling Technology to the Limit. *International Journal of Pavement Research & Technology*, 6(2).
- Orešković, M., Pires, G. M., Bressi, S., Vasconcelos, K., & Presti, D. L. (2020). Quantitative assessment of the parameters linked to the blending between reclaimed asphalt binder and recycling agent: A literature review. *Construction and Building Materials*, 234, 117323.
- Oshone, M., Sias, J. E., Dave, E. V., Epps Martin, A., Kaseer, F., & Rahbar-Rastegar, R. (2019). Exploring master curve parameters to distinguish between mixture variables. *Road*

- Materials and Pavement Design*, 20(sup2), S812-S826.
doi:10.1080/14680629.2019.1633784
- Osmari, P. H., Aragão, F. T. S., Leite, L. F. M., Simão, R. A., da Motta, L. M. G., & Kim, Y.-R. (2017). Chemical, Microstructural, and Rheological Characterizations of Binders to Evaluate Aging and Rejuvenation. *Transportation research record*, 2632(1), 14-24.
doi:10.3141/2632-02
- Pahlavan, F., Hung, A., & Fini, E. H. (2018). Evolution of molecular packing and rheology in asphalt binder during rejuvenation. *Fuel*, 222, 457-464. doi:10.1016/j.fuel.2018.02.184
- Petersen, J. C. (2009). A review of the fundamentals of asphalt oxidation: chemical, physicochemical, physical property, and durability relationships. *Transportation Research Circular(E-C140)*.
- Podolsky, J. H., Saw, B., Elkashef, M., Williams, R. C., & Cochran, E. W. (2021). Rheology and mix performance of rejuvenated high RAP field produced hot mix asphalt with a soybean derived rejuvenator. *Road Materials and Pavement Design*, 22(8), 1894-1907.
doi:10.1080/14680629.2020.1719190
- Rajib, A. I., Samieadel, A., Zalghout, A., Kaloush, K. E., Sharma, B. K., & Fini, E. H. (2020). Do all rejuvenators improve asphalt performance? *Road Materials and Pavement Design*, 1-19. doi:10.1080/14680629.2020.1826348
- Rathore, M., & Zaumanis, M. (2020). Impact of laboratory mixing procedure on the properties of reclaimed asphalt pavement mixtures. *Construction and Building Materials*, 264, 120709.
doi:<https://doi.org/10.1016/j.conbuildmat.2020.120709>
- Reed, J. (2010). *Evaluation of the effects of aging on asphalt rubber pavements*. Arizona State University. Retrieved from <https://repository.asu.edu/items/8798>
- Rinaldini, E., Schuetz, P., Partl, M., Tebaldi, G., & Poulidakos, L. (2014). Investigating the blending of reclaimed asphalt with virgin materials using rheology, electron microscopy and computer tomography. *Composites Part B: Engineering*, 67, 579-587.
- Rodezno, C., & Brown, R. (2017). Improving accuracy of asphalt content determination by ignition test. *Road Materials and Pavement Design*, 18(sup4), 112-127.
- Rodezno, C., Moraes, R., Yin, F., & Fortunatus, M. (2021). Recycled Asphalt Binder Study.
- Rowe, G. (2011). Prepared discussion for the AAPT paper by Anderson et al.: Evaluation of the relationship between asphalt binder properties and non-load related cracking. *Journal of the Association of Asphalt Paving Technologists*, 80, 649-662.
- Sánchez, D., Caro, S., & Alvarez, A. (2020). Determining optimum doses of palm oil rejuvenators for recycled blends *Advances in Materials and Pavement Performance Prediction II* (pp. 339-342): CRC Press.

- Santos, F. B., Faxina, A. L., & Soares, S. d. A. (2021). Soy-based rejuvenated asphalt binders: Impact on rheological properties and chemical aging indices. *Construction and Building Materials*, 300, 124220. doi:<https://doi.org/10.1016/j.conbuildmat.2021.124220>
- Shen, J., Amirkhanian, S., & Tang, B. (2007). Effects of rejuvenator on performance-based properties of rejuvenated asphalt binder and mixtures. *Construction and Building Materials*, 21(5), 958-964. doi:10.1016/j.conbuildmat.2006.03.006
- Shirodkar, P., Mehta, Y., Nolan, A., Sonpal, K., Norton, A., Tomlinson, C., . . . Sauber, R. (2011). A study to determine the degree of partial blending of reclaimed asphalt pavement (RAP) binder for high RAP hot mix asphalt. *Construction and Building Materials*, 25(1), 150-155.
- Sobieski, T., Arámbula-Mercado, E., & Epps Martin, A. (2021). A method for characterising RAP degree of binder activity. *Road Materials and Pavement Design*, 1-21. doi:10.1080/14680629.2021.1963817
- Sreeram, A., Leng, Z., Zhang, Y., & Padhan, R. K. (2018). Evaluation of RAP binder mobilisation and blending efficiency in bituminous mixtures: An approach using ATR-FTIR and artificial aggregate. *Construction and Building Materials*, 179, 245-253.
- Sun, Z., Yi, J., Huang, Y., Feng, D., & Guo, C. (2016). Properties of asphalt binder modified by bio-oil derived from waste cooking oil. *Construction and Building Materials*, 102, 496-504. doi:10.1016/j.conbuildmat.2015.10.173
- Tabatabaee, H. A., & Kurth, T. L. (2017). Analytical investigation of the impact of a novel bio-based recycling agent on the colloidal stability of aged bitumen. *Road Materials and Pavement Design*, 18(sup2), 131-140. doi:10.1080/14680629.2017.1304257
- Tabatabaee, H. A., Velasquez, R., & Bahia, H. U. (2012). Predicting low temperature physical hardening in asphalt binders. *Construction and Building Materials*, 34, 162-169. doi:<https://doi.org/10.1016/j.conbuildmat.2012.02.039>
- Tran, N. (2020). Compounding Mixture Durability by Making Incremental Specification Improvements *NCAT Newsletters* (Vol. Fall 2020, pp. 11-13).
- Tran, N. (2021). Lessons Learned from the First Mixture Rejuvenator Evaluation on the Test Track. *NCAT Newsletters*.
- Tran, N., Huber, G., Leiva, F., & Pine, B. (2019a). Mix Design Strategies for Improving Asphalt Mixture Performance NCAT Report 19-08.
- Tran, N., Xie, Z., Julian, G., Taylor, A., Willis, R., Robbins, M., & Buchanan, S. (2017). Effect of a Recycling Agent on the Performance of High-RAP and High-RAS Mixtures: Field and Lab Experiments. *Journal of Materials in Civil Engineering*, 29(1), 04016178. doi:10.1061/(asce)mt.1943-5533.0001697

- Tran, N., Yin, F., Leiva, F., Rodezno, C., Huber, G., & Pine, W. (2019b). Adjustments to the Superpave Volumetric Mixture Design Procedure for Selecting Optimum Asphalt Content. *Project NCHRP*, 20-07.
- Tran, N. H., Taylor, A., & Willis, R. (2012). *Effect of rejuvenator on performance properties of HMA mixtures with high RAP and RAS contents*:NCAT Report.
- Valdés, G., Pérez-Jiménez, F., Miró, R., Martínez, A., & Botella, R. (2011). Experimental study of recycled asphalt mixtures with high percentages of reclaimed asphalt pavement (RAP). *Construction and Building Materials*, 25(3), 1289-1297.
doi:10.1016/j.conbuildmat.2010.09.016
- Wang, C., Xue, L., Xie, W., You, Z., & Yang, X. (2018). Laboratory investigation on chemical and rheological properties of bio-asphalt binders incorporating waste cooking oil. *Construction and Building Materials*, 167, 348-358.
doi:10.1016/j.conbuildmat.2018.02.038
- Wang, F., Wang, Z., Li, C., Xiao, Y., Wu, S., & Pan, P. (2017). The rejuvenating effect in hot asphalt recycling by mortar transfer ratio and image analysis. *Materials*, 10(6), 574.
- West, R., Rodezno, C., Leiva, F., & Taylor, A. (2018a). *Regressing Air Voids for Balanced HMA Mix Design*
- West, R., Rodezno, C., Leiva, F., & Yin, F. (2018b). *Development of a framework for balanced mix design*:Project NCHRP.
- West, R., Timm, D., Powell, B., Heitzman, M., Tran, N., Rodezno, C., . . . Vargas, A. (2019). *Phase VI (2015-2017) NCAT Test Track Findings*
- West, R., Timm, D., Powell, B., Tran, N., Yin, F., Bowers, B., . . . Nakhaei, M. (2021a). *Phase VII (2018-2021) NCAT Test Track Findings*
- West, R., Yin, F., Rodezno, C., & Taylor, A. (2021b). *Balanced Mixture Design Implementation Support*
- West, R. C. (2015). *Best practices for RAP and RAS management*
- West, R. C., & Copeland, A. (2015). *High RAP asphalt pavements: Japan practice-lesson learned*
- Williams, B. A., Willis, J. R., & Shacat, J. (2020). *proportionedAsphalt Pavement Industry Survey on Recycled Materials and Warm-Mix Asphalt Usage: 2019*
- Willis, J. R., Turner, P., Julian, G., Taylor, A. J., Tran, N., & Padula, F. (2012). Effects of changing virgin binder grade and content on RAP mixture properties. *NCAT Report*(12-03).
- WisDOT. (2021). Standard Specification *Hot Mix Asphalt*.

- Xie, Z., Rizvi, H., Purdy, C., Ali, A., & Mehta, Y. (2019). Effect of rejuvenator types and mixing procedures on volumetric properties of asphalt mixtures with 50% RAP. *Construction and Building Materials*, 218, 457-464.
doi:<https://doi.org/10.1016/j.conbuildmat.2019.05.093>
- Xie, Z., Tran, N., Julian, G., Taylor, A., & Blackburn, L. D. (2017). Performance of asphalt mixtures with high recycled contents using rejuvenators and warm-mix additive: field and lab experiments. *Journal of Materials in Civil Engineering*, 29(10), 04017190.
- Xu, G., & Wang, H. (2018). Diffusion and interaction mechanism of rejuvenating agent with virgin and recycled asphalt binder: A molecular dynamics study. *Molecular Simulation*, 44(17), 1433-1443.
- Xu, G., Wang, H., & Sun, W. (2018a). Molecular dynamics study of rejuvenator effect on RAP binder: Diffusion behavior and molecular structure. *Construction and Building Materials*, 158, 1046-1054. doi:10.1016/j.conbuildmat.2017.09.192
- Xu, J., Hao, P., Zhang, D., & Yuan, G. (2018b). Investigation of reclaimed asphalt pavement blending efficiency based on micro-mechanical properties of layered asphalt binders. *Construction and Building Materials*, 163, 390-401.
- Xu, M., Yi, J., Feng, D., & Huang, Y. (2019). Diffusion characteristics of asphalt rejuvenators based on molecular dynamics simulation. *International Journal of Pavement Engineering*, 20(5), 615-627.
- Xu, M., & Zhang, Y. (2020). Study of rejuvenators dynamic diffusion behavior into aged asphalt and its effects. *Construction and Building Materials*, 261, 120673.
- Yan, Y., Roque, R., Cocconcelli, C., Bekoe, M., & Lopp, G. (2017). Evaluation of cracking performance for polymer-modified asphalt mixtures with high RAP content. *Road Materials and Pavement Design*, 18(sup1), 450-470.
doi:10.1080/14680629.2016.1266774
- Yildirim, Y. (2007). Polymer modified asphalt binders. *Construction and Building Materials*, 21(1), 66-72. doi:<https://doi.org/10.1016/j.conbuildmat.2005.07.007>
- Yin, F., Arambula, E., Lytton, R., Martin, A. E., & Cucalon, L. G. (2014). Novel method for moisture susceptibility and rutting evaluation using Hamburg wheel tracking test. *Transportation Research Record*, 2446(1), 1-7.
- Yin, F., Chen, C., West, R., Martin, A. E., & Arambula-Mercado, E. (2020). Determining the Relationship Among Hamburg Wheel-Tracking Test Parameters and Correlation to Field Performance of Asphalt Pavements. *Transportation Research Record*, 2674(4), 281-291.
- Yin, F., Gu, F., Moraes, R., & Hanz, A. (2021). *Impact of Polymer Modification on IDEAL-CT and I-FIT for Balanced Mix Design*.

- Yin, F., Kaseer, F., Arámbula-Mercado, E., & Epps Martin, A. (2017). Characterising the long-term rejuvenating effectiveness of recycling agents on asphalt blends and mixtures with high RAP and RAS contents. *Road Materials and Pavement Design*, 18(sup4), 273-292. doi:10.1080/14680629.2017.1389074
- Yin, F., & Moraes, R. (2021). *Novel Methods for Adding Rejuvenators in Asphalt Mixtures with High Recycled Binder Ratios*.
- Yu, S., Shen, S., Zhang, C., Zhang, W., & Jia, X. (2017). Evaluation of the blending effectiveness of reclaimed asphalt pavement binder. *Journal of Materials in Civil Engineering*, 29(12), 04017230.
- Yu, X., Zaumanis, M., Dos Santos, S., & Poulikakos, L. D. (2014). Rheological, microscopic, and chemical characterization of the rejuvenating effect on asphalt binders. *Fuel*, 135, 162-171. doi:10.1016/j.fuel.2014.06.038
- Zadshir, M., Hosseinezhad, S., & Fini, E. H. (2019). Deagglomeration of oxidized asphaltenes as a measure of true rejuvenation for severely aged asphalt binder. *Construction and Building Materials*, 209, 416-424. doi:10.1016/j.conbuildmat.2019.03.090
- Zadshir, M., Oldham, D. J., Hosseinezhad, S., & Fini, E. H. (2018). Investigating bio-rejuvenation mechanisms in asphalt binder via laboratory experiments and molecular dynamics simulation. *Construction and Building Materials*, 190, 392-402. doi:10.1016/j.conbuildmat.2018.09.137
- Zaumanis, M., Boesiger, L., Kunz, B., Cavalli, M. C., & Poulikakos, L. (2019). Determining optimum rejuvenator addition location in asphalt production plant. *Construction and Building Materials*, 198, 368-378. doi:10.1016/j.conbuildmat.2018.11.239
- Zaumanis, M., & Mallick, R. B. (2013). Finite element modeling of rejuvenator diffusion in RAP binder film—simulation of plant mixing process *Multi-Scale Modeling and Characterization of Infrastructure Materials* (pp. 407-419): Springer.
- Zaumanis, M., Mallick, R. B., & Frank, R. (2013). Evaluation of Rejuvenator's Effectiveness with Conventional Mix Testing for 100% Reclaimed Asphalt Pavement Mixtures. *Transportation Research Record: Journal of the Transportation Research Board*, 2370(1), 17-25. doi:10.3141/2370-03
- Zaumanis, M., Mallick, R. B., & Frank, R. (2014a). Determining optimum rejuvenator dose for asphalt recycling based on Superpave performance grade specifications. *Construction and Building Materials*, 69, 159-166. doi:10.1016/j.conbuildmat.2014.07.035
- Zaumanis, M., Mallick, R. B., Poulikakos, L., & Frank, R. (2014b). Influence of six rejuvenators on the performance properties of Reclaimed Asphalt Pavement (RAP) binder and 100% recycled asphalt mixtures. *Construction and Building Materials*, 71, 538-550. doi:10.1016/j.conbuildmat.2014.08.073

- Zhang, K., Wen, H., & Hobbs, A. (2015). Laboratory tests and numerical simulations of mixing superheated virgin aggregate with reclaimed asphalt pavement materials. *Transportation Research Record*, 2506(1), 62-71.
- Zhang, R., Sias, J. E., & Dave, E. V. (2020). Evaluation of the cracking and aging susceptibility of asphalt mixtures using viscoelastic properties and master curve parameters. *Journal of Traffic and Transportation Engineering (English Edition)*. doi:10.1016/j.jtte.2020.09.002
- Zhang, Y., & Bahia, H. U. (2021). Effects of recycling agents (RAs) on rutting resistance and moisture susceptibility of mixtures with high RAP/RAS content. *Construction and Building Materials*, 270, 121369.
- Zhang, Y., Swiertz, D., & Bahia, H. U. (2021). Use of Blended Binder Tests to Estimate Performance of Mixtures with High Reclaimed Asphalt Pavement/Recycled Asphalt Shingles Content. *Transportation research record*, 0361198121997423.
- Zhou, F., Im, S., Morton, D., Lee, R., Hu, S., & Scullion, T. (2015). Rejuvenator characterization, blend characteristics, and proposed mix design method. *J. Assoc. Asphalt Paving Technol*, 84, 675-704.
- Zhou, F., Im, S., Sun, L., & Scullion, T. (2017). Development of an IDEAL cracking test for asphalt mix design and QC/QA. *Road Materials and Pavement Design*, 18(sup4), 405-427.
- Zhou, F., Karki, P., & Hu, S. (2019). *Rejuvenator Laboratory Characterization and Field Performance*
- Zhou, Z., Gu, X., Dong, Q., Ni, F., & Jiang, Y. (2020). Low- and intermediate-temperature behaviour of polymer-modified asphalt binders, mastics, fine aggregate matrices, and mixtures with Reclaimed Asphalt Pavement material. *Road Materials and Pavement Design*, 21(7), 1872-1901. doi:10.1080/14680629.2019.1574233
- Zhu, H., Xu, G., Gong, M., & Yang, J. (2017). Recycling long-term-aged asphalts using bio-binder/plasticizer-based rejuvenator. *Construction and Building Materials*, 147, 117-129.